Bioprocess monitoring and chemometric modelling of wine fermentations

by

Jessica Louise Garlick

Thesis presented in partial fulfilment of the requirements for the degree of
Master of Science

at
Stellenbosch University
Institute for Wine Biotechnology, Department of Viticulture and Oenology,
Faculty of Natural Sciences

Supervisor: Dr HH Nieuwoudt
Co-supervisor: Prof M du Toit

March 2013

Declaration

By submitting this thesis electronically, I declare that the entirety of the work contained therein is my own, original work, that I am the sole author thereof (unless to the extent explicitly otherwise stated), that reproduction and publication thereof by Stellenbosch University will not infringe any third party rights and that I have not previously in its entirety or in part submitted it for obtaining any qualification.

Date: 15/12/2012

SUMMARY

Wine fermentation is a continuously changing biological process whereby the raw product, grape juice is transformed into a high value product wine. In an ideal situation the fermentation kinetics of batch fermentations should follow the same trend over time. This however is not the case in industrial wine fermentations where significant batch-to-batch variation is present. The time trajectories of fermentation processes are therefore often unpredictable in absolute terms. The monitoring of substrate (sugar) and product concentrations (ethanol) as well as other quality parameters during a wine fermentation, is therefore of extreme importance to ensure effective control and management of wine fermentation processes. Conventional methods for fermentation monitoring are however costly, time consuming and often unreliable. For these reasons the modern wine industry requires rapid, reliable, non-destructive monitoring techniques which would meet the criteria of providing critical real-time process information that is displayed in easily interpretable graphical format, in order to ensure the highest quality and continuous consistency throughout all the stages of a process.

This research study in particular, addressed the current need for alternative fermentation monitoring strategies that meet these criteria, by evaluating the potential use of spectroscopy as an analytical technique for fermentation monitoring. The overall objective of this study was to use chemometric modelling of information obtained by Fourier transform mid-infrared (FT-MIR) and near-infrared (FT-NIR) spectroscopy, to quantitatively and qualitatively monitor both alcoholic (AF) and malolactic fermentation (MLF) processes. Towards this objective 11 batch fermentations elaborated with *Oenococcus oeni* and *Lactobacillus plantarum* strains in respectively a co-inoculation and sequential inoculation scenario, were sampled and analysed at regular time intervals with FT-MIR and FT-NIR spectroscopy and enzymatic reference methods during 2011.

Samples were also analysed by gas chromatography flame ionisation detection (GC-FID) and mass spectrometry (GC-MS) at two critical stages during fermentation, namely 50% completion of MLF and 100% completion of MLF, in order to obtain a profile of the evolution of the aroma compounds associated with each inoculation scenario.

Three clearly defined research objectives were set for this project. The first objective involved the expansion of the existing quantitative platform for fermentation monitoring. Towards the outcomes of this objective, partial least squares (PLS) calibration models for prediction of malic acid and lactic acid in fermenting must and wines elaborated in our study, were established, based on the MIR and NIR spectra. The models showed excellent predictive abilities in independent test set validation. This outcome made a significant contribution to our existing PLS calibration capacity, particularly towards monitoring of MLF. Quantitative data obtained with the PLS models were also used to graphically project the rate of AF in the

different batches, by non-linear fitted regression plots that easily visualised the overall patterns of sugar and ethanol metabolism in the different fermentations.

The second research objective involved the qualitative monitoring of fermentations. This approach used FT-MIR and FT-NIR spectra together with chemometrics to identify trends between the different fermentation treatments. Principal component analysis (PCA) clearly projected the time trend from the onset of fermentation, through AF and MLF. No unique bacterial trend was however observed with spectroscopy. These results illustrate the potential of these techniques to be used for modelling of fermentations in industrial situations, through providing critical information about the evolution of the process. Furthermore, these techniques provide tools for identifying problematic and deviating fermentations. A spectral conformity test based on simple calculations of the standard deviation between the absorbance at each recorded wavenumber in the spectra, further confirmed identification of the critical fermentation stages. This technique by-passes the need for spectral interpretation and is a very useful addition, particularly from the industry perspective, to the portfolio of methods established in this study.

The third research objective adressed the need to evaluate the possibility to discriminate between the different process stages and LAB treatments using univariate (ANOVA) and multivariate chemometric techniques such as PCA, PLS discriminant analysis (PLS-DA) and Soft Independent Modelling of Class Analogy (SIMCA) for possible future interpretative and classification purposes. The exploratory tool of PCA was used to investigate the similarities and differences between the chemical footprints of the different treatments. PCA showed clear differentiation between the two process stages using chemical quantified data. Differentiation between the LAB treatments was visible with PCA, showing a more prominent separation at 50% completion of MLF. Furthermore the ability of spectroscopy for potential classification was shown using PLS-DA and SIMCA. This profiling study can be seen as a preliminary study setting the ground work for further in-depth research into the profiling of different LAB treatments and inoculation strategies.

OPSOMMING

Wyngisting is ‘n voortdurend veranderende biologiese proses waarvolgens die rou produk, druiwesap, in ‘n produk van hoë waarde, naamlik wyn, verander word. Onder ideale omstandighede sou die gistingskinetika van lotgistings dieselfde tendens oor tyd volg. Dit is egter nie die geval in industriële wyngistings nie, waar noemenswaardige wisseling van lot tot lot teenwoordig is. Die tydsbaan van gistingsprosesse is dus in baie gevalle in absolute terme onvoorspelbaar. Die monitering van substraat- (suiker) en produkkonsentrasies (etanol), sowel as ander kwaliteitsparameters tydens ‘n wyngisting, is van die uiterste belang om doeltreffende beheer en bestuur van wyngistingsprosesse te verseker. Konvensionele metodes vir die monitering van gisting is egter duur, tydrowend en ook soms onbetroubaar. Om hierdie redes vereis die moderne wynbedryf vinnige, betroubare en nie-destruktiewe moniteringstegnieke wat aan die kriteria sou voldoen vir die verskaffing van kritiese, intydse prosesinligting wat in ‘n maklik interpreteerbare grafiese formaat vertoon word om die hoogste kwaliteit en voortdurende konsekwentheid tydens al die stadia van ‘n proses te verseker.

Hierdie navorsingstudie het in besonder die huidige behoefte aan alternatiewe gistingsmoniteringstrategieë wat aan hierdie kriteria voldoen, aangespreek deur die potensiële gebruik van spektroskopie as ‘n analitiese tegniek vir die monitering van gisting te evalueer. Die oorhoofse doelwit van hierdie studie was die chemometriese modellering van inligting wat met behulp van Fourier transform middel-infrarooi (FT-MIR) en naby-infrarooi (FT-NIR) spektroskopie verkry is om die prosesse van alkoholiese en appelmelksuurgisting (AMG) kwantitatief en kwalitatief te monitor. Ten einde hierdie doelwit te bereik, is 11 lotgistings met *Oenococcus oeni* en *Lactobacillus plantarum* rasse uitgevoer in scenario’s van ‘n gesamentlike inokulasie en opeenvolgende inokulasie onderskeidelik. Monsters van hierdie gistings is met gereelde tydintervalle in 2011 geneem en analises is met FT-MIR en FT-NIR spektroskopie en ensiematiese verwysingsmetodes gedoen.

Monsters is ook met gaschromatografiese vlam ionisasie-opsporing (GC-FID) en massaspektrometrie (GC-MS) op twee kritiese stadia tydens gisting geanaliseer, naamlik toe AMG 50% en 100% voltooid was, om ‘n profiel te verkry van die evolusie van die aromaverbindings wat met elke inokulasie-scenario verband hou.

Drie duidelik gedefinieerde navorsingsdoelwitte is vir hierdie studie bepaal. Die eerste doelwit het die uitbreiding van die bestaande kwantitatiewe platform vir gistingsmonitering behels. Hiervoor is gedeeltelike kleinstekwadraat [*partial least squares (PLS)*] kalibrasiemodelle vir die voorspelling van appelsuur en melksuur in die gistende mos en wyne in ons studie op die basis van MIR- en NIR-spektra bepaal. Die modelle het in onafhanklike geldigheidsbepaling van die toetsstel uitstekende voorspellingsvermoëns getoon. Hierdie uitkoms het ‘n noemenswaardige bydrae gemaak tot ons bestaande PLS kalibrasiekapasiteit, veral om AMG te monitor. Die kwantitatiewe data wat met die PLS-modelle verkry is, is ook gebruik om die

tempo van alkoholiese gisting in die verskillende lotte grafies uit te beeld deur middel van kromlynige passing van regressiepersele, waarmee dit maklik was om die algehele patrone van suiker- en etanolmetabolisme in die verskillende gistings te visualiseer.

Die tweede navorsingsdoelwit het die kwalitatiewe monitering van gistings behels. Hierdie benadering het FT-MIR en FT-NIR spektra tesame met chemometrie gebruik om tendense tussen die verskillende gistingsbehandelings te identifiseer. Hoofkomponentanalise [*principal component analysis (PCA)*] het duidelik die tydtendens vanaf die aanvang van gisting, deur alkoholiese gisting en AMG, geprojekteer. Geen unieke bakteriese tendens is egter met spektroskopie waargeneem nie. Hierdie uitslae illustreer die potensiaal van hierdie tegnieke om vir die modellering van gistings in industriële situasies gebruik te word deur kritiese inligting oor die evolusie van die proses te verskaf. Verder verskaf hierdie tegnieke gereedskap vir die identifikasie van problematiese en afwykende gistings. ‘n Spektrale gelykvormigheidstoets gebaseer op eenvoudige berekeninge van die standaardafwyking tussen die absorbansie by elke aangetekende golfgetal in die spektra het ook die identifikasie van die kritiese gistingstadia bevestig. Hierdie tegniek omloop die noodsaak vir spektrale interpretasie en is ‘n baie nuttige byvoeging tot die portefeulje van metodes wat in hierdie studie bepaal is, veral vanuit ‘n bedryfsperspektief.

Die derde navorsingsdoelwit het die behoefte aangespreek om tussen die verskillende prosesstadia en melksuurbakterie-behandelings te onderskei deur gebruik te maak van eenvariant- (ANOVA) en meervariant- chemometriese tegnieke soos PCA, PLS-diskriminantanalise en sagte onafhanklike modellering van klasanalogie [*soft independent modelling of class analogy (SIMCA)*] vir moontlike toekomstige verklarende en klassifikasiedoeleindes. Die ondersoekende gereedskap van PCA is gebruik om ooreenkomste en verskille tussen die chemiese voetspore van die verskillende behandelings te ondersoek. PCA het duidelike differensiasie tussen die twee prosesstadia getoon op grond van chemies gekwantifiseerde data. Differensiasie tussen die melksuurbakterie-behandelings was met PCA sigbaar, met ‘n meer prominente skeiding teen 50% voltooide AMG. Verder is die vermoë van spektroskopie vir potensiële klassifikasie met PLS-diskriminantanalise en SIMCA getoon. Die profielsamestelling in hierdie studie kan beskou word as ‘n voorlopige studie vir verdere diepgaande navorsing oor die profielsamestelling van verskillende melksuurbakterie-behandelings en inokulasiestrategieë.

This thesis is dedicated to my mother and best friend who has given me the strength and courage to reach my potential.

BIOGRAPHICAL SKETCH

Jessica Garlick was born on the 24 November 1987 and matriculated at Bridge House School in 2005. She obtained her BSc Food Science-degree at Stellenbosch University in 2009. After completing two industry involved harvest seasons in 2010, Jessica enrolled at the Institute for Wine Biotechnology in 2011 for her MSc-degree in Wine Biotechnology.

ACKNOWLEDGEMENTS

I wish to express my sincere gratitude and appreciation to the following persons and institutions:

DR HH NIEUWOUDT, Institute for Wine Biotechnology, Department of Viticulture and Oenology, Stellenbosch University, whom as my supervisor shared her passion and expertise in the field of spectroscopy and chemometrics and provided me with the continued support, motivation and critical insight needed to complete this manuscript. Thank you for pushing me to my fullest potential and inspiring my research.

PROF M DU TOIT, Institute for Wine Biotechnology, Department of Viticulture and Oenology, Stellenbosch University, whom as my co-supervisor encouraged me every step of the way, inspired me with her passion for wine-making and in-depth knowledge on MLF as well as gave critical input into this manuscript.

PROF M KIDD, Centre for Statistical Consultation, Deptartment of Statistics and Actuarial Sciences, Stellenbosch University, for knowledge and support in the statistical processing of the data.

EDMUND LAKEY AND THE EXPERIMENTAL CELLAR STAFF, Experimental cellar, Department of Viticulture and Oenology, for all the long hours spent together in the cellar.

ELDA LERM, for assisting with the wine-making and for all the support over the past two years.

MY LOVING SISTERS AND FATHER, for their continued love and support. Thank you for always believing in me.

RUELLE, SHEILA AND ANDRÉ DU TOIT, an amazing aunt and grandparents, for giving me the support and motivation I needed to get through this year.

ANKE VON MOLLENDORFF AND IAN STEUNENBERG, amazing friends whom without, this last year wouldn't have been possible.

KARIN VERGEER, Thank you for all your effort with the final touches of this thesis and for always having a smile.

THE NATIONAL RESEARCH FOUNDATION AND WINETECH, for the financial support.

OUR HEAVENLY FATHER, for making everything possible and for giving me the hope to keep on going.

PREFACE

This thesis is presented as a compilation of six chapters. Each chapter is introduced separately and is written according to the style of the *South African Journal of Enology and Viticulture*.

Chapter 1 **GENERAL INTRODUCTION, PROJECT AIMS AND OUTPUTS**

Chapter 2 **LITERATURE REVIEW**
Monitoring yeast and bacterial metabolites during alcoholic and malolactic fermentation

Chapter 3 **RESEARCH RESULTS**
Bioprocess monitoring and trend identification in wine fermentations with Fourier transform infrared (FT-IR) spectroscopy and chemometric modelling

Chapter 4 **RESEARCH RESULTS**
Metabolic profiling of lactic acid bacteria in a Shiraz wine matrix using FT-MIR spectroscopy, gas chromatography and multivariate data analysis

Chapter 5 **RESEARCH RESULTS**
High-throughput Fourier transform mid-infrared (FT-MIR) and near-infrared (FT-NIR) spectroscopy calibrations for the quantification of malic acid and lactic acid

Chapter 6 **GENERAL DISCUSSION AND CONCLUSIONS**

These chapters were written as independent papers with the consequence that overlapping, especially in the introductory parts and in the materials and methods sections, was unavoidable.

TABLE OF CONTENTS

Chapter 1

General Introduction, Project Aims & Outputs

CHAPTER 1. GENERAL INTRODUCTION, PROJECT AIMS AND OUTPUTS

1.1 INTRODUCTION

Wine fermentation is seen as a continuously evolving biotechnological process that is characterised by successive microbial-mediated reactions. Through alcoholic fermentation (AF) and malolactic fermentation (MLF), yeast and lactic acid bacteria (LAB) respectively, produce varying amounts of metabolites which result in continuous and rapid compositional fluctuations in a fermentation over time (Van Sprang *et al*., 2003; Blanco *et al*., 2004; Jørgensen *et al*., 2004). The time trajectories of AF and MLF processes are thus often difficult to predict in absolute terms (Cozzolino *et al*., 2006). Various other factors also contribute to these compositional changes and the subsequent batch-to-batch variation which is accompanied with wine production. These include initial must sugar concentrations, nitrogen limitations, temperature conditions and the specific oenological practices undertaken (Henschke, 1997; Bisson, 1999).

The oenological decision to directly inoculate LAB as starter cultures for the induction of MLF was realised by winemakers as a means to ensure rapid and complete MLF (Henick-Kling, 1995; Nielsen *et al*., 1996; Krieger-Weber, 2009), decrease the potential negative risks associated with a spontaneous MLF and encourage a positive flavour contribution by LAB (Krieger-Weber, 2009). The specific timing of inoculation of these MLF starter cultures is also a critical decision made by the winemaker. Sequential inoculation is the long established protocol of inoculation of LAB during AF or after the completion of AF while co-inoculation involves the simultaneous inoculation of yeast and bacteria. The choice of MLF starter species and/or strain (Pozo Bayon *et al*., 2005; Lee *et al*., 2009a, b; Malherbe *et al*., 2012), as well as the specific timing of inoculation (Abrahamse & Bartowsky *et al*., 2012; Knoll *et al*., 2012) are known to influence the metabolic rate of fermentation processes as well as produce various metabolic products. These decisions subsequently produce wines with vastly distinct chemical profiles.

For these reasons, the modern wine industry looks for fast and reliable monitoring techniques which can provide critical real-time information about the metabolic state and progress of the process, in order to better manage wine production processes. Traditional off-line analysis produce delayed results (Vojinović *et al*., 2006) and are being increasingly replaced by non-destructive in-line sampling techniques for effective real-time measurements (reviewed by Karoui *et al*., 2010). Real time monitoring techniques have the advantage of providing information throughout the process, therefore giving direct insight into the state of the bioprocess (Vojinović *et al*., 2006). This has large logistical advantages as well as allowing the winemaker to identify problematic fermentations and make immediate and informed decisions about rectifying actions.

Both mid-infrared (MIR) and near-infrared (NIR) spectroscopic techniques offer cost effective, fast, non-destructive alternatives to the conventional methods used for fermentation monitoring (Urtubia *et al*., 2004; 2008). The recent developments in hardware technologies including optical sensor systems as well as software packages (chemometrics) has ensured the increasing acceptance of infrared (IR) in online applications for bioprocess monitoring purposes (reviewed by Karoui *et al*., 2010).

Modern commercial MIR and NIR instrumentation equipped with chemometric software packages has been successfully applied by the international wine industry to quantitatively detect a number of wine constituents (Patz *et al*., 2004 ; Urbano-Cuadrado *et al.,* 2005; Boulet *et al*., 2007; Cozzolino *et al*., 2011; Garde-Cerdán *et al*., 2011). Very few studies have, however, reported on the use of MIR and/or NIR spectroscopy to qualitatively monitor the complete time course of red wine fermentations covering both AF and MLF (Urtubia *et al*., 2004; Cozzolino *et al*., 2006; Di Egidio *et al*., 2010 ; Buratti *et al*., 2011 ; Cozzolino & Curtin, 2012).

To our knowledge, no reports have shown the ability of MIR and NIR spectroscopy to evaluate the influence of different inoculation strategies on the chemical composition of the wine matrix. One recent study has reported the ability of MIR and NIR spectroscopic techniques to discriminate between different *O. oeni* strains (Cozzolino *et al*., 2012).

Over the past few years, the Institute for Wine Biotechnology (IWBT), Stellenbosch University, together with industry inputs, have invested in the development of Fourier transform (FT)-IR spectroscopy based calibrations models for the monitoring of the entire wine production process including compounds found in grape constituents (Lochner, 2006; Swanepoel, 2006; Swanepoel *et al*., 2007), fermenting must (Nieuwoudt *et al*., 2006 ; Magerman, 2009), and bottled wine constituents (Nieuwoudt *et al*., 2004). The use of spectroscopy for the qualitative monitoring of a fermentation has however been limited to one study which reported the use of FT-IR in batch process monitoring of AF and the identification of problem fermentations (Magerman, 2009).

The study presented in this thesis therefore adds to the ongoing research program at the IWBT regarding the use of MIR and NIR spectroscopy for the quantitative and qualitative monitoring of critical stages of AF and MLF. Quantitative monitoring involving a large amount of wet analytical chemistry as well as the extensive establishment of calibration models is used for the quantification and future prediction of certain constituents. For the purpose of this study, qualitative monitoring evaluated how valuable the spectral data was for providing insight into fermentation processes without the use of quantified values. The spectrum produced by IR spectroscopy techniques is seen as a compositional fingerprint providing large amounts of chemical information about a sample. The use of powerful chemometric techniques captures the important information and allows us to identify trends and variations within the fermentations.

This project adressed the urgent need for the development of preliminary quantitative calibrations models for the monitoring of malic acid and lactic acid, as well as explored the possibility for MIR and NIR spectroscopy together with chemometric techniques, as rapid less expensive alternatives to extensive amounts of wet analytical chemistry for the qualitative monitoring of fermentations. Furthermore, the utility of spectroscopy, in combination with gas chromatography for the profiling of MLF starter cultures, was evaluated.

1.2 PROJECT AIMS AND OUTPUTS

OBJECTIVE 1: DEVELOPMENT OF QUANTITATIVE STRATEGIES FOR FERMENTATION MONITORING

AIM 1: Evaluate the ready-to-use commercial calibration on the FT-IR spectrometer for the quantification of malic acid in fermenting must and wine. This ready-to-use calibration model is advantageous for routine quantification purposes and easy to use for an unskilled user however the accuracy of these calibration models can be influenced by wine matrix variations such as variety and geographic location not included in the calibration sets and thus introducing spectral interferences (Nieuwoudt *et al*., 2004; Soriano *et al*., 2007). For this reason it was important to evaluate whether the commercial calibration was suitable for the prediction of malic acid in South African samples. In the absence of a commercial calibration for lactic acid, this task could only be done for malic acid.

AIM 2: Establish high sample-throughput methods for the quantification of malic acid and lactic acid using FT-MIR and FT-NIR spectroscopy. Reference data were generated using enzyme-linked spectrophotometric assays. These compounds are quantitatively two major organic acids found in wine (Volschenk *et al*., 2006) and malic acid in particular is an important parameter for quality control and the routine monitoring of MLF, being the principal indicator of MLF (Martineau *et al*., 1995).

AIM 3: Non-linear regression techniques were used to model the fermentation kinetics and predict the rate of AF. Data were obtained from newly established PLS calibration models as well as previously established models (Magerman, 2009).

OBJECTIVE 2: QUALITATIVE STRATEGIES FOR FERMENTATION MONITORING

AIM 1: Investigate the use of FT-MIR and FT-NIR spectroscopy together with principal component analysis (PCA) for the qualitative off-line monitoring and trend identification of AF and MLF processes.

AIM 2: Establish spectral conformity tests using FT-MIR and FT-NIR spectra to predict the stage of completion of AF.

OBJECTIVE 3: METABOLIC PROFILING OF MLF STARTER CULTURES

AIM 1: Evaluate the metabolic profiles at two critical process stages (50% completion of MLF and end MLF) of a co-inoculation and sequential inoculation strategy, elaborated with five different MLF starter cultures. Quantitative monitoring of malic acid and lactic acid, major volatile compounds, carbonyl compounds and routine wine parameters (pH, titratable acidity and volatile acidity) was carried out using enzyme-linked spectrophotometric assays, gas chromatography flame ionisation detection (GC-FID), gas chromatography mass spectrometry (GC-MS) and established PLS calibration models respectively. A combined univariate and multivariate approach was followed to evaluate the contribution of the selected MLF starter cultures on the chemical composition of the wine.

AIM 2: Evaluate the ability of different multivariate techniques including PCA, PLS-discriminant analysis (DA) and Soft Independent Modelling of Class Analogy (SIMCA) as tools to profile the contribution of different MLF species and strains on the Shiraz wine matrix.

AIM 3: Evaluate the ability of chemical quantified data, qualitative FT-MIR spectral data and PCA scores to discriminate between wine LAB using techniques such as PLS-DA and SIMCA.

Conference outputs

(1) **Garlick, J**., M. du Toit & H. Nieuwoudt. **2012**. Bioprocess monitoring and trend identification in wine fermentations using FT-IR spectroscopy and chemometric modelling. 34th SASEV Conference, Allée Bleue, Simondium.
(2) Garlick, J., **M. du Toit** & H. Nieuwoudt. **2012**. Bioprocess monitoring and trend identification in wine fermentations with FT-IR spectroscopy and chemometric modelling. Macrowine 2012, Bordeaux, France.

Publication under preparation

Currently the preparation of a popular article to be published in the South African Wineland is underway for the dissemination of the information regarding the application of this study for industrial significance.

1.3 LITERATURE CITED

Abrahamse, C.E. & Bartowsky, E.J., 2012. Timing of malolactic fermentation inoculation in Shiraz grape must and wine: Influence on chemical composition. *World J. Microbiol. Biotechnol*. 28, 1-11.

Bisson, L.F.,1999. Stuck and sluggish fermentations. *Am. J. Enol. Vitic.* 150, 1-13.

Blanco, M., Peinado, A.C. & Mas, J., 2004. Analytical monitoring of alcoholic fermentation using NIR spectroscopy. *Biotechnol. Bioeng*. 88, 536-542.

Boulet, J.C., Williams, P. & Doco, T., 2007. A Fourier transform infrared spectroscopy study of wine polysaccharides. *Carbohydr. Polym*. 69, 79-85.

Buratti, S., Ballabio, D., Giovanelli, G., Dominguez, C.M.Z., Moles, A., Benedetti, S. & Sinelli, N., 2011. Monitoring of alcoholic fermentation using near infrared and mid infrared spectroscopies combined with electronic nose and electronic tongue. *Anal. Chim. Acta* 697, 67-74.

Cozzolino, D., Parker, M., Dambergs, R.G., Herderich, M. & Gishen, M., 2006. Chemometrics and visible-near infrared spectroscopic monitoring of red wine fermentation in a pilot scale. *Biotechnol. Bioeng*. 95, 1101-1107.

Cozzolino, D., Cynkar, W., Shah, N. & Smith, P., 2011. Feasibility study on the use of attenuated total reflectance mid-infrared for analysis of compositional parameters in wine. *Food Res. Int*. 44, 181-186.

Cozzolino, D. & Curtin, C., 2012. The use of attenuated total reflectance as tool to monitor the time course of fermentation in wild ferments. *Food Control* 26, 241-246.

Cozzolino, D., McCarthy, J. & Bartowsky, E., 2012. Comparison of near infrared and mid infrared spectroscopy to discriminate between wines produced by different *Oenococcus Oeni* strains after malolactic fermentation: A feasibility study. *Food control* 26, 81-87.

Di Egidio, V., Sinelli, N., Giovanelli, G., Moles, A. & Casiraghi, E., 2010. NIR and MIR spectroscopy as rapid methods to monitor red wine fermentation. *Eur. Food. Res. Technol*. 230, 947-955.

Garde-Cerdán, T., Lorenzo, C., Alonso, G.L. & Salinas, M.R., 2011. Near infrared spectroscopy: Easy and rapid tool to determine different volatile compounds in wines. *Curr. Bioact. Compd.* 7, 93-105.

Henick-Kling, T., 1995. Control of malolactic fermentation in wine: energetics, flavour modification and methods of starter culture preparation. *J. Appl. Bacteriol. Symp. Supp*. 79, 29S-37S.

Henschke, P.A., 1997. Stuck fermentation: causes, prevention and cure. In: Allen, M., Leske, P. & Baldwin, G. (eds). Proc. Seminar: Advances in Juice Clarification and Yeast Inoculation, *Aust. Soc. Vitic. Oenol.,* Melbourne, Vic. Adelaide SA. pp. 30-41.

Jørgensen, P., Pedersen, J.G., Jensen, E.P. & Esbensen, K.H., 2004. On line batch fermentation process monitoring (NIR)—Introducing biological process time. *J. Chem*. 18, 81–91.

Karoui, R., Downey, G., & Blecker, C., 2010. Mid-infrared spectroscopy coupled with chemometrics: a tool for the analysis of Intact food systems and the exploration of their molecular structure-quality relationships - a review. *Chem. Rev*. 110, 6144-6168.

Knoll, C., Fritsch, S., Schnell, S., Grossmann, M., Krieger-Weber, S., du Toit, M. & Rauhut, D., 2012. Impact of different malolactic fermentation inoculation scenarios on Riesling wine aroma. *World J. Microbiol. Biotechnol*. 28, 1143-1153.

Krieger-Weber, S., 2009. Application of yeast and bacteria as starter cultures. In: König, H., Unden, G. & Fröhlich, J. (eds). Biology of microorganisms on grapes, in must and in wine. Springer, Berlin. pp. 498-511.

Lee, J.E., Hong, Y.S & Lee, C.H., 2009a. Characterization of fermentative behaviors of lactic acid bacteria in grape wines through ^{1}H-NMR- and GC-based metabolic profiling. *J. Agric. Food Chem*. 57, 4810-4817.

Lee, J.E., Hwang, G.S., Lee, C.H. & Hong, Y.S., 2009b. Metabolomics reveals alterations in both primary and secondary metabolites by wine bacteria. *J. Agric. Food Chem*. 57, 10772-10783.

Lochner, E., 2006. The evaluation of Fourier transform infrared (FT-IR) spectroscopy for the determination of total phenolics and total anthocyanins concentrations of grapes. Thesis, Stellenbosch University, Private Bag X1, 7602, Matieland (Stellenbosch), South Africa.

Magerman, C.M., 2009. The evaluation of Fourier transform infrared (FT-IR) spectroscopy for quantitative and qualitative monitoring of alcoholic wine fermentation. Thesis, Stellenbosch University, Private Bag X1, 7602, Matieland (Stellenbosch), South Africa.

Malherbe, S., Tredoux, A.G.J., Nieuwoudt, H.H. & du Toit, M., 2012. Comparative metabolic profling to investigate the contribution of *O. oeni* MLF starter cultures to red wine composition. *J. Ind. Microbiol. Biotechnol*. 39, 477–494.

Martineau, B., Henick-Kling, T. & Acree, T., 1995. Reassessment of the influence of malolactic fermentation on the concentration of diacetyl in wines. *Am. J. Enol. Vitic*. 46, 385-388.

Nielsen, J.C., Prahl, C. & Lonvaud-Funel, A., 1996. Malolactic fermentation in wine by direct inoculation with freeze-dried *Leuconostoc oenos* cultures. *Am. J. Enol. Vitic*. 47, 42-48.

Nieuwoudt, H.H., Prior, B.A., Pretorius, I.S., Manley, M. & Bauer, F.F., 2004. Principal component analysis applied to Fourier transform infrared spectroscopy for the design of calibration sets for glycerol prediction models in wine and for the detection and classification of outlier samples. *J. Agric. Food Chem*. 52, 3726-3735.

Nieuwoudt, H.H., Pretorius, I.S., Bauer, F.F., Nel, D.G. & Prior, B.A., 2006. Rapid screening of the fermentation profiles of wine yeasts by Fourier transform infrared spectroscopy. *J. Microbiol. Methods* 67, 248-256.

Patz, C. D., Blieke, A., Ristow, R. & Dietrich, H., 2004. Application of FT-MIR spectrometry in wine analysis. *Anal. Chim. Acta* 513, 81-89.

Pozo-Bayón, M.A., Alegría, E.G., Polo, M.C., Tenorio, C., Martín-Álvarez, P.J., Calvo de la Banda, M.T., Ruiz-Larrea, F. & Moreno-Arribas, M.V., 2005. Wine volatile and amino acid composition after malolactic fermentation: Effect of *Oenococcus oeni* and *Lactobacillus plantarum* starter cultures. *J. Agric. Food Chem*. 53, 8729-8735.

Soriano, A., Pérez-Juan, P.M., Vicario, A., González, J.M. & Pérez-Coello, M.S., 2007. Determination of anthocyanins in red wine using a newly developed method based on Fourier transform infrared spectroscopy. *Food Chem.* 104 (3), 1295-1303.

Swanepoel, M., 2006. Monitoring the quality control chain from vineyard to wine: An industrial case study. MSc Thesis, Stellenbosch University, Stellenbosch, South Africa.

Swanepoel, M., du Toit, M. & Nieuwoudt, H. H., 2007. Optimisation of the quantification of total soluble solids, pH and titratable acidity in South African grape must using Fourier transform Mid-infrared spectroscopy. *S. Afr. J. Enol. Vitic.* 28 (2), 140-149.

Urbano Cuadrado, M., Luque de Castro, M., Perez Juan, P. & Gómez-Nieto, M., 2005. Comparison and joint use of near infrared spectroscopy and Fourier transform mid infrared spectroscopy for the determination of wine parameters. *Talanta* 66, 218-224.

Urtubia, A., Ricardo Pérez-Correa, J., Meurens, M. & Agosin, E., 2004. Monitoring large scale wine fermentations with infrared spectroscopy. *Talanta* 64, 778-784.

Urtubia, A., Pérez-correa, J.R., Pizarro, F. & Agosin, E., 2008. Exploring the applicability of MIR spectroscopy to detect early indications of wine fermentation problems. *Food control* 19, 382-388.

Van Sprang, E.N.M., Ramaker, H.J., Westehuis, J.A., Smilde, A.K., Gurden, S.P. & Wienke, D., 2003. Near infrared spectroscopic monitoring of a series of industrial batch processes using a bilinear grey model. *App Spectrosc*. 57, 1007–1019.

Vojinović, V., Cabral, J.M.S. & Fonseca, L.P., 2006. Real-time bioprocess monitoring: Part I: In situ sensors. *Sensors actuators B: Chem*. 114, 1083-1091.

Volschenk, H., van Vuuren, H.J.J. & Viljoen-Bloom, M., 2006. Malic acid in wine: Origin, function and metabolism during vinification. *S. Afr. J. Enol. Vitic*. 27, 123-136.

Chapter 2

Literature Review

Monitoring yeast and bacterial metabolites during alcoholic and malolactic fermentation

CHAPTER 2. LITERATURE REVIEW

Monitoring yeast and bacterial metabolites during alcoholic and malolactic fermentation

2.1 INTRODUCTION

Wine fermentation, involving both alcoholic and malolactic fermentation is a rapidly changing biotechnological process characterised by successive microbial-mediated reactions and can thus be considered a true bioprocess. The microbial species present during fermentation specifically yeast and bacterial species produce a vast array of fermentation-derived metabolites which contribute to the overall aroma and quality of wine (Swiegers *et al.*, 2005; Bartowsky & Pretorius, 2009). These complex fermentation processes are critically important for the bioconversion of raw products into the high valued end product, wine (Cozzolino *et al*., 2006).

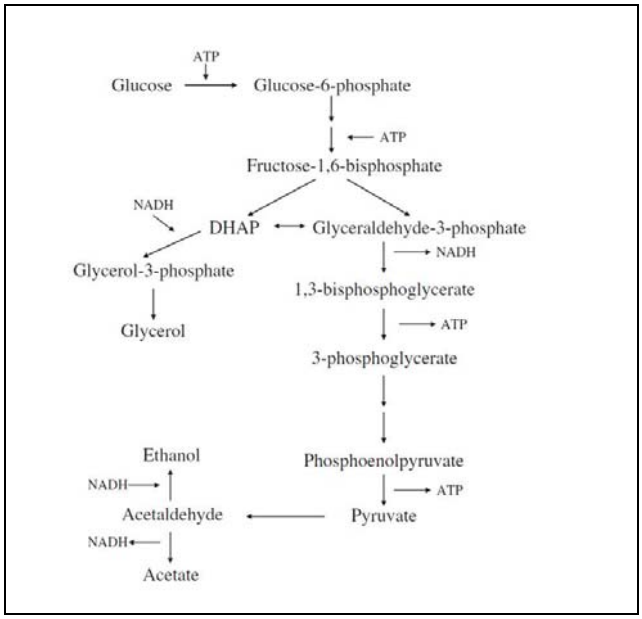

Figure 2.1 Conversion of glucose into ethanol during alcoholic fermentation by yeast *Saccharomyces cerevisiae* showing the relationship between energy production and the processes linked to the redox state of the coenzyme NAD^+/NADH. DHAP is dihydroxyacetone phosphate (adapted from Norbeck & Blomberg, 1997)

During alcoholic fermentation (AF) yeasts drive the transformation of sugars (mainly glucose and fructose) to firstly increase their biomass while secondly producing the major end products ethanol, glycerol and CO_2 (**Figure 2.1**) (Blanco *et al*., 2004). The primary objective of the secondary fermentation in wine namely malolactic fermentation (MLF) via lactic acid bacteria (LAB) metabolism, is the biological de-acidification of the wine matrix, converting L-malic acid to L-lactic acid and CO_2 with a simultaneous increase in pH, while improving the biological stability in wine (**Figure 2.2**) (Bartowsky *et al*., 2002).

Apart from these two important reactions producing major fermentation metabolites other transformations also take place during the winemaking process. Yeast and bacterial metabolism also produce a vast array of sensorially significant aromatic metabolites produced in

mg/L or µg/L quantities (Rapp, 1998; Lambrechts & Pretorius, 2000; Swiegers *et al*., 2005). These compounds include, amongst others, organic acids, higher alcohols, esters, fatty acids, carbonyl compounds, sulphur compounds and volatile phenols which can have either a positive or negative impact on the final wine quality (Bartowsky & Pretorius, 2009).

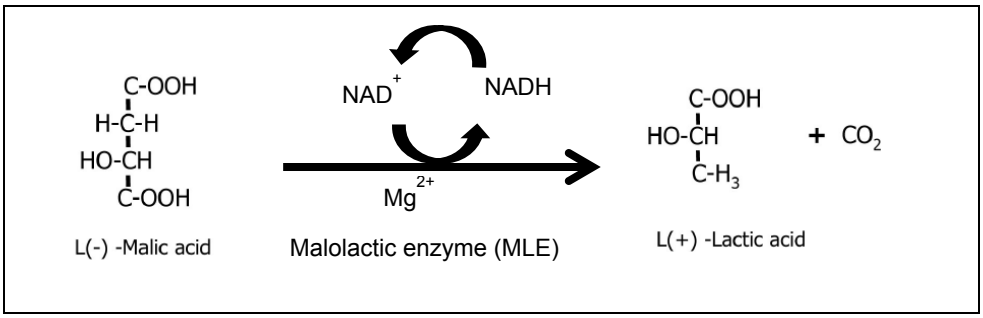

Figure 2.2 Conversion of L-Malic acid to L-Lactic acid catalysed by the malolactic enzyme during MLF (adapted from Costello, 2005).

The production of several intermediary metabolites and end products during fermentation results in rapid and continuous compositional fluctuations in a ferment over time. For this reason considerable batch-to-batch variation is indicative of industrial fermentation processes (Blanco *et al*., 2004; Jørgensen *et al*., 2004; Van Sprang *et al*., 2003) and the time course of fermentation processes are thus often difficult to predict in absolute terms (Cozzolino *et al*., 2006).

For the effective control and management of fermentation processes the modern wine industry needs fast, reliable monitoring techniques capable of providing critically important real-time information about the metabolic state and progress of fermentation. In other words the monitoring of important marker compounds specific to AF and MLF would therefore give the winemaker insight into the stage of completion of the processes respectively. This real-time information would allow the winemaker to identify problematic or deviating fermentations and subsequently make informed process decisions.

To date both near- and mid-infrared (NIR and MIR) spectroscopic techniques together with chemometrics have been used to reliably predict and quantify the concentration of wine constituents (Patz *et al*., 2004; Urbano-Cuadrado *et al.,* 2005; Boulet *et al*., 2007; Cozzolino *et al*., 2008b; Cozzolino *et al*., 2011). More recently these analytical methods are seen as the techniques of choice for monitoring of bioprocesses, providing means to reliably predict the concentration of compounds and monitoring the evolution of processes. The application of these infrared spectroscopic techniques for on-line monitoring is being more readily applied with the continual development in sensor technologies, specifically with regards to NIR spectroscopy (Reviewed by Scarff *et al*., 2006; Fernańdez-Novales *et al*., 2008).

The aim of this review is therefore to highlight the important marker compounds specific to AF and MLF which are necessary to be monitored, for the identification of critical stages of these processes respectively. The techniques used to monitor and model the changes taking

place during these fermentation processes will be provided. Monitoring will focus mainly on MIR and NIR spectroscopy together with various chemometric methods.

2.2 YEAST AND BACTERIA ASSCOIATED WITH ALCOHOLIC AND MALOLACTIC FERMENTATION

Wine fermentation presents a highly complex and selective medium evolving from grape juice into wine. The selective conditions which prevail during fermentation allows for the growth of only a certain number of microorganisms which are able to overcome these conditions (Henschke, 1997; Pretorius, 2000; Bartowsky & Pretorius, 2009).

Numerous yeast species are known to be associated with the production of wine including *Brettanomyces (Dekkera), Candida, Cryptococcus, Debaryomyces, Hanseniaspora (Kloeckera), Kluyveromyces, Metschnikowia, Pichia, Rhodotorula, Saccharomyces, Saccharomycodes, Schizosaccharomyces, Torulaspora*, *Zygosaccharomyces* (Pretorius *et al*., 1999). *Saccharomyces cerevisiae* is, however, known worldwide as the 'wine yeast' and is predominantly used as the selected dry yeast starter culture responsible for AF (Heard, 1999; Pretorius, 2000).

LAB and acetic acid bacteria are the only two bacterial families commonly found in grape must and wine. Four genera of LAB have been shown to be associated with winemaking including *Lactobacillus, Oenococcus, Pediococcus* and *Leuconostoc* (Wibowo *et al.,* 1985). The natural occurrence of MLF and the complete degradation of malic acid may take weeks or even months. Winemakers therefore recognize the advantages of direct inoculation of the wine with a particular commercial starter culture in order to ensure rapid and complete MLF (Henick-Kling, 1995; Nielsen *et al*., 1996; Krieger-Weber, 2009), decrease the potential negative risks associated with a spontaneous MLF and encourage a positive flavour contribution by LAB (Krieger-Weber, 2009). *O. oeni* is the best adapted LAB for the hostile wine conditions of high alcohol, low pH and the presence of SO_2 (Matthews *et al*., 2006) and subsequently represents the majority of commercially available MLF starter cultures on the market (reviewed by du Toit *et al*., 2010). *Lactobacillus* spp. have, however, shown the potential to be used as MLF starter cultures (Bou & Krieger, 2004; du Toit *et al*., 2010).

The prevalence of yeast and bacteria during fermentation are affected by various factors, which in turn affect the rate and successful completion of AF and MLF as well as the production of specific metabolites. These include amongst others, the choice of AF and MLF starter cultures, inoculation strategies, nutrient availability, pH, temperature, ethanol, SO_2 and microbial interactions (reviewed by Pretorius *et al*., 2000; Fleet, 2003; du Toit *et al*., 2010; Lerm *et al*., 2010). These factors subsequently lead to the variation which is observed between different batches in an industrial winemaking situation.

The following section details the metabolic marker compounds which are indicative of yeast and bacterial metabolism and are important for identifying critically important process stages of

AF and MLF. Furthermore factors influencing their concentrations in the final product are detailed. The monitoring of these interesting marker compounds can give insight into the metabolic state of a fermentation for effectively monitoring the rate of these processes.

2.3 YEAST AND BACTERIAL METABOLITES ASSOCIATED WITH ALCOHOLIC AND MALOLACTIC FERMENTATION

2.3.1 SUGARS

Sugars (principally glucose and fructose) are the major raw materials which are bioconverted during the production of wine. Glycolysis (Embdem-Meyerhoff pathway) is the principal process used by yeasts for the catabolism of these sugars (Pronk *et al*, 1996). This process used to produce energy in the form of ATP generates pyruvic acid as its final product. Pyruvic acid is a key metabolite used by yeasts for a variety of metabolic pathways. During AF pyruvic acid is converted to the major fermentation product ethanol together with CO_2 (**Figure 2.3**). Under certain conditions yeasts cannot direct pyruvic acid to the formation of ethanol, and therefore produce glycerol via the glycopyruvic fermentation pathway to maintain the redox balance (**Figure 2.3**) (Constenoble *et al*., 2000). Pyruvate subsequently evolves to form secondary metabolic products including amongst others succinic acid, α-ketoglutaric acid, acetic acid, lactic acid, 2,3-butanediol, diacetyl and acetoin (Overkamp *et al*., 2002).

The heterolactic metabolism of sugars by *O. oeni* results in the production of equimolar quantities of lactic acid, ethanol, acetic acid and CO_2 (**Figure 2.4**) as well as one ATP molecule when metabolising one mole of glucose (Ribéreau-Gayon *et al*., 2006).

The wide variety of intermediary metabolites and end products produced during AF raises the need for monitoring techniques to provide real-time information about the progress of AF (Blanco *et al*., 2004).

The residual sugar content of wine determines the specific style and can therefore be seen as an important quality parameter in wine production. The maximum residual sugar content of South African dry red wine is 4 g/L while South African noble late harvest dessert wines have a minimum sugar content of 50 g/L (Nieuwoudt *et al*., 2002). Sugars are therefore the most obvious marker compound to monitor the progress of AF, however, the monitoring of other compounds would provide a more complete overview of the metabolic state of the AF process.

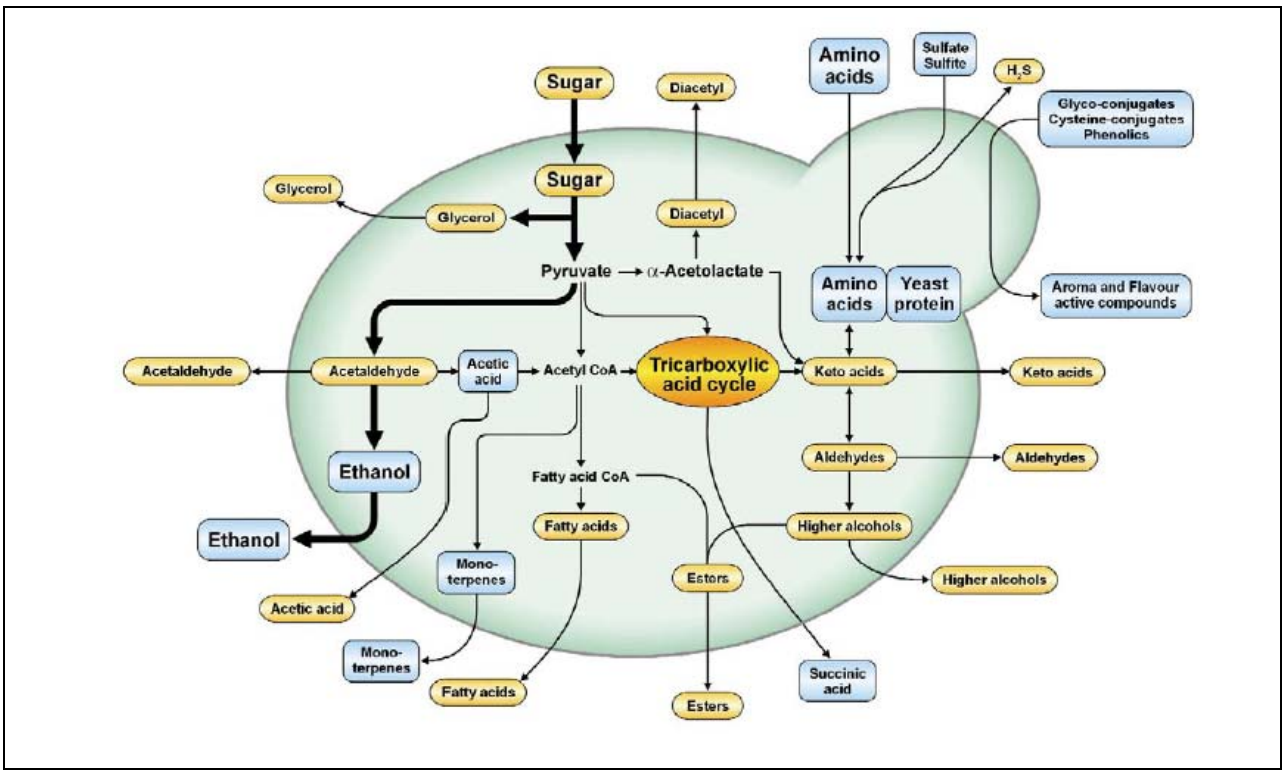

Figure 2.3 Yeast-derived flavour active compounds (used with permission, Swiegers *et al*., 2005)

2.3.2 ALCOHOLS

Ethanol

In modern day winemaking there is an increased interest to harvest fully ripened grapes to produce wines characterised by full fruit and intense varietal flavours (de Barros Lopes *et al*., 2003). These increased sugar concentrations subsequently results in wines with high ethanol levels (Bauer & Pretorius, 2000; de Barros Lopes *et al*., 2003; de Orduña, 2010). The presence of excessive ethanol concentrations has been shown to negatively affect the overall perception of flavour and aroma (Guth & Sies, 2002). In the presence of higher ethanol levels the fruity aroma of a wine was perceived as herbaceous (Goldner *et al*., 2009). Increased levels of ethanol have also shown to influence the perceived astringency of tannins and the bitterness, roughness and hotness of wine (Jones *et al*., 2008; Obreque-Slìer *et al*., 2010) and well as yeast metabolism (Hallsworth, 1998; Alexandre *et al*., 2001).

Besides being the major end product produced during AF and a critical marker compound for the progress of AF, ethanol is essential for enhancing the flavour and aroma attributes of other wine components and subsequently influences the quality of the final product.

Furthermore, issues pertaining to the legal limits regarding the ethanol content of certain wine styles are critical reasons why the evolution of ethanol should be monitored.

Glycerol

Glycerol is a major product produced during AF (**Figure 2.3**) (Pronk *et al*., 1996) and after ethanol and water is the third major component in dry wines. It is one of many polyols found in

wine with a colourless, odourless and viscous nature. The levels found in white wines are typically lower than the concentrations found in red wines (7 g/L versus 10 g/L; Nieuwoudt *et al*., 2002) while noble late harvest wines have concentrations up to 16 g/L (Nieuwoudt *et al*., 2002).

In yeasts the metabolism of glycerol plays three important roles during the anaerobic fermentation of sugars, it maintains the redox ($NADH/NAD^+$) balance (Constenoble *et al*., 2000), it synthesizes precursors for phospholipid synthesis and it protects yeasts against high osmotic stress due to high sugar concentrations (Pronk *et al*., 1996).

The factors influencing the glycerol concentrations of small-scale laboratory fermentations included the nitrogen source and yeast strain used for inoculation, pH and temperature (Scanes *et al*., 1998).

The metabolism of glycerol by wine LAB has been reported in *L. casei* and *Pediococcus pentosaceus* subsequently producing acetoin, diacetyl, 2,3-butanediol and acetic acid (Pasteris & Strasser de Saad, 2009). Furthermore, the metabolism of glycerol by LAB has been implicated in wine spoilage to produce 3-hydroxy-propionaldehyde that leads to the formation of acrolein (**Figure 2.4**) (Pasteris & Strasser de Saad, 2009).

Glycerol has been shown to contribute to the overall mouthfeel of wine, enhance the complexity and add to the apparent sweetness of wine, however, very little research has been done on the interaction of glycerol and other wine flavour constituents and the subsequent contribution of glycerol to the overall aroma profile.

The monitoring of glycerol production during fermentation could therefore provide insight into the contribution of glycerol to the final quality of wine.

Higher alcohols

Higher alcohols (fusel alcohols) are secondary metabolites found in wine mainly due to yeast metabolism (**Figure 2.3**). Although found in vastly smaller quantities to the major metabolites, monitoring the evolution of these compounds could provide the winemaker with information pertaining to the final wine quality.

These metabolites have a characteristic strong pungent aroma at excessive levels, however, they can have a positive influence at lower levels. It has been reported that at levels below 300 mg/L they can add to the complexity of the wine and impart fruity characters while at high levels (> 400 mg/L) they can have a detrimental effect on wine quality (Rapp & Versini, 1991).

The metabolism of amino acids by yeasts results in the production of these important aroma compounds together with their associated esters and volatile acids (Lambrechts & Pretorius, 2000). The assimilation of amino acids by yeasts involves a deamination reaction producing an α-keto acid. The α-keto acid can be discreted from the cell or it can be further decarboxylated into an aldehyde (**Figure 2.3**). The aldehyde can either be reduced to the respective alcohol or oxidised into a volatile carboxylic acid. This catabolic mechanism which

produces higher alcohols from the corresponding amino acids is known as the Ehrlich reaction (Ribéreau-Gayon *et al*., 2006).

The transamination of the amino acid to the respective α-keto acid is catalysed by the branched-chain amino acid transferases encoded by BAT1 and BAT2 (Eden *et al*., 2001). A study by Lilly *et al*. (2006b) showed that the wines produced with yeast strains in which these genes were overexpressed resulted in higher concentrations of certain higher alcohols. Sensory analysis of these wines also showed that these wines had more fruity characteristics (peach and apricot aromas).

Higher alcohols may also be produced during the anabolic pathway from glucose via pyruvate (Ribéreau-Gayon *et al*., 2006). It has been reported that the amino acid concentrations in the grape must affects the final higher alcohol composition in wine (Schulthess & Ettlinger, 1978). Fermentation with different strains of *S. cerevisiae* has shown to produce different variations of higher alcohols (Giudici *et al*., 1990). In a study comparing wine produced with a mixed starter culture (*Pichia fermentans* and *S. cerevisiae*) and with *S. cerevisiae* alone, the wine produced with the mixed culture had higher levels of the higher alcohols namely 1-propanol, n-butanol and 1-hexanol *(*Clemente-Jimenez *et al*., 2005).

Literature, however, shows inconclusive theories on the contribution of LAB to the production of higher alcohols. Some reports have shown strain dependant increases in certain higher alcohol concentrations (Maicas *et al*., 1999; Ugliano & Moio, 2005; Lee *et al*., 2009b). However, other authors (De Revel *et al*., 1999; Jeromel *et al*., 2008; Boido *et al*., 2009; Abrahamse & Bartowsky, 2012) have reported insignificant changes in terms of higher alcohols after MLF, except for the significant increases in isoamyl alcohol (De Revel *et al*., 1999) and isobutanol and 2-phenyl ethanol (Jeromel *et al*., 2008) as well as strain dependant increases observed for hexanol and 2-phenyl ethanol (Boido *et al*., 2009). In contrast, Herjavec *et al*. (2001) found no significant changes in isoamyl alcohol, 2-phenylethanol, isobutanol and propanal concentrations after MLF.

These varying reports show the clear need for metabolic profiling studies to gain a more in-depth analysis of the metabolic footprints of different LAB starter cultures.

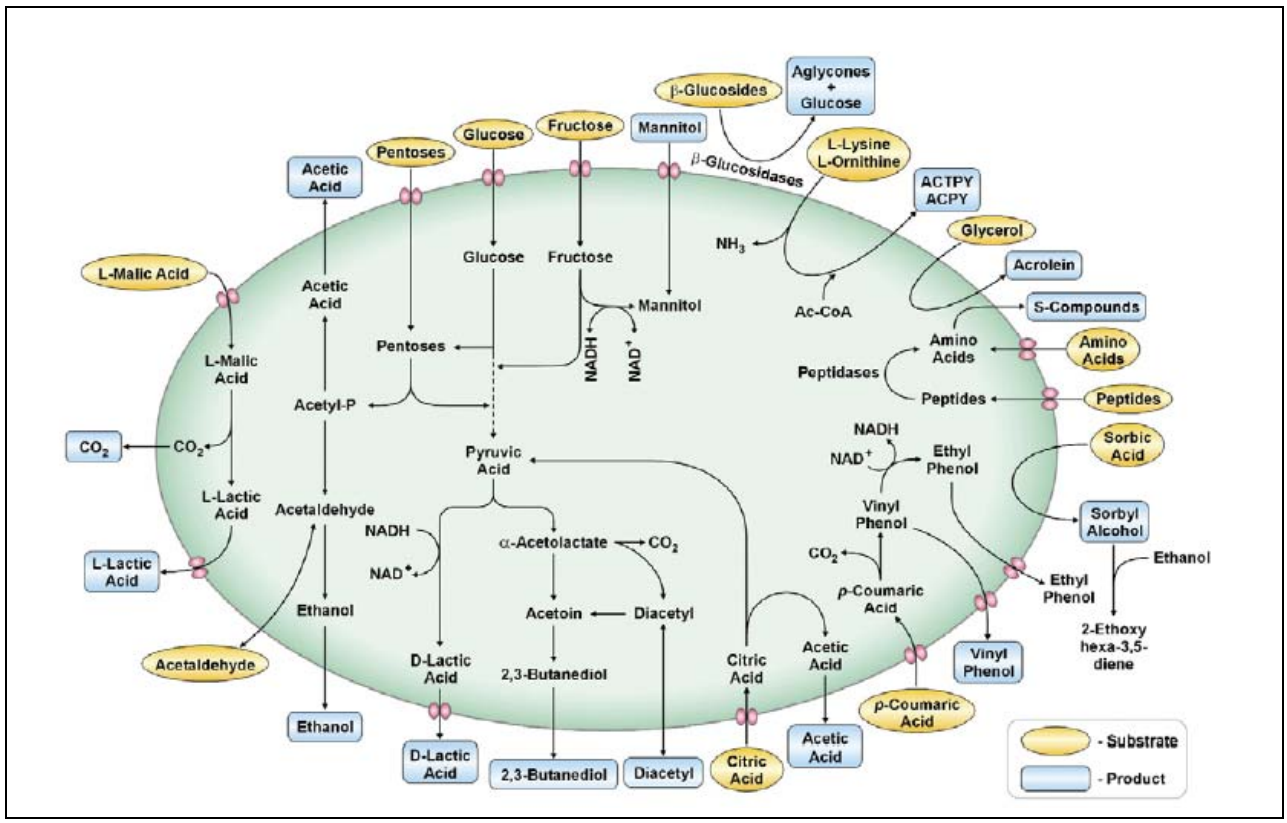

Figure 2.4 Bacterial-derived flavour active compounds (used with permission, Swiegers *et al*., 2005)

2.3.3 ACIDS

NON VOLATILE ORGANIC ACIDS

The acidity of the grape must and wine influences the final quality of wine by contributing to the microbial stability, colour, taste and the occurrence of MLF. The acidity of wine is influenced by the extraction of organic acids from the grapes as well as the metabolism of certain organic acids by yeasts and bacteria.

The major organic acids present in grapes include tartaric acid, malic acid and citric acid (Volschenk *et al*., 2006) (**Table 2.1**). The non-volatile organic acids namely tartaric and malic acid make up 90% of the titratable acidity of grape must (Swiegers *et al*., 2005).

Tartaric acid

Tartaric acid is metabolised by very few organism and thus the concentrations of this acid remains relatively constant during fermentation (Swiegers *et al*., 2005). Certain LAB can degrade tartaric acid which always results in the lowering of the wine quality and is associated with wine spoilage. *Lactobacillus* species have been shown to metabolise tartaric acid resulting in the production of acetic acid, lactic acid and succinic acid (du Toit *et al*., 2010).

Malic acid

Most yeast strains can metabolise malic acid, however, the degree of degradation is strain dependent. The principal pathway used by yeasts for the degradation of malic acid involves AF.

Malic acid is transformed into pyruvate which is catalysed by the malic enzyme. Pyruvate is subsequently decarboxylated into acetaldehyde which is further reduced to ethanol (Ribéreau-Gayon *et al*., 2006). *S. cerevisiae* strains can partially degrade grape must malic acid (3-45%) during AF (Radler, 1993), while strains of *S. paradoxus* have shown to completely degrade malic acid (Mocke, 2005).

The metabolism of L-malic acid to L-lactic acid and CO_2 is the major reaction taking place during MLF (**Figure 2.4**). This reaction is catalysed by the malolactic enzyme using NAD^+ and Mg^{2+} as cofactors (Lonvaud-Funel, 1999). The removal of malic acid confers biological stability to the wine and decreases the risk of bacterial spoilage (Henick-Kling, 1995). The MLF reaction deacidifies the wine and subsequently raises the pH by 0.1 to 0.3 units (Margalit, 1997) which subsequently affects the quality of the final product (Lonvaud-Funel, 1999).

Spontaneous MLF by natural flora has shown to be unpredictable and can take many weeks to completely degrade malic acid. This loss of time can be extremely costly to winemakers. Furthermore the delay in onset and completion of MLF can increase the possibility of the production of off-odours and flavours by spoilage bacteria. For these reasons winemakers have realised the advantages for the inoculation of starter cultures for the management of MLF (Nielsen *et al*., 1996). With this said, however, failures in terms of the adaptation of starter cultures to the wine conditions can occur, while the rate of MLF can also depend on the LAB starter culture (Lee *et al*., 2009 a; b). MLF is therefore seldom predictable in absolute terms. Rapid and low cost monitoring strategies monitoring the degradation of malic acid would therefore provide tools for effective management of MLF (Esti *et al*., 2004).

Citric acid

Citric acid is a grape-derived acid which is metabolised by most LAB species after malic acid depletion (Nielsen & Richelieu, 1999). Some yeasts have also been shown to metabolise citric acid (Swiegers *et al*., 2005).

All heterofermentative cocco-bacilli including *Leuconostoc* and *O. oeni* species, as well as facultative heterofermentative lactobacilli, namely *L. plantarum* and *L. casei*, have the ability to degrade citric acid (Lonvaud-Funel, 1999). The metabolism of citric acid in *O. oeni* has been previously described (Ramos *et al*., 1995).

The metabolism of citric acid by LAB results in the formation of diacetyl, acetic acid, lactic acid, acetoin, 2,3-butanediol, diacetyl and aspartic acid (**Figure 2.5**). Citric acid metabolism is therefore responsible for the changes in the carbonyl compounds during MLF (Sauvageot & Vivier, 1997). Pyruvate produced as an intermediary product during citric acid metabolism can be metabolised to either lactic acid, acetic acid or α-acetolactic acid, all depending on the conditions of the environment including aeration, pH and carbohydrate availability (Starrenburg & Hugenholtz, 1991). The acetic acid produced during citric acid metabolism can thus affect the volatile acidity of the wine.

In modern day winemaking, it is common practice to monitor the conversion of malic acid to lactic acid for monitoring MLF. However, there is a clear need to monitor the production of minor but sensorially significant aroma compounds including carbonyl compounds. This holistic approach to monitoring of MLF would provide the winemaker with more information regarding the quality and style of the final product.

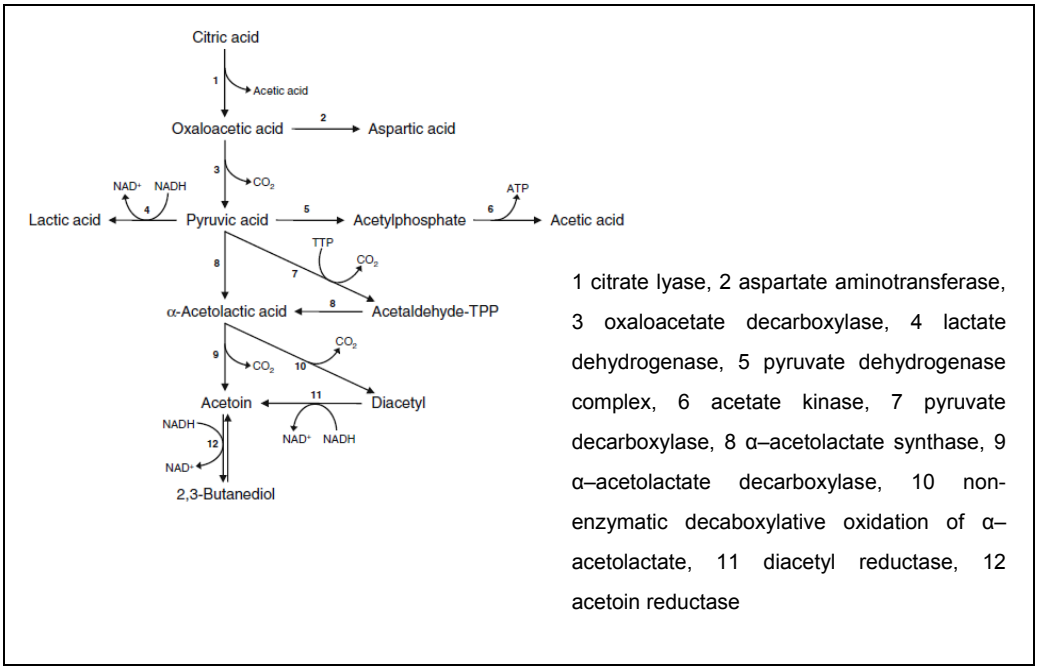

Figure 2.5 The metabolic pathway for citric acid metabolism by *O. oeni* (adapted from Ramos *et al*., 1995).

Succinic acid

Succinic acid is found in trace quantities in grapes (Volschenk *et al*., 2006) and is present in wine mainly as a result of yeast driven AF fermentation (**Figure 2.3**). It reaches concentrations of about 2 g/L (Coulter *et al*., 2004). *S. cerevisiae* strains have shown differences in the production of succinate (Eglinton *et al*., 2000). Succinic acid has been described to impart a characteristic salty bitter taste to wine (Whiting, 1976).

Strong evidence exists that during anaerobic fermentation the production of succinic acid is most likely via the reductive branch (via oxaloacetate and malate) of the tri-carboxylic acid (TCA) cycle (Roustan & Sablayrolles, 2002; Camarasa *et al*., 2003).

Aeration, yeast strain, fermentation temperature, must composition and clarification, nutrient content, SO_2 concentration and titratable acidity have all be shown to be associated with the incidence of abnormally high succinic acid levels during fermentation (Coulter *et al*., 2004).

VOLATILE ACIDS

The volatile acids (**Table 2.1**) are characterised by organic compounds with short carbon chain lengths which are found in wine in concentrations between 500 and 1000 mg/L (Swiegers *et al*.,

2005). Acetic acid is the predominant volatile acid of wine and contributes approximately 90% to the volatile acidity (Radler, 1993). Acetic acid is mainly produced by aerobic acetic acid bacteria, however, both bacteria (**Figure 2.4**) and yeasts (**Figure 2.3**) can produce this volatile acid.

Acetic acid imparts a characteristic pungent vinegar aroma if it is present in concentrations above its sensory threshold of 0.7 g/L (Francis & newton, 2005), however, it can add complexity to the wine at concentrations between 0.2 and 0.6 g/L depending on the type and style of wine (Bartowsky & Henschke, 1995; Lonvaud-Funel, 1999). Acetic acid is a clear parameter pertaining to wine quality and is seen as a spoilage indictor in the wine industry. The stringent monitoring of this wine constituent throughout fermentation would ensure the effective management of fermentations, providing the winemaker with information about problematic or deviating fermentations.

During AF yeasts produce acetic acid via the pyruvate dehydrogenase (PDH) bypass pathway. This pathway catalysis the conversion of pyruvate to acetyl-CoA which is an intermediary product needed for anabolic processes such as lipid biosynthesis (Pronk *et al*., 1996). The subsequent reducing equivalents produced during this pathway are also needed for other metabolic pathways and for redox reactions (Swiegers *et al*., 2005).

The reported acetic acid concentrations produced by yeasts have been varied producing concentrations from 100 mg/L to 2 g/L during fermentation (Radler, 1993). Strain differences have been reported with results showing *S. bayanus* and *S. uvarum* to produce less acetic acid than *S. cerevisiae* (Giudici *et al*., 1995; Eglinton *et al*., 2000). The choice of yeast culture for the induction for AF is therefore a critical choice made by the winemaker, which allows for a degree of control over the final acetic acid concentrations.

MLF is generally associated with a 0.1- 0.2 g/L increase in acetic acid concentration (Bartowsky & Henschke, 1995). The production of acetic acid by LAB during MLF can occur during the first reaction of citric acid metabolism (Bartowsky & Henschke, 2004) or during the metabolism of hexoses via the phosphoketolase pathway (Lonvaud-Funel, 1999). A higher pH has been shown to favour the production of acetic acid during citric acid metabolism (Ramos *et al*., 1995).

Furthermore, straight chain and branched chain fatty acids predominantly propionic acid and hexanoic acid make up the remaining volatile acidity of wine. These volatile acids are produced as a result of the hydrolysis of lipids by yeasts during fatty acid metabolism from acetyl-CoA (**Figure 2.3**) (Lui, 2002) and contribute to the aroma and flavour of wine. Fatty acids are found in trace quantities in wine, however, these aroma compounds are of interest due to their low sensory thresholds. At high concentrations they can be detrimental to wine quality resulting in cheesy, rancid, pungent, fat-like, sweaty aromas (Francis & Newton, 2005).

The contribution of LAB to the production of fatty acids in wine is limited, however, studies have reported differences in the volatile fatty acid profiles due to MLF (Maicas *et al*., 1999,

Herjavec *et al*., 2001). In a more recent study *O. oeni* strains were differentiated in terms of their metabolic profiles. Significant differences were observed between LAB strains after MLF in terms of hexanoic acid, isobutyric acid and octanoic acid (Lee *et al*., 2009a). In a second study Lee *et al*. (2009b) reported significant differences for acetic acid and butyric acid between the genera namely *O. oeni* and *L. plantarum.*

These preliminary studies have shown the possibility for LAB specie and strain differences in terms of the production of fatty acids. Further metabolic studies are needed to make concrete conclusions about the influence of different LAB starter cultures on the production of these constituents. Furthermore, monitoring the evolution of these aroma compounds during wine production would provide more solid information pertaining to the factors affecting the concentrations of these constituents as well as the issues regarding their relationship to the final wine quality.

Table 2.1 Organic acids present in grapes and wine (adapted from Volschenk *et al.*, 2006)

Fixed acids		**Volatile acids**	
Major acids	**Minor acids**	**Major acids**	**Minor acids**
L-tartaric acid (5-10 g/L)	Pyruvic acid	Acetic acid	Formic acid
L-malic acid* (2-6.5 g/L)	α -Keto-glutaric acid		Propionic acid
L-lactic acid (1-3 g/L)	Isocitric acid		2-methylpropionic acid
Citric acid** (0.5-1g/L)	2-oxoglutaric acid		Butyric acid
Succinic acid (0.5-1.5 g/L)	Dimethyl glyceric acid		2-methylbutyric acid
Amino acids	Citramalic acid		3-methylbutyric acid
	Gluconic acid***		Hexanoic acid
	Galacturonic acid		Octanoic acid
	Mucic acid		Decanoic acid
	Coumaric acid		
	Ascorbic acid		

*15-16 g/L has been reported in cool climate regions
**> 0.3 g/L when wines have been stabilised for metal precipitation
***Present in wines infected with *Botrytis cinerea*

2.3.4 CARBONYL COMPOUNDS

Acetaldehyde

Acetaldehyde is one of the major metabolites formed during yeast fermentation and the last precursor before ethanol formation (**Figure 2.3**). Pyruvate is converted to acetaldehyde which is subsequently converted to ethanol, a crucial step in maintaining the redox balance in a cell (Pronk *et al*., 1996). Sugar is the major precursor for acetaldehyde production, however, the metabolism of amino acids also contributes to its formation (Henschke & Jiranek, 1993). The presence of acetaldehyde may also be a sign of oxidation of ethanol by film yeasts (Fleet & Heard, 1993). Acetaldehyde is a precursor metabolite for the production of acetate, acetoin and ethanol (Lambrechts & Pretorius, 2000).

Acetaldehyde is quantitatively the most abundant volatile aroma compound found in wine comprising more than 90% of the total aldehyde concentrations (Liu & Pilone, 2000). At low levels acetaldehyde can impart a pleasant fruity aroma to the wine, however, at higher levels it can have a grassy, green apple-like off-flavour (Liu & Pilone, 2000).

The ability of wine LAB to metabolise acetaldehyde has been reported (**Figure 2.4**) (Osborne *et al*., 2000). Acetaldehyde metabolism by *O. oeni* in a synthetic wine medium produced ethanol and acetic acid (Osborne *et al*., 2000). Osborne *et al*. (2006) reported the degradation of acetaldehyde in white wines by two commercial *O. oeni* strains. The ability of LAB to metabolise acetaldehyde is seen as an alternative approach to the traditional methods of adding SO_2 to remove acetaldehyde, however, in red wine making this can have a negative effect on colour development (Liu & Pilone, 2000).

Diacetyl

The carbonyl compound diacetyl (2,3-butanedione) is the most important flavour compound associated with MLF and produced during citric acid metabolism (**Figure 2.5**). The production of diacetyl by yeasts involve the metabolism of pyruvate, however, these concentrations are at levels below its detection threshold (Martineau & Henick-Kling, 1995).

Diacetyl is responsible for the characteristic MLF aromas including buttery, butterscotch, nutty and toasty aromas when present at concentrations above its sensory threshold (Bartowsky & Henschke, 1995; 2004). The final concentration of diacetyl in wine and its sensory perception, however, depends on several factors including wine type, inoculation rate, bacterial strain, pH, contact with yeast lees, aeration and SO_2 concentration. These factors have been reviewed by Bartowsky & Henschke (2004). Martineau *et al*. (1995) has reported variations in the diacetyl concentration for different wine styles varying from 0.2 mg/L in Chardonnay, 0.9 mg/L in Pinot noir and 2.8 mg/L in Cabernet Sauvignon wines. Diacetyl can be further metabolised by both yeast and bacteria to acetoin and 2,3-butanediol (Martineau & Henick-Kling, 1995; Nielsen & Richelieu, 1999). These end products have higher sensory thresholds compared to diacetyl (approximately 150 and 600 mg/L respectively; Etiévant, 1991).

As previously mentioned the monitoring of carbonyl compounds is of extreme importance to ensure further control over MLF and the production of a certain style and quality of wine. More specifically the importance of monitoring the major carbonyl compound, diacetyl is clear.

2.3.5 ESTERS

Esters, an important group of volatile aroma compounds are mainly produced via yeast metabolism during AF (**Figure 2.3**) and contribute largely to the fruity aroma in wine (Lilly *et al*., 2000). Esters can either be formed via the chemical esterification of an alcohol and an acid or via lipid and acetyl-CoA metabolism (Lambrechts & Pretorius, 2000). The balance between the ester synthesizing enzymes and the ester degrading enzymes has shown to have an influence

on the final ester concentrations in wine (Lilly *et al*., 2006a). The amount of esters produced also depends on the yeast strain (Marais *et al*., 2001), as well as other factors such as the wine type (Smyth *et al*., 2005).

Esters in wine can be classified as acetate esters of higher alcohols, ethyl esters of fatty acids or esters of organic acids. Acetate esters are usually found in higher concentrations to that of ethyl esters and contribute more to the fruity aromas, while ethyl esters tend to contribute more to the apple flavours in wine (Saerens *et al*. 2008).

The contribution of wine LAB to the ester concentrations in wine following MLF is not fully understood, however, genetic studies on *O. oeni* (Sumby *et al*., 2009) and *Lactobacillus* (Mtshali *et al*., 2010) have identified and characterised the genes involved in esterase activities. Studies have shown that esters such as ethyl lactate and diethyl succinate are typically associated with MLF (Ugliano & Moio, 2005).

Research into the metabolic profiling and monitoring of different LAB strains regarding their production of volatile compounds namely esters, higher alcohols and fatty acids, is undoubtedly necessary to fully understand the differences and/or similarities between different LAB starter cultures. This would provide a means for the winemaker to make more informed decisions regarding the choice of MLF starter cultures for the production of a certain style of wine.

As presented in this review, the biological fermentation processes of AF and MLF are extremely complex and are characterised by the rapidly and continuously changing chemical composition, from grape juice into wine. These processes are accompanied by the production of various major and minor by-products and end product metabolites which can be influenced by a variety of different factors. The monitoring of AF and MLF in each fermentation tank is therefore a key element in the effective control of the winemaking process.

2.4 ANALYTICAL TECHNIQUES USED FOR BIOPROCESS MONITORING OF FERMENTATIONS

The rapidly changing biotechnological processes presented during wine production has led to a growing interest in the critical control and monitoring of fermentation processes in order to effectively manage the wine production process (Di Egidio *et al*., 2010; Buratti *et al*., 2011). These major and minor metabolites presented in this review all directly or indirectly pertain to the quality of wine, and the monitoring of many of these metabolites are therefore important to gain full insight into the complete fermentation process.

An “ideal” bioprocess monitoring system should be sensitive, rapid, non-destructive, capable of automation, robust, operate in (near) real-time and generate multi-analyte data which should be able to be integrated with data generated from other sensors (Vaidyanathan *et al*., 1999). An ideal monitoring system would require on-line detection techniques which provide the following advantages: i) early detection of possible deviations, ii) can be established within the fermentation and provide real-time information, iii) the permanent and continual monitoring of

the process, and iv) evaluation of the conditions at any desired point in the fermentation (Pemen *et al*., 1998). Together with chemometric techniques this monitoring system would provide real-time quantitative and qualitative information of the process (Huang *et al*., 2008). This would allow the winemaker to critically evaluate the quality changes from the raw materials to the final product.

Traditional analysis involves off-line measurements whereby a sample is removed from the bioreactor to be analysed in a laboratory. At-line sampling can occur if the equipment is located near the bioreactor (Vojinović *et al*., 2006). These laborious sampling procedures result in infrequent and delayed results which is not ideal for effective monitoring of a bioprocess (Cozzolino *et al*., 2006). The shift toward non-invasive sampling, with rapid developments in biosensor technology such as spectroscopic probes has provided the application to perform in-line measurements. The advantages being no sample withdrawal and pretreatment and thus sampling can take place continuously without any time delay (reviewed by Scarff *et al*., 2006). Furthermore the application of real-time methods is seen as the most attractive method for an effective bioprocess monitoring system (reviewed by Vojinovic *et al*., 2006.).

The traditional wet analytical techniques used for fermentation monitoring in at-line and off-line applications such as gas chromatography (GC) and high performance liquid chromatography (HPLC) (**see section 2.4.1**) are reliable and highly selective. The use of these techniques for process control are, however, often hindered by the lack of automation, highly specific analytical instrumentation, sample preparation requirements, long run times and the generation of toxic waste. These techniques can, however, be used for online applications provided that the instruments are interfaced with the bioreactor (van de Merbel *et al*., 1996).

Vibrational spectroscopy is the technology which seems to meet the requirements for an "ideal" monitoring system most closely (Roychoudhury *et al*., 2006). Both NIR and MIR spectroscopy offer a quick alternative to traditional methods (Urtubia *et al*., 2004; 2008) offering a wealth of information about a process (Harms *et al*., 2002). The fundamental principles of vibrational spectroscopy are detailed in **section 2.4.3** together with the quantitative and qualitative applications in wine production.

2.4.1. CHROMATOGRAPHIC ANALYTICAL METHODS

A number of chromatographic techniques are applied for the accurate separation and quantification of molecules within food samples (Reid *et al*., 2006). Liquid chromatography (LC), more specifically HPLC is applied for the detection of compounds including proteins, amino acids, phenolic compounds and carbohydrates while GC techniques are more suited for volatile or semi-volatile components (Reid *et al*., 2006).

Chromatographic techniques including GC and HLPC are the most common chromatographic methods used for the quantification of wine components (de Villiers *et al*.,

2011). A number of studies have shown the use of GC coupled with flame ionization detection (GC-FID) and mass spectrometry (GC-MS) together with extraction techniques including solid phase extraction (SPE), solid phase micro extraction (SPME) and solid phase dynamic extraction (SPDE) for the detection and quantification of major volatile aroma compounds namely esters, alcohols and acids in wine (reviewed by Ebeler, 2001; de Villiers *et al*., 2011). Studies evaluating the contribution of malolactic bacteria to the volatile composition of wine have used these applications in order to gain a better insight into the volatile fermentation metabolites and the subsequent impact on wine aroma (Pozo-Bayón *et al*., 2005; Ugliano & Moio, 2005; Izquierdo Cañas *et al*., 2008; Boido *et al*., 2009; Vilanova *et al*., 2010; García-Carpintero *et al*., 2011). Knoll *et al*. (2012) investigated differences in the production of major volatile compounds pertaining to different LAB inoculation strategies using a GC-MS method. Another study quantified the major volatile compounds using GC-MS while the carbonyl compounds namely diacetyl and acetoin where quantified using a GC-SPME method to evaluate the influence of pH and ethanol on the volatile profile (Knoll *et al*., 2011).

These well-established analytical separation techniques have great potential in bioprocess monitoring (Matz *&* Lennemann, 1996). The use of on-line chromatographic detectors have been successfully applied for monitoring of a bioprocess (reviewed by van de Merbel *et al*., 1996), including amongst others GC detectors (Flilippini *et al*., 1991; Mathis *et al*., 1993).

A study by Boe *et al.* (2007) developed a method for the online detection of volatile fatty acids in an anaerobic process using headspace GC-FID. In an anaerobic process the volatile fatty acids are important indicators to be monitored as certain volatile compounds are known to be early warning indictors for possible process failure. It was reported that other online techniques are available for the analysis of volatile fatty acids including the use of titration (Steyer *et al*., 2002), however, the development of this GC based technique would provide the exact concentrations of individual volatile fatty acids and therefore give more detailed information about the process status for subsequent process control.

To our knowledge the use of GC techniques for online applications in wine analysis are limited. The constituents of wine are found in varying concentrations and the presence of major components such as water and ethanol (Rapp *et al*., 1998) can mask minor components such as aroma compounds. This therefore poses as a challenge when trying to quantify compounds found in these small quantities (Ionescu *et al*., 1999). A technique was developed whereby GC coupled with electronic nose was used to quantify volatile aroma compounds. The GC technique was used for sample dehydration and dealcoholisation before subsequent aroma detection by the electronic nose (Ragazzo-Sánchez *et al*., 2004a, b; Rogazzo *et al*., 2006). In this case GC wasn't used directly for quantification purposes, however, it was used successfully as a complementary technique to separate ethanol and water and therefore allow for a more accurate determination of volatile aroma compounds in wine.

These studies therefore show the potential for GC based techniques to be incorporated into monitoring systems, giving highly accurate and detailed information about the process state.

2.4.2 BIOSENSOR TECHNOLOGIES

The rapid need for low cost, non-destructive techniques which can be easily automated and provide reliable real-time information for quality control purposes has led to the growing development of sensor techniques (Esbensen *et al*., 2004; Buratti *et al*., 2011). The various biosensor techniques available have shown applications for on-line bioprocess monitoring on an industrial scale in both the food and beverage industries (Reviewed by Mello & Kubota, 2002; Vojinović *et al*., 2006).

The application of biosensor technologies is based on the recognition of a specific analyte within a complex system via a recognition system, the subsequent transduction of the signal via an optical, thermal or electrochemical transducer and lastly the processing of the signal (**Figure 2.6**) (McDonagh *et al*., 2008). Sensors are therefore specific for a specific analyte and produce a signal which relates specifically to the concentration of the measured analyte.

Biosensors have been successfully used to monitor fermentations which quantified AF marker analytes including glycerol (Compagnone *et al*., 1998) as well as MLF marker compounds including L-malic acid and L-lactic acid (Esti *et al*., 2004). The use of enzyme based biosensors was successfully used for the determination of D, L-lactic acid and L-malic acid in red and white wines (Mazzei *et al*., 2007).

The suitability of these biosensors to monitor these marker compounds can provide insight into the metabolic state of a process. The analysis of these marker compounds during AF and MLF would allow for the detection and prevention of unwanted metabolic changes taking place, which would subsequently affect the quality of the final product. Monitoring of malic acid in particular would provide information about the stage of completion of MLF. This would ensure a rapid and complete MLF process without the production of off-odours and flavours which can be as a result of delayed MLF. Furthermore monitoring would provide more information about the parameters which affect the production and/or degradation of these compounds.

More recently, the use of the electronic nose and tongue (multisensory systems) has received much attention. These techniques are based on trying to mimic the human olfactory system thereby producing a signal which is a combination of various sensor responses. The electronic nose consists of an array of gas sensors with various selectivities for liquid or solid samples (Dickinson *et al*., 1998), while the sensors of the electronic tongue are selective for liquid samples and are based on conductometric, voltametric and potentiometric techniques (Winquist *et al*., 2000).

A number of reports have shown the use of the electronic nose for wine analysis and discrimination purposes (Natale *et al*., 2004; Garcia *et al*,. 2006; Lozano *et al*., 2008; Ragazzo-Sanchez *et al*., 2008). Studies have combined these electronic sensor systems in monitoring the sensory profile of wines by following the evolution of aroma compounds throughout fermentation (Pinheiro *et al*., 2002; Buratti *et al*., 2007; 2011). Another study (Cozzolino *et al*., 2005) coupled mass spectrometry with electronic nose (MS e_nose) to determine sensory properties of wine as a rapid alternative to GC-MS analysis of wine aroma compounds. To the authors knowledge the only online application of this technique for monitoring aroma was included in the study by Pinheiro *et al*. (2002).

Apetrei and co-workers (2012) were the first group to report on the use of an electronic sensory system involving an electronic nose, tongue and electronic eye for the characterisation of wines. The electronic eye system involved an optical system to measure the colour with the use of CIE Lab coordinates. Apetrei *et al*. (2012) used this electronic sensory system as a means to discriminate between wines aged in barrels and wines aged with oak chips.

This study shows the clear move towards complex monitoring systems for fermentation monitoring whereby one global analysis can provide reliable information pertaining to colour, aroma and taste in a similar way as human experts do. These techniques can be regarded as rapid alternatives to traditional chemical analysis techniques.

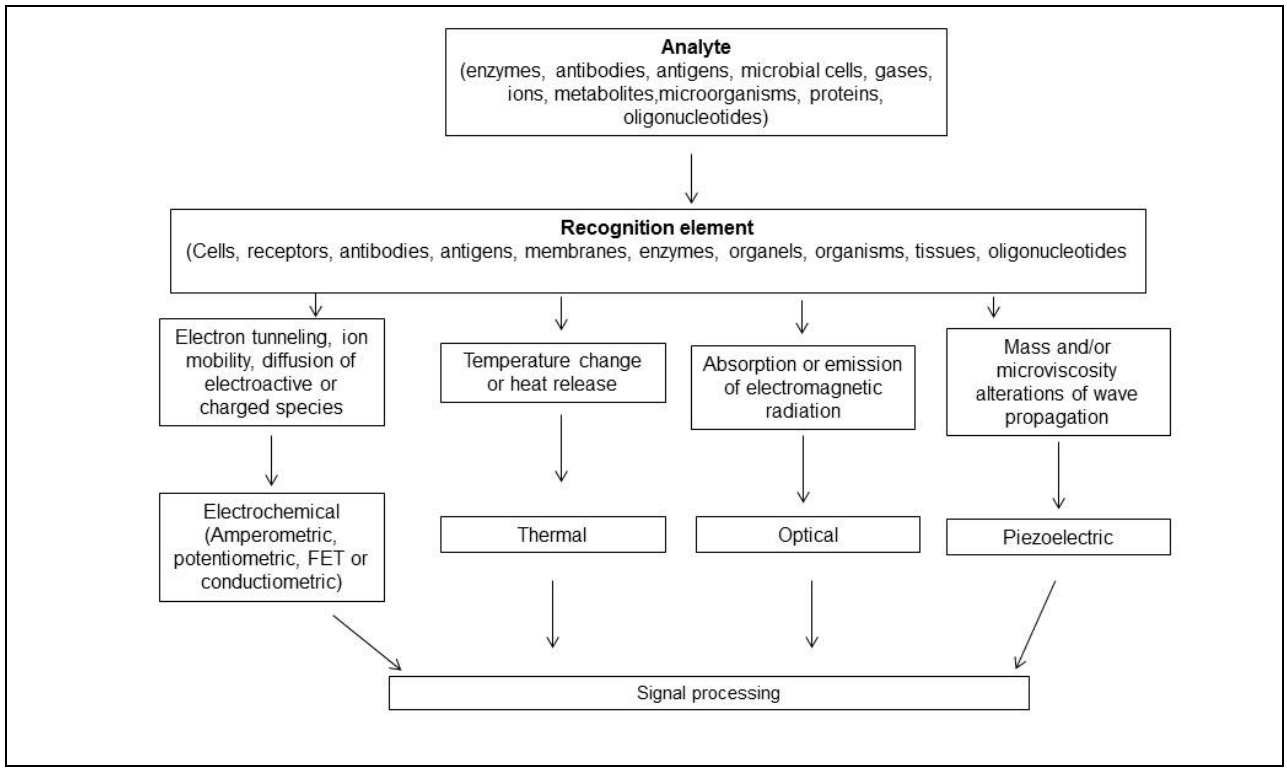

Figure 2.6 Components of a biosensor (adapted from Mello & Kubota, 2002).

2.4.3 SPECTROSCOPY

Spectroscopy has been long used as an analytical technique for the monitoring of processes in various industries. Recently it has been recognized by the wine industry as a fast alternative to traditional chemical analysis, which has the potential to provide important real-time information about a process in an on-line situation (Cozzolino & Curtin, 2012).

Infrared (IR) spectroscopy is based on the study of the interaction of matter with electromagnetic radiation in the infrared region and the subsequent measurement of the intensity of absorbance, transmission or reflectance at predefined wavenumbers (cm^{-1}) or wavelengths (nm). The principle involves the vibration of covalent bonds in functional groups present in a sample upon the exposure to IR radiation. Covalent bonds exhibiting a dipole moment (C-C, C-H, O-H, C=O and N-H) can absorb IR radiation at different frequencies which subsequently results in vibrational motions including the stretching, bending and twisting of the bonds (Pavia *et al*., 2009). The frequencies are subsequently transformed through various mathematical calculations to produce a characteristic absorbance- or transmittance spectrum which characterizes the specific bonds present in a sample. Various organic and inorganic compounds have optical properties and absorb in the IR region. The characteristic spectrum produced is seen as a chemical "fingerprint" and provides critically important information with regards to the sample (Pavia *et al*., 2009).

The IR regions of the electromagnetic spectrum are divided into the near-, mid- and far-IR regions (**Table 2.2**). The IR region lies at wavelengths longer than those characteristic of

visible light. These ranges, however, differ in literature depending on the instrumentation and the specific applications of these techniques (Smith, 1999; Pavia *et al*., 2009). In theor, mid IR waves are expressed as wavenumbers while near IR waves are expressed as wavelengths.

Table 2.2 The infrared regions of the electromagnetic spectrum (adapted from Pavia *et al*., 2009).

Region	Wavenumber ($\bar{v}$) range (cm^{-1})	Wavelength (λ) range (nm)
Near	12800 to 4000	780 to 2500
Mid	4000 to 200	2500 to 50000
Far	200 to 10	50000 to 1000000

Both MIR and NIR spectroscopy have been widely used for applications in routine wine analysis (reviewed by Cozzolino & Dambergs, 2009). This involves the use of spectroscopy together with powerful chemometric software to quantitatively predict the concentration of wine constituents. Chemometric techniques such as principal component analysis (PCA) and partial least squares (PLS) regression are, however, indispensable for the interpretation of spectral data. PLS regression is used to find correlations between the spectrum of a sample and the corresponding concentration of the wine constituent, for the future prediction of unknown samples (Næs *et al*., 2002; Esbensen, 2006). The use of the PLS regression technique is detailed in **section 2.4.4.2**. **Tables 2.3 and 2.4** give an overview of some recent quantitative applications of MIR and NIR respectively in the wine industry.

It is clear from **Table 2.3** and **Table 2.4** that extensive research has been carried out on the quantitative prediction of wine constituents using both MIR and NIR spectroscopy. The prediction of several wine constituents including amongst others ethanol, pH, glycerol, malic acid, organic acids and volatile compounds (Patz *et al*., 2004; Urbano-Cuadrado *et al.,* 2004; Moreira & Santos, 2005; Nieuwoudt *et al*., 2006; Garde-Cerdán *et al*., 2011) have been reported using NIR and MIR spectroscopy techniques.

Table 2.3 Quantitative applications of MIR spectroscopy in viticulture and oenology.

Applications	References
Determination of organic acids in wine, vinegars and spirits	Regmi *et al*., 2012
Determination of red wine anthocyanins	Romera-Fernández *et al*., 2012
Compositional analysis of wine	Cozzolino *et al*., 2011
Quantification of sugars and acids in Chinese rice wine	Shen *et al*., 2011
Determination on red wine polysaccharides	Boulet *et al*., 2007
Determination of red wine anthocyanins	Soriano *et al*., 2007
Quantification of total soluble solids (TSS), pH and TA in South African grape must	Swanepoel *et al*., 2007
Quantification of fermentation compounds namely ethanol, glycerol, volatile acidity, reducing sugar and glucose in Chenin blanc wines and synthetic musts.	Nieuwoudt *et al*., 2006
Organic acid analysis	Moreira & Santos, 2005
Determination of wine parameters including alcoholic degree, volumic mass, total acidity, glycerol, total polyphenol index, lactic acid and total sulphur dioxide	Urbano-Cuadrado *et al.,*2005
Glycerol determination in in South African table wines	Nieuwoudt *et al*., 2004
Routine wine analysis of carbohydrates, alcohols and organic acids	Patz *et al*., 2004
Determination of ethanol, titratable acidity, pH, volatile acidity, reducing sugars, tartaric acid, malic acid and lactic acid	Kupina & Shrikhande, 2003
Determination of AF compounds namely glucose, fructose, glycerol and ethanol	Fayolle *et al*., 1996

Table 2.4 Quantitative applications of NIR spectroscopy in viticulture and oenology.

Applications	References
Determination of volatile compounds	Garde-Cerdán *et al*., 2011
Volatile compound determination in aged red wines	Lorenzo *et al.,* 2009
Assessing the sensory properties of Australian red wines	Cozzolino *et al*., 2008a
Determination of wine elements including calcium, potassium, magnesium, phosphorus, sodium, sulphur, iron, boron and manganese in Australian wines	Cozzolino *et al*., 2008b
Determination of volatile aroma compounds in Riesling wine	Smyth *et al*., 2008
Determination of wine parameters including alcoholic degree, volumic mass, total acidity, glycerol, total polyphenol index, lactic acid and total sulphur dioxide	Urbano-Cuadrado *et al.,* 2005
Prediction of malvidin-3-glucoside, pigmented polymers and tannins in Australian red varieties namely Shiraz and Cabernet Sauvignon	Cozzolino *et al*., 2004
Determination of 15 wine parameters including amongst others ethanol, volumic mass, total acidity, pH, glycerol, colour, tonality and total polyphenol index	Urbano-Cuadrado *et al.,* 2004
Determination of total anthocyanins, pH and TSS in different grape varieties	Dambergs *et al*., 2003
Methanol determination in grape spirits	Dambergs *et al*., 2002
Determination of sugar, malic acid, lactic acid, YAN and ethyl carbamate in must and wine samples	Manley *et al*., 2001

The direct interpretation of spectral features in both the MIR and NIR region is difficult (Cozzolino *et al*., 2011), however, they can both provide unique advantages (Pavia *et al*., 2009). MIR radiation gives rise to fundamental vibrations characterized by stretching and bending modes producing a high resolution spectrum. Sharp peaks produced in the MIR region (4000 to 200 cm^{-1}) are easier interpreted and assigned to specific chemical components or compounds than bands in the NIR region (Wilson *et al*., 1994). The fingerprint region (1,500 – 500 cm^{-1}) is an information rich region of the MIR region mainly used for the identification of specific compounds producing specific absorbance patterns. The MIR region, however, is complicated by the prominent absorption of water (Vaidyanathan *et al*., 1999). The NIR region utilizes the spectral range from 780 to 2500 nm and is characterized by overtone and combination bands when irradiated with NIR frequencies. NIR instruments therefore provide information related to vibrations of the combinations of the fundamental absorptions (Cen & He, 2007) and thus produce a spectrum which is less defined. The advantages of NIR spectroscopy include, low absorptivity and low reflectivity. This allows samples with a longer path length to be analysed by NIR, particularly in reflectance modes and therefore less sample preparation is needed compared with MIR analysis (Manley *et al*., 2001). NIR radiation can also penetrate through visually opaque samples (Bauer *et al*., 2008).

Studies relating the spectral properties of wine samples to the determination of actual concentrations, via linear regressions are able to evaluate the spectral regions which are important for the prediction of the respective constituents.

The MIR analysis of wine samples has shown that characteristic bands in the wavenumber region 1500 – 900 cm^{-1} correspond to sugars and organic acids (Patz *et al*., 2004; Nieuwoudt *et al*., 2004; Bevin *et al*, 2006; Cozzolino *et al*., 2011a). The regions associated with sugars include the C-O stretch for fructose at 1060 cm^{-1} and glucose at 1030 cm^{-1} (Bevin *et al*., 2006; 2008). It has also been shown that the absorption peaks of ethanol and water dominate the spectrum, while the C-O stretch for primary alcohols was prominent at wavenumber 1050 cm^{-1}. The wavenumbers from (2850 - 2960 cm^{-1}) showing the contribution of C-H stretch of ethanol was also significant. Furthermore, the region from 1690 - 1760 cm^{-1} contains information relating to esters, aldehydes and carboxylic acids (Bevin *et al*., 2006; 2008).

In the NIR region, bands have been observed at 1450 nm and 1950 nm which are related to the O-H second overtone and O-H stretch first overtone of ethanol and water (Cozzolino *et al*., 2003; 2012). The absorption band at 2266 nm is likely related to the C-H combinations and O-H stretch overtone while the band at 2305 nm to the C-H overtones. The absorption bands at 2266 and 2302 nm are most like related to methanol (Cozzolino *et al*., 2003). Furthermore, absorption bands around 1900 - 2000 nm are also associated with S-H overtones while bands around 2150 - 2250 nm with C-S overtones, respectively (Cozzolino *et al*., 2003; 2012)

The major development regarding the instrumentation used for spectroscopy has involved the development of Fourier transformation (FT) based systems based on a Michelson interferometer (**Figure 2.7**) compared with the conventional dispersive type instruments. These dispersive instruments based on a monchromator system, select parts of the spectrum to be detected, while FT allows all the frequencies over the entire wavenumber range to reach the detector. The radiation from the light source passes through an interferometer before it reaches the sample and subsequently the detector producing a time-domain (intensity versus time) response called an interferogram. The response is subsequently transformed by FT to produce a frequency-domain (intensity versus frequency) spectrum (Smith, 1999; Pavia *et al*., 2009). FT instruments produce spectra with a better signal to noise ratio and have a faster sample throughput than dispersive instruments (Smith, 1999; Pavia *et al*., 2009). The developments in sample presentation modes [e.g. attenuated total reflectance (ATR)] have further improved these technologies. ATR has also minimised the necessity of sample preparation techniques and has made it easier to acquire a MIR spectrum of an aqueous sample (Roychoudhury *et al*., 2006). ATR also eliminates the possibility of water complicating an MIR spectrum (Wilson *et al*., 1994).

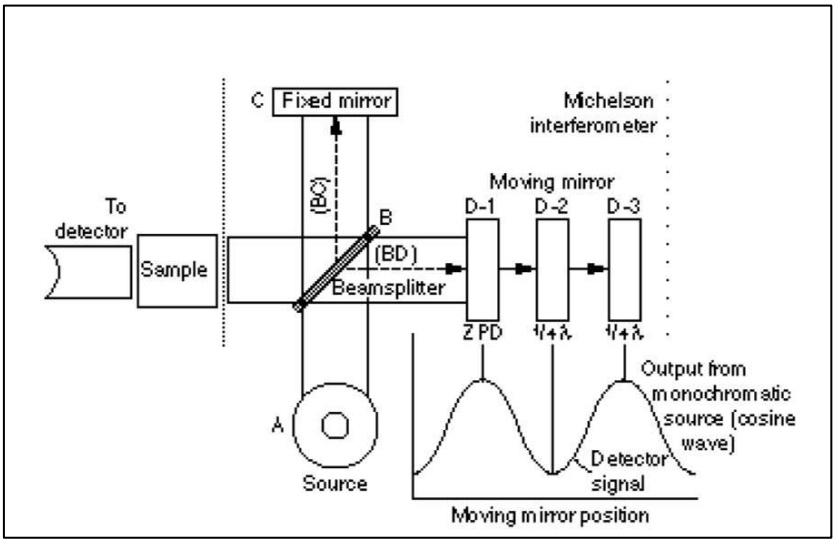

Figure 2.7 Typical layout of an FT-IR spectrometer (Adapted from Nicolet Instrument Corporation; www.thermonicolet.com).

The commercially available MIR instrument namely The WineScan FT120 instrument (Foss Analytical, Denmark, http://www.foss.dk) has shown excellent performance in terms of precision, accuracy and the speed of analysis since its release on the market in 1998 (Gishen & Holdstock, 2000; Patz *et al*., 2004; Nieuwoudt *et al*., 2004). Commercially available NIR instrumentation includes diode array spectrometers and the FOSS NIRSystems.

Up to now it is clear that spectroscopy as a quantitative tool has shown huge success in the wine industry. With this said, however, these quantitative techniques don't come without difficulties. Quantitative analysis involves extensive amounts of wet chemistry methods to produce quantified values which are used to develop robust calibration models. These techniques are seen as laborious, expensive and delay obtaining results in real-time (Cozzolino *et al*., 2006).

For this reason research has moved towards using spectroscopy as a qualitative tool for the monitoring of fermentations. This involves interpreting spectral data alone without the generation of quantified values. Studies have shown the potential for spectroscopic techniques together with chemometrics to qualitatively monitor fermentations, however, these studies are very limited. These studies have provided the ground work for the further developments in IR spectroscopy, as fast, non-destructive alternatives for on-line fermentation applications in the future (Urtubia *et al*., 2004; 2008; Cozzolino *et al*., 2011).

Off-line attenuated total reflectance (ATR)-MIR (4000 and 375 cm^1) spectroscopy was successfully used to qualitatively monitor the time course of wild fermentations. The second derivative of the spectra showed a time course trend while the same trend was observed using PCA. PLS discriminant analysis (PLS-DA) was used to model the time course of the fermentation with a coefficient of determination (R^2) of 0.93 and a standard error of prediction (SEP) of 1.21 days (Cozzolino & Curtin, 2012).

Off-line red wine fermentation samples were collected and data was generated using FT-NIR (12,500 to 3600 cm^{-1}), ATR-MIR (4000 to 700 cm^{-1}), as well as electronic nose and tongue instruments. Using the 1st and 2nd derivative of the fermentation kinetics the maximum acceleration and maximum rate of the process for sugar consumption and ethanol and glycerol production were determined. PCA scores showed a clear time trend on principal component (PC) 1 and the significant wavenumbers responsible for the separation were identified using the PCA loadings plot. The same time related trends were observed with the electronic nose and tongue data on PC1 and PC2. The results showed that interpretation of spectral data and the PC1 scores of the spectra was successful in evaluating the chemical changes taking place throughout fermentation and were in agreement with the results obtained by modelling the sugar consumption and alcohol production using HPLC reference analysis (Buratti *et al*., 2011).

FT-MIR (4,000 to 700 cm^{-1}) and FT-NIR (12,500 to 3,600 cm^{-1}) data generated for red wine fermentations were used to monitor the time related changes using PCA score values and spectral loadings. The stage of the fermentation was successfully predicted using linear discriminant analysis (LDA) with 87% and 100% correct classification for NIR and MIR regions respectively (Di Egidio *et al*., 2010).

Off-line NIR spectroscopy (400 to 2500 nm) together with multivariate data analysis (PCA, DPLS and LDA) was successfully applied to monitor the progress of red wine

fermentations. PCA identified time related trends using PCA scores while LDA successfully classified samples in terms of the time point of fermentation (Cozzolino *et al*., 2006).

Reports have shown the use of data analysis techniques such as MPCA and MPLS in the prediction and early recognition of problematic fermentations in an industrial scale (Urtubia *et al*., 2007; 2008; 2012; Emparán *et al*., 2012).

To the authors knowledge only one recent study has evaluated the ability of MIR and NIR spectroscopic techniques to qualitatively identify metabolic differences between LAB treatments. In this study Cabernet Sauvignon and Chardonnay wine fermentations were elaborated with eight different *O. oeni* strains for MLF. Wine samples were scanned using MIR (400 - 4000 cm^{-1}) and NIR (400 – 2500 nm). The evaluation of the raw spectral data showed no clear variation between the LAB treatments. No visual differences between the bacterial strains were observed in the raw spectra. PCA showed clear separation between the bacterial strains independent of the wine with PC1 explaining 68% of the variation with both MIR and NIR spectroscopy. The loadings of the first three PC's were used in order to determine the wavenumbers which were contributing to the separation. Successful classification was achieved using linear discriminant models based on the spectral data. Classification rates between 67% and 100% were achieved for both MIR and NIR spectroscopy depending on the specific strains (Cozzolino *et al*., 2012).

This one preliminary study points to a clear gap for further studies, evaluating the ability to discriminate between different LAB. Such studies would provide information about the metabolic differences or similarities between different LAB.

Furthermore, the move towards the application of vibrational spectroscopic techniques for on-line process monitoring have been made available by developments in fibre optic probes and robust chemometric models. These applications are non-invasive and generate information about the process instantaneously with the detection of several analytes. The optical materials available for MIR applications are, however, expensive and are complicated by the absorptions of water in the MIR region. NIR spectroscopic techniques are, however, easier to apply with fibre optics with cheaper more robust instrumentation available (Vojinović *et al*., 2006). Very few studies have reported the use of fibre optics for the online monitoring applications using IR spectroscopy.

Short-wavelength NIR spectroscopy (700 to 1100nm) was used for the detection of ethanol during fermentations. The measurements were performed using a photodiode array spectrometer equipped with a fibre optic probe which was placed on the outside of the fermentation tank (Cavinato *et al*., 1990).

NIR spectroscopy was applied for the online determination of lactic acid, glucose and biomass during lactic acid production in batch, fed-batch and continuous fermentation scenarios (Vaccari *et al*., 1994).

More recently the alcohol content during AF was monitored using on-line NIR spectroscopy. Samples were scanned in transmission mode over the range 200 to 2500 nm at 2 nm intervals. PLS regression techniques were used to develop the calibration models (Zeaiter *et al*., 2006).

Blanco *et al*. (2004) used NIR spectroscopy for on-line monitoring of AF products in small-scale synthetic wine fermentations.

2.4.4 MULTIVARIATE DATA ANALYSIS TECHNIQUES USED FOR BIOPROCESS MONITORING

Analytical techniques used routinely in wine anlaysis and fermentation monitoring generate huge complex data sets (Kaufmann, 1997). Complex data (such as a MIR and NIR specta of wine) involve complex interactions between a large number of variables which characterise the chemical and physical properties of a wine sample. In order to extract the most relevant information from the spectrum to be able to quantify a specific component(s), it is necessary to carry out extensive multivariate calibration which involves techniques such as PLS (Esbensen, 2006). For on-line applications and for process analytical technology (PAT) systems the use of regression modelling is necessary for future prediction purposes.

The focus of this study involved an extensive amount of multivariate analysis carried out on spectral data (FT-MIR and FT-NIR), as well as on volatile aroma data quantified by the GC-FID and GC-MS instruments. The multivariate calibration technique included PLS regression. Exploratory techniques included PCA, while supervised classification techniques involved PLS-DA and Soft Independent Modelling of Class Analogy (SIMCA).

PCA identifies trends and groupings in the data without any prior knowledge of the data structure. Supervised classification techniques (also known as discriminant analysis) are used to classify samples into known classes (groups, clusters) based on their similarity (or dissimilarity) to the predefined classes (Esbensen, 2006). **Figure 2.8** highlights the multivariate methods discussed in this section.

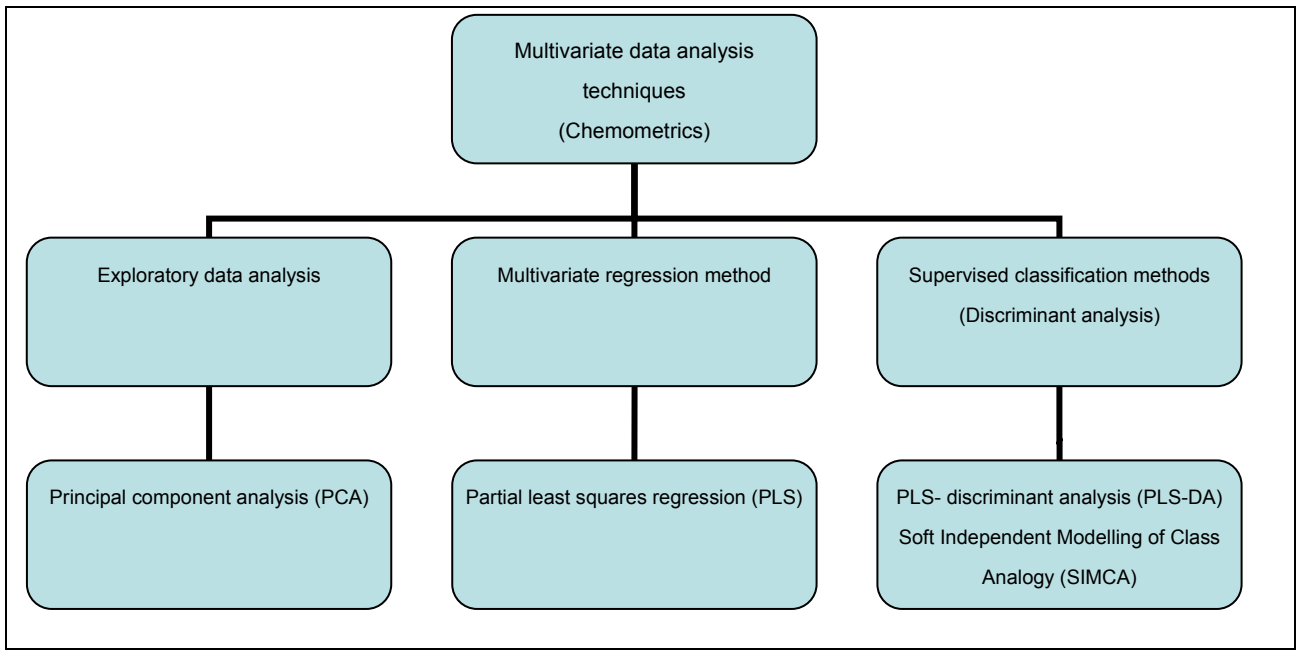

Figure 2.8 Multivariate data analysis methods discussed**.**

2.4.4.1 EXPLORATORY DATA ANALYSIS

PRINCIPAL COMPONENT ANALYSIS (PCA)

PCA is an unsupervised statistical technique frequently used as an explorative tool for data structure modeling and data description (Esbensen, 2006). It is known as the "workhorse" of multivariate data analysis and is frequently employed as the first exploratory technique for multivariate data analysis. The use of PCA in wine fermentation monitoring and discrimination has been widely reported (Urtubia *et al*., 2004; Buratti *et al*., 2011).

The main aim of PCA is to reduce the dimensionality of large and complex data sets, i.e. data reduction or data compression without losing any relevant information. This is achieved by transforming the original variables showing co linearity to a reduced number of new variables called principal components (PC's) (Esbensen, 2006).

The first step in PCA is to plot the original data matrix (X matrix) characterized by *n* objects (samples) and *p* variables, which collectively characterize the *n* objects (which can be measurements e.g. absorbance at a certain wavelength) into a p-dimensional plot. This new space will have *n* number of data points. If the variables associated with the swarm of data points correlate to each other in any way (co-vary) the data points will show some degree of a linear trend in this p-dimensional space. In the p-dimensional space, PC1 lies along the direction that explains the maximum amount of variance in the data set and contains the largest amount of information regarding similarities and differences between samples. The following PC's in order explain the residual unexplained variation not explained by the previous PC, until the maximum amount of variation in the data set is explained. PC's therefore describe in decreasing order the maximum variance among the observations. PC's therefore model the

hidden phenomena in a data set by describing the "unknown" variance resulting in this linear behaviour. Higher PC's lie in the direction where little variation between the data points exist and can therefore be seen as the "noise" directions. PC's are orthogonal to each other and can therefore be interpreted independently. PC's are linear combinations of the original X variables. The number of PC's needed to best describe the data set depends on the correlation between the original variables.

The object scores are the co-ordinates of the objects in the new space while the loadings are the coefficients by which the original variables must be multiplied by to obtain the PC's and gives an indication of the importance of a variable to a specific PC (Esbensen, 2006).

PCA decomposes the original data matrix (X matrix) into a "structure" part and a "noise" part. The following algorithm is used for the decomposition of the data matrix:

$$X(n,p) = T(n,k)P(k,p)^T + E(n,p) \quad (2.1)$$

Where the original data set (X) is decomposed into the structured part characterized by the scores matrix (T) and the loadings matrix (P^T), plus the noise part, the error matrix (E), *n* the number of objects, *p* the number of variables and *k* the number of PC's used (Esbensen, 2006).

The score and loading matrices for any two PC's can be plotted in two dimensional plots called score and loadings plots respectively. These graphical representations are used to evaluate the structure of the data and establish the relationships between the samples, variables as well as the relationship between sample and variables. Samples with similar characteristics will have scores which are located close to one another on the score plot. The loadings plot, however, will indicate which variables are closely related. Thus it is important to evaluate the score and loadings plot together.

Throughout this study PCA analysis was used as the preliminary tool to identify similarities, clustering's and subsequent correlations between samples and variables and evaluate trends in the data over time. PCA allowed us to identify outliers within the data set as well as evaluate biological repeatability.

2.4.4.2 PARTIAL LEAST SQUARES (PLS) REGRESSION

PLS is an unsupervised multivariate calibration technique used to find the relationship between two sets of data namely x variables and y variables using a regression algorithm (Figure 2.9) (Næs *et al*., 2002). This method projects the original x variables onto a smaller number of PLS components also known as "latent variables" or "factors". The factors are calculated in the same way as PC's are calculated in PCA with the incorporation of the y variable into the calculation. PLS finds the maximum covariance between the X spectral matrix and y response

variables. PLS1 deals with only one response y variable at a time (In this study, the reference data for malic acid or lactic acid). The Y matrix consists of the dependant variable whereas the X matrix is made up of independent variables (In this study, FT-MIR and FT-NIR spectral measurements). PLS-regression models are used for the prediction of new y values from new x measurements of unknown samples (i.e. to predict y from x). The NIPALS algorithm used for the calculation of the PLS regression is described in *Multivariate data analysis in practice* (Esbensen, 2006).

For the purpose of prediction, PLS regression models need to be validated in order to evaluate their performance. Validation should be performed using a test set which is most representative of future prediction samples in order to gain a fair estimate of the error level to be expected in the future (Esbensen, 2006). **Figure 2.9** details the steps that were followed in this study to setup calibration models.

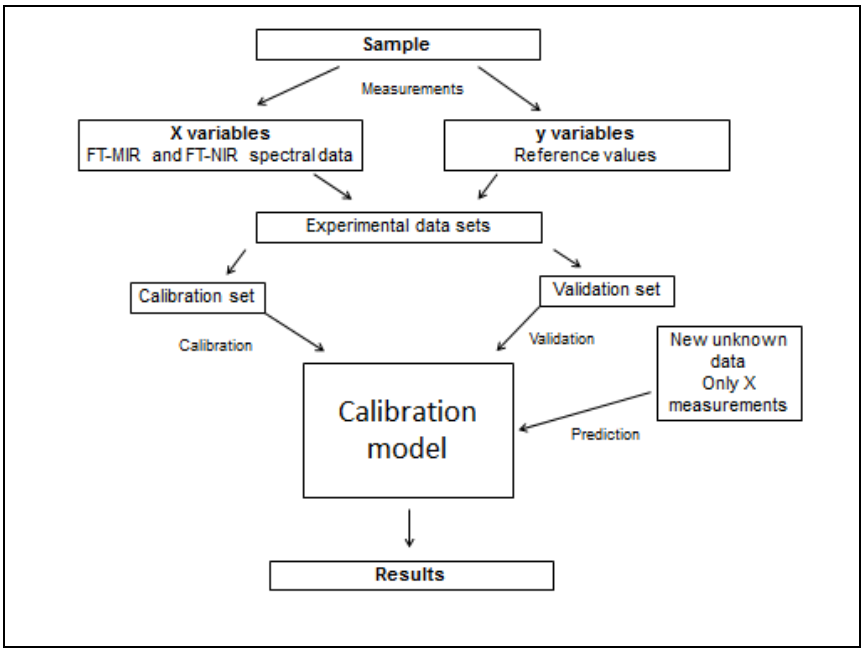

Figure 2.9 Basic steps followed to establish a quantitative PLS model using FT-MIR and FT-NIR spectroscopy (adapted from Swanepoel, 2006).

Current analytical instrumentation such as the WineScan FT 120 instrument (FOSS Analytical A/S software version 2.2.1, Denmark, 2001) is supplied with extended software options that provide ready-to-use calibration models for the quantification of various components of a sample. These calibration models supplied with the instrument include amongst others those for quantifying glucose, fructose, ethanol, glycerol, reducing sugars, malic acid, lactic acid, pH, volatile acidity and total acidity.

Previous studies have shown the poor prediction ability of the global model to predict constituents in the South African grape must and wine matrix (Nieuwoudt *et al*., 2004; Swanepoel *et al*., 2007). For this reason it was important to evaluate the ability of the ready-to-

use calibration model for the prediction of malic acid in our samples for the subsequent monitoring of MLF in our study.

2.4.4.3 SUPERVISED CLASSIFICATION METHODS

PLS-DISCRIMINANT ANALYSIS (*PLS-DA*)

PLS-DA is a supervised classification technique which uses PLS regression to model the differences between two or more classes and subsequently discriminates between these classes. The classes are established by assigning a dummy y variable to each class. In the case where there are only two classes, objects (samples) which belong to a specific class will be assigned a +1 y-value and -1 y-value if the objects do not belong to that class. PLS1 regression is used when there are only two classes. In a dataset where more than two classes exist PLS2 regression is used and several y variables, one for each class are assigned to the objects. For example, if an object belongs to class one out of four classes it will have this specific variable set : [+1 ; -1 ; -1 ;-1] (Esbensen, 2006). PLS-DA therefore models between class variation and does not capture within class variablity.

In this study PLS-DA was used as a technique to discriminate between the two LAB strains namely, *O. oeni* and *Lb. plantarum* using spectral data and well as predicted data from the GC-FID and GC-MS instruments. This profiling technique would provide critical information pertaining to the metabolic difference or similarities between the LAB treatments. In other words, this technique would provide a means to monitor the metabolic footprints of the different LAB treatments.

SOFT INDEPENDENT MODELLING OF CLASS ANALOGY (SIMCA)

SIMCA is a supervised classification method used to evaluate whether samples are similar to existing predefined groups of samples or classes. The training stage of building a SIMCA model is based on making individual PCA models for each class. These PCA models will each have their own optimum number of PC's which explains the data for the individual classes. The classification of new samples involves evaluating their proximity to the training samples and subsequently assigning these unknown samples to a specific class. SIMCA can classify samples as belonging to one class, many classes or not belonging to any of the classes. SIMCA can therefore be used as an application in product quality prediction. For example if an unknown sample belongs to a class it can be accepted or if it doesn't it can be rejected as it lies out of specification (Esbensen, 2006).

2.4.4.4 CONFORMITY TEST

The conformity test is a method used for quality control purposes to test deviations from defined limits. These limits are established by using a specific set of reference spectra depicting the final product. The reference samples vary and form a confidence band in the spectral range, which reflect the different sample variations. The confidence band defines the amount of variation on each spectral wavelength which is acceptable for the particular product. The test spectra taken at regular time intervals throughout the fermentation can be tested for their conformity to the specific reference spectra by evaluating whether the spectrum of new samples falls within the confidence band on each wavelength.

This is done by calculating the average (A) and standard deviations (σ) of the absorbance values for each wavelength (*i*). The confidence band within the specific spectral range is subsequently calculated by taking the mean value plus/minus the standard deviation. This defines the amount of variation on each spectral wavelength which is acceptable for the particular product. To determine whether the test spectra falls within the defined confidence band in the spectral range, the difference between the average of the test sample and the average of the reference sample is calculated on each wavelength, *i*. This absolute deviation is subsequently weighted by the corresponding standard deviation of the reference sample on the respective wavelength resulting in a relative deviation referred to as the Conformity Index (CI). The calculation is as follows:

$$CI = A_{reference,i} - A_{sample,i})/\sigma_{reference,i} \quad (2.2)$$

The test result is the maximum of all the CI values.

For the purpose of this study qualitative conformity models based on FT-MIR and FT-NIR spectral data were established to predict the completion of AF. This technique is a simple and rapid technique to be used for the prediction of a process stage for future on-line applications using only qualitative data. This technique by-passes the need for extensive calibration, as well the need for spectral interpretation that is normally done with PCA.

2.5 CONCLUSIONS

The wine industry and more specifically winemakers, are continually searching for new fermentation monitoring techniques which would deliver reliable real-time information in order to effectively monitor and manage fermentation processes. Spectroscopy has shown to be a fast, non-destructive alternative to the traditional laborious fermentation monitoring techniques.

For monitoring purposes the quantification of wine constituents using spectroscopy provides important information about a specific metabolite at a specific point in the fermentation. This, however, involves an extensive amount of calibration work with large amounts of wet

analytical chemistry. The accuracy of these models also involves continual evaluation and modification as well as ensuring their stability for practical on-line applications.

The focus of wine fermentation monitoring is now moving in the direction of qualitative applications involving the evaluation of spectra by chemometric techniques such as conformity tests or SIMCA for the identification of trends and deviating problem fermentations. These qualitative applications have shown excellent potential for on-line applications to provide real-time information about wine fermentation processes.

This literature review has therefore laid the groundwork for which this research study is based upon.

2.6 LITERATURE CITED

Abrahamse, C.E. & Bartowsky, E.J., 2012. Timing of malolactic fermentation inoculation in Shiraz grape must and wine: Influence on chemical composition. *World J. Microbiol. Biotechnol*. 28, 1-11.

Alexandre, H., Ansanay-Galeote, V., Dequin, S. & Blondin, B., 2001. Global gene expression during short-term ethanol stress in *Saccharomyces cerevisiae*. *FEBS Lett*. 498, 98–103.

Apetrei, I.M., Rodríguez-Méndez, M.L, Apetrei, C., Nevares, I., del Alamo, M. & de Saja, J.A., 2012. Monitoring of evolution during red wine aging in oak barrels and alternative method by means of an electronic panel test. *Food Res. Int*. 45, 244–249.

Bartowsky, E. & Henschke, P., 1995. Malolactic fermentation and wine flavour. *Aust. Grapegrower Winemaker* 378a, 83-94.

Bartowsky, E.J., Costello, P. & Henschke, P., 2002. Management of malolactic fermentation-wine flavour manipulation. *Aust. N.Z. Grapegrower Winemaker*.7-8, 10–12.

Bartowsky, E.J. & Henschke, P.A., 2004. The 'buttery' attribute of wine – diacetyl-desirability, spoilage and beyond. *Int. J. Food Microbiol*. 96, 235-252.

Bartowsky, E.J. & Pretorius, I.S., 2009. Microbial formation and modification of flavor and off-flavor compounds in wine. In: König, H., Unden, G. & Fröhlich, J. (eds). *Biology of microorganisms on grapes, in must and in wine*. Springer-Verlag, Berlin Heidelberg. pp 209-231.

Bauer, F.F. & Pretorius, I.S., 2000. Yeast stress response and fermentation efficiency: how to survive the making of wine. *S. Afr. J. Enol. Vitic.* 21, 27–51.

Bauer, R., Nieuwoudt, H., Bauer, F.F., Kossmann, J., Koch, K.R. & Esbensen, K.H., 2008. FTIR spectroscopy for grape and wine analysis. *Anal. Chem*. 80, 1371-1379.

Bevin, C.J., Fergusson, A.J., Perry, W.B., Janik, L.J. & Cozzolino, D., 2006. Development of a rapid "fingerprinting" system for wine authenticity by mid-infrared spectroscopy. *J. Agric. Food Chem*. 54, 9713-9718.

Bevin, C.J., Dambergs, R.G., Fergusson, A.J. & Cozzolino, D., 2008. Varietal discrimination of Australian wines by means of mid-infrared spectroscopy and multivariate analysis. *Anal. Chim. Acta* 621, 19-23.

Blanco, M., Peinado, A.C. & Mas, J., 2004. Analytical monitoring of alcoholic fermentation using NIR spectroscopy. *Biotech. Bioeng*. 88, 536-542.

Boe, K., Batstone, D.J. & Angelidaki, I., 2007. An innovative online VFA monitoring system for the Anerobic Process, Based on headspace gas chromatography. *Biotech. Bioeng*. 96, 712-721.

Boido, E., Medina, K., Fariña, L., Carrau, F., Versini, G. & Dellacassa, E., 2009. The effect of bacterial strain and aging on the secondary volatile metabolites produced during malolactic fermentation of Tannat red wine. *J. Agric. Food Chem*. 57, 6271-6278.

Bou, M. & Krieger, S., 2004. Alcohol-tolerant malolactic strains for the maturation of wines with average or high pH. (Pub. N: WO/2004/111179; PCT/FR2004/001421).

Boulet, J.C., Williams, P. & Doco, T., 2007. A Fourier transform infrared spectroscopy study of wine polysaccharides. *Carbohydr. Polym*. 69, 79-85.

Buratti, S., Ballabio, D., Benedetti, S. & Cosio, M., 2007. Prediction of Italian red wine sensorial descriptors from electronic nose, electronic tongue and spectrophotometric measurements by means of genetic algorithm regression models. *Food Chem*. 100, 211-218.

Buratti, S., Ballabio, D., Giovanelli, G., Dominguez, C.M.Z., Moles, A., Benedetti, S. & Sinelli, N., 2011. Monitoring of alcoholic fermentation using near infrared and mid infrared spectroscopies combined with electronic nose and electronic tongue. *Anal. Chim. Acta* 697, 67-74.

Camarasa, C., Grivet, J. & Dequin, S., 2003. Investigation by ^{13}C-NMR and tricarboxylic acid (TCA) deletion mutant analysis of pathways for succinate formation in *Saccharomyces cerevisiae* during anaerobic fermentation. *Microbiology* 149, 2669–2678.

Cavinato, A.G., Mayes, D.M., Ge, Z.H. & Callis, J.B., 1990. Noninvasive method for monitoring ethanol in fermentation processes using fiberoptic near infrared spectroscopy. *Anal. Chem*. 62, 1977–1982.

Cen, H. & He, Y., 2007. Theory and application of near infrared reflectance spectroscopy in determination of food quality. *Trends Food Sci. Technol*. 18, 72-83.

Clemente-Jimenez, J.M., Mingorance-Cazorla, S., Martinez-Rodriguez, S., Las Heras-Vazquez, F.J. & Rodriguez-Vico, F., 2005. Influence of sequential yeast mixtures on wine fermentation. *Int. J. Food Microbiol.* 98, 301–308.

Compagnone, D., Esti, M., Messia, M.C., Peluso, E. & Palleschi, G., 1998. Development of a biosensor for monitoring of glycerol during alcoholic fermentation. *Biosens. Bioelectron*. 13, 875-880.

Costello, P., 2005. The chemistry of malolactic fermentation. In: Morenzoni, R (ed). Malolactic fermentation in wine. Lallemand Inc, Montréal, Canada. pp. 4:2.

Costenoble, R., Valadi, H., Gustafsson, L., Niklasson, C. & Johan Franzén, C., 2000. Microaerobic glycerol formation in *Saccharomyces cerevisiae*. *Yeast* 16, 1483-1495.

Coulter, A.D., Godden, P.W. & Pretorius, I.S., 2004. Succinic acid –how it is formed, what is its effect on titratable acidity, and what factors influence its concentration in wine? *Aust. N.Z. Wine Ind. J*.19, 16–20, 21–25.

Cozzolino, D., Smyth, H.E. & Gishen, M., 2003. Feasibility study on the use of visible and near-infrared spectroscopy together with chemometrics to discriminate between commercial white wines of different varietal origins. *J. Agric. Food Chem*. 51, 7703-7708.

Cozzolino, D., Kwiatkowski, M., Parker, M., Cynkar, W., Dambergs, R., Gishen, M. & Herderich, M.J., 2004. Prediction of phenolic compounds in red wine fermentations by visible and near infrared spectroscopy. *Anal. Chim. Acta* 513, 73-80.

Cozzolino, D., Smyth, H.E., Cynkar, W., Dambergs, R.G. & Gishen, M., 2005. Usefulness of chemometrics and mass spectrometry-based electronic nose to classify Australian white wines by their varietal origin. *Talanta* 68, 382-387.

Cozzolino, D., Parker, M., Dambergs, R.G., Herderich, M. & Gishen, M., 2006. Chemometrics and visible-near infrared spectroscopic monitoring of red wine fermentation in a pilot scale. *Biotech. Bioeng*. 95, 1101-1107.

Cozzolino, D., Cowey, G., Lattey, K. A., Godden, P., Cynkar, W. U., Dambergs, R. G., Janik, L. & Gishen, M., 2008a. Relationship between wine scores and visible near infrared spectra of Australian red wines. *Anal. Bioanal. Chem.* 391, 975-981.

Cozzolino, D., Kwiatkowski, M. J., Dambergs, R. G., Cynkar, W. U., Janik, L. J., Skouroumounis, G. & Gishen, M., 2008b. Analysis of elements in wine using near infrared spectroscopy and partial least squares regression. *Talanta* 74, 711-716.

Cozzolino, D. & Dambergs, R.G., 2009. Wine and beer. In: Sun, D. (ed). *Infrared spectroscopy for food quality analysis and control*. Academic Press. New York, USA. pp. 377-397.

Cozzolino, D., Cynkar, W., Shah, N. & Smith, P., 2011. Feasibility study on the use of attenuated total reflectance mid-infrared for analysis of compositional parameters in wine. *Food Res. Int*. 44, 181-186.

Cozzolino, D. & Curtin, C., 2012. The use of attenuated total reflectance as tool to monitor the time course of fermentation in wild ferments. *Food Control* 26, 241-246.

Cozzolino, D., McCarthy, J. & Bartowsky, E., 2012. Comparison of near infrared and mid infrared spectroscopy to discriminate between wines produced by different *Oenococcus Oeni* strains after malolactic fermentation: A feasibility study. *Food Control* 26, 81-87.

Dambergs, R.G., Kambouris, A., Francis, I.L. & Gishen, M., 2002. Rapid analysis of methanol in grape-derived distillation products using near-infrared transmission spectroscopy. *J. Agric. Food Chem. 50, 3079*.

Dambergs, R.G., Cozzolino, D., Esler, M.B., Cynkar, W.U., Kambouris, A., Francis, I.L., Hoj, P. & Gishen, M., 2003. The use of near infrared spectroscopy for grape quality measurements. *Aust. N.Z. Grapegrower Winemaker.* 476A, 69-76.

de Barros Lopes, M.A., Eglinton, J., Henschke, P.A., Høj, P.B. & Pretorius, I.S., 2003. The connection between yeast and alcohol reduction in wine: managing the double-edged sword of bottled sunshine. *Aust. N.Z. Wine Indust. J*. 18, 17–18, 20, 22.

de Orduña, R.M., 2010. Climate change associated effects on grape and wine quality and production. *Food Res. Int*. 43, 1844–1855.

De Revel, G., Martin, N., Pripis-Nicolau, L., Lonvaud-Funel, A. & Bertrand, A., 1999. Contribution to the knowledge of malolactic fermentation influence on wine aroma. *J. Agric. Food Chem*. 47, 4003-4008.

de Villiers, A., Alberts, P., Tredoux, A.G.J. & Nieuwoudt, H.H., 2011. Analytical techniques for wine analysis: An African perspective. *Anal. Chim. Acta* 730, 1-22.

Dickinson, T.A., White, J., Kauer, J.S. & Walt, D.R., 1998. Current trend in artificial nose technology. *Trends Biotechnol*. 16, 250–258.

Di Egidio, V., Sinelli, N., Giovanelli, G., Moles, A. & Casiraghi, E., 2010. NIR and MIR spectroscopy as rapid methods to monitor red wine fermentation. *Eur. Food Res. Technol*. 230, 947-955.

du Toit, M., Engelbrecht, L., Lerm, E. & Krieger-Weber, S., 2010. *Lactobacillus*: The next generation of malolactic fermentation starter cultures-an overview. *Food Bioprocess Technol*. 4, 876-906.

Ebeler, S.E., 2001. Analytical chemistry: Unlocking the secrets of wine flavor. *Food Rev. Int*. 17, 45-64.

Eden A., Van Nedervelde L., Drukker M., Benvenisty N. & Debourg A., 2001. Involvement of branched-chain amino acid aminotransferases in the production of fusel alcohols during fermentation in yeast. *Appl. Microbiol. Biotechnol*. 55:296–300.

Eglinton, J.M., McWilliam, S.J., Fogarty, M.W., Francis, I.L., Kwiatkowski, M.J., Høj, P.B. & Henschke, P.A., 2000. The effect of *Saccharomyces bayanus*-mediated fermentation on the chemical composition and aroma profile of Chardonnay wine. *Aust. J. Grape Wine Res*. 6, 190–196.

Emparán, M., Simpson, R., Almonacid, S., Teixeira, A. & Urtubia, A., 2012. Early recognition of problematic wine fermentations through multivariate data analyses. *Food Control* 27, 248-253.

Esbensen, K., Kirsanov, D., Legin, A., Rudnitskaya, A., Mortensen, J., Pedersen, J., Vognsen, L., Makarychev-Mikhailov, S. & Vlasov, V., 2004. Fermentation monitoring using multisensor systems: Feasibility study of the electronic tongue. *Anal. Bioanal. Chem.* 378, 391-395.

Esbensen, K.H. (ed). 2006. *Multivariate Data Analysis – In Practice*. 5th Ed. Camo ASA, Oslo, Norway.

Esti, M., Volpe, G., Micheli, L. Delibato, E., Compagnone, D. Moscone, D. & Palleschi, G., 2004. Electrochemical biosensors for monitoring malolactic fermentation in red wine using two strains of *Oenococcus oeni*. *Anal. Chim. Acta* 513, 357-364.

Etiévant, P., 1991. Wine. In: Maarse, H. (ed). *Volatile compounds in food and beverages*. Marcel Dekker, New York. pp 483–546.

Fayolle, P., Picque, D., Perret, B., Latrille, E. & Corrieu, G., 1996. Determination of major compounds of alcoholic fermentation by middle-infrared spectroscopy: Study of temperature effects and calibration methods. *Appl. Spectrosc*. 50, 1325-1330.

Fernández-Novales, J., López, M., Sánchez, M., García, J. & Morales, J., 2008. A feasibility study on the use of a miniature fiber optic NIR spectrometer for the prediction of volumic mass and reducing sugars in white wine fermentations. *J. Food Eng*. 89, 325–329.

Filippini, C., Moser, J., Sonnleitner, B. & Fiechter, A., 1991. On-line capillary gas chromatography with automated liquid sampling, a powerful tool in biotechnology. *Anal. Chim. Acta* 255, 91-96.

Fleet, G.H. & Heard, G.M., 1993. Yeasts: Growth during fermentation. In: Fleet, G.H. (ed). *Wine Microbiology and Biotechnology*. Harwood Academic Publishers, Chur, Switzerland. pp. 27–54.

Fleet, G.H. 2003., Yeast interactions and wine flavour. *Int. J. Food Microbiol*. 86, 11 – 22.

Francis, I.L. & Newton, J.L., 2005. Determining wine aroma from compositional data. *Aust. J. Grape Wine Res*. 11, 114-126.

García, M., Aleixandre, M., Gutiérrez, J. & Horrillo, M., 2006. Electronic nose for wine discrimination. *Sens. Actuators, B* 113, 911-916.

García-Carpintero, E.G., Sánchez-Palomo, E. & González-Viñas, M.A., 2011. Aroma characterization of red wines from cv. Bobal grape variety grown in La Mancha region. *Food Res. Int*. 44, 61–70.

Garde-Cerdán, T., Lorenzo, C., Alonso, G.L. & Salinas, M.R., 2011. Near infrared spectroscopy: Easy and rapid tool to determine different volatile compounds in wines. *Curr. Bioact Compd*. 7, 93-105.

Gishen, M. & Holdstock, M., 2000. Preliminary evaluation of the performance of the Foss WineScan FT 120 instrument for the simultaneous determination of several wine analyses. *Aust. Grapegrower Winemaker 438a,* 75-81.

Giudici P., Romano P. & Zambonelli C., 1990. A biometric study of higher alcohol production in *Saccharomyces cerevisiae*. *Can. J. Microbiol*. 36, 61–64.

Giudici, P., Zambonelli, C., Passarelli, P. & Castellari, L., 1995. Improvement of wine composition with cryotolerant *Saccharomyces* strains. *Am. J. Enol. Viti.* 46, 143–147.

Goldner M.C., Zamora, M., Di Leo Lira, P., Gianninoto, H. & Bandoni, A., 2009. Effect of ethanol level in the perception of aroma attributes and the detection of volatile compounds in red wine. *J. Sens. Stud*. 24, 243–257.

Guth, H. & Sies, A., 2002. Flavour of wines: Towards an understanding by reconstitution experiments and an analysis of ethanol's effect on odour activity of key compounds. Proc. 11th Aust. Wine Ind. Tech. Conf., 7–11 October 2001, Adelaide, Australia, S.A. pp. 128–139.

Hallsworth, J.E., 1998. Ethanol-induced water stress in yeast. *J. Ferm. Bioeng*. 85, 125–137.

Harms, P., Kostov, Y. & Rao, G., 2002. Bioprocess monitoring. *Curr. Opin. Biotechnol*. 13, 124-127.

Heard, G., 1999. Novel yeasts in winemaking-looking to the future. *Food Aust*. 51, 347-352.

Henick-Kling, T., 1995. Control of malolactic fermentation in wine: energetics, flavour modification and methods of starter culture preparation. *J. Appl. Bacteriol. Symp. Supp*. 79, 29S-37S.

Henschke, P.A. & Jiranek, V., 1993. Yeasts-metabolism of nitrogen compounds. In: Fleet, G.H. (ed). *Wine Microbiology and Biotechnology*. Harwood Academic, Chur, Switzerland. pp. 77-164.

Henschke, P.A., 1997. Wine yeast. In: Zimmermann, F.K. & Entian K-D (eds). *Yeast Sugar Metabolism*. Technomic Publishing, Lancaster, PA. pp. 527-560.

Herjavec, S., Tupajić, P. & Majdak, A., 2001. Influence of malolactic fermentation on the quality of Riesling wine. *Agric. Conspec. Sci*. 66, 59-64.

Huang, H., Yu, H., Xu, H. & Ying, Y., 2008. Near infrared spectroscopy for on/in-line monitoring of quality in foods and beverages: A review. *J. Food Eng*. 87, 303-313.

Ionescu, R., Vancu, A., Moise, C. & Tomescu, A. 1999. Role of water vapour in the interaction of SnO_2 gas sensors with CO and CH_4. *Sens. Actuators, B* 61, 39-42.

Izquierdo Cañas, P., García Romero, E., Gómez Alonso, S. & Palop Herreros, M., 2008. Changes in the aromatic composition of Tempranillo wines during spontaneous malolactic fermentation. *J. Food Comp. Anal*. 21, 724-730.

Jeromel, A., Herjavec, S., Orlić, S., Redžepović, S. & Wondra, M., 2008. Changes in volatile composition of Kraljevina wines by controlled malolactic fermentation. *J. Cent. Eur. Agric*. 9, 363-372.

Jones, P.R., Gawel, R., Francis, I. & Waters E.J., 2008. The influence of interactions between major white wine components on the aroma, flavour and texture of model white wine. *Food Qual Prefer*. 19, 596–607.

Jørgensen, P., Pedersen, J.G., Jensen, E.P. & Esbensen, K.H., 2004. On line batch fermentation process monitoring (NIR)—Introducing biological process time. *J. Chemom*. 18, 81–91.

Kaufmann, A., 1997. Multivariate statistics as a classification tool in the food laboratory. *J. AOAC Int.* 80, 665-675.

Knoll, C., Fritsch, S., Schnell, S., Grossmann, M., Rauhut, D. & du Toit, M., 2011. Influence of pH and ethanol on malolactic fermentation and volatile aroma compound composition in white wines. *LWT-Food Sci. Technol*. 44, 2077-2086.

Knoll, C., Fritsch, S., Schnell, S., Grossmann, M., Krieger-Weber, S., du Toit, M. & Rauhut, D., 2012. Impact of different malolactic fermentation inoculation scenarios on Riesling wine aroma. *World J. Microbiol. Biotechnol*. 28, 1143-1153.

Krieger-Weber, S., 2009. Application of yeast and bacteria as starter cultures. In: König, H., Unden, G. & Fröhlich, J. (eds). *Biology of microorganisms on grapes, in must and in wine*. Springer, Berlin. pp. 498-511.

Kupina, S.A. & Shrikhande, A.J., 2003. Evaluation of a Fourier transform infrared instrument for rapid quality-control wine analyses. *Am. J. Enol. Vitic*. 54, 131-134.

Lambrechts, M.G. & Pretorius, I.S., 2000. Yeast and its importance to wine aroma-a review. *S. Afr. J. Enol. Vitic*. 21, 97-129.

Lee, J.E., Hong, Y.S & Lee, C.H., 2009a. Characterization of fermentative behaviors of lactic acid bacteria in grape wines through ^{1}H-NMR- and GC-based metabolic profiling. *J. Agric. Food Chem*. 57, 4810-4817.

Lee, J.E., Hwang, G.S., Lee, C.H. & Hong, Y.S., 2009b. Metabolomics reveals alterations in both primary and secondary metabolites by wine bacteria. *J. Agric. Food Chem*. 57, 10772-10783.

Lerm, E., Engelbrecht, L. & du Toit, M., 2010. Malolactic fermentation: The ABC's of MLF. *S. Afr. J. Enol. Vitic.* 31, 186-212.

Lilly, M., Lambrechts, M.G. & Pretorius, I.S., 2000. Effect of increased yeast alcohol acetyltransferase activity on flavor profiles of wine and distillates. *Appl. Environ. Microbiol*. 66, 744–753.

Lilly, M., Bauer, F.F., Lambrechts, M.G., Swiegers, J.H., Cozzolino, D. & Pretorius, I.S., 2006a. The effect of increased yeast alcohol acetyltransferase and esterase activity on the flavour profiles of wine and distillates. *Yeast* 23, 641–659.

Lilly, M., Bauer, F.F., Styger, G., Lambrechts, M.G. & Pretorius, I.S., 2006b. The effect of increased branched-chain amino acid transaminase activity in yeast on the production of higher alcohols and on the flavour profiles of wine and distillates. *FEMS Yeast Res*. 6, 726–743.

Liu, S.Q. & Pilone, G.J., 2000. An overview of formation and roles of acetaldehyde in winemaking with emphasis on microbiological implications. *Int. J. Food Sci. Technol.* 35, 49-61.

Liu, S.Q., 2002. Malolactic fermentation in wine - beyond deacidification. A review. *J. Appl. Microbiol*. 92, 589-601.

Lonvaud-Funel, A., 1999. Lactic acid bacteria in the quality improvement and depreciation of wine. *Antonie Leeuwenhoek* 76, 317-331.

Lorenzo, C., Garde-Cerdán, T., Pedroza, M.A., Alonso, G.L. & Salinas, M.R., 2009. Determination of fermentative volatile compounds in aged red wines by near infrared spectroscopy. *Food Res. Int*. 42, 1281-1286.

Lozano, J., Arroyo, T., Santos, J.P., Cabellos, J.M. & Horrillo, M.C., 2008. Electronic nose for wine ageing detection. *Sens. Actuators, B* 133, 180–186.

Maicas, S., Gil, J.V., Pardo, I. & Ferrer, S., 1999. Improvement of volatile composition of wines by controlled addition of malolactic bacteria. *Food Res. Int*. 32, 491-496.

Manley, M., Van Zyl, A. & Wolf, E., 2001. The evaluation of the applicability of Fourier transform near-infrared (FT-NIR) spectroscopy in the measurement of analytical parameters in must and wine. *S. Afr. J. Enol. Vitic*. 22, 93-100.

Marais, J., 2001. Effect of grape temperature and yeast strain on Sauvignon blanc wine aroma composition and quality. *S. Afr. J. Enol. Vitic*. 22, 47–51.

Margalit, Y., 1997. In: J. Crum (ed). *Concepts in Wine Chemistry*. Wine Appreciation Guild Ltd., San Fransisco, USA. pp. 16-18; 76-82.

Martineau, B., Acree, T.E. & Henick-Kling, T., 1995. Effect of wine type on the detection threshold for diacetyl. *Food Res. Int*. 28, 139-143.

Martineau, B. & Henick-Kling, T., 1995. Formation and degradation of diacetyl in wine during alcoholic fermentation with *Saccharomyces cerevisiae* strain EC 1118 and malolactic fermentation with *Leuconostoc oenos* strain MCW. *Am. J. Enol. Viti*. 46, 442–448.

Mathis, C., Pons, M., Engasser, J. & Lenoel, M., 1993. Development of an on-line method for the monitoring of vicinal diketones and their precursors in beer fermentation. *Anal. Chim. Acta* 279, 59-66.

Matthews, A., Grbin, P.R. & Jiranek, V., 2006. A survey of lactic acid bacteria for enzymes of interest to oenology. *Aust. J. Grape Wine Res.* 12, 235-244.

Matz, G. & Lennemann, F., 1996. On-line monitoring of biotechnological processes by gas chromatographic-mass spectrometric analysis of fermentation suspensions. *J. Chrom. A.* 750, 141-149.

Mazzei, F., Botrè, F. & Favero, G., 2007. Peroxidase based biosensors for the selective determination of D, L-lactic acid and L-malic acid in wines. *Microchem. J.* 87, 81-86.

McDonagh, C., Burke, C.S. & MacCraith, B.D., 2008. Optical chemical sensors. *Chem. Rev.* 108, 400-422.

Mello, L.D. & Kubota, L.T., 2002. Review of the use of biosensors as analytical tools in the food and drink industries. *Food Chem*. 77, 237-256.

Mocke, B.A., 2005. The breeding of yeast strains for novel oenological outcomes. MSc Thesis, Stellenbosch University, Stellenbosch, South Africa.

Moreira, J.L. & Santos, L., 2005. Analysis of organic acids in wines by Fourier-transform infrared spectroscopy. *Anal. Bioanal Chem*. 382, 421-425.

Mtshali, P.S. Divol, B., van Rensburg, P. & du Toit, M., 2010. Genetic screening of wine-related enzymes in *Lactobacillus* species isolated from South African wines. *J. Appl. Microbiol*. 108, 1389-1397.

Næs, T., Isaksson, T. Fearn, T. & Davis, T. (eds). 2002. *A user-friendly guide to multivariate calibration and classification*. NIR Publications, Chichester, UK.

Natale, C.D, Paolesse, R., Bugio, M., Martinelli, E., Pennazza, G. & D'Amico, A., 2004. Application of metalloporphyrins-based gas and liquid sensor arrays to the analysis of red wine. *Anal. Chim. Acta* 513, 49–56.

Nielsen, J.C., Prahl, C. & Lonvaud-Funel, A., 1996. Malolactic fermentation in wine by direct inoculation with freeze-dried *Leuconostoc oenos* cultures. *Am. J. Enol. Vitic*. 47, 42-48.

Nielsen, J.C. & Richelieu, M., 1999. Control of flavor development in wine during and after malolactic fermentation by *Oenococcus oeni*. *Appl. Environ. Microbiol.* 65, 740–745.

Nieuwoudt, H. H., Prior, B. A., Pretorius, I. S. & Bauer, F. F., 2002. Glycerol in South African table wines: an assessment of its relationship to wine quality. *S. Afr. J. Enol. Vitic*. 23 (1), 22-30.

Nieuwoudt, H.H., Prior, B.A., Pretorius, I.S., Manley, M. & Bauer, F.F., 2004. Principal component analysis applied to Fourier transform infrared spectroscopy for the design of calibration sets for glycerol prediction models in wine and for the detection and classification of outlier samples. *J. Agric. Food Chem*. 52, 3726-3735.

Nieuwoudt, H.H., Pretorius, I.S., Bauer, F.F., Nel, D.G. & Prior, B.A., 2006. Rapid screening of the fermentation profiles of wine yeasts by Fourier transform infrared spectroscopy. *J. Microbiol. Methods* 67, 248-256.

Norbeck, J. & Blomberg, A.,1997. Metabolic and regulatory changes associated with growth of *Saccharomyces cerevisiae* in 1.4 M NaCl. *J. Biol. Chem*. 272, 5544-5554.

Obreque-Slìer, E., Peña-Neira, A. & Lopez-Solis, R., 2010. Enhancement of both salivary protein-enological tannin interactions and astringency perception by ethanol. *J. Agric. Food Chem*. 58, 3729–3735.

Osborne, J. P., Mira de Orduña, R., Pilone, G. J. & Liu, S.-Q., 2000. Acetaldehyde metabolism by wine lactic acid bacteria. *FEMS Microbiol. Lett.* 191, 51–55.

Osborne, J. P., Dubé Morneau, A. & Mira de Orduña, R., 2006. Degradation of free and sulfur-dioxide-bound acetaldehyde by malolactic lactic acid bacteria in white wine. *J. Appl. Microbiol*. 101, 474–479.

Overkamp, K.M., Bakker, B.M., Köteer, P., Luttik, M.A.H., Van Dijken, J.P. & Pronk, J.T., 2002. Metabolic engineering of glycerol production in *Saccharomyces cerevisiae*. *Appl. Environ. Microbiol*. 68, 2814-2821.

Pasteris, S. E. & Strasser de Saad, A. M. 2009. Sugar-glycerol cofermentations *by Lactobacillus hilgardii* isolated from wine. J. Agric. Food Chem. 57, 3853-3858.

Patz, C. D., Blieke, A., Ristow, R. & Dietrich, H., 2004. Application of FT-MIR spectrometry in wine analysis. *Anal. Chim. Acta* 513, 81-89.

Pavia, L.P., Lampman, G.M. & Kriz, G.S. (eds). 2009. *Introduction to Spectroscopy: A Guide for Students of Organic Chemistry*. 4th Ed. Harcourt College Publishers, Belmont, USA. pp. 15-104.

Pemen, A.J.M., van der Laan, P.C.T. & Kema, A., 1998. On-line detection of partial discharges in statorwindings of largeturbine generators. IEE colloquium on discharges in large machines. pp. 3/1–3/4.

Pinheiro, C., Rodrigues, C.M., Schäfer, T. & Crespo, J.G., 2002. Monitoring the aroma production during wine-must fermentation with an electronic nose. *Biotech. Bioeng*. 77, 632-640.

Pozo-Bayón, M.A., Alegría, E.G., Polo, M.C., Tenorio, C., Martín-Álvarez, P.J., Calvo de la Banda, M.T., Ruiz-Larrea, F. & Moreno-Arribas, M.V., 2005. Wine volatile and amino acid composition after malolactic fermentation: Effect of *Oenococcus oeni* and *Lactobacillus plantarum* starter cultures. *J. Agric. Food Chem*. 53, 8729-8735.

Pretorius, I.S., van der Westhuizen, T.J. & Augustyn, O.P.H., 1999. Yeast biodiversity in vineyards and wineries and its importance to the South African wine industry. *S. Afr. J. Enol. Vitic*. 20, 61–74.

Pretorius, I.S., 2000. Tailoring wine yeast for the new millennium: Novel approaches to the ancient art of winemaking. *Yeast* 16, 675-729.

Pronk, J.T., Steensma, H.Y. & van Dijken, J.P., 1996. Pyruvate metabolism in *Saccharomyces cerevisiae*. *Yeast* 12, 1607–1633.

Radler, F., 1993. Yeast: metabolism of organic acids. In: Fleet, G.H. (ed). *Wine Microbiology and Biotechnology*. Harwood Academic, Chur, Switzerland. pp 165–182.

Ragazzo-Sánchez, J.A., Baldet, P., Ghommidh, C., Chalier, P., Deratani, A., Boulet, J.C., Grenier, P., Persin, M., Crouzet, J., Chanié, E. & Perrain, A., 2004a. Sampler of volatile components. European Patent no. 02 291 627.4.

Ragazzo-Sánchez, J.A., Chalier, P. & Ghommidh, C., 2004b. Coupling GC and electronic nose for dehydration and desalcoholization of alcoholised beverages. Application to off-flavour detection in wine. *Sens. Actuators, B* 106, 253-257.

Ragazzo, J.A., Chalier, P., Chevalier, D. & Ghommidh, C., 2006. Electronic nose discrimination of aroma compounds in alcoholised solutions. *Sens. Actuators, B* 104, 665-673.

Ragazzo-Sanchez, J.A., Chalier, P., Chevalier, D., Calderon-Santoyo, M. & Ghommidh, C., 2008. Identification of different alcoholic beverages by electronic nose coupled to GC. *Sens. Actuators, B* 134, 43–48.

Ramos, A., Lolkema, J.S., Konings, W.N. & Santos, H., 1995. Enzyme basis for pH regulation of citrate and pyruvate metabolism by *Leuconostoc oenos*. *Appl. Environ. Microbiol*. 61, 1303–1310.

Rapp, A. & Versini, G., 1991. Influence of nitrogen compounds in grapes on aroma compounds in wine. Proceedings of the international symposium on nitrogen in grapes and wine; Seattle, USA; 18-19 June 1991: American Society of Enology and Viticulture, Davis, C.A. pp. 156–164.

Rapp, A., 1998. Volatile flavour of wine: Correlation between instrumental analysis and sensory perception. *Nahrung* 42, 351-363.

Regmi, U., Palma, M. & Barroso, C., 2012. Direct determination of organic acids in wine and wine-derived products by Fourier transform infrared (FT-IR) spectroscopy and chemometric techniques. *Anal. Chim. Acta* 732, 137-144.

Reid, L.M., O'Donnell, C.P. & Downey, G., 2006. Recent technological advances for the determination of food authenticity. *Trends Food Sci. Technol*. 17. 344–353.

Ribéreau-Gayon, P., Dubourdieu, D., Doneche, B. & Lonvaud, A. (eds). 2006. *Handbook of Enology. The microbiology of wine and vinfications*, vol 1. 2nd Ed .Wiley, New York. pp. 53-78; 139-160.

Romera-Fernández, M., Berrueta, L.A., Garmón-Lobato, S., Gallo, B., Vicente, F. & Moreda, J.M., 2012. Feasibility study of FT-MIR spectroscopy and PLS-R for the fast determination of anthocyanins in wine. *Talanta* 88, 303-310.

Roustan, J.L. & Sablayrolles, J.M., 2002. Impact of the addition of electron acceptors on the by-products of alcoholic fermentation. *Enzyme Microb. Technol*. 31, 142–152.

Roychoudhury, P., Harvey, L.M. & McNeil, B., 2006. The potential of mid infrared spectroscopy (MIRS) for real time bioprocess monitoring. *Anal. Chim. Acta* 571, 159-166.

Saerens, S.M.G., Delvaux, F., Vertrepen, K.J., Van Dijck, P., Thevelein, J.M. & Delvaux, F.R., 2008. Parameters affecting ethyl ester production by *Saccharomyces cerevisiae* during fermentation. *Appl. Environ. Microbiol*. 74, 454-461.

Sauvageot, F. & Vivier, P., 1997. Effect of malolactic fermentation on sensory properties of four Burgundy wines. *Am. J. Enol. Vitic.* 48, 187-192.

Scanes, K., Hohmann, S. & Prior, B., 1998. Glycerol production by the yeast *Saccharomyces cerevisiae* and its relevance to wine: A review. *S. Afr. J. Enol. Vitic*. 19, 17-24.

Scarff, M., Alison Arnold, S., Harvey, L.M. & McNeil, B., 2006. Near Infrared spectroscopy for bioprocess monitoring and control: Current status and future trends. *Crit. Rev. Biotechnol*. 26, 17–39.

Schulthess, D. & Ettlinger, L, 1978.Influence of the concentration of branched chain amino acids on the formation of fusel alcohols. *J. Inst. Brew*. 84, 240–243.

Shen, F., Ying, Y., Li, B., Zheng, Y. & Hu, J., 2011. Prediction of sugars and acids in Chinese rice wine by mid-infrared spectroscopy. *Food Res. Int*. 44, 1521-1527.

Smith, B.C. (ed.). 1999. *Infrared spectral interpretation: A systematic approach*. CRC Press LLC, Boca Raton, Florida, USA. pp. 67-152.

Smyth, H., Cozzolino, D., Herderich, M.J, Sefton, M.A. & Francis, I.L., 2005. Relating volatile composition to wine aroma: identification of key aroma compounds in Australian white wines. Proc. 12th Aust. Wine Ind. Tech. Conf., 24–29 July 2004, Melbourne, Australia, S.A. pp. 31–33.

Smyth, H.E., Cozzolino, D., Cynkar, W.U., Dambergs, R.G., Sefton, M. & Gishen, M., 2008. Near infrared spectroscopy as a rapid tool to measure volatile aroma compounds in Riesling wine: possibilities and limits. *Anal. Bioanal. Chem*. 390, 1911-1916.

Soriano, A., Pérez-Juan, P.M., Vicario, A., González, J.M. & Pérez-Coello, M.S., 2007. Determination of anthocyanins in red wine using a newly developed method based on Fourier transform infrared spectroscopy. *Food Chem.* 104 (3), 1295-1303.

Starrenburg, M.J.C. & Hugenholtz, J., 1991. Citrate fermentation by *Lactococcus* and *Leuconostoc spp*. *Appl. Environ. Microbiol*. 57, 3535-3540.

Steyer, J-P., Bouvier, J.C., Conte, T., Gras, P. & Sousbie, P., 2002. Evaluation of a four year experience with a fully instrumented anaerobic digestion process. *Water Sci. Technol*. 45, 495-502.

Sumby, K.M., Matthews, A.H., Paul R. Grbin, P.R. & Jiranek, V., 2009. Cloning and characterization of an intracellular esterase from the wine-associated lactic acid bacterium *Oenococcus oeni*. *Appl. Environ. Microbiol*. 75, 6729-6735.

Swanepoel, M., 2006. Monitoring the quality control chain from vineyard to wine: An industrial case study. MSc Thesis, Stellenbosch University, Stellenbosch, South Africa.

Swanepoel, M., du Toit, M. & Nieuwoudt, H. H., 2007. Optimisation of the quantification of total soluble solids, pH and titratable acidity in South African grape must using Fourier Transform Mid-infrared spectroscopy. *S. Afr. J. Enol. Vitic.* 28 (2), 140-149.

Swiegers, J., Bartowsky, E.J., Henschke, P. & Pretorius, I.S., 2005. Yeast and bacterial modulation of wine aroma and flavour. *Aust. J. Grape Wine Res*. 11, 139-173.

Ugliano, M. & Moio, L., 2005. Changes in the concentration of yeast-derived volatile compounds of red wine during malolactic fermentation with four commercial starter cultures of *Oenococcus oeni*. *J. Agric. Food Chem*. 53, 10134-10139.

Urbano-Cuadrado, M., Luque de Castro, M., Pérez-Juan, P., García-Olmo, J. & Gómez-Nieto, M., 2004. Near infrared reflectance spectroscopy and multivariate analysis in enology: Determination or screening of fifteen parameters in different types of wines. *Anal. Chim. Acta* 527, 81-88.

Urbano Cuadrado, M., Luque de Castro, M., Perez Juan, P. & Gómez-Nieto, M., 2005. Comparison and joint use of near infrared spectroscopy and Fourier transform mid infrared spectroscopy for the determination of wine parameters. *Talanta* 66, 218-224.

Urtubia, A., Ricardo Pérez-Correa, J., Meurens, M. & Agosin, E., 2004. Monitoring large scale wine fermentations with infrared spectroscopy. *Talanta* 64, 778-784.

Urtubia, A., Pérez-Correa, J.R., Soto, A., Pszczólkowski, P., 2007. Using data mining techniques to predict industrial wine problem fermentations. Food control 18, 1512-1517.

Urtubia, A., Pérez-correa, J.R., Pizarro, F. & Agosin, E., 2008. Exploring the applicability of MIR spectroscopy to detect early indications of wine fermentation problems. *Food control* 19, 382-388.

Urtubia, A., Hernández, G. & Roger, J.M., 2012. Detection of abnormal fermentations in wine process by multivariate statistics and pattern recognition techniques. *J. Biotechnol*. 159, 336-341.

Vaccari, G., Dosi, E., Campi, A.L., Gonzalezvara, A., Matteuzzi, D. & Mantovani, G. 1994. A near-infrared spectroscopy technique for the control of fermentation processes—an application to lactic-acid fermentation. *Biotech. Bioeng*. 43. 913–917.

Vaidyanathan, S., Macaloney, G., Vaughan, J., McNeil, B. & Harvey, L.M., 1999. Monitoring of submerged bioprocesses. *Crit. Rev. Biotechnol*. 19, 277-316.

Van de Merbel, N., Lingeman, H. & Brinkman, U., 1996. Sampling and analytical strategies in on-line bioprocess monitoring and control. *J. Chrom. A* 725, 13-27.

Van Sprang, E.N.M., Ramaker, H.J., Westehuis, J.A., Smilde, A.K., Gurden, S.P. & Wienke, D., 2003. Near infrared spectroscopic monitoring of a series of industrial batch processes using a bilinear grey model. *Appl Spectrosc*. 57, 1007–1019.

Vilanova, M., Genisheva, Z., Masa, A. & Oliveira, J.M., 2010. Correlation between volatile composition and sensory properties in Spanish Albariño wines. *Microchem. J*. 95, 240-246.

Vojinović, V., Cabral, J.M.S. & Fonseca, L.P., 2006. Real-time bioprocess monitoring: Part I: In situ sensors. *Sens. Actuators, B* 114, 1083-1091.

Volschenk, H., van Vuuren, H.J.J. & Viljoen-Bloom, M., 2006. Malic acid in wine: Origin, function and metabolism during vinification. *S. Afr. J. Enol. Vitic*. 27, 123-136.

Whiting, G.C., 1976. Organic acid metabolism of yeasts during fermentation of alcoholic beverages– a review. *J. Inst. Brew*. 82, 84–92.

Wibowo, D., Eschenbruch, R., Davis, C., Fleet, G. & Lee, T., 1985. Occurrence and growth of lactic acid bacteria in wine: A review. *Am. J. Enol. Vitic*. 36, 302-313.

Wilson, R.H., Holland, J.K. & Potter, J., 1994. Lining up for FTIR analysis. *Chem. Br*. 30, 993-996.

Winquist, F., Holmin, S., Krantz-Rulker, C., Wide, P. & Lundstrom, I., 2000. A hybrid electronic tongue. *Anal. Chim. Acta* 406, 147–157.

Zeaiter, M., Roger, J.M. & Bellon-Maurel, V., 2006. Dynamic orthogonal projection. A new method to maintain the on-line robustness of multivariate calibrations. Application to NIR-based monitoring of wine fermentations. *Chemom. Intell. Lab. Syst*. 80, 227–235.

Chapter 3

Research Results

Bioprocess monitoring and trend identification in wine fermentations with Fourier transform infrared (FT-IR) spectroscopy and chemometric modelling

CHAPTER 3. RESEARCH RESULTS

Bioprocess monitoring and trend identification in wine fermentations with Fourier transform infrared (FT-IR) spectroscopy and chemometric modelling

Jessica Garlick[1], Maret du Toit[1], Hélène Nieuwoudt[1]

[1]Institute for Wine Biotechnology, Department of Viticulture and Oenology, Stellenbosch University, Private Bag X1, Matieland, 7602 South Africa

ABSTRACT

Wine fermentation, characterised by successive microbial-mediated reactions, is accompanied by rapidly changing biological processes. The time trajectories for alcoholic and malolactic fermentation are seldom predictable in absolute terms, and significant batch-to-batch variation is characteristic of wine production. Effective management of wine fermentations therefore requires monitoring strategies which would provide real-time graphical displays to assess the metabolic state of the process stage and to identify problematic fermentations. Infrared (IR) spectroscopy coupled to chemometric modelling is the strategy of choice, producing information rich spectra, fast accurate measurements at low cost and data that can be easily interpreted by graphical displays of the fermentation processes. The aim of this study was to evaluate the use of Fourier transform (FT) mid-infrared (MIR, 929 – 5,011 cm^{-1}) and near-infrared (NIR, 800 – 2,500 nm) spectroscopy together with various chemometric modelling techniques to quantitatively and qualitatively follow the trends of alcoholic and malolactic fermentation and to identify the stages of completion of these processes. The experimental design was set up to explore the differences and/or similarities in the fermentation trends of *Oenococcus oeni* (*O. oeni*) and *Lactobacillus plantarum* (*L. plantarum*) treatments, used in both a co-inoculation and a sequential inoculation scenario. The results obtained showed that it was possible to monitor the time course trend throughout alcoholic and malolactic fermentation with both FT-MIR and FT-NIR spectroscopy. PCA analysis confirmed this time course trend, and the main variation in the fermentations was dominated by the conversion of sugar to ethanol. No trends were observed based on the different LAB treatments. The time course trend could also be modelled by a conformity test of IR spectra alone, thereby bypassing the need for spectral interpretation. The predicted concentrations of sugars and ethanol over the duration of the fermentation were modelled by non-linear response curves and reflected the fermentation kinetics in an easily interpretable graphic display to predict the rate of

fermentations. In the particular fermentations reported here, the co-inoculated fermentations proceeded significantly faster than the sequential fermentations.

3.1 INTRODUCTION

Wine fermentation is a rapidly changing biotechnological process characterised by successive microbial-mediated reactions and can thus be considered a true bioprocess. The primary fermentation of wine, alcoholic fermentation (AF), is most commonly initiated by the yeast strain *Saccharomyces cerevisiae* in inoculated fermentations. Together with being the fundamental process whereby ethanol and CO_2 are produced from grape sugars (mainly glucose and fructose), the metabolic process of AF also contributes to, amongst other changes, the formation of aroma compounds such as higher alcohols, esters, fatty acids and aldehydes. These compounds contribute to the final chemical composition and sensory attributes of wine (Lambrechts & Pretorius, 2000). The secondary fermentation in wine, malolactic fermentation (MLF), conducted by several lactic acid bacteria (LAB), is a deacidification reaction where harsher tasting L-malic acid is converted into the softer tasting L-lactic acid and CO_2 with a simultaneous increase in pH (Margalit, 1997). Together with reducing wine acidity, MLF is used by winemakers as a means to ensure microbial stability and alter the complexity and aroma profile of some wine styles (Drici-Cachon *et al*., 1996; Lonvaud-Funel, 1999). It has become common practice to inoculate fermentations with starter cultures in order to ensure a rapid and complete fermentation with the production of desirable flavours (Krieger-Weber, 2009). Several starter cultures are commercially available and the choice of starter culture for the induction of MLF is of particular interest to the winemaker, specifically due to the various influences on the final aroma and quality.

Wine fermentations are accompanied by continuous and often rapid changes in the chemical composition of the ferment over time. The time courses for AF and MLF are seldom predictable in absolute terms, and significant batch-to-batch variation as a result of various viticultural and oenological factors, is characteristic of wine production. The time course of MLF and the metabolic products produced during MLF are known to be affected by, amongst other factors, the timing of LAB inoculation (Abrahamse & Bartowsky, 2012; Knoll *et al*., 2012) as well as by the bacterial species and/or strains used as MLF starter cultures (Pozo-Bayón *et al*., 2005; Boido *et al*., 2009; Cozzolino *et al*., 2012; Knoll *et al*., 2012).

The long established protocol of sequential inoculation involves the inoculation of starter cultures during AF or after the completion of AF, while the relatively new practice of co-inoculation involves the simultaneous inoculation for AF and MLF. Besides the practical advantage of reducing the total fermentation time (Rosi *et al*., 2003; Massera *et al*., 2009;

Abrahamse & Bartowsky, 2012), co-inoculation has shown to produce wines with different chemical compositions and aromatic profiles, compared with wines produced using sequential inoculation of LAB (Bartowsky *et al*., 2008; Abrahamse & Bartowsky, 2012; Knoll *et al*., 2012). Research has revealed significant differences in the metabolic behaviour of *Oenococcus oeni* (*O. oeni*) and *Lactobacillus plantarum* (*L. plantarum*) strains and species subsequently producing different metabolic end products (Pozo-Bayón *et al*., 2005; Lee *et al*., 2009a, b).

For this reason the modern wine industry looks for cost effective techniques which can provide real-time information about that status of fermentation processes in order to monitor the quality of the final product. Real-time analysis would provide large advantages in terms of logistical considerations as well as giving the winemaker the opportunity to identify problematic fermentations and make informed decisions about the fermentation at each specific stage of the bioprocess.

Traditional methods of fermentation monitoring involve off-line chemical analysis performed on samples removed from fermentation tanks (Vojinović *et al*., 2006). These laborious measurements result in delayed infrequent results which is inefficient for an effective real time bioprocess monitoring system. Recent developments in sensor systems including the rapid applications of on-line electronic nose and tongue techniques (Buratti *et al*., 2011) meets the demands for automisation and non-destructive real time process monitoring. Furthermore, infrared (IR) spectroscopy also offers an excellent alternative to these conventional methods for the fast non-destructive monitoring of a fermentation process (Urtubia *et al*., 2004; 2008).

IR techniques record the response of the frequencies of vibrations upon the absorption of radiation by chemical bonds of constituents (C-C, C-H, O-H, C=O and N-H) (Pavia *et al*., 2009) and subsequently establish a characteristic spectrum, seen as a unique chemical fingerprint of the sample (Stuart, 2004). Chemometric techniques involving principal component analysis (PCA) and partial least squares (PLS) regression are indispensable for the interpretation of spectral data. PLS finds correlations between the spectrum and the corresponding concentration of known constituents in the wine matrix for the future prediction of unknown samples (Naes *et al*., 2002; Esbensen, 2006).

Both Fourier transform mid-infrared (FT-MIR), 929 – 5,011 cm^{-1} and near-infrared (FT-NIR), 800 – 2,500 nm or 12,999 – 4000 cm^{-1} spectroscopic techniques have been widely recognized as fast non-destructive techniques and are frequently employed by the wine industry to quantitatively predict the concentration of wine constituents (reviewed by Bauer *et al*., 2008). The application of these spectroscopic techniques for on-line bioprocess monitoring has been made available mainly due to the rapid developments in hardware such

as fibre optic probes specifically for NIR spectroscopy as well as appropriate chemometric techniques which accompany the instrumentation (reviewed by Landgrebe *et al*., 2010).

The use of both MIR and NIR techniques for monitoring purposes are seen as complementary with both these regions providing unique advantages (Pavia *et al*., 2009). The fundamental vibrations characteristic of the MIR region yield distinct spectral features which are easier assigned to specific chemical components or compounds, than spectral bands in the NIR region (Wilson *et al*., 1994), however, the strong absorbance by water in the MIR region complicates sample preparations, especially in aqueous samples (Karoui *et al*., 2010). The complexity of the spectral data in the NIR region with characteristic weak and broad signals from overtones and combination bands makes interpretation difficult (Cen & He, 2007). NIR spectroscopy, however, requires very little sample preparation compared with MIR analysis and can penetrate deeper into samples (Bauer *et al*., 2008). It terms of on-line applications the optical materials available for MIR are expensive and are complicated by the absorptions of water in the MIR region while NIR spectroscopic techniques are easier to apply with fibre optics and cheaper more robust instrumentation is available (Vojinović *et al*., 2006).

Reports have shown the successful application of IR spectroscopy for wine fermentation monitoring, however, to our knowledge, very few studies report on the qualitative interpretation of spectral loadings and scores for monitoring the progression of red wine fermentations.

Using MIR spectroscopy and NIR spectroscopy together with chemometrics such as PCA and PLS discriminant analysis (PLS-DA) the time course of red wine fermentations have been successfully monitored and samples have been successfully classified in terms of the time point of fermentation (Cozzolino *et al*., 2006; Di Egidio *et al*., 2010; Buratti *et al*., 2011; Cozzolino & Curtin, 2012). Furthermore, reports have shown the use of data analysis techniques such as MPCA and MPLS in the prediction and early recognition of problematic fermentations in an industrial scale (Urtubia *et al*., 2007; 2008; 2012; Emparán *et al*., 2012). To our knowledge no qualitative reports have shown the ability of MIR and NIR spectroscopy to evaluate the influence of different inoculation strategies on the chemical composition of the wine matrix while only one recent study has reported the ability of MIR and NIR spectroscopic techniques to discriminate between different *O. oeni* strains (Cozzolino *et al*., 2012).

The overall objective of this study was therefore to evaluate the potential of FT-MIR and FT-NIR spectroscopy to qualitatively monitor AF and MLF. More specifically spectroscopy together with chemometrics was used to evaluate the trends of *Oenococcus oeni* (*O. oeni*) and *Lactobacillus plantarum* (*L. plantarum*) treatments in a co-inoculation and sequential inoculation strategy. Non-linear fitted graphs were used to evaluate the rate of

the different fermentations. PCA was used as a tool to identify trends in the different fermentations and inoculation strategies by providing easy interpretable graphic displays of the data. Furthermore a spectral conformity test based on IR spectra alone was used to predict the state of a fermentation process. This is a fast and easy technique bypassing the need for spectral interpretation such as PCA.

3.2 MATERIALS AND METHODS

3.2.1 BACTERIAL STRAINS

The bacterial strains and their abbreviations used in this study are listed in **Table 3.1.**

Table 3.1 Lactic acid bacterial cultures used in this study

LAB genera	Bacterial treatment	Treatment label	Producer/Source
O. oeni	S5	S5	IWBT[a]
	Lalvin VP41®	VP	Lallemand, South Africa
L. plantarum	56	56	IWBT[a]
	V22	V2	Lallemand, South Africa
O. oeni and *L. plantarum*	NT 202 Co-inoculant	MX	Anchor Yeast, South Africa
	Spontaneous[b]	CN	

[a]Institute of Wine Biotechnology (Stellenbosch University, South Africa)
[b]A fermentation not receiving any MLF inoculation. This treatment served as a control

3.2.2 EXPERIMENTAL DESIGN

3.2.2.1 SMALL SCALE VINIFICATION PROCEDURES

Vinification was carried out on the Shiraz cultivar in 2011. One and a half tonnes of grapes (Welgevallen experimental farm, Stellenbosch region, South Africa) were crushed and destemmed. The skins and juice were homogenously divided and standard red winemaking procedures were followed to assess two inoculation scenarios, namely co-inoculation and sequential inoculation. **Figure 3.1A** and **Figure 3.1B** show the experimental layout and biological triplicates for both inoculation strategies respectively.

Before the onset of AF, SO_2 was added to the must at 20 ppm. The SO_2 (total and free) (ppm) was analysed using the Metrohm titration unit (Metrohm Ltd., Switzerland). The *S. cerevisiae* strain, NT 202 (Anchor Yeast, South Africa) and the nutrient supplement GO-FERM® (inactive yeast product) (Lallemand) (0.3 g/L), were rehydrated and inoculated according to the manufacturer's specifications. AF was carried out at 25 °C. The blended yeast nutrient FERMAID K® (Lallemand) (0.3 g/L) was added on the third day of AF

according to the manufacturer's specifications. AF was considered complete at a residual sugar concentration of less than 5 g/L as predicted by the WineScan FT 120 spectrometer (FOSS Analytical A/S software version 2.2.1, Denmark, 2001). On completion of AF the wine was lightly pressed using a hydraulic press and transferred to 20 L fermentation canisters.

Freeze-dried bacterial starter cultures (0.01 g/L) were rehydrated and inoculated according to the manufacturer's specifications to initiate MLF. MLF took place at 20 °C. Co-inoculation involved the inoculation of the bacterial strains concurrently with the inoculation of the yeast starter culture, while sequential inoculation involved the inoculation of the bacterial strains after the completion of AF. The bacterial nutrient supplement OptimaloPlus (Lallemand) (0.2 g/L) was rehydrated and was added straight after LAB inoculation in the sequential inoculation strategy. MLF was regarded as complete at a malic acid concentration of less than 0.3 g/L.

After MLF, all the wines were racked and the total SO_2 levels adjusted to 80 mg/L with an average free sulphur level of ±40 mg/L. The wines were cold stabilized at -4 °C for 10 days. Prior to bottling the wines were once again racked and filtered through a K700 filter. Bottled wines were stored at 15 °C.

3.2.2.2 SAMPLING

Figure 3.2 shows the sampling carried out in this study. Samples (50 mL) were collected at different stages of the fermentation process for different analysis. During AF manual punch downs were carried out while during MLF fermentation canisters were mixed by shaking prior to sampling.

The samples were immediately used for microbial analysis and further prepared for spectral analysis in the laboratory. Samples were subsequently frozen at -20 °C until organic acid analysis could be done.

3.2.3 FT-MIR SPECTROSCOPY

Sample preparation involved filtration and subsequent degassing of samples under vacuum as described by Louw *et al*. (2009). FT-MIR spectra of the samples was generated using a WineScan FT 120 spectrometer (FOSS Analytical A/S software version 2.2.1, Denmark, 2001) equipped with a purpose-built Michelson interferometer (FOSS Analytical A/S, Hillerød, Denmark, 2001) using the validated method as described by Nieuwoudt *et al*. (2006). The samples (37 mL) were pumped through a CaF_2-lined cuvette with a fixed optical path length of 37 µm. Duplicate spectra were generated in the spectral range of 5011 - 929

cm^{-1} at 4 cm^{-1} intervals for each sample (i.e, 1056 data points per spectrum). The FT-MIR data were treated as seen in **Figure 3.2A** for further data analysis.

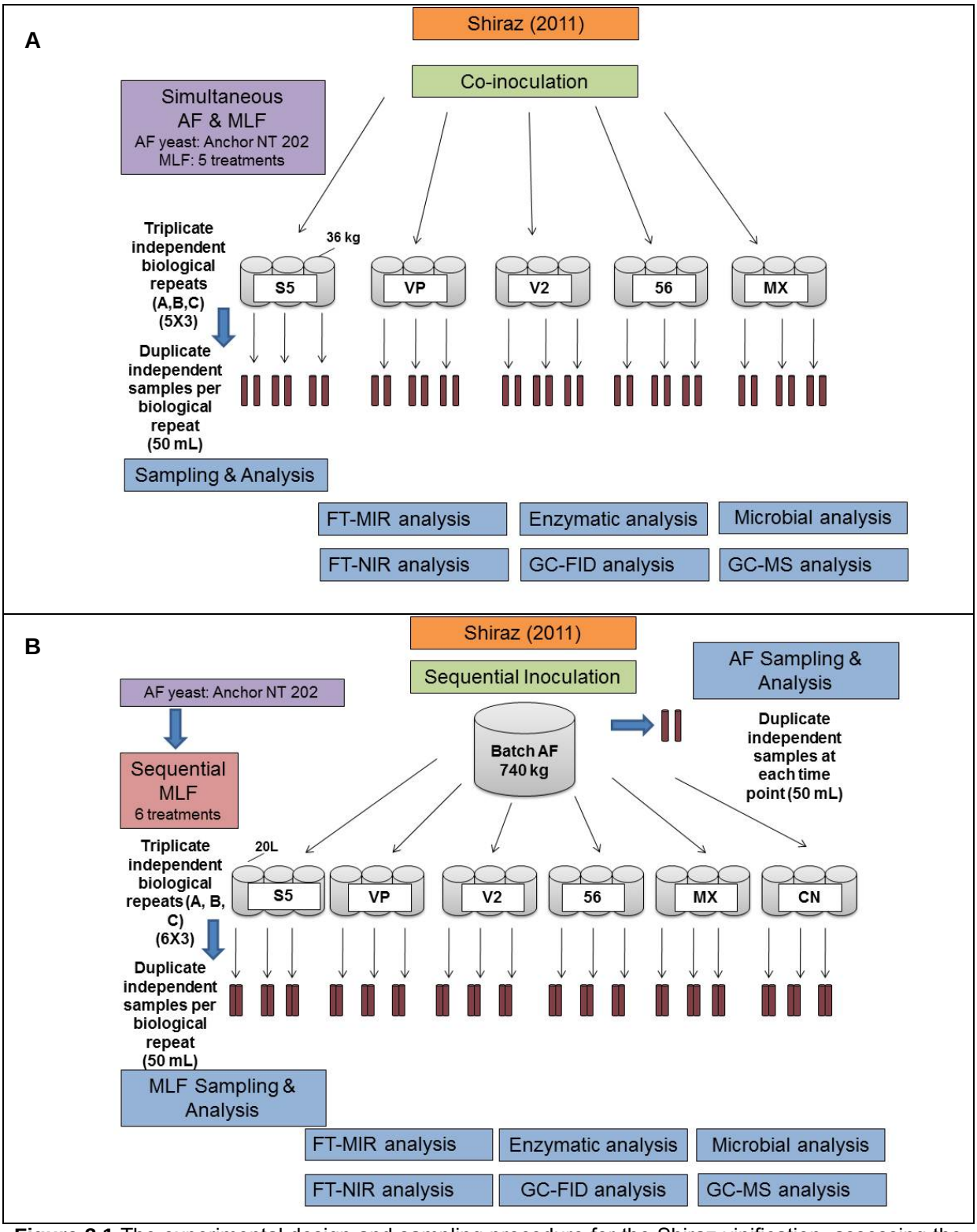

Figure 3.1 The experimental design and sampling procedure for the Shiraz vinification, assessing the two inoculation strategies **A)** co-inoculation and **B)** sequential inoculation elaborated with five bacterial strains. A spontaneous MLF (CN) (A fermentation not receiving any MLF starter culture) served as a control in this experiment. Analysis in this study involved FT-MIR, FT-NIR, enzymatic and microbial analysis. GC-FID and GC-MS analysis was carried out in the study reported in Chapter 4.

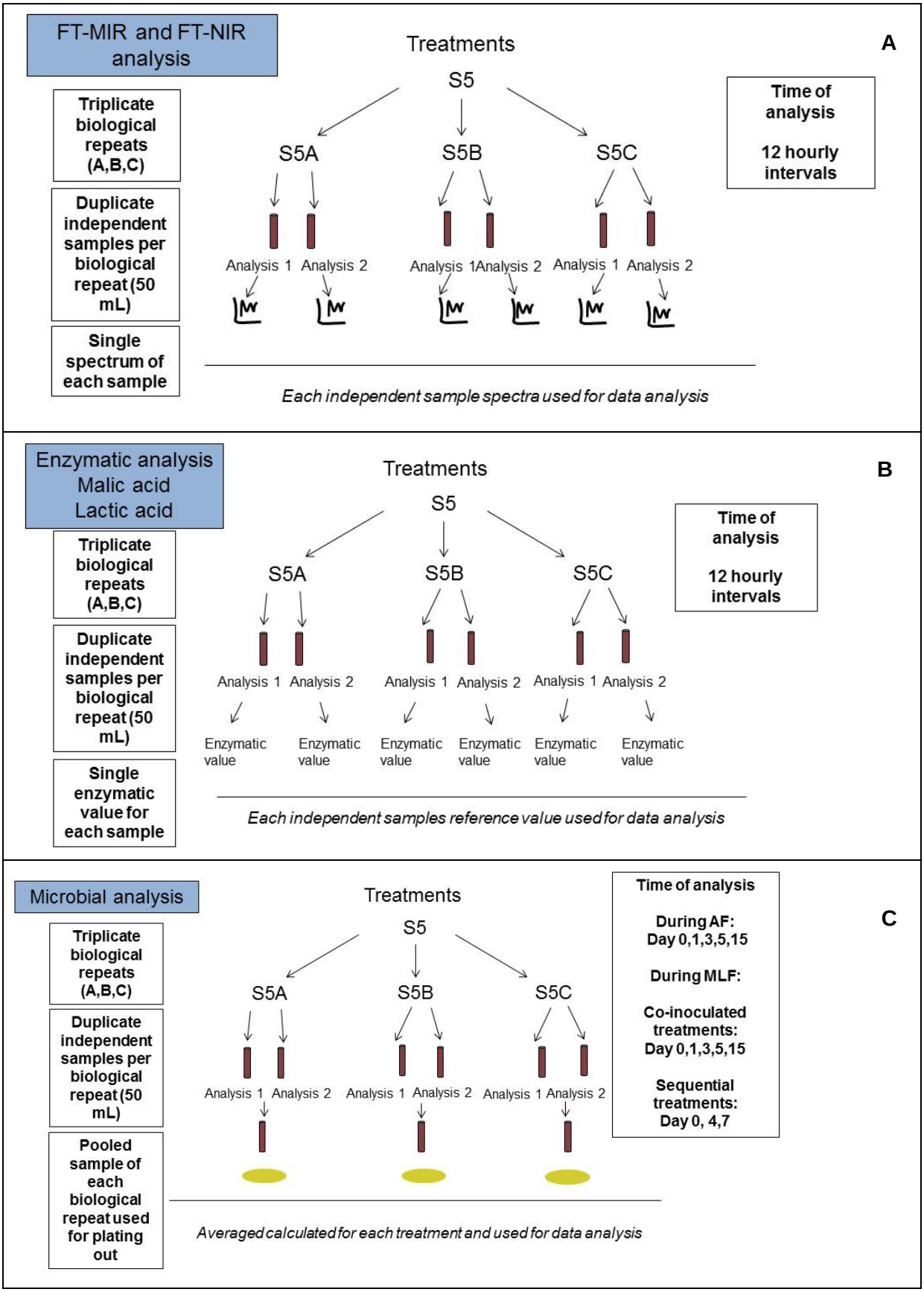

Figure 3.2 Experimental design illustrating the chemical analysis **A)** FT-MIR and FT-NIR spectroscopy, **B)** enzymatic reference analysis and **C)** microbial analysis and further data handling using treatment S5 as an example. All the LAB treatments were handled in the same way. Yellow dots represent the plates for microbiological analysis.

3.2.4 FT-NIR SPECTROSCOPY

NIR spectral data were generated on the samples using a FT-NIR spectrometer (MPA, Multi Purpose FT-NIR analyser instrument, Bruker Optics, Ettlingen, Germany) equipped with OPUS software version 6.5 (Bruker Optics, Ettlingen, Germany). The spectral data were collected over the range 12,499 – 3,999 cm^{-1} in transmission mode using a quartz cuvette with a 1 mm path length. Samples were scanned at a resolution of 8 cm^{-1} at a controlled temperature (21 °C±2 °C). Each spectrum is based on an average of 16 repeat scans (air background). The FT-NIR data were treated as shown in **Figure 3.2A** for further data analysis.

3.2.5 QUANTIFICATION OF ROUTINE WINE PARAMETERS

Malic acid and lactic acid were quantified using the established in-house enzyme-linked assay on the automated Arena konelab 20 XT Photometric analyser (Part number: 984163, Thermo Electron Oy, Finland) as reported in **section 5.2.3 in Chapter 5**. **Figure 3.2B** shows the handling of the enzymatic data for further data analysis.

Existing in-house PLS calibration models (Magerman, 2009) were used to predict the routine wine parameters including ethanol (% v/v), reducing sugars (RS) (g/L), glucose (g/L) and fructose (g/L), titratable acidity (expressed as g/L tartaric acid), pH and volatile acidity (expressed as g/L acetic acid) from the MIR spectra using the WineScan FT 120 instrument (FOSS Analytical A/S software version 2.2.1, Denmark, 2001).

3.2.6 MICROBIAL ANALYSIS

The evolution of microflora (yeast and LAB) was monitored throughout AF and MLF (**Figure 3.2C**). A ten-fold dilution series of the wine sample was made in sterile distilled water and 100 µL was plated out on selective media. Plating out was done on MRST for the analysis of *O. oeni* while MRS agar was used for the analysis of other wine LAB. Yeast growth was monitored using YPD Agar plates.

MRST plates contained 50 g/L De Man, Rogosa and Sharpe (MRS; Biolab, Merck, Wadeville, Gauteng) and 20 g/L Bacteriological agar (Biolab, Merck) which was supplemented with 10% preservative free tomato juice (All Gold, South Africa) adjusted to a pH of 5.0 using hydrochloric acid (HCl). MRS plates contained 50 g/L MRS broth (Biolab, Merck) and 15 g/L Bacteriological agar (Biolab, Merck). Both media contained 50 mg/L Delvocid Instant (DSM Food Specialties, The Netherlands) dissolved in 1mL of sterile dH_20 to prevent yeast growth and 25 mg/L kanamycin sulphate (Roche Diagnostics GmbH, Mannheim, Germany) dissolved in 1mL of sterile dH_20 to suppress the growth of acetic acid bacteria. YPD plates contained 70 g/L yeast peptone dextrose agar and contained 50 mg/L

Chloramphenicol dissolved in 1mL of 96% ethanol to prevent bacterial growth as well as 25 mg/L kanamycin sulphate (Roche Diagnostics GmbH, Mannheim, Germany) dissolved in 1mL of sterile dH_20.

MRST and MRS agar plates were anaerobically cultivated using Microbiology Anaerocult pads in anaerobic jars (Merck, Darmstadt, Germany) for approximately 7 to 10 days at 30 °C whereas the YPD agar plates were kept in an aerobic environment for approximately 3 days at 30 °C.

3.2.7 DATA ANALYSIS

In order to determine the rate of the different fermentations, the major AF parameters were modelled using non-linear response curves in the Statistica software (version 10, StatSoft Inc., Tulsca, USA) according to the general sigmoidal regression equation (Motulsky & Christopoulos, 2003):

$$Y=Bottom + (Top-Bottom)/(1+10^{[(EC50-X)*HillSlope)]} \quad (3.1)$$

Where, X is the time in days, Y is the response concentration, Top is the maximum response parameter, Bottom is the baseline response parameter and HillSlope is the slope of the regression. The EC 50 parameter characterised the time taken (in days) for each treatment to reach half the complete utilisation or production for a specific compound.

The regression coefficient (R^2) was used to quantify the goodness of fit of the regression to the data. Confidence intervals ($p<0.05$) determined whether significant differences were present between the different treatments over time, based on the EC 50 parameter.

PCA was applied to the spectral data as an exploratory tool (Esbensen, 2006) to evaluate trends in the fermentation process using The Unscrambler® X software (version 10.2, Camo, Nedre Vollgate, Norway). PCA provides an excellent tool for the visual interpretation of the data therefore allowing us to identify difference or similarities between the different LAB treatments and inoculation strategies. All spectral data sets were mean centred. No spectral pre-processing was used for the MIR spectral data. NIR spectral pre-processing evaluated first derivative and standard normal variate (SNV) as well as multiplicative scatter correction (MSC).

Qualitative conformity models (**as detailed in Chapter 2 section 2.4.4.4**) based on FT-MIR and FT-NIR spectral data were established using the OPUS software version 6.5 (Bruker Optics, Ettlingen, Germany) to test deviations from certain defined limits. These limits were established using reference spectra depicting the end of AF. Based on standard

deviations alone test spectra taken at regular time intervals throughout the fermentation were tested for their conformity to the reference spectra in order to predict the end of AF. The interactive region selection and spectral pre-processing techniques provided by the OPUS software were evaluated to produce the best possible model. These conformity tests provide a fast, easy tool to predict the state of processes without requiring spectral interpretations.

3.3 RESULTS AND DISCUSSION

3.3.1 QUANTITATIVE MONITORING OF FERMENTATIONS

Quantitative monitoring of the small scale Shiraz fermentations involved monitoring the routine wine parameters as well as microbial analysis.

3.3.1.1 MONITORING OF ROUTINE WINE PARAMETERS

MONITORING SUGAR DEGRADATION AND ETHANOL PRODUCTION

The quantified values for sugars and ethanol obtained from the existing MIR PLS models on the WineScan FT 120 instrument (FOSS Analytical A/S software version 2.2.1, Denmark, 2001) were used to monitor AF. **Figure 3.3** shows the sugar degradation (RS) and ethanol production of the raw data plotted over time (hours) for both the inoculation strategies.

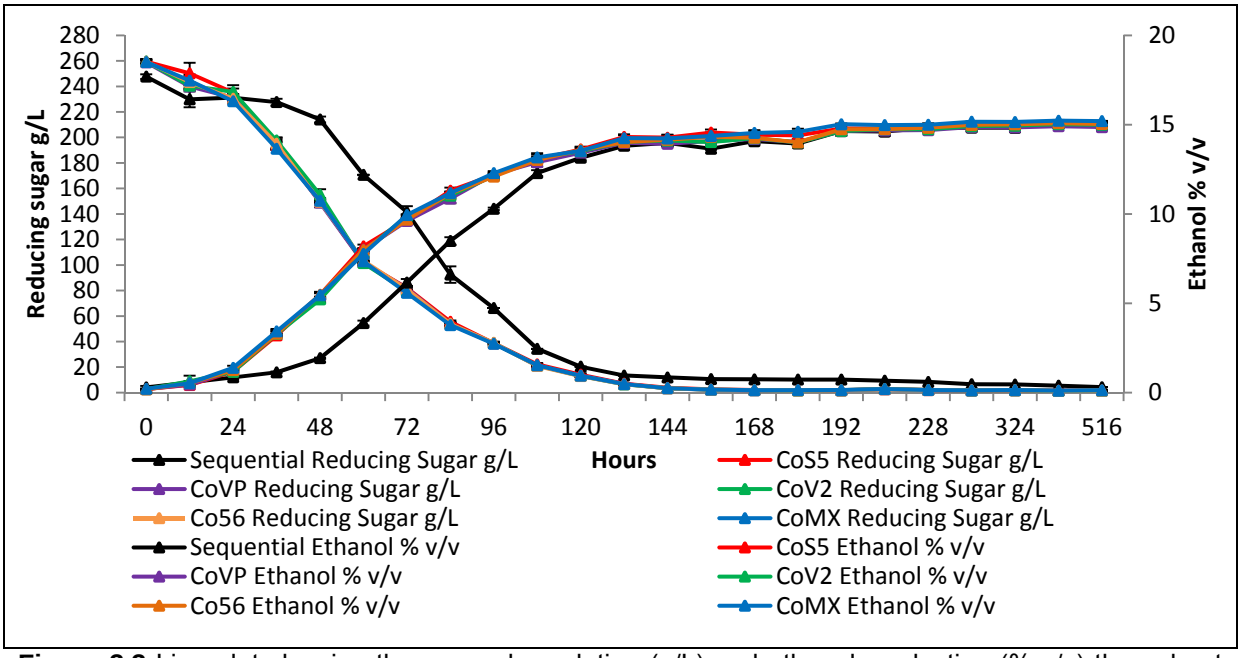

Figure 3.3 Line plot showing the sugar degradation (g/L) and ethanol production (% v/v) throughout AF fermentation for both the inoculation strategies. Each value represents the average of triplicate repeats. Co refers to the different co-inoculation strategy treatments.

The initial RS concentration ranged between 247 to 259 g/L at the beginning of the fermentation (**Figure 3.3**). At the beginning of AF the sequential tank had a lower RS concentration compared with the co-inoculated treatments. A certain degree of biological variation is already visible at this stage of fermentation. The ethanol concentration at the end of the alcoholic fermentation was approximately 15 % v/v for all the treatments. AF of the co-inoculated treatments was complete at 144 hours of the fermentation whereas the sequential tank had a RS of approximately 11.86 g/L at this point. The sequential tank experienced a slight stuck or sluggish fermentation from 144 hours with residual fructose still present. The sequential tank was seen as dry at 516 hours of AF (**Figure 3.3**). These treatment differences clearly show batch-to-batch variation in terms of the time trajectories of AF which is indicative of biological fermentation processes (Jørgensen *et al*., 2004).

The non-linear response curves obtained by fitting data of the routine wine parameters according to the non-linear regression **equation 3.1** are shown in **Figure 3.4**.

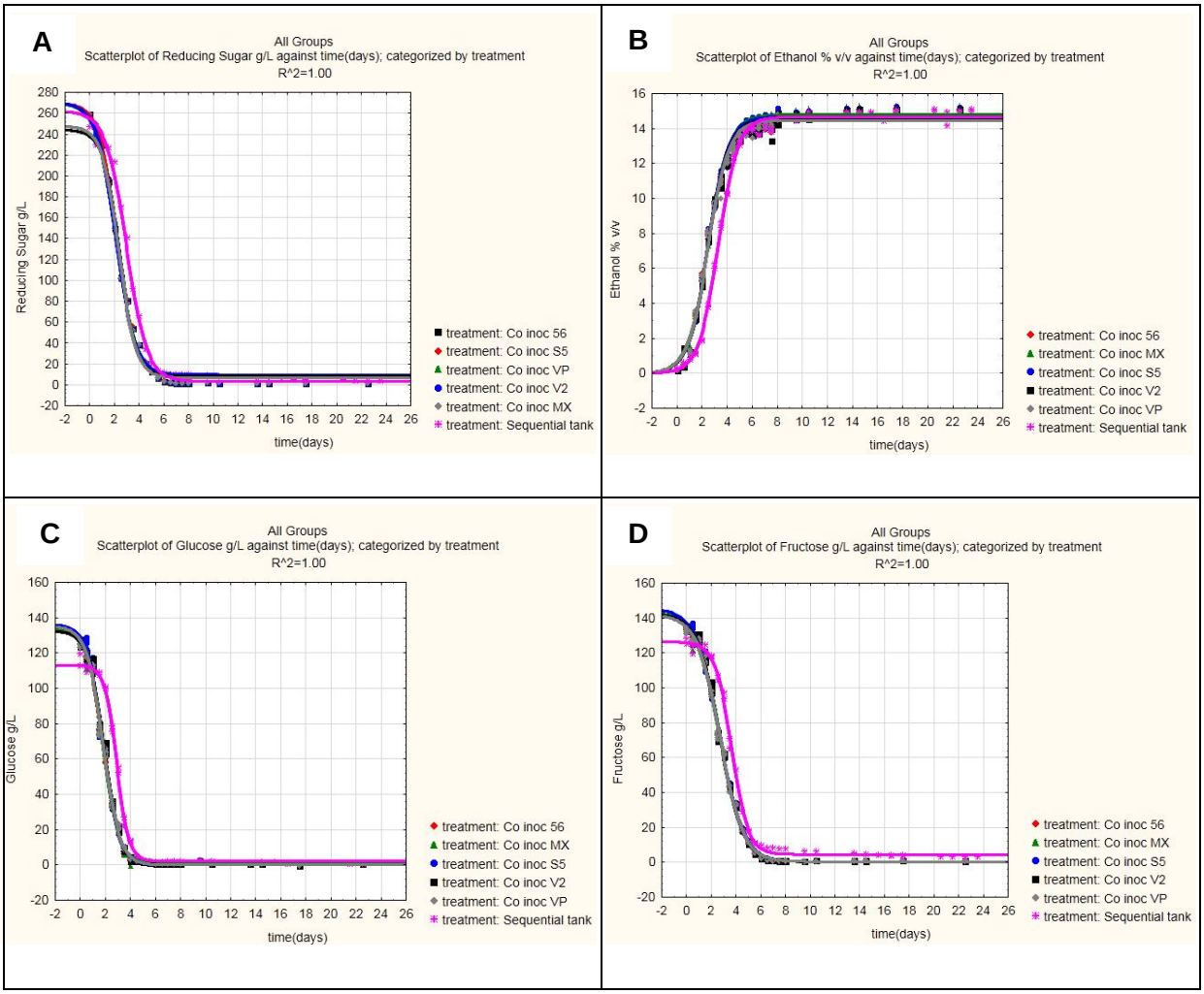

Figure 3.4 Non-linear response curves modelling the fermentation kinetics of **A)** reducing sugar (g/L), **B)** ethanol (% v/v), **C)** glucose (g/L) and **D)** fructose (g/L) for both the inoculation strategies. Co inoc refers to the different co-inoculation strategies.

Equation 3.1 fits well to the quantified data with an R^2 value of 1 in all cases (**Figure 3.4**). The time taken for each treatment to reach half the complete utilisation or production of a fermentation parameter, relating to the rate of fermentation (EC 50 parameter) was calculated and is reported in **Table 3.2**. The significant differences ($p<0.05$) between the treatments in terms of the EC 50 parameter is shown in **Figure 3.5**.

Table 3.2 The EC 50 parameter value (in days) for glucose, fructose, reducing sugars and ethanol.

Treatment	Glucose	Fructose	Reducing Sugar	Ethanol
S5	1.841	2.681	2.227	2.497
VP	1.832	2.726	2.159	2.495
V2	1.896	2.725	2.118	2.499
56	1.817	2.717	2.401	2.499
MX	1.809	2.677	2.365	2.519
Sequential	2.901	3.651	2.972	3.295

The co-inoculated treatments all had similar efficiency's in terms of their conversion of sugars to ethanol (**Figure 3.5**). Significantly different rates between the co-inoculated treatments and the sequential treatment were, however, observed for RS, ethanol, glucose and fructose (**Figures 3.5A, 3.5B, 3.5C and 3.5D**). The degradation of RS and production of ethanol was faster in the co-inoculated treatments compared to that of the sequential treatment (**Figures 3.5A and 3.5B**). The co-inoculated treatments took on average two and a half days to degrade half the RS and reach half the completion of ethanol production whereas the sequential tank took on average three days (**Table 3.2**).

The techniques used to monitor these fermentations, specifically the non-linear fitted graphs clearly showed more subtle differences between the fermentation treatments. This is of major relevance in industrial applications where the identification of even the smallest deviations are necessary for effective monitoring purposes to ensure consistency and product quality.

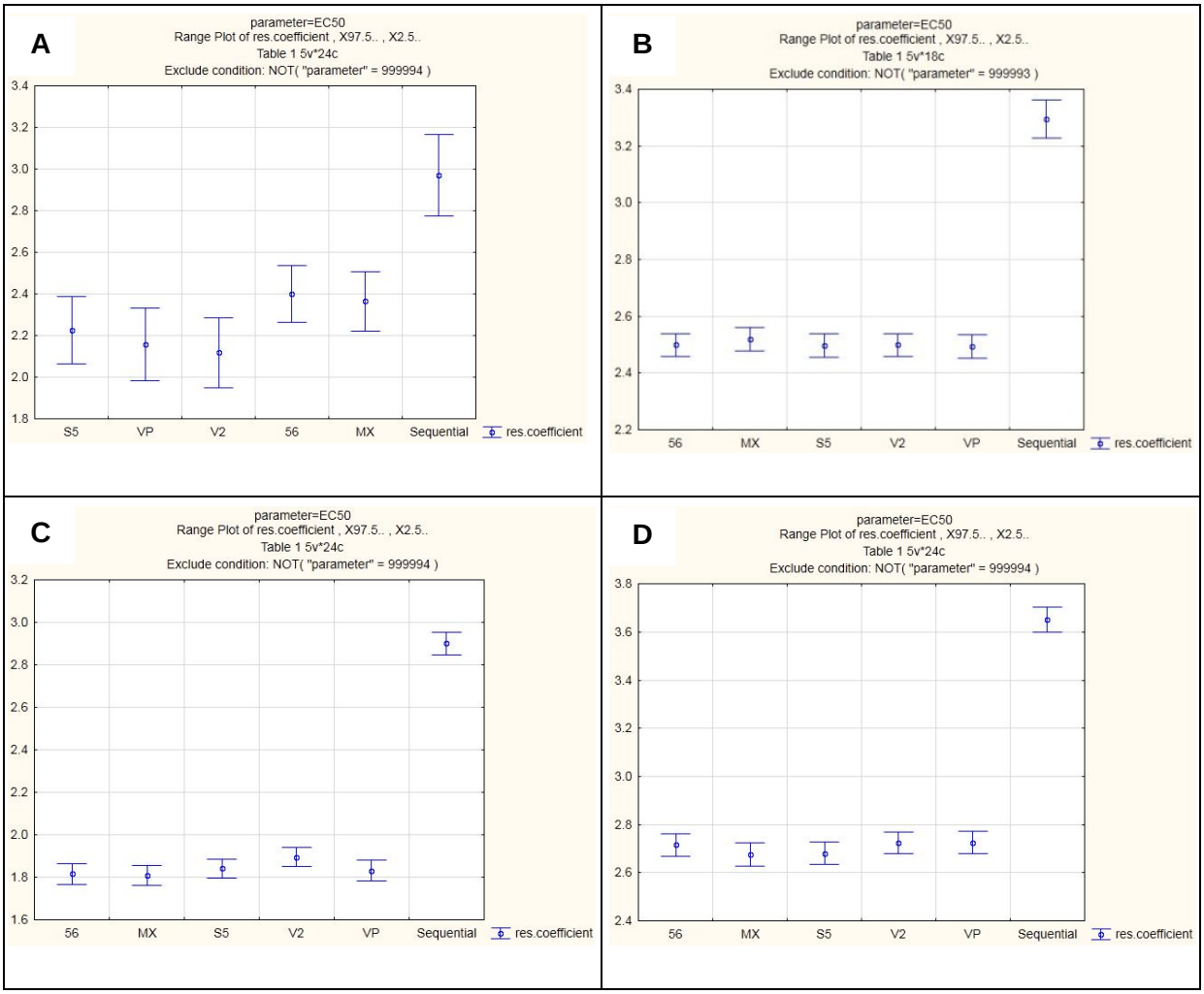

Figure 3.5 Estimate bars showing 95% confidence intervals for **A)** reducing sugar (g/L), **B)** ethanol (% v/v), **C)** glucose (g/L) and **D)** fructose (g/L) for each fermentation treatment in terms of the EC 50 parameter. The treatment labels depict the co-inoculated treatments while sequential refers to the sequential tank.

MONITORING VOLATILE ACIDITY, pH AND TITRATABLE ACIDITY

Titratable acidity (expressed as g/L tartaric acid), pH and volatile acidity (expressed as g/L acetic acid) monitored during fermentation are reported in **Table 3.3** for both the inoculation strategies. These parameters are critical quality parameters used during fermentation monitoring and it was therefore necessary to monitor these parameters throughout AF and MLF. **Figure 3.6** shows the trends observed over time for these parameters.

Table 3.3 The average quantified values for titratable acidity (expressed as g/L tartaric acid), pH and volatile acid (expressed as g/L acetic acid) obtained during AF and MLF showing both inoculation strategies.

Treatment	Co-inoculation				Sequential inoculation			
Titratable acidity	**Start AF**	**End AF**	**Middle MLF**	**End MLF**	**Start AF**	**End AF**	**Middle MLF**	**End MLF**
S5	3.63	3.96	4.15	3.41	3.86	3.53	3.20	2.92
VP	3.64	3.81	3.73	3.41	3.86	3.53	3.16	2.91
V2	3.75	4.14	3.92	3.39	3.86	3.53	3.28	2.89
56	3.66	4.19	3.95	3.45	3.86	3.53	3.33	2.90
MX	3.71	4.03	3.92	3.39	3.86	3.53	3.33	2.89
CN					3.86	3.53	3.43	2.90
pH								
S5	3.86	3.68	3.59	3.75	3.86	3.84	3.90	3.93
VP	3.86	3.68	3.70	3.78	3.86	3.84	3.90	3.93
V2	3.85	3.64	3.68	3.82	3.86	3.84	3.88	3.92
56	3.85	3.64	3.70	3.73	3.86	3.84	3.87	3.93
MX	3.85	3.66	3.68	3.78	3.86	3.84	3.88	3.94
CN					3.86	3.84	3.85	3.93
Volatile acid								
S5	0.21	0.15	0.14	0.25	0.21	0.28	0.33	0.40
VP	0.19	0.14	0.15	0.28	0.21	0.28	0.32	0.40
V2	0.19	0.13	0.19	0.28	0.21	0.28	0.31	0.40
56	0.18	0.14	0.22	0.28	0.21	0.28	0.31	0.41
MX	0.20	0.15	0.16	0.28	0.21	0.28	0.33	0.41
CN					0.21	0.28	0.30	0.41

A gradual decrease was noticed in the titratable acidity for all the treatments from the beginning of AF to the end of MLF (**Figure 3.6A**). This corresponds to the fact that MLF is a known de-acidification reaction (Lee *et al*., 2009b). The titratable acidity of the co-inoculated treatments did, however, first increase during AF after which the decrease was observed. A bigger decrease in titratable acidity was noticed in the sequential treatments (~0.9 g/L) from the beginning of AF to the end of MLF compared to the co-inoculated treatments (~0.3 g/L). The sequential treatments had a lower titratable acid concentration (~2.9 g/L) than the co-inoculated treatments (~3.41 g/L) at the end of MLF (**Figure 3.6A**)

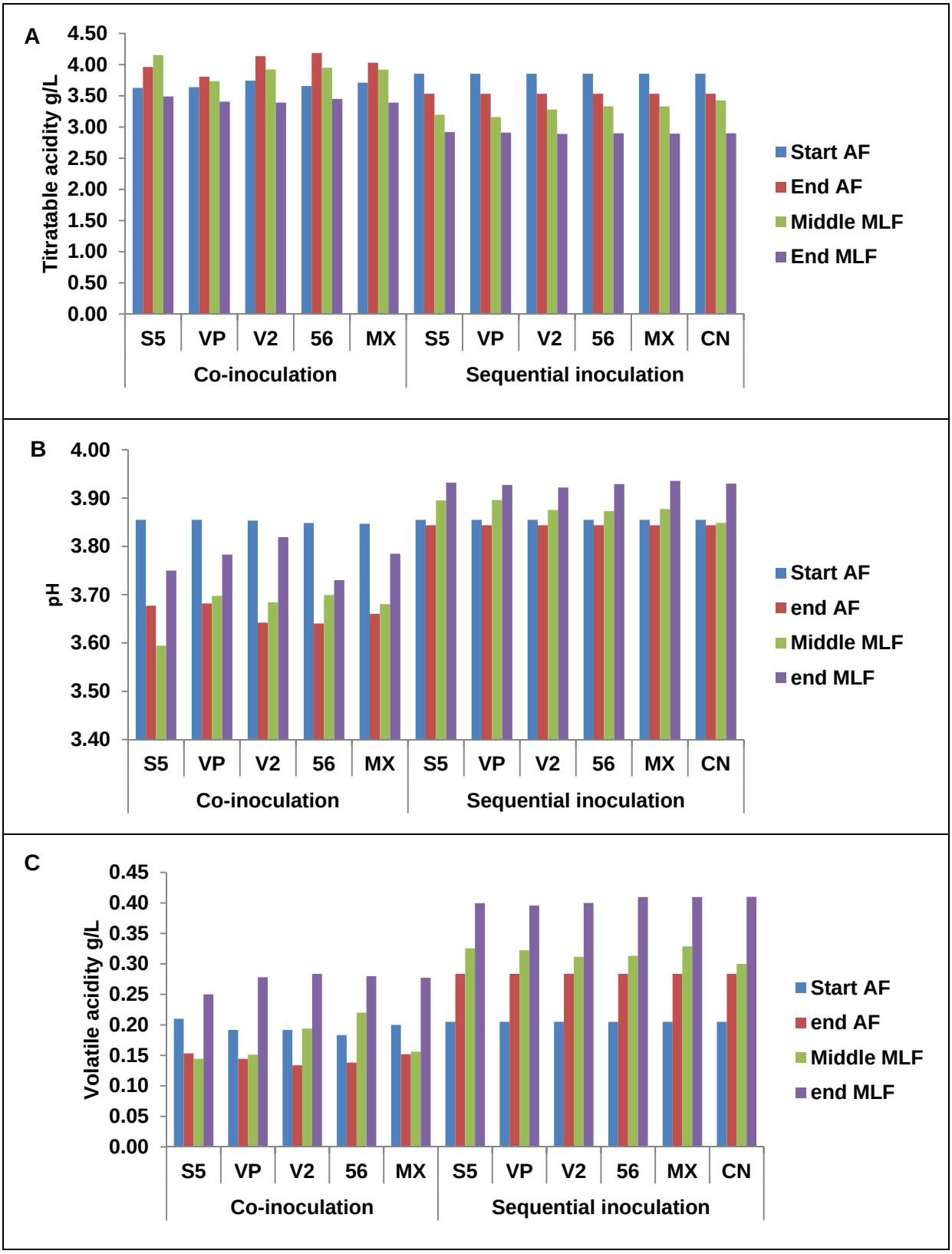

Figure 3.6 Bar graphs showing **A)** titratable acidity (g/L), **B)** pH and **C)** volatile acidity (g/L) over time for both the inoculation strategies. Each value represents the average of triplicate repeats.

The co-inoculated treatments showed a drop in pH by 0.19 units during AF while the pH of the sequential treatments remained relatively constant (**Figure 3.6B**). An increase in pH of

approximately 0.1 units was seen for all the treatments during MLF which corresponds to previous literature (Margalit, 1997), however, the pH for the co-inoculated treatments at the end of MLF was lower than that observed at the beginning of AF. The co-inoculated treatments had a lower final pH at the end of MLF compared to that of the sequential treatments (**Figure 3.6B**).

There was an expected increase in the volatile acidity concentration following MLF for all the treatments (**Figure 3.6C**) due to either the metabolism of residual sugars or citric acid metabolism (Lee *et al*., 2009b). No significant differences were noticed in terms of the increase in volatile acidity for all the treatments from the end of AF to the end of MLF. The values for the co-inoculated treatments increased on average by 0.14 g/L whereas the increase by the sequential treatments was on average 0.12 g/L. Although the change in concentration was comparable for all the treatments, the sequential treatments had a higher volatile acidity concentration at the end of MLF of 0.4 g/L compared to the co-inoculation treatments which had an average concentration of 0.28 g/L at the end of MLF. Despite speculations that co-inoculation can result in an increase in the acetic acid concentrations and subsequently the volatile acidity (Knoll *et al*., 2012), the results of this study show that the inoculation regime didn't have an effect on the amount of volatile acidity produced. This corresponds to results found by Abrahamse & Bartowsky (2012).

MONITORING MALIC ACID AND LACTIC ACID

The quantified values for organic acids (malic acid and lactic acid) (g/L) obtained using the automated Arena Konelab 20 XT photometric analyser (Thermo Electron Oy, Finland) were used to monitor the stage of completion of MLF. Malic acid is a critical indicator for the completion of MLF and for this reason it was monitored throughout fermentation. LAB are also known to have different metabolic rates of malic acid degradation (Lee *et al*., 2009a). For this reason it was important to evaluate rate of malic acid degradation and the subsequent production in lactic acid for the different LAB treatments in this study as well as evaluate if the inoculation scenario influenced their metabolic rates. **Figure 3.7A** and **Figure 3.7B** shows the malic acid degradation and lactic acid production respectively for the co-inoculated treatments while **Figure 3.8A** and **Figure 3.8B** reports the trends in malic acid degradation and lactic acid production respectively in the sequential treatments.

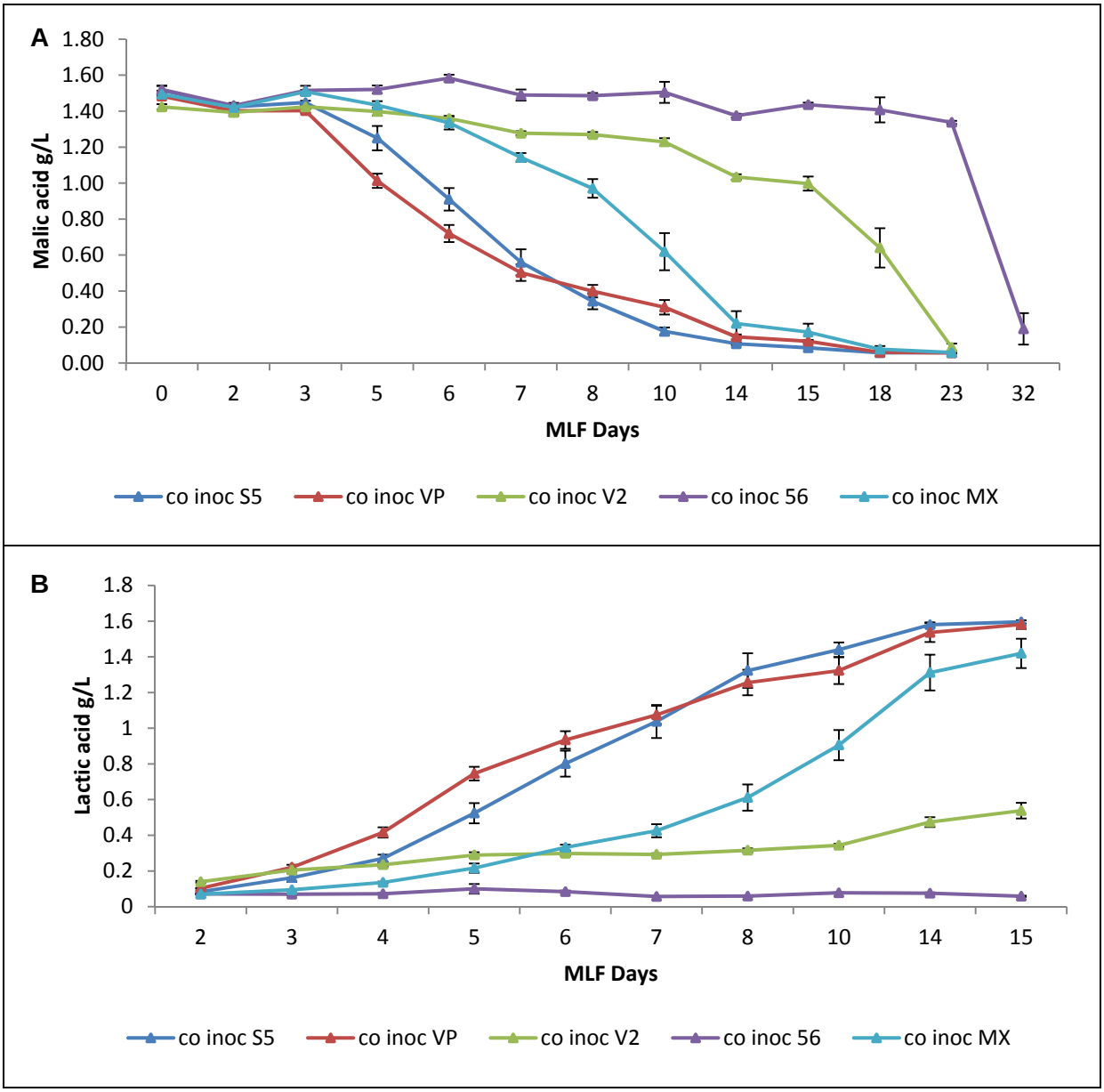

Figure 3.7 Line graph showing **A)** the degradation of malic acid and **B)** the production of lactic acid during MLF for the co-inoculated treatments. Each value represents the average of triplicate repeats.

The malic acid concentration at the beginning of MLF ranged between 1.42 and 1.52 g/L for the co-inoculated treatments (**Figure 3.7A**). The lactic acid content at day two of MLF ranged between 0.07 and 0.14 g/L (**Figure 3.7B**).

The degradation of malic acid in the co-inoculated treatments shows significant differences between all the bacterial strains (**Figure 3.7A**). The *O. oeni* strains showed the best performance in the co-inoculation scenario with S5 and VP completing MLF within 10 and 14 days respectively. Treatment MX finished MLF within 14 days. The fermentation kinetics show that treatment MX had a slow degradation of malic acid between day 0 and day eight with a rapid degradation noticed between days eight to 14. Treatments S5, VP and MX all showed a sigmoidal trend in the degradation of malic acid. The *L. plantarum*

strains, however, took much longer to complete MLF. *L. plantarum* strain, V22 completed MLF in 23 days. The trend seen for the degradation of malic acid in this treatment differed from the sigmoidal trend noticed in the other treatments. *L. plantarum* strain, 56 was the least efficient strain in the co-inoculation scenario in terms of malic acid degradation and eventually completed MLF in 32 days. The degradation of malic acid by treatment 56 was mainly seen between day 23 and 32.

The treatment trends observed for lactic acid production (**Figure 3.7B**) corresponds to the treatment trends observed for malic acid degradation. With this said, however, malic acid degradation isn't the only source for lactic acid production in a wine fermentation (Pronk *et al*., 1996). A significant difference in the lactic acid concentration was observed between treatments S5, VP and MX compared to treatments V2 and 56 at day 15 of MLF. This is due to the fact that treatments V2 and 56 had not completed MLF by day 15 as reported. Treatments S5, VP and MX all had completed MLF at this stage and had similar lactic acid concentrations of 1.6 g/L,1.6 g/L and 1.5 g/L respectively. Treatment V2 showed a very slow production of lactic acid from day 0 to day 15 producing approximately 0.5 g/L. Treatment 56 showed no production of lactic acid between day 0 and 15 which corresponds to the absence of malic acid degradation reported during this time.

The malic acid concentration at MLF day 0 for all the sequential strains was lower than those reported for the co-inoculated treatments and ranged from 0.95 g/L to 1.26 g/L (**Figure 3.8A**). This is due to the fact that malic acid would have been degraded to a certain extent by yeast metabolism during AF.

The malic acid degradation observed in the sequential inoculated treatments showed significant differences between the bacterial strains (**Figure 3.8A**). The trends were similar to the trends observed in the co-inoculated treatments. The treatments showed the biggest difference in their malic acid values at MLF day 8. Treatment S5 and VP once again showed a rapid rate of degradation in malic acid from day 0 to day 14 followed by MX, V2 and 56 in that order. All the sequential treatments, however, completed MLF by day 14.

The treatment trends observed for lactic acid production in the sequential treatments (**Figure 3.8B**) corresponds to the treatment trends observed for malic acid degradation. The treatments showed the biggest difference in their lactic acid values at MLF day five. All the sequential treatments had similar lactic acid values at the end of MLF (day 14) which ranged from 1.27 to 1.30 g/L. The lactic acid concentrations reported for the sequential treatments were considerably lower than those reported for the co-inoculation treatments on the same day.

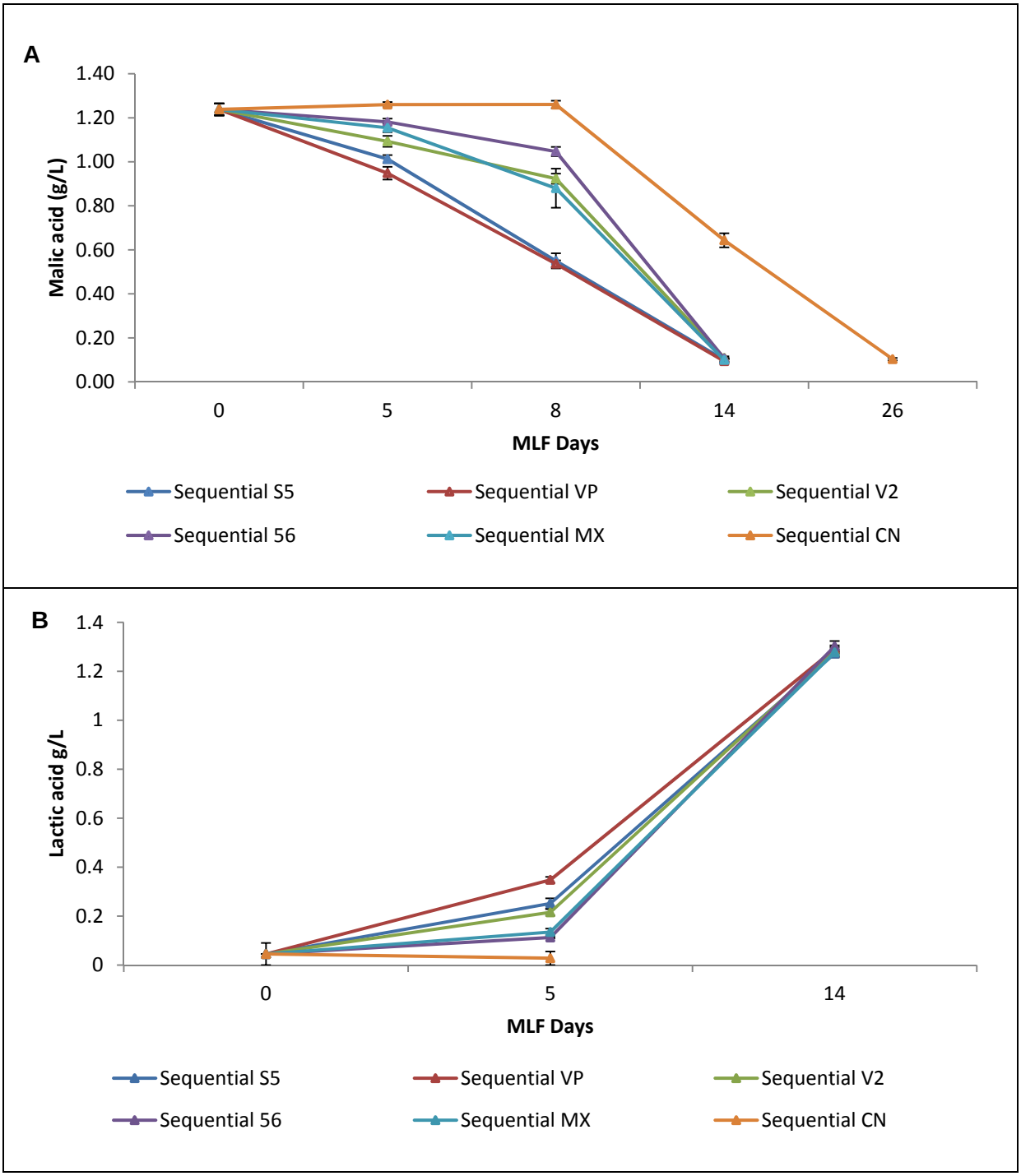

Figure 3.8 Line graph showing **A)** the degradation of malic acid and **B)** the production of lactic acid during MLF for the sequential treatments. Each value represents the average of triplicate repeats.

The spontaneous control (CN) was considered separately. No degradation in malic acid was observed for treatment CN from day 0 to day eight of MLF (**Figure 3.8A**). The spontaneous control degraded malic acid much slower than the other treatments and subsequently took 26 days to complete MLF. No lactic acid production was recorded for the control treatment between day 0 and five of MLF. Furthermore no other data was recorded for this treatment.

The organic acid values reported in this study correspond to the concentrations found in wine by other authors (Moreira & Santos, 2005). In this study MLF seemed to be more efficient in the sequential inoculation taking 14 days from the onset of MLF. However, it is known that co-inoculation greatly reduces the fermentation time due to the faster onset of MLF (Abrahamse & Bartowsky, 2012). Definite treatment differences were noticed in both the co-inoculated and sequential treatments showing expected differences in malic acid metabolism for each specific bacterial strain. The main reaction during MLF is the degradation of L- malic acid into the softer L-lactic acid by the malolactic enzyme produced by LAB (Lerm *et al*., 2010). The rate of malic acid degradation by LAB is highly correlated to the enzyme activity of the bacterial cell (Bartowsky, 2005). The *O. oeni* strains, VP, S5 as well as MX showed to be the most efficient treatments in this particular study. This corresponds with previous research stating that *O. oeni* is the dominant LAB isolated from MLF (du Toit *et al*., 2011). With this said, however, the *L. plantarum* strains, V22 and 56 both completed MLF.

3.3.1.2 MICROBIOLOGICAL ANALYSIS

YEAST ANALYSIS

From a microbiological point of view AF was monitored through the analysis of yeast cell numbers (cfu/mL) over time. **Figure 3.9** shows the evolution of yeast cfu/mL for both inoculation strategies.

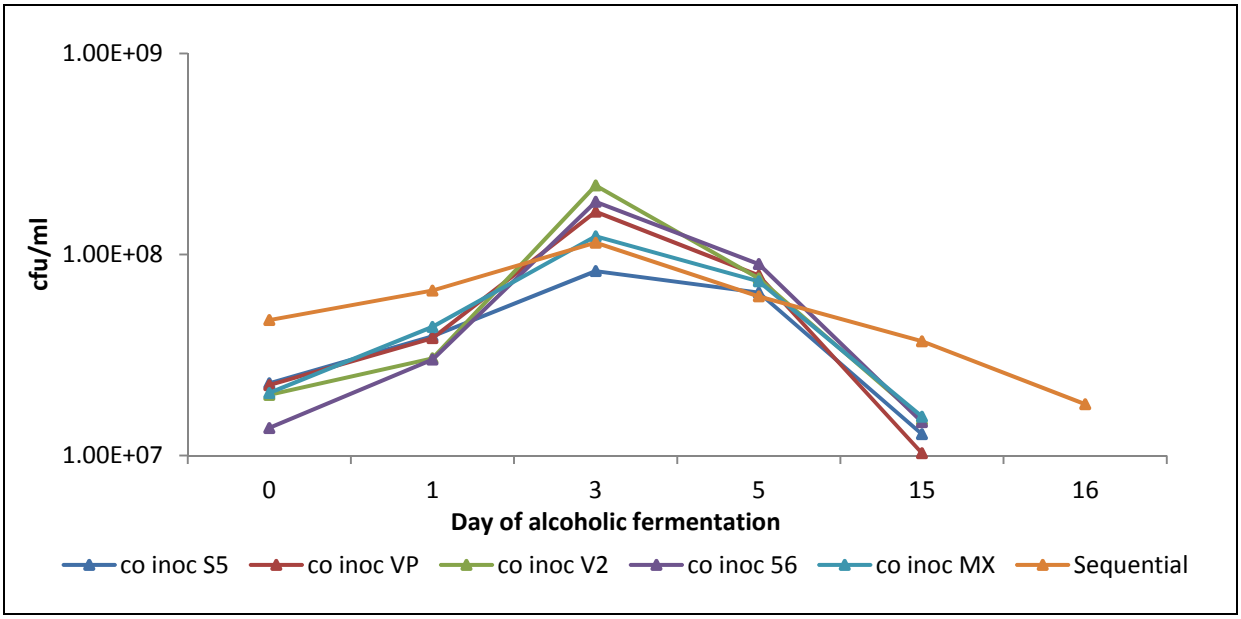

Figure 3.9 Line graph showing the evolution of yeast cell numbers (cfu/mL) as recorded throughout AF for the co-inoculated and sequential inoculated treatments. Each value represents the average of triplicate repeats. co inoc refers to the different co-inoculation strategies.

All the treatments were adequately inoculated for AF with yeast counts greater than 10^6 cfu/mL (**Figure 3.9**). The co-inoculated treatments were inoculated at approximately $1x10^7$ to $2x10^7$ cfu/mL whereas the sequential tank had a substantially higher cell count of $4x10^7$ cfu/mL upon inoculation. The higher inoculation of yeasts in the sequential tank could be a reason why the RS was lower in the sequential tank at the beginning of the fermentation to that of the co-inoculated treatments.

The yeast counts (cfu/mL) (**Figure 3.9**) showed the same growth pattern for all the treatments. An increase was noticed in the biomass formation of all the treatments with the growth phase being most prominent between day one and three of AF. The highest yeast cell count of approximately 10^8 cfu/mL was reached at day three of the fermentation.

The inoculation strategy showed no significant difference in terms of the yeast growth rate. The co-inoculation of bacteria with yeast had no antagonistic effects on the rate of yeast growth.

BACTERIAL ANALYSIS

Microbial analysis during MLF monitored the evolution of LAB (cfu/mL) over time. **Figures 3.10A and 3.10B** shows the bacterial counts (cfu/mL) of the co-inoculated and sequential treatments respectively during MLF.

All the co-inoculated treatments were efficiently inoculated at approximately $1x10^6$ to $4x10^6$ cfu/mL (**Figure 3.10A**). The sequential treatments were, however, inoculated at a lower dosage with the sequential treatment MX inoculated at a substantially lower amount (**Figure 3.10B**).

All the bacterial treatments in both the inoculation strategies followed the typical growth of LAB during fermentation (**Figures 3.10A and 3.10B**). The *L. plantarum* strains V22 and 56 showed the same tendency to decrease in cell numbers (cfu/mL) in the first four days of fermentation (**Figures 3.10A and 3.10B**). This corresponded to the slower degradation of malic acid reported for these strains. However, it was expected that *L. plantarum* 56 would have had much lower cell numbers (cfu/mL) due to its extremely slow degradation of malic acid. The cell numbers (cfu/mL) of the *O. oeni* treatments S5 and VP, however, increased over this period corresponding to the reported efficiency of these strains in the malic acid degradation. The initial decrease in bacterial numbers seen in treatment MX in the co-inoculated scenario is typical of the *L. plantarum* strain in wine fermentation conditions (**Figure 3.10A**). The increase in cell numbers from day three is possibly be due to the *O. oeni* strain which dominates most of the fermentation especially in higher alcohol environments (**Figures 3.10A and 3.10B**).

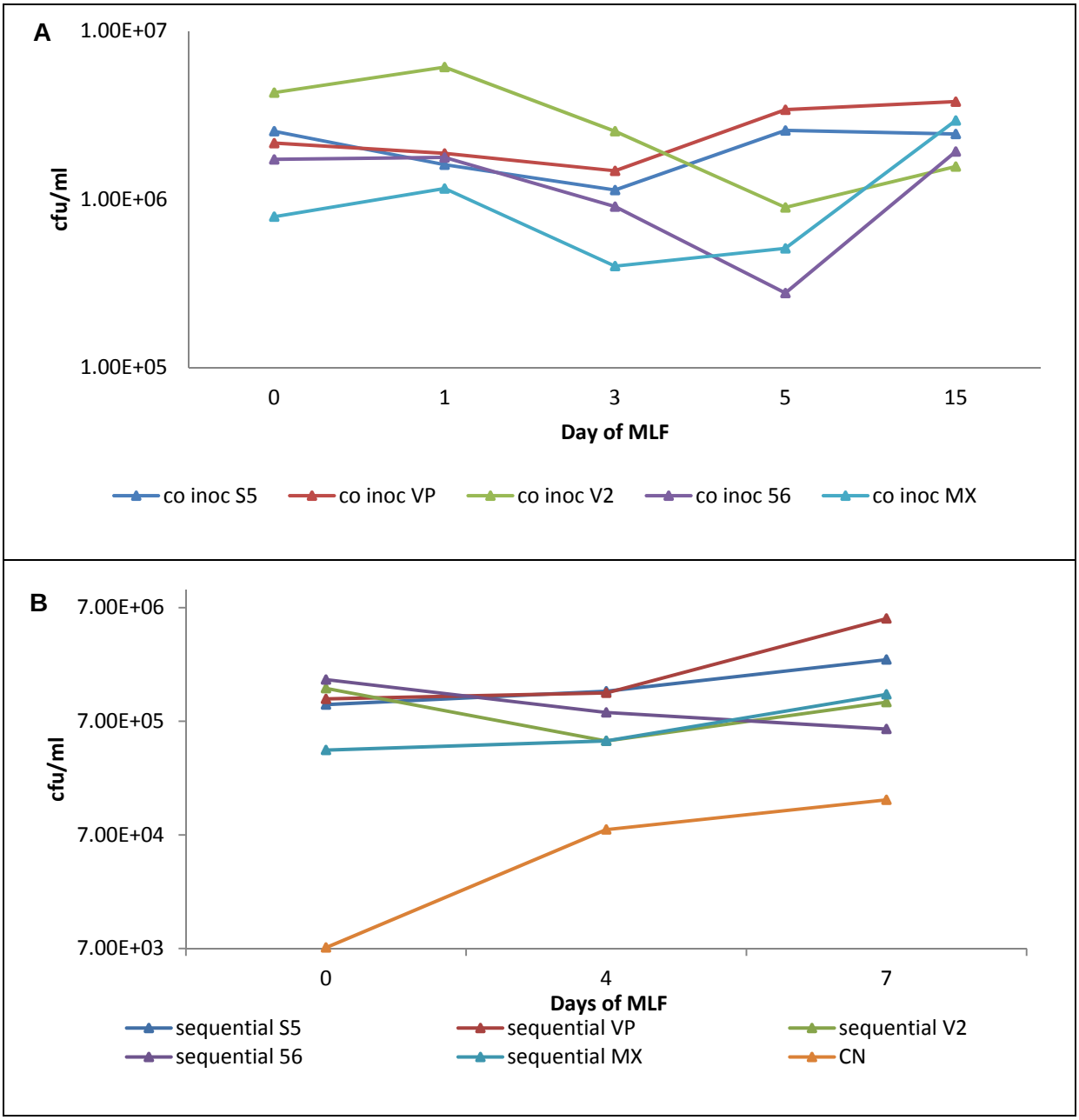

Figure 3.10 Line graph showing the evolution of LAB (cfu/mL) as recorded throughout MLF for the **A)** co-inoculated and **B)** sequential treatments. Each value represents the average of triplicate repeats.

The control (**Figure 3.10B**) had substantially lower bacterial values throughout the fermentation compared to the other treatments as no inoculation of bacteria was carried out in this treatment. Malic acid degradation previously observed was slow in this treatment as the natural flora needed time to increase.

3.3.2 QUALITATIVE APPROACH TO FERMENTATION MONITORING

The qualitative monitoring of the Shiraz fermentations involved the interpretation of the FT-MIR and FT-NIR spectra as well as using PCA analysis for trend identification. This qualitative approach will evaluate how valuable the spectral data is for monitoring purposes without the use of quantitative data.

3.3.2.1 TREND IDENTIFICATION USING FT-IR SPECTRA

FT-MIR SPECTRA

Figure 3.11A shows the change in the FT-MIR spectrum (5011 - 929 cm^{-1}) over the course of the fermentation using day 0 (inoculation of yeast and bacteria) and day 23 of the co-inoculated treatment V2 as an example.

Although the entire MIR spectral range (5011 - 926 cm^{-1}) was scanned for each sample at each sampling time point (**Figure 3.11A**) it is clear that the MIR spectrum is dominated by intense absorption at wavenumbers 1698 - 1582 cm^{-1} and wavenumbers in the region 3627 – 2971 cm^{-1}. These wavenumber regions are characterised by the intense absorbance by water. The region from 3627 cm^{-1} onwards contains very little useful information (Patz *et al*., 2004). After the removal of these "noise" regions, further data analysis included only wavenumbers regions: 1582 - 965 cm^{-1}, 2006 – 1698 cm^{-1} and 2971 - 2701 cm^{-1} (**Figure 11B**).

The visual inspection of the FT-MIR spectrum clearly shows changes at specific spectral ranges which are related to the time course of the fermentation. Most of the spectroscopic variation was observed around the region 1500 – 960 cm^{-1} as well as the region from 2900 – 2700 cm^{-1} (**Figure 3.11B**). The former region known as the "fingerprint region" is particularly important in providing information about particular C-O, C-C, C-H and C-N bonds which produce characteristic IR bands in this region (Stuart, 2004). The observed variation included a broad range of several hundred wavenumbers but could also be attributed to single wavenumbers where individual prominent peaks were present.

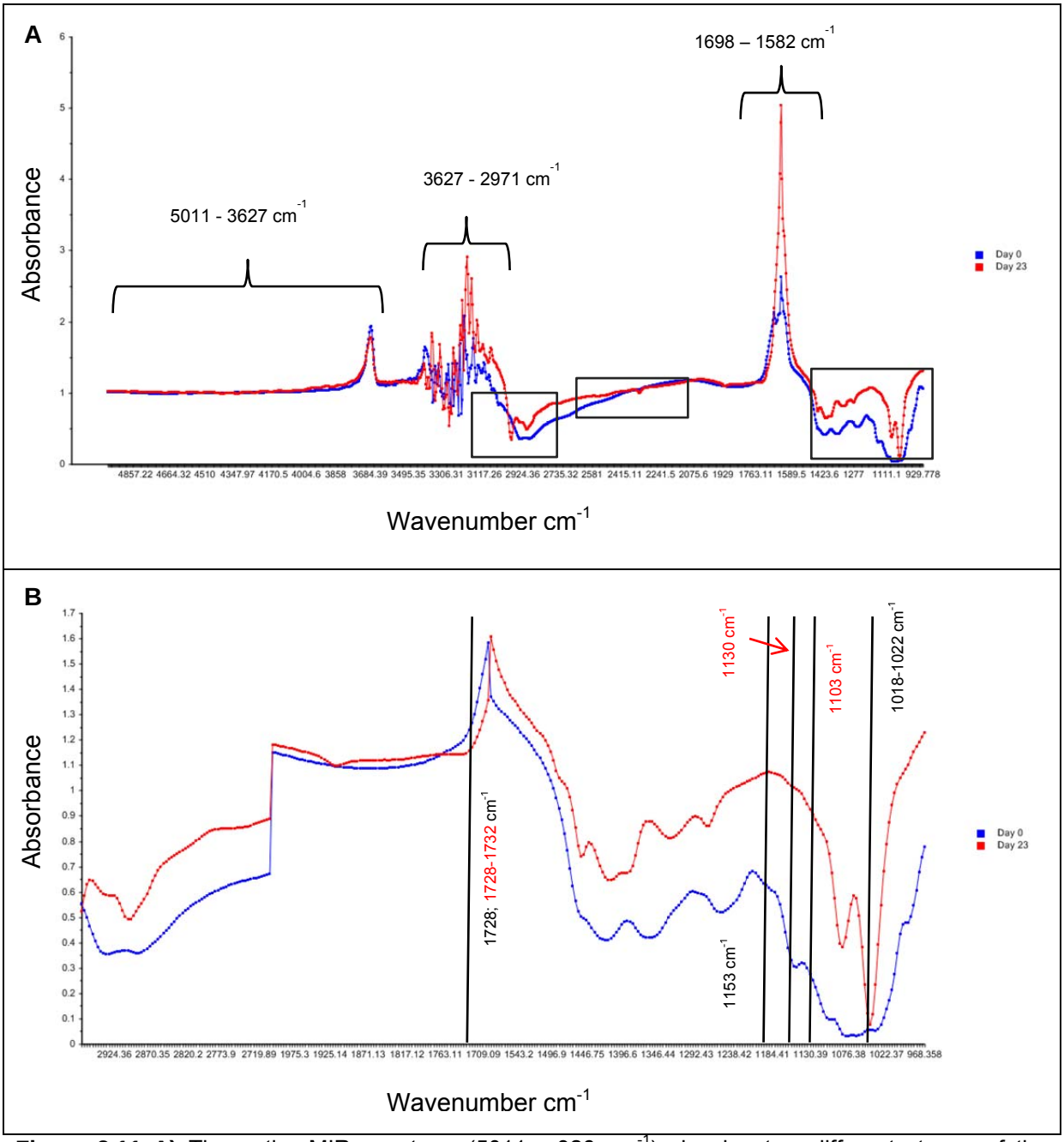

Figure 3.11 A) The entire MIR spectrum (5011 - 926 cm^{-1}) showing two different stages of the fermentation (day 0 and 23). Boxed areas include the wavenumber regions which were used in B and **B)** The MIR spectrum excluding bracketed wavenumber regions shown in A (noise regions due to the absorption of water and insignificant information). Vertical lines indicate the filters which collectively explained 73% and 88% of the variation in malic acid (black wavenumbers) and lactic acid (red wavenumbers) respectively (**See Table 5.5 in Chapter 5**).

Changes related to fermentation time are characterised by prominent peaks at the end of fermentation (day 23) at wavenumbers 1045 cm^{-1} and 1084 cm^{-1} (**Figure 3.11B**) related to the absorption by the C-O and C-C bands of primary alcohols and organic compounds produced during fermentation (Smith, 1999; Stuart, 2004). Characteristic peaks associated with sugars include the C-O stretch for fructose and glucose at 1060 cm^{-1} and 1030 cm^{-1}

respectively (Bevin *et al*., 2008). The contribution of the C-H stretch of ethanol at day 23 is also observed between wavenumbers 2960 – 2850 cm^{-1} (**Figure 3.11B**). The bands present between 3300 - 2500 cm^{-1} are also characteristic of the broad intense O-H stretching band as well as the weaker C-H stretching band of carboxylic acids (Silverstein *et al*., 1991). In addition, spectral bands found in the region 1760 – 1690 cm^{-1} contain information relating to the C=O stretching bands of carboxylic acids, aldehydes and esters (Stuart, 2004).

MIR calibration work discussed in **Chapter 5 section 5.3.2** allowed for the evaluation of the wavenumber regions which were highly correlated to the prediction of malic acid and lactic acid. Collectively, more than 73% and 88% of the variation in malic acid and lactic acid content of the samples respectively could be correlated to the absorbance at the filters shown in **Figure 3.11B** (**See Table 5.5 in Chapter 5**). These filters corresponded to prominent spectral peaks visually observed in the MIR spectrum (**Figure 3.11B**). The most prominent filters for malic acid were at 1728 cm^{-1}, 1018 cm^{-1} to 1022 cm^{-1} and at 1153 $cm^{-1,}$ in this order. For lactic acid the filters were present at 1130 cm^{-1}, 1103 cm^{-1} and from 1728 cm^{-1} to 1732 cm^{-1} in this order.

The selection of filters in this study show clear differences between the two organic acids. This could be due to the fact that these compounds are found in different concentrations in the fermenting must and wine matrix (Moreira & Santos, 2005).

The filter at wavenumber 1728 cm^{-1} explaining the highest variation of malic acid can be attributed to the absorption of the C=O stretch band of carboxylic acids (Silverstein *et al*., 1991). This result corresponds to that of work done by Moreira & Santos (2005). In this study the filter at wavenumber 1728 cm^{-1} is a common filter between the two organic acids, however, it is the most important filter for the determination of malic acid. The C=O functional group is of less importance when calibrating for organic acids present at smaller concentrations, such as lactic acid (Moreira & Santos, 2005).

The wavenumber at 1103 cm^{-1} found to be highly correlated to lactic acid in this study corresponds to this work done by Picque *et al*. (1993). Sivakesava *et al*. (2001) showed high correlation bands at wavenumber regions 2950 - 2800 cm^{-1} and 1800 - 1625 cm^{-1} for lactic acid.

FT-NIR SPECTRA

Figure 3.12 shows an example of a typical raw FT-NIR spectrum (12, 000 – 3,999 cm^{-1}) of fermenting must and wine over the course of the fermentation using day one and day 15 of the co inoculated treatment V2.

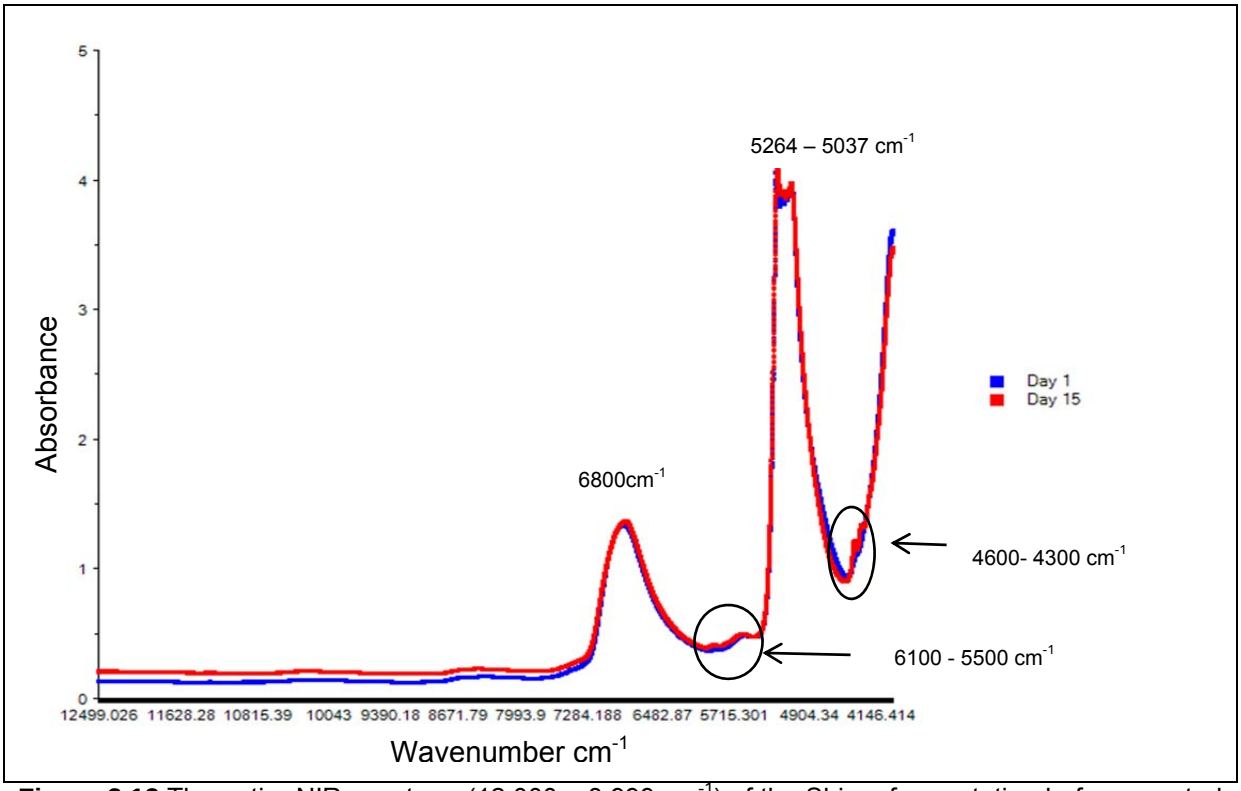

Figure 3.12 The entire NIR spectrum (12,000 – 3,999 cm^{-1}) of the Shiraz fermentation before spectral transformation showing two different stages of fermentation (day 1 and 15). Circles show the wavenumber regions where visual variation was observed.

The visual evaluation of the entire raw NIR region (12,000 – 3,999 cm^{-1}) (**Figure 3.12**) shows dominant absorption bands at 6800 cm^{-1} and 5264 – 5037 cm^{-1} for both time points which are related to the first overtone of the O-H stretch of water and a combination of stretch and deformation of the OH group in water and ethanol respectively (Dambergs *et al*., 2002; Cozzolino *et al*., 2004; 2006; Liu *et al*., 2006). Changes related to the fermentation time were visually observed in the spectral regions 4600 – 4300 cm^{-1} and 6100 - 5500 cm^{-1} (**Figure 3.12**). The wavenumber regions 5264 – 5037 cm^{-1} and 4055 - 3999 cm^{-1} were regarded as noise regions and were subsequently removed from the NIR spectrum before further spectral interpretation and subsequent spectral pre-processing.

The transformation of the spectra by first derivative results in spectral peaks where the original spectra had a maximum slope and zero crossing points at peaks in the original spectrum. SNV also corrects for multiplicative scatter effects by centring and scaling each individual spectrum (Naes *et al*., 2002). The visual inspection of **Figure 3.13** clearly shows that the first derivative and SNV transformation reduced the scatter and additive baseline effects and exposed the important spectral information. The variation at spectral regions 4600 – 4300 cm^{-1} and 6100 - 5500 cm^{-1} was subsequently more prominent in the transformed spectra using first derivative and SNV (**Figure 3.13**). More prominent

differences over time are noticed at these specific wavenumber regions where a succession of alternate maxima and minima are observed in the transformed spectra.

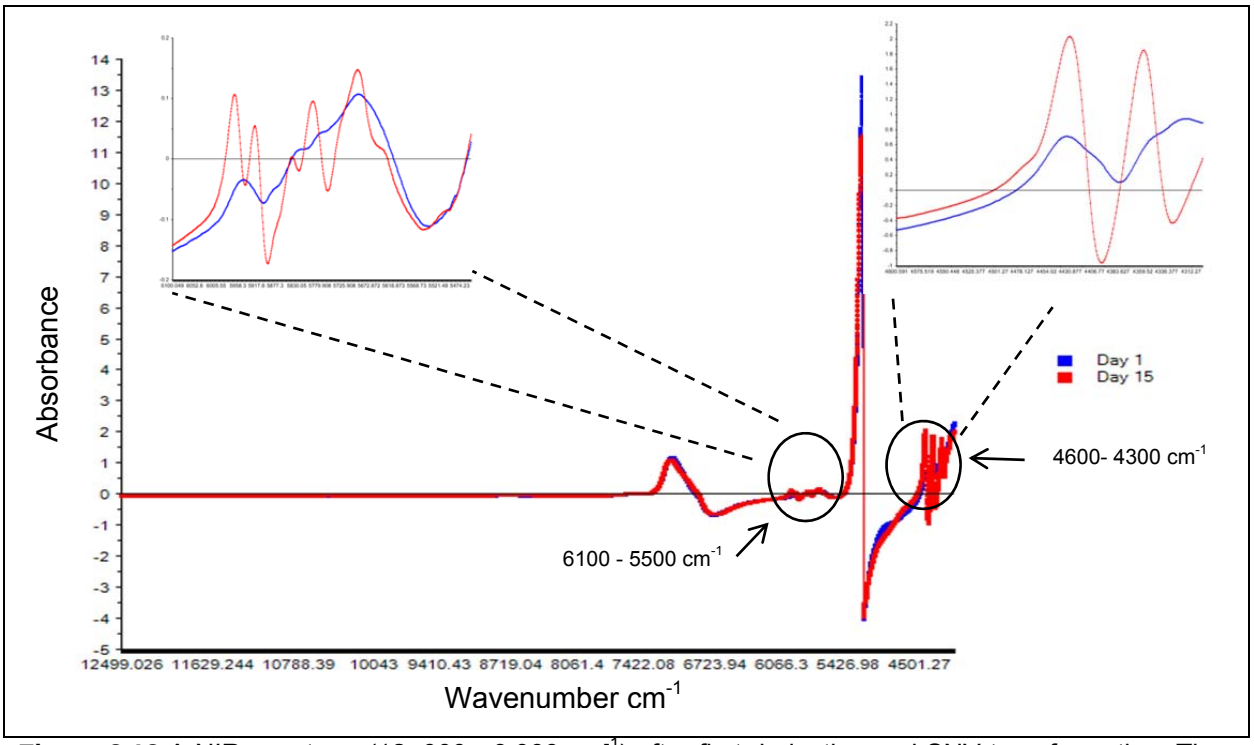

Figure 3.13 A NIR spectrum (12, 000 - 3,999 cm^{-1}) after first derivative and SNV transformation. The noise region (5264 - 5037 and 4055 - 3999 cm^{-1}) was removed before spectral pre-processing. Insert: wavenumber region 6100 - 5500 cm^{-1} and 4600 - 4300 cm^{-1} after first derivative and SNV transformation.

The visual inspection of the NIR spectra transformed by MSC (**Figure 3.14**) showed a slight improvement of the NIR spectra with the removal of baseline scatter, however, the variation over time wasn't as prominent as the transformation with first derivative and SNV (**Figure 3.13**).

The variation observed in the region 4600 – 4300 cm^{-1} (**Figures 3.13 and 3.14**) over time is most likely due to the degradation of sugar and the subsequent production of ethanol over time in the fermentation (Cozzolino *et al*., 2004; 2006). The peaks observed in this wavenumber region were assigned to the CH-stretch and the CH-deformation combination from the CH_3 and CH_2 group of ethanol which increased in concentration throughout fermentation (Dambergs *et al*., 2002; Cozzolino *et al*., 2006). Peaks in this region also correspond to the absorption of C-H stretching and C=O combination band of carbohydrates and O-H and C-O from glucose (Di Egidio *et al*., 2010). Changes observed in the region 6100 - 5500 cm^{-1} correspond to the CH-stretch first overtones of CH_3 and CH_2 groups (Dambergs *et al*., 2002; Cozzolino *et al*., 2004; 2006). The absorption peak at 5900 cm^{-1} is

related to the C-H stretch first overtones associated with sugars and ethanol (Dambergs *et al*., 2002; Liu *et al*., 2006; Di Egidio *et al*., 2010).

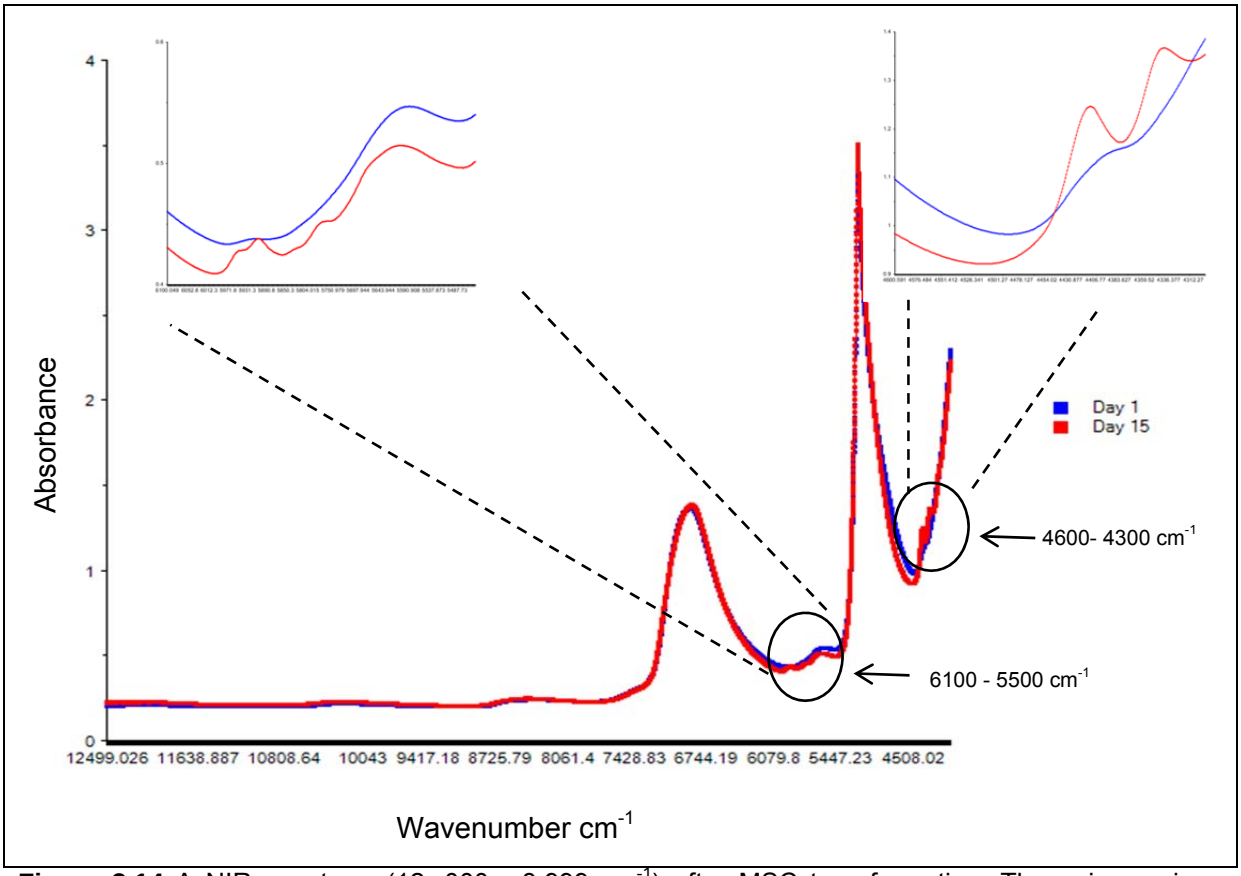

Figure 3.14 A NIR spectrum (12, 000 - 3,999 cm^{-1}) after MSC transformation. The noise regions (5264 - 5037 and 4055 - 3999 cm^{-1}) were removed before spectral pre-processing. Insert: Region 6100 - 5500 cm^{-1} and 4600 - 4300 cm^{-1} after MSC transformation.

NIR calibration work discussed in **Chapter 5 section 5.3.2** allowed for the evaluation of the wavenumber regions which were highly correlated to the prediction of malic acid and lactic acid. Unlike MIR calibrations these were not individual wavenumbers but rather combinations of wavenumbers together with a specific spectral pre-processing technique.

The wavenumber region 6100 – 5449 cm^{-1} transformed by first derivative and SNV was proposed as the most suitable combination for constructing the calibration models for lactic acid using the OPUS QUANT 2 optimization software (**Figure 3.13 insert**). The combination of the wavenumber regions 7500.2 – 5449.2 cm^{-1} and 4600.6 – 4291.1 cm^{-1} transformed by MSC produced a model with comparable results (**Figure 3.14 insert**). For the malic acid calibration model the wavenumber region 6100 – 5449 cm^{-1} transformed by MSC was proposed as the most suitable combination yielding the most optimum results (**Figure 3.14 insert**).

Due to the complexity of the must and wine matrix as well as the complexity of band assignment in the NIR region of the electromagnetic spectrum, it is a difficult task to ascertain why these relatively large wavenumber regions were used for the calibration models of carboxylic acids namely, malic acid and lactic acid. However, it is clear that these regions do correlate to the spectral variation visually observed in the raw and transformed NIR spectra of this study. However, it is known that the C-H stretch, O-H stretch, C-O stretch and C=O stretch overtones of carboxylic acids have characteristic peaks in the region 7500 – 5449 cm^{-1} (Shenk *et al*., 2008). These wavenumber regions therefore certainly do include the absorption bands for carboxylic acids like malic acid and lactic acid.

The work carried out by other authors showed good correlations between NIR and lactic acid determination. Work by Sivakesava *et al*. (2001) showed good correlations using the wavenumber region 14, 285 – 6250 cm^{-1}. Urbano Cuadrado *et al*. (2005) showed that the biggest absorbance differences in the NIR region were noticed at wavenumber regions 25,000 – 9090 cm^{-1} as well as at 5235 – 5102 cm^{-1}.

A FT-IR spectrum illustrates the collective absorbance of all the IR active components present in a sample and is subsequently used to evaluate the molecular changes taking place throughout fermentation.

Our results show that FT-MIR and FT-NIR spectra are powerful tools to identifiy trends within the fermentation. The interpretation of the MIR and NIR spectral data showed time related trends. No variation was identified according to the different LAB treatments or inoculation strategies.

FT-IR spectra were used to identify the spectral bands characteristic of the major AF parameters namely, sugars and ethanol as well as the carboxylic acids malic acid and lactic acid. Work done by other authors was used to guide the identification of sugars and ethanol. Interesting spectral regions for malic acid and lactic acid determination was guided by the preliminary calibration work done in this study as well as to compare these spectral regions with regions identified by previous studies.

The characteristic spectral bands present in the MIR region can be directly interpreted whereas the interpretation of NIR region is considered a difficult task. The NIR region is more complex than the MIR region due to vibrational molecular overlapping of the overtone and combination vibrational modes characteristic of this region (Ben-Dor *et al*., 1997).

Due to the complexity of the fermenting must and wine matrix under analysis the assignment of specific IR peaks to specific compounds also sets up a challenging task. Functional groups (C-H, C-O) aren't compound specific and are shared between compounds found in fermenting must and wine. It can, however, be presumed that the largest peaks

found in the spectral data represent chemical bond vibrations of the most abundant compounds in the mixture (Urtubia *et al*., 2008).

3.3.2.2 TREND IDENTIFICATION USING PCA

FT-MIR and FT-NIR spectral data was subjected to PCA in order to further monitor and explore the time trends throughout the fermentations. PCA was used to compare the spectroscopic fingerprints and chemical changes along the fermentation process. PCA is a powerful tool which allows us to visualise in an easily interpretable graphic format the trends pertaining to the different LAB treatments and inoculation strategies.

PCA OF FT-MIR SPECTRA

The explorative stage of PCA included the modelling of the complete data set involving all the samples and all the wavenumbers.

The score plot of the complete data set explained 83% of the variance on PC1 and 4% on PC 2 (**Figure 3.15A**). Although a relatively high level of variation in the sample set was explained by PC1 no distinct clustering of the samples was observed. This was not unexpected, since all the wavenumbers were included in the model. The model therefore included the background noise due to the absorbance of water. The PC1 loadings plot (**Figure 3.15B**) showed high loadings at wavenumber regions, 3627 – 2971 cm^{-1} and 1698 – 1582 cm^{-1} where water is known to absorb (regions B). The region C, 5011 - 3627 cm^{-1} showed very low loadings and confirms the interpretation that this region shows very little useful information and can contribute to noise in the spectra (Patz *et al*., 2004). Very low loadings were observed in region A, known as the “fingerprint region” (1500 – 929 cm^{-1}), however it is known that many IR bands relating to the vibration of C-O, C-C, C-H and C-N bonds found in sugar, ethanol, glycerol and organic acids are known to absorb in this region (Smith, 1999). Subsequently the suppression of the loadings in this fingerprint region was due to the dominant water absorbance in the spectra.

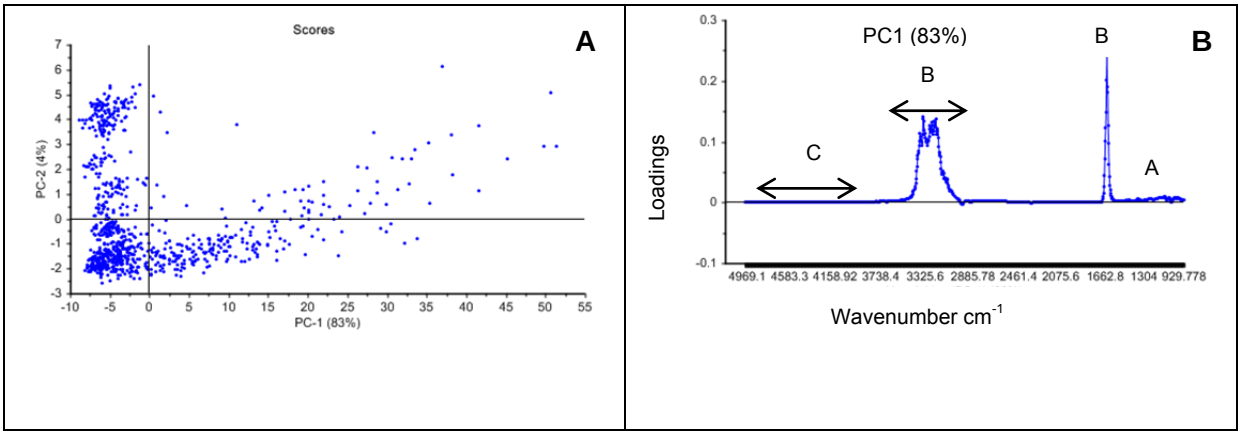

Figure 3.15 A) PCA score plot, PC1 versus PC2 of the FT-MIR spectra of the complete data set including all the wavenumber variables and **B)** Corresponding PC1 loadings plot. Region A: "fingerprint region", 1500 – 929 cm^{-1}, Regions B: 3627 – 2971 cm^{-1} and 1698 – 1582 cm^{-1} where water is known to absorb and Regions C: 5011 - 3627 cm^{-1} containing very little useful information.

In order to evaluate the influence of other wavenumbers, subsequent PCA analysis excluded regions where water absorbs (regions B, **Figure 3.15B**) as well as the region which showed very little useful information (region C, **Figure 3.15B**). Further interpretation was done modelling the co-inoculation samples separately from the sequential inoculation samples.

The PCA plot modelling the co-inoculation and sequential samples together showed very little difference between the scores of the fermentations on a specific day, however, a slight separation between the sequential samples and the co-inoculated samples were observed on PC1 (data not shown).

CO-INOCULATED FERMENTATIONS

The PCA model of the complete fermentation had an excellent explained variance of 99% on PC1 with only 1% explained by PC2 (**Figure 3.16A**).

When investigating the specific trends in the data matrix no specific clustering was observed related to the specific bacterial treatments. The chronological separation of the fermentation samples on PC1 from left to right was based according to fermentation time. Clustering of samples was clearly defined into specific days and the stage of fermentation was clearly noticeable (**Figure 3.16A**). A clear separation was also noticed between samples taken in the morning (am) from those taken in the evening (pm) of a specific day (**Figure 3.16A**). The clustering into the specific days was highly noticeable from day 0 to day five. From day six onwards no specific clustering was noticed. It was observed that towards the end of fermentation there was a convergence of scores and the differences between the scores of a specific day were no longer so prominent (**Figure 3.16A**). The scores were therefore more similar with respect to their absorbance spectra and therefore

cannot be differentiated. The decrease in variation between the scores towards the end of fermentation shows the slowing down of the chemical changes taking place during fermentation at this stage.

The separate model including samples from day 0 to five also resulted in an explained variance of 99% (**Figure 3.16C**). The separation by time from left to right on PC1 is seen more clearly in this model. The model including day six onwards explained 78% of the variance on PC1 with PC2 explaining 15% (**Figure 3.16E**). No clear separation was noticed between the scores for day six onwards, however, the scores of day ten deviated from the trend and did not fall in the chronological time order noticed. Day 18 was separated from the rest of the samples on PC1.

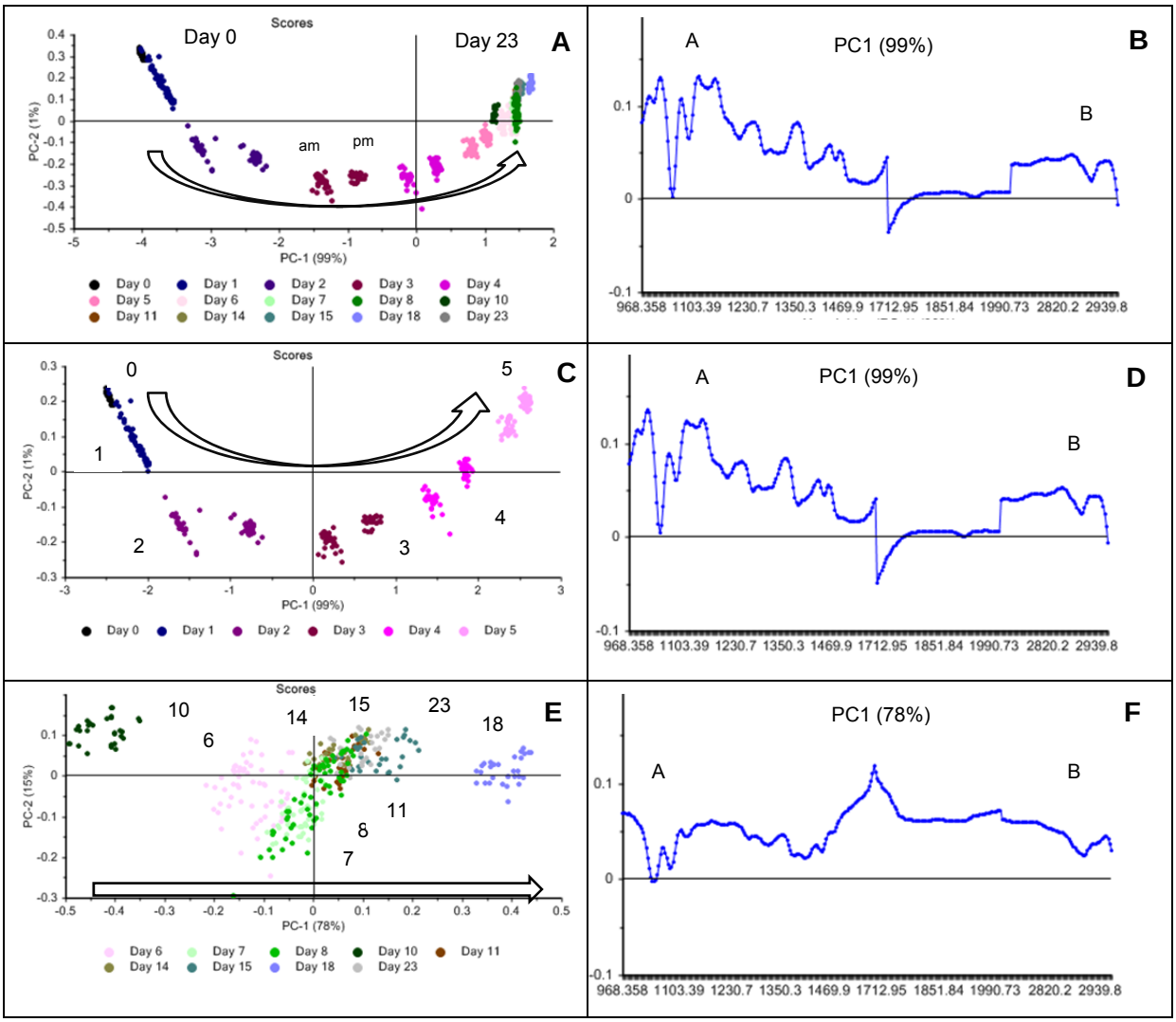

Figure 3.16 A) PCA score plot of FT-MIR spectra (PC 1 & 2) showing the complete fermentation (day 0 to 23) of the co-inoculation strategy and **B)** Corresponding PC1 (99%) loadings plot. **C)** PCA score plot showing day 0 to 5 and **D)** Corresponding PC1 (99%) loadings plot. **E)** PCA score plot showing day 6 to 23 and **F)** Corresponding PC1 (78%) loadings plot. Region A is the "fingerprint region", 1500 - 960 cm^{-1} and region B is the wavenumber region 2900 - 2700 cm^{-1}. Arrows show the separation of samples based on a time course trend while the numbers denote the days. An example of the am and pm separation is shown for day 3.

SEQUENTIAL INOCULATED FERMENTATIONS

The same time trends reported above for the co-inoculation strategy were noticed for the sequential fermentations (data not shown). Clear separation was observed from day 0 to five with a convergence in the scores noticed from day six onwards. Once again, day ten deviated from the chronological time trend.

The fact that day ten deviates from the time trend is difficult to explain, however, our results show that chemometric techniques such as PCA can detect these abnormalities. In an industrial situation the identification of such abnormalities within fermentations is exactly what the winemaker would want for a monitoring system in order to make immediate rectifying decisions.

The interpretation of the loadings plots of PC1 for both the co-inoculated (**Figures 3.16B, 3.16D and 3.16F**) and the sequential treatments (data not shown) showed similar profiles. Obvious differences were observed between the loadings plots modelling day one to five (**Figure 3.16D**) and that of day six onwards (**Figure 3.16F**) showing the change in the chemistry as the fermentation progresses. The samples from day one to day five were highly explained by the wavenumbers in the fingerprint region (Region A) (**Figure 3.16D**) whereas samples from day six onwards were explained by high loadings scattered throughout the MIR region with a noticeable difference around the region 1700 cm^{-1} (**Figure 3.16F**).

TREND IDENTIFICATION OF MLF

PCA was used to explore the differences between the two inoculation strategies during MLF. **Figure 3.17A** shows MLF day 5, 8 and 14 for the co-inoculated fermentations while **Figure 3.17C** reports the sequential fermentations.

The interpretation of the PCA score plot showed that the co-inoculated treatments separated from left to right on PC1 (91%) (**Figure 3.17A**). Very little difference was observed between the scores of MLF 8 and MLF 14 (**Figure 3.17A**). The same trend was noticed for the sequential treatments, however, the separation was from right to left (**Figure 3.17C**). Once again, very little difference was noticed between the scores of MLF 8 and MLF 14 for the sequential treatments (**Figure 3.17C**).

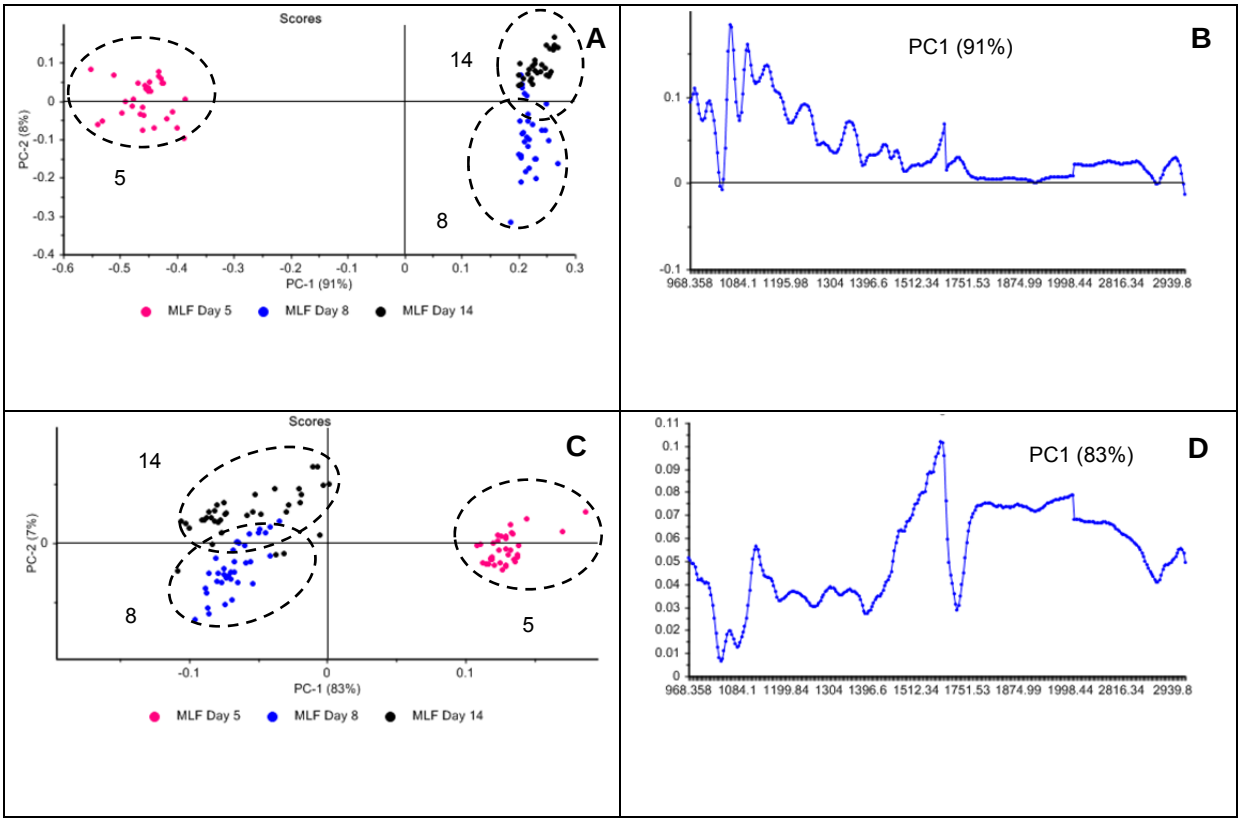

Figure 3.17 A) PCA score plot modelling MLF day 5, 8 and 14 for the co-inoculation strategy and **B)** Corresponding PC1 (91%) loadings plot. **C)** PCA score plot modelling MLF day 5, 8 and 14 of the sequential inoculation strategy and **D)** Corresponding PC1 (83%) loadings plot. The numbers denote the day of MLF.

Visual inspection of the loadings plot showed obvious differences in the chemistry of these two fermentations. The separation in the co-inoculated treatments (**Figure 3.17B**) was dominated by high loadings in the fingerprint region whereas the loadings plot of the sequential treatments (**Figure 3.17D**) showed lower loadings in the fingerprint region with higher loadings scattered throughout the MIR region with high loadings clearly noticeable at wavenumber 1700 cm^{-1} which could be characterised by the absorption of the C=O stretch band of carboxylic acids (Silverstein *et al*., 1991) as well as at 2900 cm^{-1} characterised by the C-H stretch of ethanol (Silverstein *et al*., 1991).

However, comparing these two fermentations in terms of their chemistry is difficult as their stages of fermentation are different due to the specific timing of inoculation of the bacterial cultures.

PCA OF FT-NIR SPECTRA

As with the MIR PCA of the NIR data included the modelling of the complete data set involving all the samples and all the wavenumbers. The score plot of the complete data set explained 93% of the variance on PC1 and 4% on PC 2 (data not shown). Although a

relatively high amount of variation in the sample set was explained by PC1 no distinct clustering of the samples was observed. This was not unexpected, since all the wavenumbers were included in the model.

Subsequent PCA analysis was done on first derivative and SNV transformed spectra and included the wavenumber region 6100 - 5449 cm^{-1}. The model showing the complete fermentation of the transformed NIR spectra explained 99% of the variation on PC1 with PC2 explaining only 1% of the variation (**Figure 3.18A**).

The trends observed in the NIR PCA models were similar to those of the MIR data. No bacterial trend could be observed in the data. The separation of the samples observed on PC1 from left to right was once again based on a time trend. Clear separation into days was noticed between day one and day four of the fermentation and once again there was a convergence of the scores from day five onwards (**Figure 3.18A**).

The NIR data were modelled separately as done for the MIR data. The separate modelling of samples from day one to four also resulted in an explained variance of 99% (**Figure 3.18C**). The separation by time from left to right on PC1 was seen more clearly in this model (**Figure 3.18C**). The model including day five onwards explained 86% of the variation on PC1 with PC2 explaining 5% (**Figure 3.18E**). The time trend observed from day five onwards was clearer than that observed for the MIR data and the scores of day 10 did not deviate from the trend as in the MIR data.

Spectral variation over time was visible with both MIR and NIR spectroscopy. However, NIR spectra were transformed and specific wavenumber regions were selected before trends could be identified.

It is clear that the infrared spectral data collected can provide us with important information on the infrared active components present in the sample and subsequently the underlying chemistry of the fermentation. The spectral variation observed in both the MIR and NIR spectra can be attributed to the changes observed in specific compounds relating to the time course of fermentation and could therefore be due to the joint influence from both yeast and bacterial metabolism. The spectra reflect changing concentrations of many different products and by products characteristic of a wine fermentation and more specifically of microbial metabolism.

The clear separation and spectral differences observed from day 0 to day five therefore reflect the dominant conversion of sugar into ethanol throughout the fermentation process as well as the changing concentrations of other fermentation compounds such as organic acids, aldehydes, esters, phenolics and tannins present in much lower concentrations. The subsequent convergence of scores noticed from day six onwards clearly shows a slowing down of the chemical changes taking place during the fermentation

at this stage. These trends are in accordance with the chemical changes reported during the quantitative modelling specifically for sugars and ethanol in **section 3.3.1**.

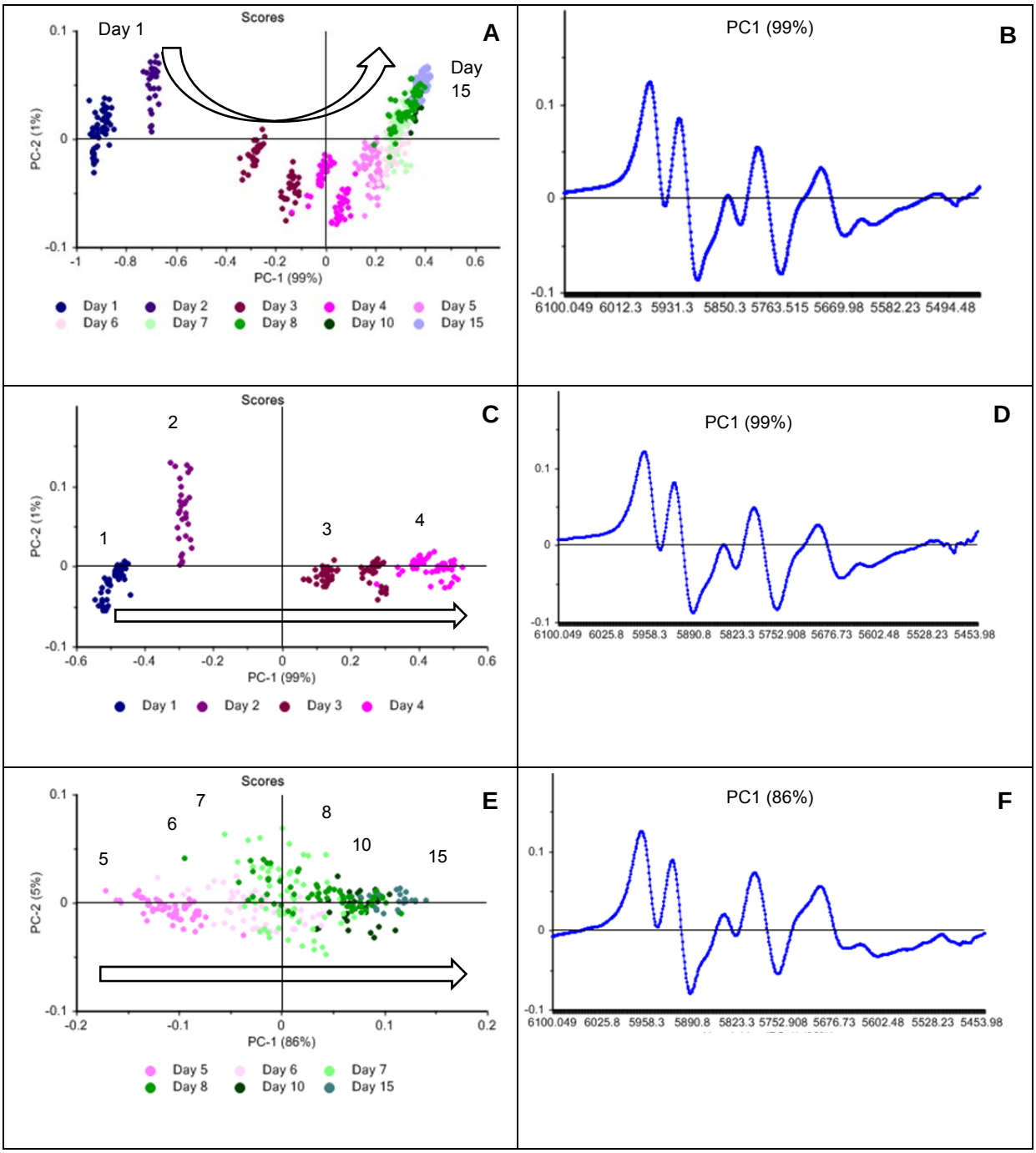

Figure 3.18 A) PCA score plot of transformed FT-NIR spectra (PC 1 & 2) showing the complete fermentation (day 1 to 15) of the co-inoculation strategy and **B)** Corresponding PC1 (99%) loadings plot and **C)** PCA score plot showing day 1 to 4 and **D)** Corresponding PC1 (99%) loadings plot. E**)** PCA score plot showing day 5 to 15 and F**)** Corresponding PC1 (86%) loadings plot. The FT-NIR spectra was transformed by 1st derivative and SNV. The wavenumber region 6100 - 5449 cm^{-1} was used. Arrows show the separation of scores based on a time course trend while the numbers denote the days.

Our results are in accordance with the very limited studies using spectroscopy to qualitatively monitor fermentations.

Off-line attenuated total reflectance (ATR)-MIR spectroscopy was used to scan 648 samples between the range 4000 and 375 cm^1. Spectral interpretation after second derivative transformation clearly showed changes related to the time of fermentation. PCA score plots explained 90% of the variation on four PC's relating to the time course. PLS discriminant analysis (PLS-DA) was used to predict the time course of the fermentation with a coefficient of determination (R^2) of 0.93 and a standard error of prediction (SEP) of 1.21 days (Cozzolino & Curtin, 2012).

Off-line fermentation samples were collected and scanned using FT-NIR, ATR-MIR, electronic nose and electronic tongue instruments. NIR spectral data was generated in transmission mode over the range 12,500 to 3600 cm^{-1} (resolution 8 cm^{-1}) while MIR data was collected over the range 4000 to 700 cm^{-1} (resolution 16 cm^{-1}). The 1st and 2nd derivatives of the fermentation kinetics was successfully used to determine the maximum acceleration and maximum rate of the process for sugar consumption and ethanol and glycerol production. PCA scores showed clear time related trends on PC1 while the evaluation of the spectral loadings identified the main wavenumbers responsible for the separation. Time related trends were also observed for the electronic nose and tongue data on PC1 and PC2. PC1 scores were modelled and 1st and 2nd derivative of the curves determined the maximum acceleration and rate of these processes. Excellent linear correlations were determined between the PC1 score kinetics and the kinetics of sugar degradation and ethanol production showing the ability of NIR, MIR, electronic nose and tongue techniques to evaluate the chemical changes within the fermentation (Buratti *et al*., 2011).

Seventy five samples scanned using MIR (4,000 to 700 cm^{-1}) and NIR (12,500 to 3,600 cm^{-1}) spectroscopy were successfully used to monitor the time related changes in red wine fermentations using PCA score and spectral loadings. Results of the linear discriminant analysis (LDA) to predict the stage of fermentation showed correct classification for 87% and 100% of the samples for NIR and MIR respectively. Good PLS correlations were established for glucose, fructose, ethanol, glycerol and phenolic compounds (Di Egidio *et al*., 2010).

The progress of red wine fermentations was monitored using off-line NIR spectroscopy (400 to 2500 nm) together with chemometric analysis (PCA, DPLS and LDA). PCA identified time related trends while LDA successfully classified samples in terms of the time point of fermentation (Cozzolino *et al*., 2006). Furthermore, reports have shown the use of data analysis techniques such as MPCA and MPLS in the prediction and early recognition

of problematic fermentations in an industrial scale (Urtubia *et al*., 2007; 2008; 2012; Emparán *et al*., 2012).

3.3.2.3 CONFORMITY TEST

Conformity models established with FT-MIR (**Figure 3.19A**) and FT-NIR (**Figure 3.19B**) spectral data were used to predict the stage of completion of alcoholic fermentation (e.g. co-inoculated MX treatment). This technique of monitoring using IR spectra alone is a fast easy test which by-passes the need for spectral interpretation such as PCA in order to monitor the state of the process. The use of this technique would considerably reduce the cost and time needed for fermentation monitoring.

The models were established using reference spectra which included samples from the end of AF (RS < 5 g/L). Samples taken at day 10 of the fermentation (RS < 5 g/L) were therefore used as reference spectra for both the models (green diamonds) (**Figure 3.19A and 3.19B**). Sixty one samples were used as reference spectra for the MIR model (**Figure 3.19A**), whereas 30 samples were used for the NIR model (**Figure 3.19B**). Test spectra included spectra taken at specific time intervals for a specific fermentation (in this case the co-inoculation treatment MX) (Blue pentagons). The test spectra included 108 spectral samples used for the MIR model (**Figure 3.19A**) and 96 spectral samples for the NIR model (**Figure 3.19B**).

The interactive region selection was used to select the wavenumber regions for establishing the model. The MIR model was established with the following wavenumber regions 3036 – 1732 cm^{-1} and 1539 – 960 cm^{-1} and the NIR model was established with wavenumber regions 12,486 – 7422, 6062 – 5402 and 4643 – 4217 cm^{-1}. Spectral pre-processing included first derivative and vector normalization (SNV) with 17 smoothing points for both MIR and NIR spectra.

The results of the MIR model shows that the spectra at day seven for treatment MX conforms to that of the reference spectra (**Figure 3.19A**). The spectra taken at day six for treatment MX conforms to the reference spectra in the NIR model (**Figure 3.19B**).

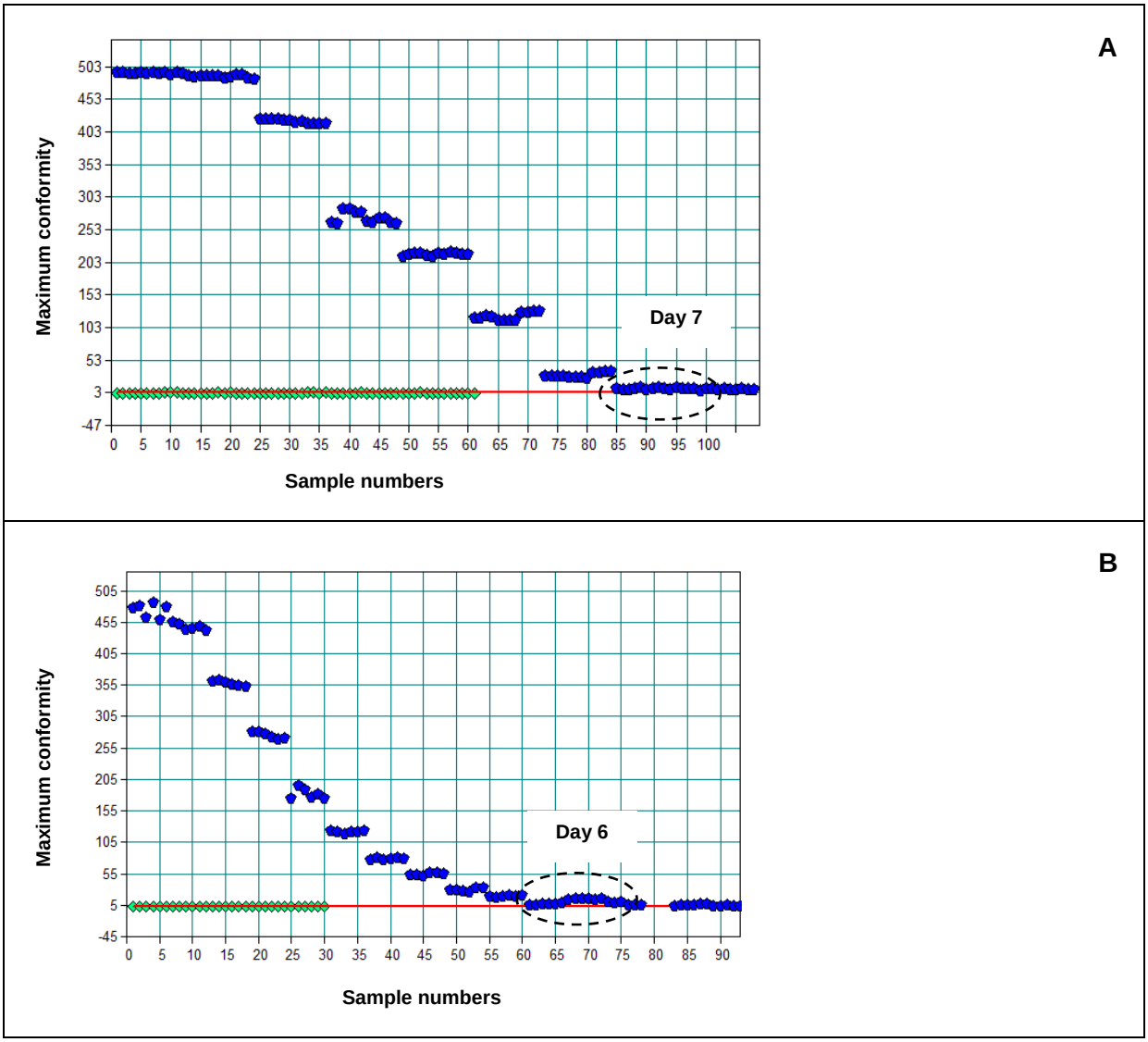

Figure 3.19 A) Conformity model predicting the stage of completion of AF using FT-MIR spectral data and **B)** Conformity model predicting the stage of completion of AF using FT-NIR spectral data. Reference spectra (green diamonds) included spectra where RS<5g/L. Test spectra (Blue pentagons) were taken at regular intervals during the fermentation. The circled test spectra shows the specific day which conforms to the reference spectra.

3.4 CONCLUSIONS

The results of this work show the excellent ability of both MIR and NIR spectroscopy together with the powerful chemometric techniques to monitor a bioprocess and identify the molecular time-related changes involved with alcoholic and malolactic fermentations. Both qualitative and quantitative approaches have shown promise in determining trends within fermentations using different inoculation strategies. Infrared spectroscopy has shown its capability of quantitatively reliably predicting AF and MLF fermentation parameters and qualitatively predicting a stage in the fermentation process.

The quantitative approach to the monitoring of the Shiraz fermentations subsequently allowed for the accurate and stringent monitoring and trend identification of the fermentation parameters including RS, glucose, fructose, ethanol, volatile acidity, titratable acidity, pH, malic acid and lactic acid over time. In an industrial setup the modelling of the fermentation kinetics using techniques such as non-linear response curves can be seen as advantageous from a monitoring point of view to predict the rate of a fermentation. These quantitative applications, however, involve extensive calibration work with large amounts of wet analytical chemistry which is laborious and costly.

The trends identified by the qualitative approach involving only infrared spectra were in agreement with the specific trends noticed in the quantitative models specifically for sugars and ethanol. For this reason these techniques can surpass the timely, expensive traditional techniques of quantitative fermentation monitoring by providing a platform for real-time process analysis and the subsequent monitoring of the chemical changes taking place in a fermentation. The approach of using infrared spectra alone to predict the stage of AF using spectral conformity models provides a fast reliable alternative to the timely and costly quantitative calibration models used to predict fermentation parameters.

These modelling techniques show promise in an online industrial setup whereby fast generation of spectra can provide the winemaker with insight into the progress of the fermentation as well as a technique to identify stuck/sluggish fermentations, subsequently providing a platform for stringent control of the bioprocess for excellent product quality.

Although the measurements of this study were carried out in off-line mode these techniques can be applied in future, to on-line measurements using sensor techniques to monitor fermentations providing the winemaker with fast reliable real-time information for subsequent quality and process control.

3.5 LITERATURE CITED

Abrahamse, C.E. & Bartowsky, E.J., 2012. Timing of malolactic fermentation inoculation in Shiraz grape must and wine: Influence on chemical composition. *World J. Microbiol. Biotechnol*. 28, 1-11.

Bartowsky, E.J., 2005. *Oenococcus oeni* and malolactic fermentation–moving into the molecular arena. *Aust. J. Grape Wine Res*. 11, 174-187.

Bartowsky, E., Costello, P. & McCarthy, J., 2008. MLF-adding an extra dimension to wine flavour and quality. *Aust. N.Z. Grapegrower Winemaker* 533, 60–65.

Bauer, R., Nieuwoudt, H., Bauer, F.F., Kossmann, J., Koch, K.R. & Esbensen, K.H., 2008. FTIR spectroscopy for grape and wine analysis. *Anal. Chem*. 80, 1371-1379.

Ben-Dor, E., Inbar, Y. & Chen, Y., 1997. The reflectance spectra of organic matter in the visible near-infrared and short wave infrared region (400-2500 nm) during a controlled decomposition process. *Remote Sens. Environ*. 61, 1-15.

Bevin, C.J., Dambergs, R.G., Fergusson, A.J. & Cozzolino, D., 2008. Varietal discrimination of Australian wines by means of mid-infrared spectroscopy and multivariate analysis. *Anal. Chim. Acta* 621, 19-23.

Boido, E., Medina, K., Farina, L., Carrau, F., Versini, G., & Dellacassa, E., 2009. The effect of bacterial strain and aging on the secondary volatile metabolites produced during malolactic fermentation of Tannat red wine. *J. Agric. Food Chem.* 57, 6271-6278.

Buratti, S., Ballabio, D., Giovanelli, G., Dominguez, C.M.Z., Moles, A., Benedetti, S. & Sinelli, N., 2011. Monitoring of alcoholic fermentation using near infrared and mid infrared spectroscopies combined with electronic nose and electronic tongue. *Anal. Chim. Acta* 697, 67-74.

Cen, H. & He, Y., 2007. Theory and application of near infrared reflectance spectroscopy in determination of food quality. *Trends Food Sci. Technol*. 18, 72-83.

Cozzolino, D., Kwiatkowski, M., Parker, M., Cynkar, W., Dambergs, R., Gishen, M. & Herderich, M.J., 2004. Prediction of phenolic compounds in red wine fermentations by visible and near infrared spectroscopy. *Anal. Chim. Acta* 513, 73-80.

Cozzolino, D., Parker, M., Dambergs, R.G., Herderich, M. & Gishen, M., 2006. Chemometrics and visible-near infrared spectroscopic monitoring of red wine fermentation in a pilot scale. *Biotech. Bioeng*. 95, 1101-1107.

Cozzolino, D. & Curtin, C., 2012. The use of attenuated total reflectance as tool to monitor the time course of fermentation in wild ferments. *Food Control* 26, 241-246.

Cozzolino, D., McCarthy, J. & Bartowsky, E., 2012. Comparison of near infrared and mid infrared spectroscopy to discriminate between wines produced by different *Oenococcus Oeni* strains after malolactic fermentation: A feasibility study. *Food Control* 26, 81-87.

Dambergs, R.G., Kambouris, A., Francis, I.L. & Gishen, M., 2002. Rapid analysis of methanol in grape-derived distillation products using near-infrared transmission spectroscopy. *J. Agric. Food Chem. 50, 3079*.

Di Egidio, V., Sinelli, N., Giovanelli, G., Moles, A. & Casiraghi, E., 2010. NIR and MIR spectroscopy as rapid methods to monitor red wine fermentation. *Eur. Food Res. Technol*. 230, 947-955.

Drici-Cachon, A., Guzzo, J., Cavin, F., & Diviès, C., 1996. Acid tolerance in *Leuconostoc oenos*. Isolation and characterisation of an acid resistant mutant. *Appl. Microbiol. Biotechnol*. 44, 785–789.

du Toit, M., Engelbrecht, L., Lerm, E. & Krieger-Weber, S., 2011. *Lactobacillus*: The next generation of malolactic fermentation starter cultures-an overview. *Food Bioprocess Technol*. 4, 876-906.

Emparán, M., Simpson, R., Almonacid, S., Teixeira, A. & Urtubia, A., 2012. Early recognition of problematic wine fermentations through multivariate data analyses. *Food Control* 27, 248-253.

Esbensen, K.H. (ed). 2006. *Multivariate Data Analysis – In Practice*. 5th Ed. Camo ASA, Oslo, Norway. pp. 19-97; 115-153.

Jørgensen, P., Pedersen, J.G., Jensen, E.P. & Esbensen, K.H., 2004. On line batch fermentation process monitoring (NIR)-Introducing biological process time. *J. Chemom*. 18, 81–91.

Karoui, R., Downey, G. & Blecker, C., 2010. Mid-infrared spectroscopy coupled with chemometrics: A tool for the analysis of intact food systems and the exploration of their molecular structure−quality relationships− A review. *Chem. Rev*. *110,* 6144-6168.

Knoll, C., Fritsch, S., Schnell, S., Grossmann, M., Krieger-Weber, S., du Toit, M. & Rauhut, D., 2012. Impact of different malolactic fermentation inoculation scenarios on Riesling wine aroma. *World J. Microbiol. Biotechnol*. 28, 1143-1153.

Krieger-Weber, S., 2009. Application of yeast and bacteria as starter cultures. In: König, H., Unden, G. & Fröhlich, J. (eds). *Biology of microorganisms on grapes, in must and in wine*. Springer, Berlin. pp. 498-511.

Lambrechts, M.G. & Pretorius, I.S., 2000. Yeast and its importance to wine aroma-a review. *S. Afr. J. Enol. Vitic*. 21, 97-129.

Landgrebe, D., Haake, C., Höpfner, T., Beutel, S., Hitzmann, B., Scheper, T., Rhiel, M. & Reardon, K.F., 2010. On-line infrared spectroscopy for bioprocess monitoring. *Appl. Microbiol. Biotechnol*. 88, 11-22.

Lee, J.E., Hong, Y.S & Lee, C.H., 2009a. Characterization of fermentative behaviors of lactic acid bacteria in grape wines through ^{1}H-NMR- and GC-based metabolic profiling. *J. Agric. Food Chem*. 57, 4810-4817.

Lee, J.E., Hwang, G.S., Lee, C.H. & Hong, Y.S., 2009b. Metabolomics reveals alterations in both primary and secondary metabolites by wine bacteria. *J. Agric. Food Chem*. 57, 10772-10783.

Lerm, E., Engelbrecht, L. & du Toit, M., 2010. Malolactic fermentation: The ABC's of MLF. *S. Afr. J. Enol. Vitic.* 31, 186-212.

Liu, L., Cozzolino, D., Cynkar, W.U., Gishen, M. & Colby, C.B., 2006. Geographic classification of Spanish and Australian Tempranillo red wines by visible and near-infrared spectroscopy combined with multivariate analysis. *J. Agric. Food Chem*. 54, 6754.

Lonvaud-Funel, A., 1999. Lactic acid bacteria in the quality improvement and depreciation of wine. *Antonie Leeuwenhoek* 76, 317–331.

Louw, L., Roux, K., Tredoux, A., Tomic, O., Naes, T., Nieuwoudt, H.H. & van Rensburg, P., 2009. Characterization of selected South African young cultivar wines using FTMIR spectroscopy, gas chromatography, and multivariate data analysis. *J. Agric. Food Chem*. 57, 2623-2632.

Magerman, C.M., 2009. The evaluation of Fourier transform infrared (FT-IR) spectroscopy for quantitative and qualitative monitoring of alcoholic wine fermentation. Thesis, Stellenbosch University, Private Bag X1, 7602, Matieland (Stellenbosch), South Africa.

Margalit, Y., 1997. In: J. Crum (ed). *Concepts in Wine Chemistry*. Wine Appreciation Guild Ltd., San Fransisco, USA. pp. 16-18; 76-82.

Massera, A., Soria, A., Catania, C., Krieger, S. & Combina, M., 2009. Simultaneous inoculation of Malbec (Vitis vinifera) musts with yeast and bacteria: Effects on fermentation performance, sensory and sanitary attributes of wines. *Food Technol. Biotechnol*. 47(2), 192–201.

Moreira, J.L. & Santos, L., 2005. Analysis of organic acids in wines by Fourier-transform infrared spectroscopy. *Anal. Bioanal. Chem.* 382, 421-425.

Motulsky, H.J. & Christopoulos, A. (eds). 2003. *Fitting models to biological data using linear and nonlinear regression. A practical guide to curve fitting*. Graphpad Software Inc., San Diego CA, www.graphpad.com. pp. 13-46.

Naes, T., Isaksson, T. Fearn, T. & Davis, T. (eds). 2002. *A user-friendly guide to multivariate calibration and classification*. NIR Publications, Chichester, UK. pp. 5-18; 124.

Nieuwoudt, H.H., Pretorius, I.S., Bauer, F.F., Nel, D.G. & Prior, B.A., 2006. Rapid screening of the fermentation profiles of wine yeasts by Fourier transform infrared spectroscopy. *J. Microbiol. Methods* 67, 248-256.

Patz, C.D., Blieke, A., Ristow, R. & Dietrich, H., 2004. Application of FT-MIR spectrometry in wine analysis. *Anal. Chim. Acta* 513, 81-89.

Pavia, L.P., Lampman, G.M. & Kriz, G.S. (eds). 2009. *Introduction to Spectroscopy: A Guide for Students of Organic Chemistry*. 4th Ed. Harcourt College Publishers, Belmont, USA. pp. 15-104.

Picque, D., Lefier, D., Grappin, R. & Corrieu, G., 1993. Monitoring of fermentation by infrared spectrometry: Alcoholic and lactic fermentations. *Anal. Chim. Acta* 279, 67-72.

Pronk, J.T., Steensma, H.Y. & van Dijken, J.P., 1996. Pyruvate metabolism in *Saccharomyces cerevisiae*. *Yeast* 12,1607–1633.

Pozo-Bayón, M.A., Alegría, E.G., Polo, M.C., Tenorio, C., Martín-Álvarez, P.J., Calvo de la Banda, M.T., Ruiz-Larrea, F. & Moreno-Arribas, M.V., 2005. Wine volatile and amino acid composition after malolactic fermentation: Effect of *Oenococcus oeni* and *Lactobacillus plantarum* starter cultures. *J. Agric. Food Chem*. 53, 8729-8735.

Rosi, I., Fia, G. & Canuti, V., 2003. Influence of different pH values and inoculation time on the growth and malolactic activity of a strain of *Oenococcus oeni*. *Aust. J. Grape Wine Res.* 9(3), 194–199.

Shenk, JS, Workman, J.J & Westerhaus, M.O., 2008. Application of NIR Spectroscopy to Agricultural Products. In: Burns, D.A. & Ciurczak, E.W. (eds). *Handbook of Near-Infrared Analysis*. 3rd Ed. Marcel Dekker, New York, pp. 347-386.

Silverstein, R.M., Clayton Bassler, G. & Morrill, T.C. (eds). 1991. Infrared spectrometry. In: *Spectrometric identification of organic compounds*. 5th Ed. Wiley, New York. pp. 91-164.

Sivakesava, S., Irudayaraj, J. & Ali, D., 2001. Simultaneous determination of multiple components in lactic acid fermentation using FT-MIR, NIR, and FT-Raman spectroscopic techniques. *Process Biochem*. 37, 371-378.

Smith, B.C. (ed.). 1999. *Infrared spectral interpretation: A systematic approach*. CRC Press LLC, Boca Raton, Florida, USA. pp. 67-152.

Statsoft, Inc. (2011) STATISTICA (data analysis software system), version 10. www.statsoft.com.

Stuart, B., 2004. *Infrared spectroscopy: Fundamentals and applications*. Wiley, Chichester, West Sussex, England. pp 71-80.

Urbano Cuadrado, M., Luque de Castro, M., Perez Juan, P. & Gómez-Nieto, M., 2005. Comparison and joint use of near infrared spectroscopy and Fourier transform mid infrared spectroscopy for the determination of wine parameters. *Talanta* 66, 218-224.

Urtubia, A., Ricardo Pérez-Correa, J., Meurens, M. & Agosin, E., 2004. Monitoring large scale wine fermentations with infrared spectroscopy. *Talanta* 64, 778-784.

Urtubia, A., Pérez-Correa, J.R., Soto, A., Pszczólkowski, P., 2007. Using data mining techniques to predict industrial wine problem fermentations. *Food control* 18, 1512-1517.

Urtubia, A., Pérez-correa, J.R., Pizarro, F. & Agosin, E., 2008. Exploring the applicability of MIR spectroscopy to detect early indications of wine fermentation problems. *Food control* 19, 382-388.

Urtubia, A., Hernández, G. & Roger, J.M., 2012. Detection of abnormal fermentations in wine process by multivariate statistics and pattern recognition techniques. *J. Biotechnol*. 159, 336-341.

Vojinović, V., Cabral, J.M.S. & Fonseca, L.P., 2006. Real-time bioprocess monitoring: Part I: In situ sensors. *Sens. Actuators, B* 114, 1083-1091.

Wilson, R.H., Holland, J.K. & Potter, J., 1994. Lining up for FTIR analysis. *Chem. Br*. 30, 993-996.

WineScan FT 120 Type 77110 and 77310 Reference Manual, Issue 4 GB Foss Electric, Denmark, 2001. http://www.foss.dk.

Chapter 4

Research Results

Metabolic profiling of lactic acid bacteria in a Shiraz wine matrix using FT-MIR spectroscopy, Gas Chromatography and multivariate data analysis

CHAPTER 4. RESEARCH RESULTS

Metabolic profiling of lactic acid bacteria in a Shiraz wine matrix using FT-MIR spectroscopy, Gas Chromatography and multivariate data analysis

Jessica Garlick[1], Maret du Toit[1], Hélène Nieuwoudt[1]

[1]Institute for Wine Biotechnology, Department of Viticulture and Oenology, Stellenbosch University, Private Bag X1, Matieland, 7602 South Africa

4.1 INTRODUCTION

The aroma and flavour of wine are major characteristics in determining the style and quality of a wine (Swiegers *et al*., 2005). The volatile composition of a wine which is directly linked to wine aroma is the most important distinguishing characteristic between wines and in essence determines the consumer's perception of a wine.

Amongst other factors the volatile composition of wine can be affected by the biological changes taking place during both alcoholic fermentation (AF) and malolactic fermentation (MLF) by yeasts and bacteria respectively. During AF yeasts not only convert sugars to ethanol and CO_2, but also produce sensorially important volatile metabolites contributing to wine aroma (Rapp, 1998; Lambrechts & Pretorius, 2000). MLF, or the secondary fermentation, of wine is applied commercially to most red wines and certain white wine styles. MLF can occur spontaneously by the action of the indigenous microflora, however, the inoculation of commercially available lactic acid bacteria (LAB) starter cultures has improved the management of MLF (Versari *et al*., 1999). While *Oenococcus oeni* is the most dominant and best adapted species to the harsh wine environment (Matthews *et al*., 2006), as well as the most selected bacteria used as starter cultures for the induction of MLF *(*Drici-Cachon *et al.,* 1996; Lonvaud-Funel, 1999), other species such as *Lactobacillus* have also shown the potential to be used as MLF starter cultures (reviewed by du Toit *et al*., 2010). Apart from its primary objective as a biological de-acidification reaction and improving the biological stability in wine, MLF via LAB metabolism plays a role in the modification of the aroma profile of wines and the subsequent wine style (Bartowsky *et al*., 2002; 2004).

The major volatile metabolites produced during MLF include esters, volatile fatty acids, higher alcohols and carbonyl compounds (reviewed by Swiegers *et al*., 2005; Lerm *et al*., 2010). It has been reported, however, that distinct differences exist amongst wines produced with varying strains and species of LAB as well as different inoculation strategies in terms of their volatile profiles. Distinct volatile profiles were observed in wines produced when inoculating

LAB at different stages during AF (Abrahamse & Bartowsky, 2012; Knoll *et al*., 2012). Metabolic profiling research has revealed significant metabolic differences between *O. oeni* and *L. plantarum* species (Pozo Bayón *et al*., 2005; Lee *et al*., 2009b) as well as differentiation between strains (Pozo Bayón *et al*., 2005; Lee *et al*., 2009a; Knoll *et al*., 2012; Malherbe *et al*., 2012).

The quantification of these volatile metabolites is routinely performed with methods using gas chromatography (GC) combined with flame ionisation detection (FID) or with mass spectrometry (MS) detection (Ebeler, 2001; Peinado *et al*., 2004a, b; Lee *et al*., 2009a, b; Antalick *et al*., 2010). These techniques are highly selective and sensitive for the analysis of these volatile compounds in wine (reviewed by de Villiers *et al*., 2012), however, the use of these techniques are costly, time consuming and labour intensive.

The use of spectroscopy and GC-based analytical data together with chemometric techniques such as principal component analysis (PCA) and partial least squares regression (PLS-DA) have been widely applied for classification and discrimination purposes in wine. Many studies have successfully used these techniques for the discrimination between wine cultivars (Edelmann *et al*., 2001; Cozzolino, 2003; Roussel *et al*., 2006; Bevin *et al*., 2008; Louw *et al*., 2009), vintages (Palma & Barroso, 2002) as well as for yeast strain classification (Osborne, 2007; Son *et al*., 2009). Studies using these techniques to discrimination between wine LAB and their impact on the wine matrix are, however, very limited (Manley *et al*., 2001; Pozo Bayon *et al*., 2005; Lee *et al*., 2009a, b; Cozzolino *et al*., 2012; Malherbe *et al*., 2012).

The aim of this study was therefore to gain insight into the metabolic profiles of different LAB species and strains assessing two different process stages within co-inoculation and sequential inoculation strategies. The assessment of the two process stages namely 50% and 100% completion of MLF, which are two critically important stages during wine production, would provide information used for quality control purposes. This study evaluated the possibility of analytical techniques involving Fourier transform mid-infrared (FT-MIR) spectroscopy and GC together with the multivariate techniques namely PCA, PLS-DA and Soft Independent Modelling of Class Analogy (SIMCA) to discriminate between the different LAB treatments for future interpretative and classification purposes. Furthermore this study evaluated the ability of FT-MIR to discriminate between LAB, as a fast alternative to the conventional GC based analysis.

The complex data sets generated by these analytical techniques are usually combined with chemometrics for interpretation purposes. Multivariate techniques such PCA and PLS-DA capture the relevant information from these complex data sets and evaluate the interactions amongst multiple variables present within a sample (Næs *et al*., 2002; Esbensen, 2006). PCA is an unsupervised statistical technique frequently used as an explorative tool for data structure modelling and data description. PCA shows variations and similarities between samples and can be used to identify the specific variables contributing to these trends (Næs *et al*., 2002; Esbensen, 2006). PLS-DA is a supervised classification technique which uses PLS regression

to model the differences between two or more classes and subsequently discriminates between these classes. In addition, SIMCA is used as a classification method and is based on classifying samples into data classes according to their similarity with the training samples of the predefined classes. SIMCA is also used for the detection of non-typical or outlying samples. Unlike DA SIMCA can classify samples not belonging to the predefined classes (Esbensen, 2006).

4.2 MATERIALS AND METHODS

4.2.1 BACTERIAL STRAINS, EXPERIMENTAL DESIGN AND SAMPLING

The experimental design and sampling procedure carried out in this study follows that which has been reported in **Chapter 3**. **Figure 3.1 in Chapter 3** gives a flow diagram of the experimental design used throughout this study. Sampling procedures and subsequent data analysis are shown in **Figure 3.2** except for the GC-FID and GC-MS analysis which is shown in **Figures 4.1A and 4.1B** respectively. The bacterial strains used are show in **Table 3.1 in Chapter 3**. Sampling involved the collection of independent duplicate samples per biological repeat at 12 hourly intervals where possible throughout alcoholic and malolactic fermentation.

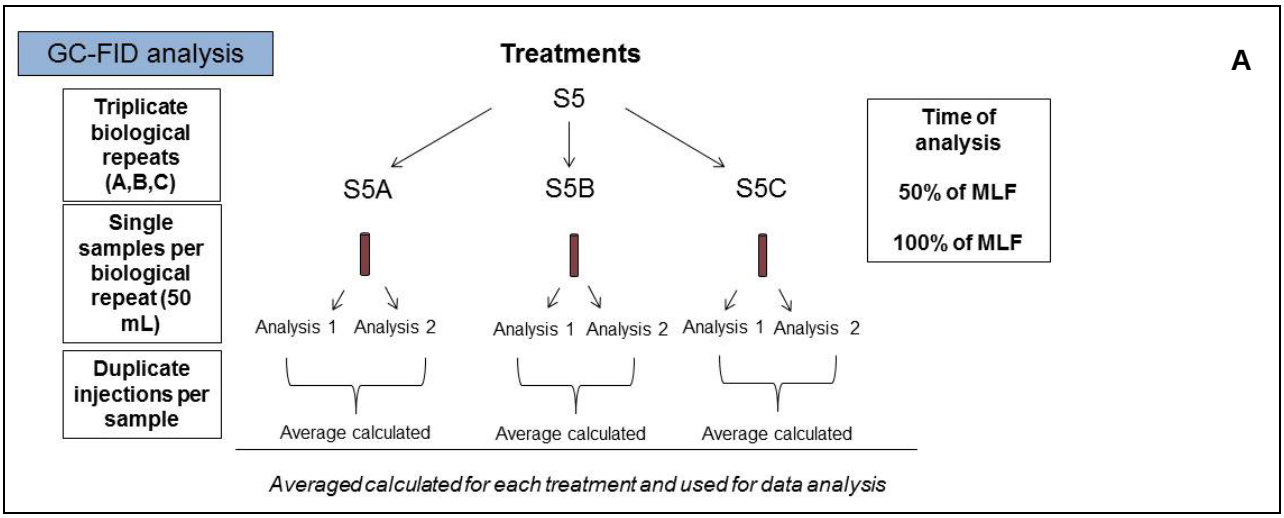

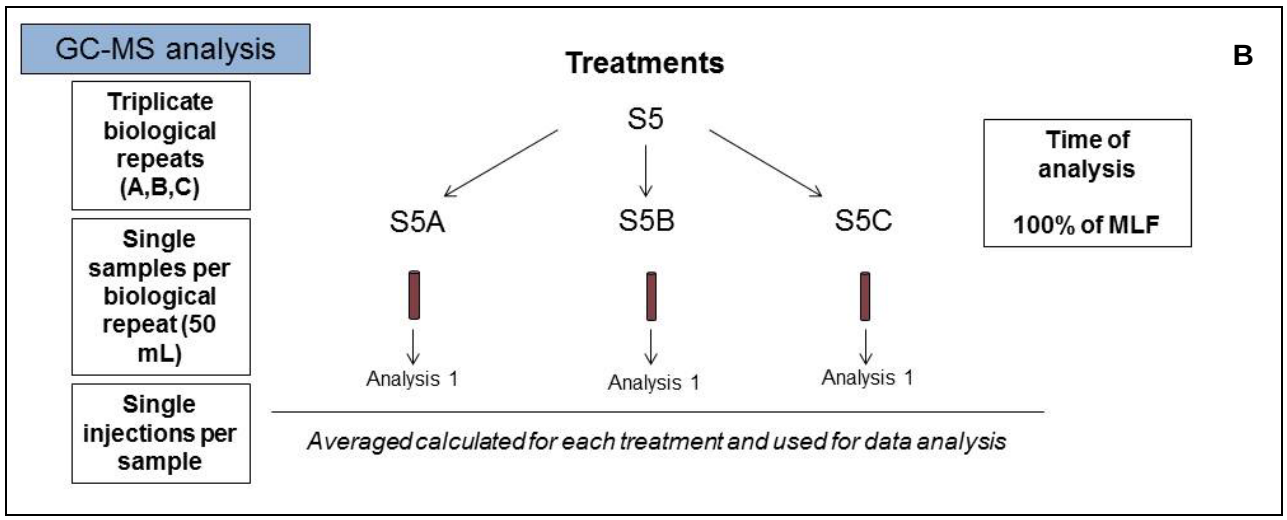

Figure 4.1 Experimental design illustrating the chemical analysis **A)** GC-FID and **B)** GC-MS and further data handling using treatment S5 as an example. All the LAB treatments were handled in the same way.

4.2.2 CHEMICAL REAGENTS, STANDARDS AND WINE SIMULANT

The reagents diethyl ether (99.5%) and absolute ethanol as well as sodium sulphate (Na_2SO_4) and sodium chloride (NaCl) used for sample preparation and GC analyses were purchased from Merck (Darmstadt, Germany). Pure water was obtained from a Milli-Q purification system (Millipore, Bedford, MA, USA). All the standards were of analytical grade (purity 95% - 99.9%). Isoamyl acetate was purchased from Riedel de Haën (Seelze, Germany). Ethyl acetate, methanol, ethyl propionate, ethyl 2-methylbutyrate, ethyl isovalerate, 3-methyl-1-pentanol, 3-ethoxy-1-propanol were from Sigma-Aldrich (Steinheim, Germany). Ethyl 2-methyl propanoate, 2-methyl propyl acetate, ethyl butyrate, propanol, isobutanol, butanol, ethyl hexanoate, pentanol, hexyl acetate, ethyl lactate, ethyl octanoate, 1-octen-3-ol, ethyl 3-hydroxybutanoate, propionic acid, isobutyric acid, butyric acid, isovaleric acid, diethyl succinate, valeric acid, ethyl phenylacetate, 2-phenylethyl acetate, diacetyl (2,3-butanedione), acetoin (3-hydroxy-2-butanone) and 2,3-pentanedione were from Fluka (Buchs, Switzerland). Isoamyl alcohol, ethyl decanoate and hexanoic acid was from Aldrich (Steinheim, Germany). Hexanol and 2-phenylethanol was from Merck (Darmstadt, Germany). Acetic acid was purchased from Saarchem and decanoic acid from Sigma (St. Louis, USA). The internal standards (2-pentanone and 4-methyl-2-pentanol, Fluka) and the volatile standards were dissolved in a wine simulant prepared according to Louw *et al*. (2009) and were subsequently used for the set up of the respective calibration curves [as described by Malherbe *et al*. (2012)].

4.2.3 FT-MIR SPECTROSCOPY

All the fermentations samples were taken to the laboratory for analysis. Sample preparation involved filtration and subsequent degassing of samples under vacuum as described by Louw *et al*., 2009. FT-MIR spectra were acquired by use of a WineScan FT 120 spectrometer (FOSS

Analytical A/S software version 2.2.1, Denmark, 2001) according to the validated method as described by Nieuwoudt *et al*. (2006).

Quantified chemical data namely titratable acidity (expressed as g/L tartaric acid), pH and volatile acidity were quantified from existing in-house FT-MIR PLS calibration models using the WineScan FT120 2001 version 2.2.1 software (Magerman, 2009).

Samples were subsequently frozen at -20 °C until enzymatic, GC-FID and GC-MS analysis could be done.

4.2.4 ORGANIC ACID ANALYSIS

Frozen samples were thawed at ambient laboratory temperature (±20 °C) and thoroughly mixed before enzymatic analysis. MLF was followed using an established in-house enzyme-linked assay for the quantification of L-Malic acid (expressed as g/L) and L-Lactic acid (expressed as g/L) as discussed in **section 5.2.3 in Chapter 5** with an automated Arena Konelab 20 XT Photometric analyser (Part number: 984163, Thermo Electron Oy, Finland). MLF was regarded as complete at a malic acid concentration of less than 0.3 g/L. 50% and 100% degradation of malic acid is hereafter referred to 50% and 100% completion of MLF respectively.

4.2.5 VOLATILE COMPOUND ANALYSIS

The samples identified by enzymatic analysis as critical process stages (50% and 100% completion of MLF) for each fermentation treatment were further analysed by GC techniques. The frozen samples were thawed and mixed prior to GC analysis.

4.2.5.1 MAJOR VOLATILE COMPOUNDS

The presence of thirty-nine major volatile compounds (**Table 4.1**) in samples were quantified in samples at 50% and 100% completion of MLF (malic acid < 0.3 g/L) using a Hewlett Packard 6890 Plus gas chromatograph (Agilent, Little Falls, Wilmington, USA) equipped with a split/splitless injector and an flame ionisation detection (FID) detector using the validated method as described by Malherbe *et al*. (2012). The GC-FID data was treated as shown in **Figure 4.1A** for further data analysis. The volatile compounds were extracted from the samples using the validated liquid-liquid extraction procedure as described by Louw *et al*. (2009). Each extract was then injected into the GC-FID in duplicate. A J & W DB-FFAP capillary GC column (Agilent, Little Falls, Wilmington, USA) with dimensions 60 m length x 0.32 mm internal diameter x 0.5 µm film thickness was used for the separation of compounds. The concentrations of the volatile compounds listed in **Table 4.1** were calculated using peak integrations by comparing their retention times and peak area with those from the calibration standard curve using the HP GC Chemstation data handling software [HP GC Chemstation, revision A.07.01 (682)].

Table 4.1 Major volatile aroma compounds quantified by GC FID analysis.

Higher Alcohols	Esters	Fatty acids
Methanol	Ethyl Acetate	Acetic Acid
Propanol	Ethyl Butyrate	Propionic Acid
Isobutanol	Isoamyl Acetate	Isobutyric Acid
Butanol	Ethyl Hexanoate	Butyric Acid
Isoamyl Alcohol	Hexyl Acetate	Isovaleric Acid
Hexanol	Ethyl Lactate	Valeric acid
2-Phenylethanol	Ethyl Caprylate	Hexanoic Acid
Pentanol	Ethyl Caprate	Octanoic Acid
4-Methyl-1-Pentanol	Diethyl Succinate	Decanoic Acid
3-Methyl-1-Pentanol	2-Phenylethyl Acetate	
1-Octen-3-ol	Ethyl Propionate	
3-Ethoxy-1-Propanol	Ethyl Phenylacetate	
	2-Methyl-propyl Acetate	
	Ethyl Isovalerate	
	Ethyl-3-hydroxybutanoate	
	Ethyl-2-methylpropanoate	
	Ethyl-2-methylbutyrate	

4.2.5.2 CARBONYL COMPOUNDS

The fermentation samples were subjected to headspace solid phase microextraction (HS-SPME) combined with gas chromatography-mass spectrometry (GC-MS) for the quantification of carbonyl compounds (diacetyl, acetoin and 2,3-pentanedione) using the validated method as described by Malherbe *et al*. (2012). Samples were subjected to GC-MS at 100% completion of MLF (malic acid < 0.3 g/L). A 60 µm polyethylene glycol (PEG) SPME fiber (Supelco, Bellefonte, PA) was used for extraction of polar compounds from the headspace. Quantitative data was obtained by calculating the absolute peak area. Further data analysis was carried out as shown in **Figure 4.1B**.

4.2.6 DATA ANALYSIS

A univariate and multivariate strategy was followed in this study in order to produce models with excellent discrimination ability.

Univariate data analysis was carried out in Statistica (version 10, StatSoft Inc., Tulsca, USA). One-way analysis of variance (ANOVA) was carried out on the major volatiles and carbonyl compounds. Statistical differences between the treatments were considered significant with a significance level of 5% (p<0.05). Post-hoc analysis included Fishers least significance difference (LSD) (Statistica version 10, StatSoft Inc., Tulsca, USA).

The multivariate approach to data analysis included PCA, PLS-DA and SIMCA performed using The Unscrambler® X software (version 10.2, Camo ASA, Norway).

PCA analysis was used as an exploratory technique to investigate the similarities and differences between the chemical footprints of the different treatments.

PLS-DA evaluated the ability to discriminate between the two LAB species/classes using different sets of data namely, quantified chemical data, FT-MIR spectral data as well as PCA score values from preliminary PCA models as x variables. A y dummy variable, -1 or + 1 was assigned to *O. oeni* (+1) and to *L. plantarum* (-1).

Full cross validation was used as the validation method for establishing models using PCA and PLS-DA. The correlation coefficient (R^2) was used to report the "goodness" of the model for future prediction purposes. The quantified chemical data was pre-treated by autoscaling (mean centering and standardisation, 1/Stdev) to avoid the interferences of differences in measurement units and to give each variable an equal chance of influencing the model components. A constant weighting of 1.00 was used for the spectroscopic data. No spectral pre-treatment was used.

Although the full spectrum (5011 - 929 cm^{-1}) was recorded a reduced spectral range was used and included wavenumbers 965 to 1582 cm^{-1}, 1698 to 2006 cm^{-1} and 2701 to 2971 cm^{-1}. The regions 1582 to 1698 cm^{-1} and 2971- 3627 cm^{-1} include a large amount of noise in the data from water absorption while the region from 3627 to 5011 cm^{-1} contains very little important information (Patz *et al*., 2004).

SIMCA analysis was used as exploratory metabolic profiling technique to investigate the ability to differentiate between LAB treatments at a particular process stage using both chemical quantified data and FT-MIR spectral data. The SIMCA analysis involved setting up two training sets respectively, "*O. oeni*" (n=4 for the quantified chemical data) (n=19 for the FT-MIR spectra) and "*L. plantarum*" (n=5 for the quantified chemical data) (n=17 for the FT-MIR spectra) which were modelled with separate PCA analyses. A test set (n=6 for the quantified chemical data) (n=24 for the FT-MIR spectra) was used to test the discrimination power of the model. The membership of test samples to the specific classes was defined at a significance level of 5%.

4.3 RESULTS AND DISCUSSION

4.3.1 COMPARISON OF THE VOLATILE COMPOSITION OF DIFFERENT TREATMENTS

Forty-one volatile compounds including higher alcohols, esters, fatty acids and carbonyl compounds were identified and quantified. **Table 4.2 and 4.3** lists the mean concentration (mg/L) ± standard deviation of the volatile compounds and chemical composition (pH, titratable acidity, volatile acidity) quantified at 50% and 100% completion of MLF for the different

treatments in both the inoculation strategies. **Figure 4.2** summarises the total mean concentrations (mg/L) of higher alcohols, esters and fatty acids for each of the treatments in both inoculation strategies at 50% and 100% completion of MLF. **Figure 4.3** shows the total mean concentration of the carbonyl compounds at 100% completion of MLF.

In general all the treatments completed MLF (**data shown in Chapter 3 section 3.3.1**). During MLF an increase was observed for the total ester and fatty acid concentrations while the higher alcohol concentration remained relatively constant (**Figure 4.2**). The spontaneous control had similar concentrations of higher alcohols and fatty acids at the end of MLF to those observed in the sequential treatments, while the control had the highest ester concentration. In general, a higher concentration of total higher alcohols, fatty acids, esters and carbonyl compounds was observed in sequential inoculation strategy compared to co-inoculation (**Figures 4.2 and 4.3**). The spontaneous control, however, had the lowest total carbonyl concentrations (**Figure 4.3**). The results (**Tables 4.2 and 4.3**) showed that the volatile composition of the Shiraz treatments was influenced due to MLF, however, the abundance of the volatile compounds was dependent on the specific LAB treatment and the inoculation strategy.

The contribution of certain volatile compounds to the discrimination between LAB treatments will be further explored by the following univariate and multivariate approach.

Table 4.2 Mean concentrations (mg/L) of volatile compounds (higher alcohols, esters, fatty acids and carbonyl compounds) and wine parameters (pH, volatile acidity and titratable acidity) determined in this study at 50% and 100% completion of MLF for the co-inoculated Shiraz treatments. Concentrations represent the means of triplicate treatment repeats, each analysed in duplicate by GC-FID and in single injections for GC-MS. The significant p-values based on the F-test are highlighted in red (p<0.05). The different alphabetic letters row-wise indicate significant differences based on the LSD post-hoc tests (p<0.05). Variable numbers are indicated.

Variable numbers		Co-inoculation											
		50% MLF						100% MLF					
		S5	VP	V2	56	MX	*p* value	S5	VP	V2	56	MX	*p* value
	Higher Alcohols												
6	Methanol	117.13 ± 35.34c	139.55 ± 2.44cb	178.1 ± 6.77a	182.19 ± 22.88a	164.15 ± 9.23ab	0.01	153.14 ± 1.36	180.34 ± 16.94	188.5 ± 11.2	189.87 ± 24.18	184.77 ± 7.45	0.06
8	Propanol	60.61 ± 15.15b	69.9 ± 1.41ab	82.91 ± 3.43a	79.01 ± 5.91a	83.5 ± 5.17a	0.02	71.29 ± 2.27c	79.16 ± 7.66cb	95.29 ± 5.16a	88.64 ± 10ab	84.37 ± 5.44ab	0.01
9	Isobutanol	23.5 ± 4.05c	27.18 ± 1.25cb	31.17 ± 1.35ab	30.05 ± 0.89ab	31.81 ± 2.65a	<0.01	28.67 ± 0.69c	31.48 ± 1.06cb	37.49 ± 0.63a	33.76 ± 3.16ab	32.57 ± 4.04cb	0.01
11	Butanol	1.9 ± 0.27c	2.42 ± 0.07b	2.83 ± 0.15a	2.78 ± 0.02a	2.89 ± 0.25a	<0.01	2.55 ± 0.02c	2.87 ± 0.06bc	3.39 ± 0.11a	3.08 ± 0.19ab	2.96 ± 0.36b	<0.01
12	Isoamyl Alcohol	234.13 ± 27.08b	272.33 ± 7.14ab	305.56 ± 20.97a	295.3 ± 6.39a	307.56 ± 36.48a	0.01	289.75 ± 1.18	302.81 ± 13.88	323.07 ± 5.03	301.51 ± 23.19	296.96 ± 39.33	0.45
17	Hexanol	3.51 ± 0.4c	4.3 ± 0.22cb	5.08 ± 0.48ab	5.22 ± 0.26a	4.94 ± 0.67ab	<0.01	4.58 ± 0.07	4.89 ± 0.4	4.44 ± 0.11	4.23 ± 0.41	4.19 ± 0.14	0.05
28	2-Phenylethanol	46.34 ± 4.53b	51.87 ± 1.57ab	57.65 ± 2.02a	57.15 ± 2.11a	56.54 ± 7.3a	0.03	54.38 ± 0.59	56.44 ± 3.44	52.18 ± 0.9	45.74 ± 11	43.42 ± 2.23	0.05
14	Pentanol	0.13 ± 0.01b	0.14 ± 0.01ab	0.16 ± 0.01a	0.15 ± 0.01a	0.16 ± 0.02a	0.03	0.15 ± 0	0.16 ± 0.01	0.18 ± 0.014	0.16 ± 0.01	0.16 ± 0.02	0.15
	4-Methyl-1-pentanol	nd	nd	nd	nd	nd		nd	nd	nd	nd	nd	
15	3-Methyl-1-Pentanol	0.07 ± 0.01b	0.1 ± 0.01a	0.13 ± 0.02a	0.13 ± 0.01a	0.12 ± 0.02a	<0.01	0.12 ± 0ab	0.14 ± 0.02a	0.12 ± 0b	0.11 ± 0.01b	0.11 ± 0.01b	0.02
	1-Octen-3-ol	nd	nd	nd	nd	nd		nd	nd	nd	nd	nd	
18	3-ethoxy-1-propanol	2.51 ± 0.59	2.53 ± 0.06	2.9 ± 0.16	2.87 ± 0.08	2.79 ± 0.39	0.46	2.7 ± 0.12	2.63 ± 0.31	2.55 ± 0.14	2.72 ± 0.03	2.46 ± 0.21	0.46
	Total higher alcohols	489.83	570.32	666.49	654.85	654.46		607.33	660.92	707.21	669.82	651.97	
	Esters												
5	Ethyl Acetate	32.97 ± 5.62c	45.22 ± 7.84b	61.7 ± 4.36a	57.45 ± 3.93a	55 ± 5.07ab	<0.01	55.9 ± 0.62b	60.79 ± 5.69b	87.84 ± 3.38a	61.26 ± 7.48b	82.26 ± 2.87a	<0.01
7	Ethyl Butyrate	0.18 ± 0.01d	0.22 ± 0.01c	0.27 ± 0b	0.3 ± 0.01a	0.25 ± 0.01b	<0.01	0.25 ± 0.01c	0.31 ± 0b	0.35 ± 0.01a	0.32 ± 0.03ab	0.3 ± 0.03b	<0.01
10	Isoamyl Acetate	0.97 ± 0.18c	1.24 ± 0.12bc	1.46 ± 0.09b	1.9 ± 0.06a	1.77 ± 0.25a	<0.01	1.4 ± 0.03c	1.88 ± 0.13ab	2.05 ± 0.08a	1.63 ± 0.1bc	1.72 ± 0.25b	<0.01
13	Ethyl Hexanoate	0.4 ± 0.05c	0.44 ± 0.02cb	0.55 ± 0.02a	0.48 ± 0.02ab	0.5 ± 0.07ab	<0.01	0.54 ± 0a	0.53 ± 0.04a	0.47 ± 0.01b	0.52 ± 0.05a	0.41 ± 0.01c	<0.01
	Hexyl Acetate	< LOQ	< LOQ	< LOQ	< LOQ	< LOQ		< LOQ	< LOQ	< LOQ	< LOQ	< LOQ	
16	Ethyl Lactate	9.45 ± 1.5	13.08 ± 0.63	10.85 ± 5.76	6.3 ± 0.02	9.11 ± 0.71	0.11	18.31 ± 0.4c	23.03 ± 0.75b	29.53 ± 1.21a	23.89 ± 2.3b	25.02 ± 2.56b	<0.01

Table 4.2 (cont.)

19	Ethyl Caprylate	0.15 ± 0.06	0.18 ± 0.06	0.19 ± 0.02	0.21 ± 0.09	0.23 ± 0.06	0.57	0.15 ± 0.01b	0.27 ± 0.03a	0.27 ± 0.02a	0.21 ± 0.05b	0.16 ± 0.04b	<0.01
	Ethyl caprate	< LOQ	< LOQ	< LOQ	< LOQ	< LOQ		< LOQ	< LOQ	< LOQ	< LOQ	< LOQ	
25	Diethyl Succinate	0.39 ± 0.02c	0.39 ± 0.01c	0.67 ± 0.03a	0.49 ± 0.02b	0.42 ± 0.03c	<0.01	0.72 ± 0.02b	0.51 ± 0.03b	0.6 ± 0.01b	1.23 ± 0.46a	0.68 ± 0.04b	0.01
26	2-Phenylethyl Acetate	0.47 ± 0.02ab	0.46 ± 0.01cd	0.42 ± 0.02d	0.43 ± 0.02cd	0.5 ± 0.03a	<0.01	0.4 ± 0	0.42 ± 0.02	0.42 ± 0	0.39 ± 0.02	0.39 ± 0.01	0.05
	Ethyl Propionate	nd	nd	nd	nd	nd		nd	nd	nd	nd	nd	
	Ethyl phenylacetate	< LOQ	< LOQ	< LOQ	< LOQ	< LOQ		< LOQ	< LOQ	< LOQ	< LOQ	< LOQ	
	2-Methyl-propyl acetate	nd	nd	nd	nd	nd		nd	nd	nd	nd	nd	
	Ethyl isovalerate	nd	nd	nd	nd	nd		nd	nd	nd	nd	nd	
	Ethyl-3-hydroxybutanoate	< LOQ	< LOQ	< LOQ	< LOQ	< LOQ		< LOQ	< LOQ	< LOQ	< LOQ	< LOQ	
	Ethyl-2-methylpropanoate	nd	nd	nd	nd	nd		nd	nd	nd	nd	nd	
	Ethyl-2-methylbutyrate	nd	nd	nd	nd	nd		nd	nd	nd	nd	nd	
	Total esters	44.98	61.23	76.11	67.56	67.78		77.67	87.74	121.53	89.45	110.94	
	Fatty Acids												
20	Acetic Acid	146.78 ± 32c	174.98 ± 8.62cb	210.88 ± 10.87a	218.07 ± 4.22a	198.05 ± 24.7ab	<0.01	204.23 ± 4.72d	261.2 ± 13.92c	337.13 ± 18.1a	272.83 ± 33.71cb	307.84 ± 31.21ab	<0.01
21	Propionic Acid	2.3 ± 0.3c	2.73 ± 0.09cb	3.44 ± 0.17a	3.64 ± 0.54a	3.19 ± 0.34ab	<0.01	2.91 ± 0.11b	2.94 ± 0.04b	2.92 ± 0.09b	3.16 ± 0.1a	3.1 ± 0.15ab	0.04
22	Isobutyric Acid	1.15 ± 0.14c	1.38 ± 0.02b	1.58 ± 0.05a	1.5 ± 0.07ab	1.43 ± 0.17ab	<0.01	1.46 ± 0.05ab	1.57 ± 0.07a	1.38 ± 0.07b	1.37 ± 0.1b	1.38 ± 0.07b	0.04
23	Butyric acid	0.64 ± 0.04c	0.78 ± 0.02b	0.9 ± 0.04a	0.88 ± 0.02a	0.82 ± 0.12ab	<0.01	0.87 ± 0.01	0.93 ± 0.07	0.86 ± 0.05	0.84 ± 0.09	0.85 ± 0.03	0.41
24	Isovaleric acid	1.88 ± 0.19	2.17 ± 0.09	1.69 ± 1.47	2.53 ± 0.02	2.39 ± 0.31	0.55	2.4 ± 0.01	2.62 ± 0.17	2.44 ± 0.06	2.24 ± 0.45	2.25 ± 0.15	0.3
	Valeric Acid	< LOQ	< LOQ	< LOQ	< LOQ	< LOQ		< LOQ	< LOQ	< LOQ	< LOQ	< LOQ	
27	Hexanoic Acid	0.91 ± 0.05d	1.16 ± 0.11c	1.42 ± 0.14ab	1.5 ± 0.11a	1.26 ± 0.2cb	<0.01	1.34 ± 0.03	1.7 ± 0.14	1.6 ± 0.01	1.27 ± 0.33	1.36 ± 0.12	0.05
29	Octanoic Acid	0.63 ± 0.07cb	0.63 ± 0.03cb	0.59 ± 0.04c	0.78 ± 0.04a	0.69 ± 0.03ab	<0.01	0.58 ± 0.03d	0.85 ± 0.08a	0.81 ± 0.04ab	0.65 ± 0.08cd	0.72 ± 0.05cb	<0.01
30	Decanoic Acid	0.65 ± 0.22	0.49 ± 0.01	0.47 ± 0	0.5 ± 0.03	0.5 ± 0	0.27	0.47 ± 0	0.63 ± 0.19	0.5 ± 0.01	0.49 ± 0.01	0.51 ± 0.04	0.27
	Total fatty acids	154.94	184.32	220.97	229.40	208.33		214.26	272.44	347.64	282.85	318.01	
	Carbonyl compounds												
31	Diacetyl							4.34 ± 0.84	4.63 ± 0.1	4.02 ± 0.76	3.83 ± 0.34	4.83 ± 0.55	0.27
33	Acetoin							3.49 ± 0.08c	3.28 ± 0.02c	7.17 ± 0.02a	5.87 ± 0.01ab	4.86 ± 0.19cb	<0.01
32	2,3 pentanedione							0.37 ± 0.39bc	0.4 ± 0.31b	0.22 ± 0.45c	0.34 ± 0.43bc	0.6 ± 1.95a	<0.01
	Total carbonyl compounds							8.20	8.31	11.41	10.04	10.29	

Table 4.2 (cont.)

	Wine parameters										
3	Titratable acidity	4.15	3.73	3.92	3.95	3.92	3.41	3.41	3.39	3.45	3.39
4	pH	3.59	3.70	3.68	3.70	3.68	3.75	3.78	3.82	3.73	3.78
1	Volatile acidity	0.14	0.15	0.19	0.22	0.16	0.25	0.28	0.28	0.28	0.28

nd: not detected; LOQ: Limit of quantification
50% MLF refers to 50% completion of malic acid degradation; 100% MLF refers to 100% completion of malic acid degradation

Table 4.3 Mean concentrations (mg/L) of volatile compounds (higher alcohols, esters, fatty acids and carbonyl compounds) and wine parameters (pH, volatile acidity and titratable acidity) determined in this study at 50% and 100% completion of MLF for the Sequential Shiraz treatments. Concentrations represent the means of triplicate treatment repeats, each analysed in duplicate by GC-FID and in single injections for GC-MS. The significant p-values based on the F-test are highlighted in red (p<0.05). The different alphabetic letters row-wise indicate significant differences based on the LSD post-hoc tests (p<0.05). Variable numbers are indicated.

Variable numbers		Sequential inoculation												
		50% MLF						100% MLF						
		S5	**VP**	**V2**	**56**	**MX**	***p* value**	**S5**	**VP**	**V2**	**56**	**MX**	**CN**	***p* value**
	Higher Alcohols													
6	Methanol	274.53 ± 17.17	254.62 ± 7.55	259.92 ± 5.18	284.05 ± 27.06	274.65 ± 9.04	0.2	273.56 ± 6.64a	273.96 ± 23.24a	243.3 ± 6.78b	263.45 ± 7.18ab	250.51 ± 7.46b	247.72 ± 5.69	0.04
8	Propanol	71.35 ± 2.43cb	69.09 ± 1.79c	71.81 ± 1.33ac	75.85 ± 3.57ab	76.23 ± 2.83a	0.02	72.77 ± 3.85	72.36 ± 4.54	71.52 ± 4.28	75.66 ± 3.18	73.72 ± 3.26	71.53 ± 3.63	0.73
9	Isobutanol	40.56 ± 1.8b	40.6 ± 0.76b	40.78 ± 0.53b	41.98 ± 1.03b	44.05 ± 0.83a	0.01	42.72 ± 1.4	42.86 ± 2.02	42.56 ± 1.63	42.591 ± 2.27	43.51 ± 2.06	42.4 ± 1.34	0.98
11	Butanol	3.05 ± 0.11ab	2.95 ± 0.07b	2.97 ± 0.04b	3.06 ± 0.13ab	3.2 ± 0.04a	0.04	3.12 ± 0.09	3.25 ± 0.2	3.16 ± 0.08	3.08 ± 0.18	3.1 ± 0.16	3.22 ± 0.17	0.65
12	Isoamyl Alcohol	273.44 ± 7.13	263.51 ± 2.97	263.78 ± 2.58	266.57 ± 12.25	276.45 ± 6.77	0.17	276.15 ± 8.85	282.77 ± 14.68	280.06 ± 6.3	273.18 ± 5.46	278.42 ± 2.22	274.97 ± 5.66	0.71
17	Hexanol	3.4 ± 0.07	3.41 ± 0.04	3.36 ± 0.02	3.35 ± 0.36	3.44 ± 0.15	0.96	3.46 ± 0.03	3.68 ± 0.17	3.52 ± 0.13	3.44 ± 0.06	3.38 ± 0.13	3.28 ± 0.08	0.08
28	2-Phenylethanol	49.97 ± 1.39	50.02 ± 0.82	50.34 ± 0.41	50.43 ± 3.09	50.87 ± 2.78	0.98	50.92 ± 3.44	52.87 ± 1.99	51.06 ± 1.28	49.32 ± 2.67	49.9 ± 0.66	50.69 ± 0.18	0.41
14	Pentanol	0.29 ± 0.05	0.244 ± 0.01	0.25 ± 0	0.24 ± 0.01	0.26 ± 0	0.2	0.26 ± 0.01	0.6 ± 0.01	0.26 ± 0	0.24 ± 0.02	0.25 ± 0	0.26 ± 0.01	0.22
	4-Methyl-1-pentanol	nd	nd	nd	nd	nd		nd	nd	nd	nd	nd	nd	
15	3-Methyl-1-Pentanol	0.0432212 ± 0	0.04 ± 0	0.04 ± 0	0.04 ± 0.01	0.04 ± 0	0.6	0.05 ± 0a	0.05 ± 0.01ab	0.05 ± 0cb	0.04 ± 0c	0.05 ± 0cb	0.04 ± 0	0.01
	1-Octen-3-ol	nd	nd	nd	nd	nd		nd	nd	nd	nd	nd	nd	
18	3-ethoxy-1-propanol	2.41 ± 0.33	2.23 ± 0.04	2.23 ± 0.02	2.37 ± 0.06	2.25 ± 0.07	0.51	2.29 ± 0.06	2.34 ± 0.17	2.12 ± 0.09	2.35 ± 0.2	2.16 ± 0.15	2.24 ± 0.07	0.25
	Total higher alcohols	719.04	686.71	695.48	727.94	731.44		725.30	734.74	697.61	713.35	705.00	696.35	

Table 4.3 (cont.)

	Esters													
5	Ethyl Acetate	64.39 ± 2.05	63.84 ± 1.23	65.75 ± 0.95	68.65 ± 3.31	65.37 ± 2.27	0.13	64.06 ± 2.75a	59.91 ± 3.51ac	57.31 ± 1.54cb	60.98 ± 1.96ab	56.76 ± 0.77c	60.23 ± 2.66	0.02
7	Ethyl Butyrate	0.24 ± 0.01	0.24 ± 0	0.23 ± 0	0.23 ± 0.01	0.24 ± 0.01	0.64	0.25 ± 0.01	0.26 ± 0.01	0.26 ± 0	0.25 ± 0	0.26 ± 0	0.264 ± 0	0.59
10	Isoamyl Acetate	0.6 ± 0.03	0.6 ± 0	0.59 ± 0	0.57 ± 0.06	0.63 ± 0.03	0.38	0.7 ± 0.01	0.72 ± 0.05	0.71 ± 0.01	0.67 ± 0.03	0.7 ± 0.02	0.7 ± 0.01	0.33
13	Ethyl Hexanoate	0.34 ± 0.01	0.33 ± 0.01	0.33 ± 0.01	0.32 ± 0.02	0.35 ± 0.01	0.33	0.39 ± 0.01	0.4 ± 0.02	0.4 ± 0.02	0.38 ± 0.01	0.4 ± 0.01	0.39 ± 0.01	0.44
	Hexyl Acetate	< LOQ	< LOQ	< LOQ	< LOQ	< LOQ		< LOQ	< LOQ	< LOQ	< LOQ	< LOQ	< LOQ	
16	Ethyl Lactate	36.7 ± 2.95	35.07 ± 2.76	36.65 ± 0.95	40.32 ± 0.97	37.9 ± 2.28	0.11	53.81 ± 1.2b	60.85 ± 4.48a	66.19 ± 0.56a	65.88 ± 3.79a	61.46 ± 4.05a	89.66 ± 0.79	<0.01
19	Ethyl Caprylate	0.16 ± 0.04	0.19 ± 0.02	0.16 ± 0.01	0.15 ± 0.03	0.16 ± 0.01	0.41	0.24 ± 0.01	0.28 ± 0.04	0.26 ± 0.03	0.22 ± 0.02	0.22 ± 0.02	0.2 ± 0.02	0.05
	Ethyl caprate	< LOQ	< LOQ	< LOQ	< LOQ	< LOQ		< LOQ	< LOQ	< LOQ	< LOQ	< LOQ	< LOQ	
25	Diethyl Succinate	0.91 ± 0.12c	0.96 ± 0.08cb	1.21 ± 0.21a	1.17 ± 0.13ab	1.09 ± 0.11ac	0.09	2.07 ± 0.02	2.55 ± 0.28	2.6 ± 0.39	2.45 ± 0.11	2.47 ± 0.3	3.37 ± 0.17	0.17
26	2-Phenylethyl Acetate	0.37 ± 0.05	0.33 ± 0	0.33 ± 0	0.33 ± 0.01	0.33 ± 0	0.21	0.34 ± 0ab	0.33 ± 0.01c	0.33 ± 0cb	0.33 ± 0c	0.34 ± 0a	0.32 ± 0	0.03
	Ethyl Propionate	nd	nd	nd	nd	nd		nd	nd	nd	nd	nd	nd	
	Ethyl phenylacetate	< LOQ	< LOQ	< LOQ	< LOQ	< LOQ		< LOQ	< LOQ	< LOQ	< LOQ	< LOQ	< LOQ	
	2-Methyl-propyl acetate	nd	nd	nd	nd	nd		nd	nd	nd	nd	nd	nd	
	Ethyl isovalerate	nd	nd	nd	nd	nd		nd	nd	nd	nd	nd	nd	
	Ethyl-3-hydroxybutanoate	< LOQ	< LOQ	< LOQ	< LOQ	< LOQ		< LOQ	< LOQ	< LOQ	< LOQ	< LOQ	< LOQ	
	Ethyl-2-methylpropanoate	nd	nd	nd	nd	nd		nd	nd	nd	nd	nd	nd	
	Ethyl-2-methylbutyrate	nd	nd	nd	nd	nd		nd	nd	nd	nd	nd	nd	
	Total esters	103.71	101.56	105.25	111.74	106.07		121.86	125.30	128.06	131.16	122.61	155.14	
	Fatty Acids													
20	Acetic Acid	497.4 ± 13a	447.32 ± 29.45cb	413.57 ± 1.31c	449.13 ± 8cb	471.29 ± 42.47ab	0.02	577.95 ± 29.79	602.66 ± 21.29	596.7 ± 19.55	571.14 ± 45.19	567.75 ± 25.16	602.04 ± 9.36	0.54
21	Propionic Acid	2.77 ± 0.36a	2.31 ± 0.06b	2.34 ± 0.02b	2.44 ± 0.08b	2.32 ± 0.08b	0.04	2.34 ± 0.06a	2.27 ± 0.13a	2.05 ± 0.13b	1.87 ± 0.15b	1.91 ± 0.05b	1.62 ± 0.04	<0.01
22	Isobutyric Acid	1.76 ± 0.1a	1.63 ± 0b	1.64 ± 0.02b	1.65 ± 0.05b	1.63 ± 0.04b	0.06	1.68 ± 0.06ab	1.68 ± 0.01a	1.62 ± 0.06ac	1.56 ± 0.05c	1.6 ± 0.04cb	1.52 ± 0.03	0.04
23	Butyric acid	1.12 ± 0.09a	0.98 ± 0.02b	1.02 ± 0.02b	1.01 ± 0.02b	0.98 ± 0.02b	0.02	0.99 ± 0.06	1.03 ± 0.06	0.96 ± 0.04	0.92 ± 0.05	0.9 ± 0.05	0.94 ± 0.06	0.08
24	Isovaleric acid	2.57 ± 0.16	2.26 ± 0.01	2.39 ± 0.08	2.37 ± 0.1	2.37 ± 0.1	0.05	2.31 ± 0.04	2.4 ± 0.04	2.33 ± 0.26	2.2 ± 0.01	2.14 ± 0.04	2.15 ± 0.09	0.16
	Valeric Acid	< LOQ	< LOQ	< LOQ	< LOQ	< LOQ		< LOQ	< LOQ	< LOQ	< LOQ	< LOQ	< LOQ	
27	Hexanoic Acid	1.93 ± 0.3a	1.52 ± 0.03b	1.54 ± 0.1b	1.43 ± 0.15b	1.45 ± 0.12b	0.02	1.72 ± 0.11	1.71 ± 0.15	1.66 ± 0.06	1.6 ± 0.01	1.55 ± 0.09	1.54 ± 0	0.34
29	Octanoic Acid	1.94 ± 1.44	1.06 ± 0.04	0.98 ± 0.03	0.89 ± 0.08	0.92 ± 0.11	0.31	1.24 ± 0.09	1.34 ± 0.1	1.2 ± 0.06	1.19 ± 0.05	1.22 ± 0.06	1.46 ± 0.08	0.16

Table 4.3 (cont.)

30	Decanoic Acid	0.6 ± 0.07a	0.53 ± 0.01b	0.5 ± 0.01b	0.5 ± 0.01b	0.5 ± 0.01b	0.01	0.61 ± 0.05	0.6 ± 0.02	0.58 ± 0.02	0.59 ± 0	0.56 ± 0.01	0.59 ± 0.01	0.26
	Total fatty acids	510.09	457.61	423.98	459.42	481.46		588.84	613.69	607.10	581.07	577.63	611.86	
	Carbonyl compounds													
31	Diacetyl							4.64 ± 0.87b	4.94 ± 2b	6.67 ± 1.05ab	8.09 ± 0.46a	6.11 ± 0.64ab	5.62 ± 0.93	0.02
33	Acetoin							10.59 ± 0.59d	10.08 ± 0.83d	17.48 ± 0.41b	19.19 ± 1.79a	13.6 ± 0.21c	0.92 ± 0.23	<0.01
32	2,3 pentanedione							0.07 ± 0.03	0.09 ± 0.05	0.08 ± 0.02	0.09 ± 0.02	0.1 ± 0.03	0.1 ± 0.01	0.83
	Total carbonyl compounds							15.30	15.11	24.23	27.37	19.81	6.64	
	Wine parameters													
3	Titratable acidity	3.20	3.16	3.28	3.33	3.33		2.92	2.91	2.89	2.90	2.89	2.90	
4	pH	3.90	3.90	3.88	3.78	3.88		3.93	3.93	3.92	3.93	3.94	3.93	
1	Volatile acidity	0.33	0.32	0.31	0.31	0.33		0.40	0.40	0.40	0.41	0.41	0.41	

nd: not detected; LOQ: Limit of quantification

50% MLF refers to 50% completion of malic acid degradation; 100% MLF refers to 100% completion of malic acid degradation

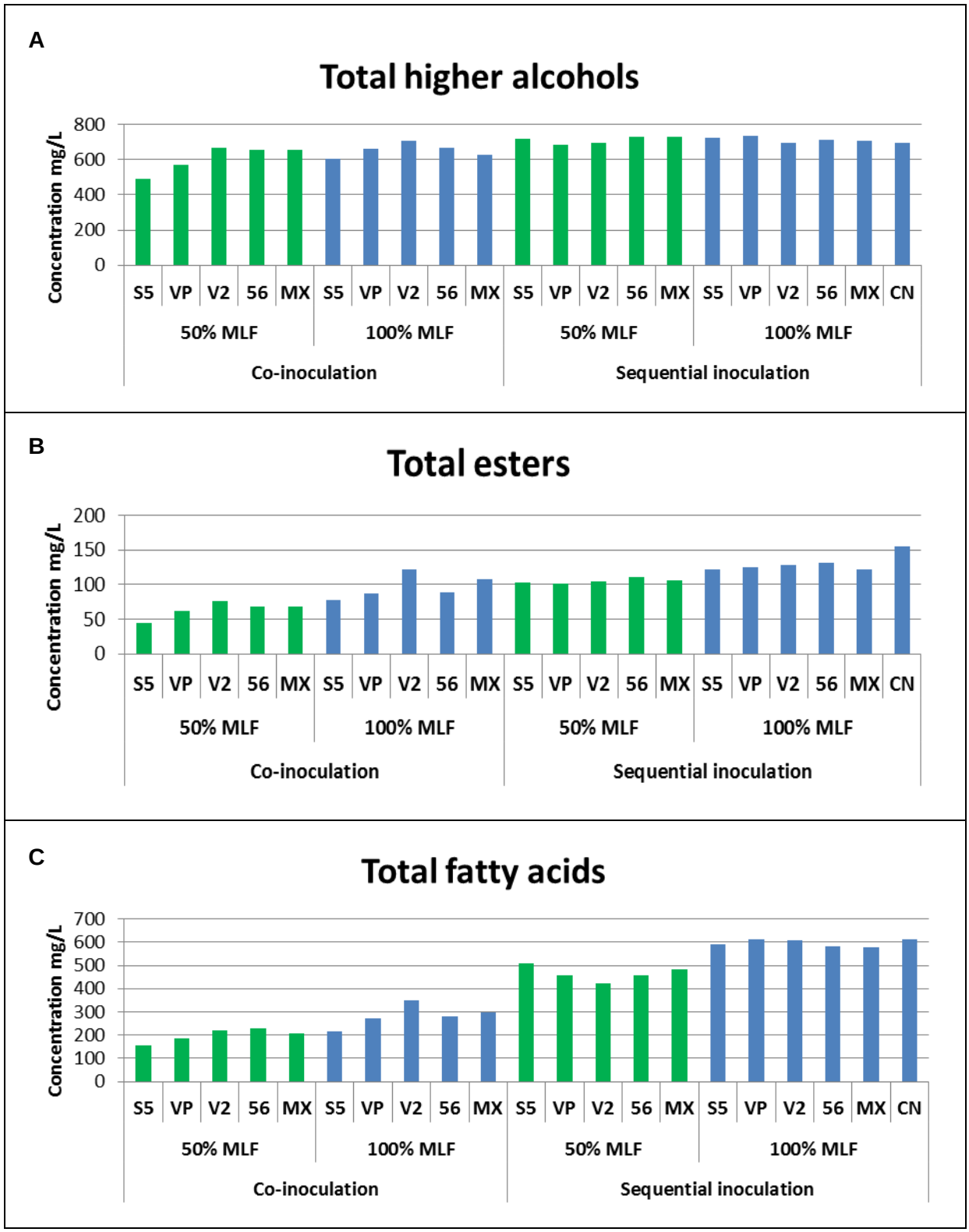

Figure 4.2 A) Total higher alcohol, **B)** ester and **C)** fatty acid changes as a result of MLF evaluating the different LAB in the co-inoculation and the sequential inoculation treatments. Each value represents the average of triplicate treatments analysed in duplicate by GC-FID.

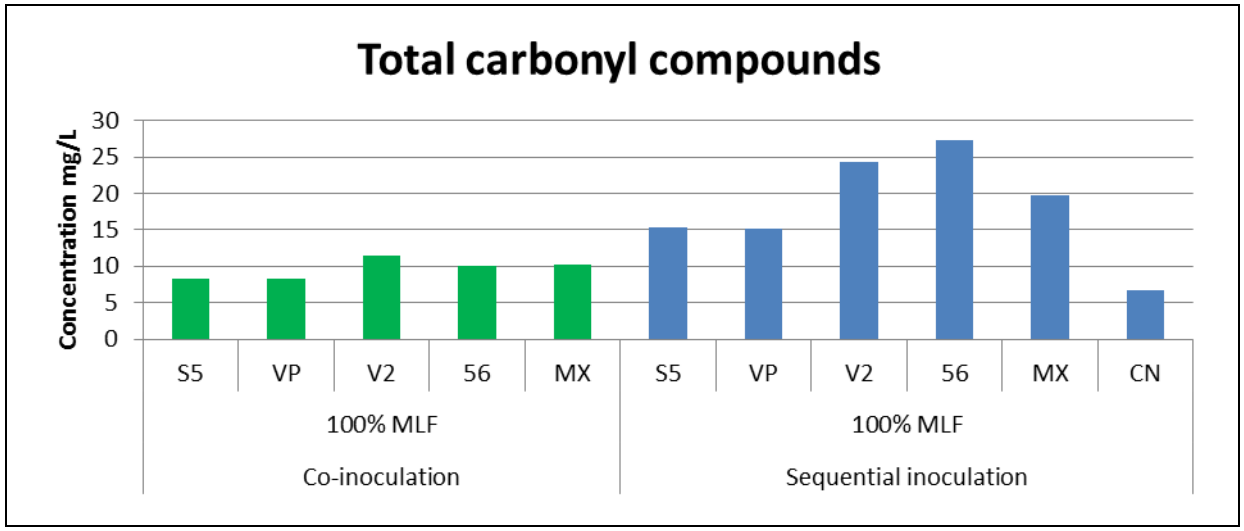

Figure 4.3 Total carbonyl compounds at the end of MLF evaluating the different LAB in the co-inoculation and the sequential inoculation treatments. Each value represents the average of triplicate treatments analysed by GC-MS.

4.3.2 PROFILING OF LAB WITHIN AN INOCULATION STRATEGY

4.3.2.1 UNIVARIATE APPROACH TO PROFILING: ANOVA

For the purpose of this study ANOVA was used as a tool to identify the quantified volatile compounds (variables) which were important for the discrimination between the different LAB treatments at each specific time point separately for the inoculation strategies (control samples excluded). **Tables 4.2 and 4.3** indicate the compounds showing significant differences between the LAB in the co-inoculation and sequential inoculation strategies respectively. Alphabetic letters indicate the significant differences between the LAB treatments based on their mean values for a specific volatile compound.

The results of this univariate study will be used for the variable selection process followed in subsequent multivariate strategy.

CO-INOCULATION STRATEGY

50% COMPLETION OF MLF

Twenty-one out of the 26 volatile compounds had significantly different means according to the LAB strains (**Table 4.2**). Only five volatile compounds were not significantly different for the LAB strains which included 3-ethoxy-1-proponol, ethyl lactate, ethyl caprylate, isovaleric acid and decanoic acid. The trends in the quantified data at 50% completion of MLF show that the *O. oeni* strains namely S5 and VP have significantly similar concentrations of higher alcohols, esters and fatty acids while the *L. plantarum* strains are significantly similar in most cases. Treatment MX tends to be similar to the concentrations found for the *L. plantarum* and *O. oeni* strains depending on the specific volatile compound. In most cases the *L. plantarum* strains

have higher concentrations to those found in the *O. oeni* strains, however, this is compound dependant. It was observed that in some cases treatment S5 was significantly lower in concentration to all the other treatments. Treatment S5 showed significantly lower concentrations for ethyl acetate, ethyl butyrate, butanol, 3-methyl-1-pentanol, isobutyric acid, butyric acid and hexanoic acid.

The differences observed at 50% completion of MLF can therefore be attributed to a large number of variables and shows the importance of the majority of the variables for the separation between LAB at 50% completion of MLF in this univariate study.

Differences in the significant ester concentrations for the LAB treatments at 50% can be observed in the radar plot (**Figure 4.4A**). Ethyl acetate was not shown due to its much higher concentrations.

100% COMPLETION OF MLF

Seventeen out of 29 compounds had significantly different means according to the LAB strains (**Table 4.2**). The compounds showing significant differences between the means of the LAB treatments included the higher alcohols namely propanol, isobutanol, butanol and 3-methyl-1-pentanol, esters namely ethyl acetate, ethyl butyrate, isoamyl acetate, ethyl hexanoate, ethyl lactate, ethyl caprylate and diethyl succinate as well as the fatty acids namely acetic acid, propionic acid, isobutyric acid and octanoic acid. The concentration of the carbonyl compound, diacetyl, was not significantly different for the different LAB treatments at 100% completion of MLF, however, significant differences between LAB were seen for acetoin and 2,3-pentanedione.

The trends in the quantified data at 100% completion of MLF show that the *O. oeni* strains and the *L. plantarum* strains are not as well distinguished as observed at 50% completion of MLF in terms of their mean values. The quantified values of *O. oeni* and *L. plantarum* are in some cases significantly similar depending on the specific volatile compound. At 100% completion of MLF the volatile profiles of these LAB are therefore more similar than at 50% completion of MLF. This was seen in a study by Knoll *et al*. (2012) where discrimination between LAB strains was more prominent with early inoculation compared with sequential inoculation.

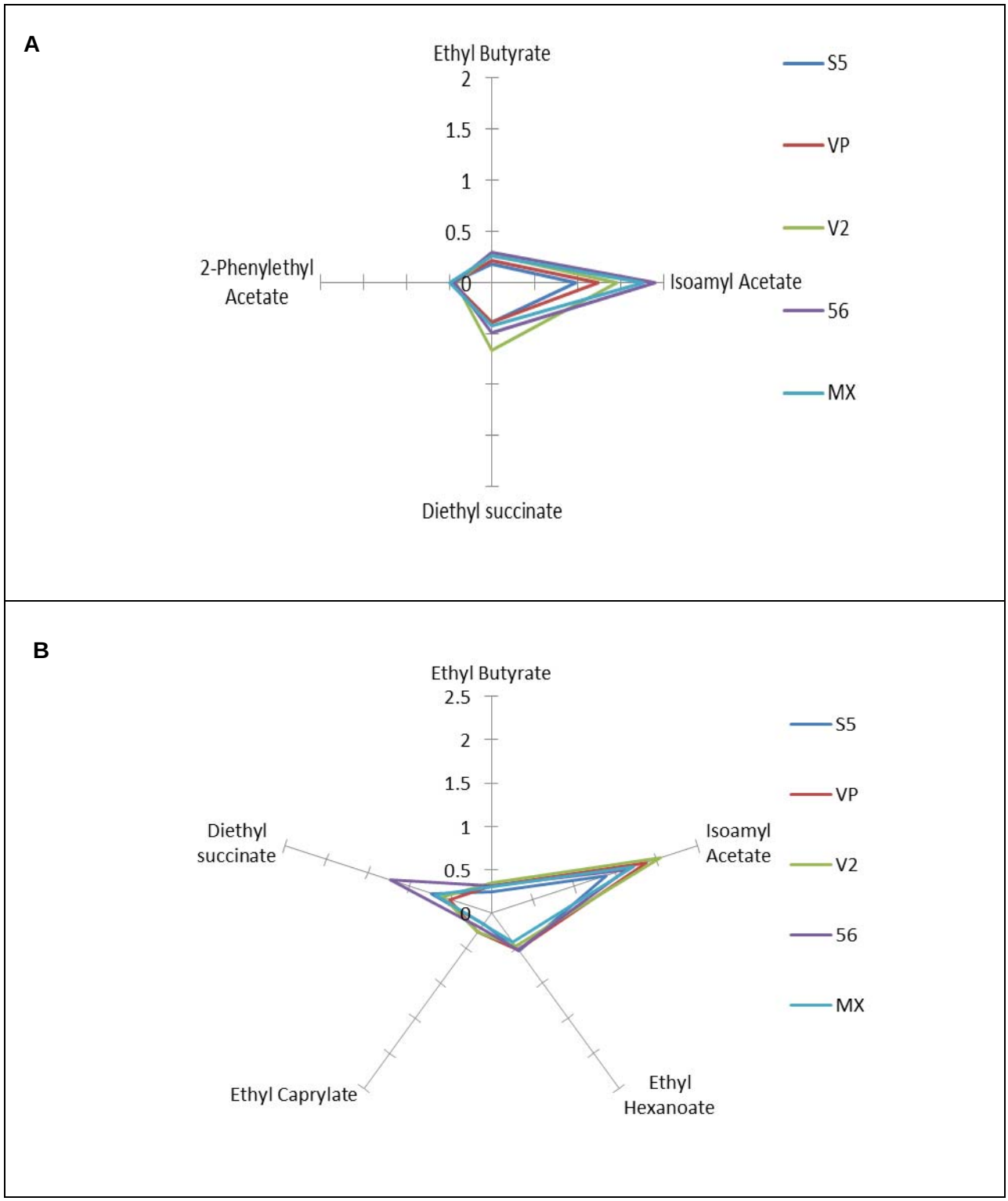

Figure 4.4 Radar plots indicating the significant esters showing mean concentration differences between the co-inoculated LAB treatments at **A)** 50% completion of MLF (ethyl acetate was removed due to its much higher concentrations) and **B)** 100% completion of MLF (ethyl acetate and ethyl lactate were removed due to their much higher concentrations).

Treatment S5 doesn't show as much difference to the other LAB treatments as that observed at 50% completion of MLF. This treatment does, however, show significantly lower values for ethyl lactate and acetic acid. Treatment V2 shows a significantly lower concentration for ethyl hexanoate while having the significantly higher ethyl lactate concentration. Treatment 56 shows the significantly highest concentration of diethyl succinate while treatment MX shows the

significantly lowest ethyl hexanoate concentration and the highest 2,3-pentanedione concentration. The *O. oeni* treatments S5 and VP (similar concentrations) showed significantly lower acetoin concentrations compared with the *L. plantarum* treatments.

Compared with the 50% completion of MLF, fewer volatile compounds showed significant differences between the LAB strains. Fewer variables are therefore contributing to the separation between the LAB strains at 100% completion of MLF compared to 50% completion of MLF in this univariate study.

Interesting to mention is the three compounds which were not significant at both process stages including 3-ethoxy-1-propanol, isovaleric acid and decanoic acid.

Differences in the significant ester concentrations for the LAB treatments at 100% can be observed in the radar plot (**Figure 4.4B**). Ethyl acetate and ethyl lactate were removed due to their much higher concentrations.

SEQUENTIAL INOCULATION STRATEGY

50% COMPLETION OF MLF

Nine out of the 26 volatile compounds quantified had significantly different means according to the LAB strains (**Table 4.3**). These included propanol, isobutanol, butanol, diethyl succinate, acetic acid, propionic acid, isobutyric acid, butyric acid, hexanoic acid and decanoic acid.

Very subtle differences were observed between the *O. oeni* strains S5 and VP as well as *L. plantarum* V2 and 56 with some degree of overlap seen for some significant volatile compounds. The main treatment contributing to the significance difference in most cases was treatment S5. Treatment S5 had significantly higher concentrations compared with other treatments for propionic acid, isobutyric acid, butyric acid, hexanoic acid and decanoic acid. Treatment MX had a significantly higher concentration of isobutanol compared to the other treatments.

100% COMPLETION OF MLF

Nine out of 29 compounds had significantly different means according to the LAB strains (**Table 4.3**). These variables included methanol, 3-methyl-1-pentanol, ethyl acetate, ethyl lactate, 2-phenylethyl acetate, propionic acid, isobutyric acid, diacetyl and acetoin.

Once again very subtle differences were observed between the *O. oeni* strains S5 and VP as well as *L. plantarum* V2 and 56 with some degree of overlap seen for these significant volatile compounds. Treatment S5 once again showed a significantly lower ethyl lactate concentration compared to the other treatments as seen in the co-inoculation treatments at 100% completion of MLF. The *O. oeni* treatments S5 and VP (similar concentrations) once again showed significantly lower acetoin concentrations compared with the *L. plantarum*

treatments and treatment MX which all differed significantly from each other. Treatment 56 had significantly higher concentrations of acetoin.

This univariate study indicated the apparent differences between the volatile profiles of LAB treatments at specific process stages within the fermentation. These results are in accordance with previous literature which shows changes in volatile compounds after MLF in red grape varietals (Maicas *et al*., 1999; Pozo-Bayón *et al*., 2005). The results of the univariate approach showed more prominent differences in the profiles between the LAB treatments in the co-inoculation strategy compared with the sequential inoculation strategy. 50% completion of MLF in the co-inoculation strategy seemed to yield the most distinct LAB profile differences. This is in accordance with a study showing that co-inoculation had the most distinct profile when comparing different inoculation strategies in Australian Shiraz wines (Abrahamse & Bartowsky, 2012).

Wine, however, is a constantly changing matrix to due to chemical equilibria and thus the significant differences that are observed should not only be ascribed to the specific treatments. Furthermore, our observations were only obtained for one year and thus it is important for us realise the possibility of over interpretation of the results. The observations reported here point to the possibility of further in-depth profiling analysis for future studies in order to make more definite conclusions.

The general trends observed for the different chemical groups namely esters, higher alcohols, fatty acids and carbonyl compounds will be discussed in the following sections.

ESTERS

Esters are mainly produced via yeast metabolism during AF and contribute largely to the fruity aroma in wine (Lilly *et al*., 2000), however, reports have also shown the ability of LAB to alter the ester content during MLF suggesting the potential esterase activities of wine LAB (Matthews *et al*., 2004). The extent to which LAB influence the ester concentration during MLF is, however, not fully understood and is still being evaluated (Swiegers *et al*., 2005).

As previously mentioned the total ester concentrations increased during MLF, however, this was dependant on the specific individual ester compound as well as the inoculation strategy and LAB strain used (**Tables 4.2 and 4.3**). The total ester concentrations at the end of MLF for the co-inoculated treatments ranged from 80 to 120 mg/L, while the sequential treatments had total ester concentrations ranging from 120 to 130 mg/L. The total ester contribution to the volatile composition was mainly due to ethyl acetate (50-90 mg/L), ethyl lactate (18-70 mg/L), isoamyl acetate (0.7-2.05 mg/L) and diethyl succinate (0.6-2.6 mg/L) concentrations. Ethyl acetate is the main ester occurring in wine, found in highest abundance (Lambrechts & Pretorius, 2000), while ethyl lactate, together with diethyl succinate, have been shown to be the two most important esters typically associated with MLF (Maicas *et al*., 1999; Herjavec *et al*.,

2001; Ugliano & Moio, 2005). The ethyl acetate concentrations reported this study are known to add to the complexity of wine as well as having a positive impact on the quality of wine by adding to the fruitiness (Ribéreau-Gayon *et al.*, 2006).

The two esters which were significantly different for the LAB treatments at the end of MLF for both inoculation strategies included ethyl acetate and ethyl lactate (**Tables 4.2 and 4.3**). In the co-inoculated treatments ethyl butyrate, isoamyl acetate, ethyl hexanoate, ethyl caprylate and diethyl succinate were significantly different for the LAB treatments at the end of MLF (**Table 4.2**) while 2-phenylethyl acetate was significant for the sequential inoculation strategy (**Table 4.3**). These results correspond to previous studies which all showed strain specific differences in ethyl acetate, ethyl lactate and diethyl succinate concentrations during MLF (Ugliano & Moio, 2005; Pozo-Bayon *et al*., 2005; Izquierdo Cañas *et al*., 2008; Boido *et al*., 2009; Knoll *et al*., 2011). The reported increase in diethyl succinate by Lee *et al*. (2009a) showed differences between different *O. oeni* strains which indicated different behaviours of esterases produced by LAB strains. Lee *et al*. (2009b) on the other hand, reported no significant differences between diethyl succinate concentrations of wines inoculated with *L. plantarum* and *O. oeni*, indicating that the esterification of succinate to diethyl succinate is not dependent on LAB genera. With this said, however, contradicting reports have shown either an increase or a decrease in the total ester concentration during MLF (Maicas *et al*., 1999; Delaquis *et al*., 2000; Matthews *et al*., 2004; Pozo Bayón *et al*., 2005; Ugliano & Moio, 2005; Izquierdo Cañas *et al*., 2008; Boido *et al*., 2009).

HIGHER ALCOHOLS

Higher alcohols are formed during fermentation due to amino acid biosynthesis by yeasts and are said to have an impact on wine aroma and flavour (Swiegers *et al*., 2005). At optimal concentrations, these higher alcohols can add to the wine complexity and fruity character, however, at higher concentrations (above 400 mg/L) these alcohols can impart harsh solvent like aromas to the wine and negatively affect the wine character (Swiegers *et al*., 2005).

In this study, higher alcohols were found to have the greatest contribution to the overall volatile concentration after completion of MLF, with isoamyl alcohol, methanol, propanol and 2-phenyl ethanol being present in the highest abundance (**Tables 4.2 and 4.3**). The co-inoculation strategy had higher alcohol concentrations ranging from 600 to 700 mg/L, while the sequential inoculation concentrations ranged from 697 to 735 mg/L. In general, the concentrations of individual alcohols were in agreement with previous studies (Francis & Newton, 2005; Malherbe *et al*., 2012).

In this study the LAB treatments showed significant differences in 3-methyl-1-pentanol at the end of MLF in both inoculation strategies (**Tables 4.2 and 4.3**). Propanol, isobutanol and butanol were also significantly different for the co-inoculated treatments at the end of MLF

(**Table 4.2**) while methanol was significantly different at the end of MLF in the sequential treatments (**Table 4.3**).

These results are in accordance with a study which showed the strain dependant production of isobutanol, propanol, butanol and isoamyl alcohol (Maicas *et al*., 1999). Lee *et al*. (2009b) also reported genera dependant increases in butanol, amongst other compounds, with increased concentrations produced by *L. plantarum* compared with *O. oeni*. In contrast, studies have found no significant changes in isoamyl alcohol, 2-phenylethanol, isobutanol and propanol concentrations after MLF (Laurent *et al*., 1994; Herjavec *et al*., 2001). Other authors (De Revel *et al*., 1999; Jeromel *et al*., 2008; Boido *et al*., 2009; Abrahamse & Bartowsky, 2012) have also shown insignificant changes in terms of higher alcohols after MLF, except for the significant increases in isoamyl alcohol (De Revel *et al*., 1999) and isobutanol and 2-phenyl ethanol (Jeromel *et al*., 2008), as well as strain dependant increases observed for hexanol and 2-phenyl ethanol (Boido *et al*., 2009).

FATTY ACIDS

Volatile short chain fatty acids are formed during fatty acid metabolism by yeasts and bacteria and are said to have an influence on wine aroma and flavour (Lui, 2002). Although found in trace quantities in wine, volatile fatty acids characterised by rancid cheesy sweaty aromas have low sensory threshold values and can have detrimental effects on the sensory properties and aroma quality of the wine (Lui, 2002; Francis & Newton, 2005). Acetic acid in particular can result in a vinegar-like aroma at high concentrations (Swiegers *et al*., 2005).

In this study the fatty acid contribution to the overall volatile concentration after MLF was dominated by acetic acid concentrations. Propionic acid, isovaleric acid and hexanoic acid also contributed considerably, however, these compounds were found in significantly smaller amounts (**Tables 4.2 and 4.3**). It is known that acetic acid makes up approximately 90% of the volatile acids in wine with propionic acid and hexanoic acid principally contributing the rest of the fatty acid profile (Swiegers *et al*., 2005).

The total fatty acid concentrations of this study were higher in the sequential inoculated treatments (ranging from 580 to 614 mg/L) (**Table 4.2**) compared to the co-inoculated treatments (ranging from 214 to 350 mg/L) (**Table 4.3**). The acetic acid concentrations found in the co-inoculated treatments are in accordance with previous studies (Francis & Newton, 2005; Malherbe *et al*., 2012) while the sequential concentrations exceed the concentrations found in young red wines (Francis & Newton, 2005). With this said, the acetic acid concentrations found in this study are, however, considered optimal (between 0.2 and 0.7 g/L) and are considerably lower than the levels considered as objectionable (0.7 – 1.1 g/L depending on the style) (Lambrechts & Pretorius, 2000).

The LAB treatments showed significant differences in propionic acid and isobutyric acid at the end of MLF in both inoculation strategies (**Tables 4.2 and 4.3**). Acetic acid and octanoic acid concentrations were only significantly different at the end of MLF for the co-inoculated LAB treatments. The contribution of LAB to the production of fatty acids in wine is limited, however, studies have reported differences in the volatile fatty acid profiles due to MLF (Maicas *et al*., 1999, Herjavec *et al*., 2001). Our results are also in accordance with a recent study by Lee *et al*. (2009a) showing significant differences between *O. oeni* strains with regards to amongst other compounds isobutyric and octanoic acid. A second study by Lee *et al*. (2009b) reported differences between *O. oeni* and *L. plantarum* in terms of acetic acid and butyric acid.

CARBONYL COMPOUNDS

The carbonyl compounds had the smallest contribution to the total volatile composition with acetoin and diacetyl being the main contributors (**Tables 4.2 and 4.3**). The carbonyl compound diacetyl (2,3-butanedione) is considered one of the most important flavour and aroma compounds produced during MLF, imparting buttery, nutty and butterscotch nuances to the wine (Bartowsky & Henschke, 1995; Lui, 2002). It is produced as an intermediate metabolite during citric acid metabolism by LAB and can be further reduced to acetoin and 2,3-butanediol (Lui, 2002; Lerm *et al*., 2010). Yeast during AF can also contribute to the diacetyl concentrations in wine although these concentrations are usually found to be below the detection threshold (Martineau & Henick-Kling, 1995).

Diacetyl was found in concentrations ranging from 4 to 5 mg/L in the co-inoculated treatments and from 5 to 8 mg/L in the sequential inoculated treatments. The concentration of diacetyl was significantly different for the LAB treatments in the sequential strategy at the end of MLF. The diacetyl concentrations found in the co-inoculated treatments are in accordance with concentrations in previous studies (Francis & Newton, 2005; Malherbe *et al*., 2012). The concentration of the compound 2,3 pentanedione was significantly different for the LAB treatments at the end of MLF in the co-inoculated strategy. The acetoin concentrations were significantly different between the LAB in both the inoculation strategies at the end of MLF with concentrations ranging from 3 to 7 mg/L in the co-inoculation strategy and 10 to 19 mg/L in the sequential inoculation strategy. These acetoin concentrations have been previously reported in young red wines (Francis & Newton, 2005). Literature states that wines that have undergone MLF generally have increased concentrations of diacetyl as well as acetoin (Martineau *et al*., 1995; Martineau & Henick-Kling, 1995; Fornachon & Llyod, 2006; Izquierdo Cañas *et al*., 2008; Lee *et al*., 2009b). Some authors, however, have shown no detectable levels of diacetyl in wines having undergone MLF, suggesting the enzymatic reduction to 2,3-butanediol (Maicas *et al*., 1999; Knoll *et al*., 2011).

4.3.2.2 MULTIVARIATE APPROACH TO PROFILING WINE LAB

The univariate approach showed clear differences between the treatments. To further explore the differences imparted by the LAB treatments on the wine matrix a multivariate approach was employed. The ability of multivariate techniques to discriminate between the LAB treatments will evaluate the possibilities for future classification purposes.

The ability to discriminate between the two process stages as well as the different LAB treatments at a specific process stage was explored using PCA. The ability to discriminate between the LAB treatments at a specific process stage was further explored using PLS-DA evaluating the use of different data sets, namely quantified chemical data, FT-MIR spectral data and PCA score values. SIMCA was used together with FT-MIR spectral data and chemical quantified data to further evaluate the ability to differentiate between the LAB treatments

PROFILING USING PCA

CO-INOCULATION STRATEGY

The initial PCA score and loadings plot (**Figures 4.5A and 4.5B respectively**) gave an overview of the volatile profile (higher alcohols, esters, and fatty acids) and chemical composition (pH, titratable acidity and volatile acidity) of the five different bacterial strains obtained at 50% and 100% completion of MLF.

The model was computed using cross validation with seven PC's explaining over 90% of the variation in the data set. Three PC's captured 75% of the variance between the samples, with PC1 explaining 48%, PC2 explaining 19% and PC3 explaining the last 8% of the variation. The score plot (**Figure 4.5A**) shows a clear separation between the samples at the two process stages with some degree of overlap observed for three samples. The variance explained by PC1 mostly explains the separation between the LAB treatments at 50% completion of MLF. LAB treatments at 50% completion of MLF show a large variation on PC1 separating in a diagonal fashion. This diagonal separation could be as a result of "noise" in the data by possible variables or outlying samples not well explained by the model which will be further investigated. The separation between LAB treatments is less prominent at 100% completion of MLF and is captured mainly by PC2 showing a very small separation in the vertical direction. Therefore in terms of the process stages it can be interpreted that at 50% completion of MLF there is greater variation between the LAB treatments in terms of their chemistry. As the fermentation progresses toward the end of MLF the differences between the LAB treatments become smaller and the fermentations converge. This was previously observed to a certain extent in the univariate study. These results correlate with the results of a recent study showing greater distinction between LAB treatments at early inoculation compared with sequential inoculation in Riesling wines (Knoll *et al*., 2012).

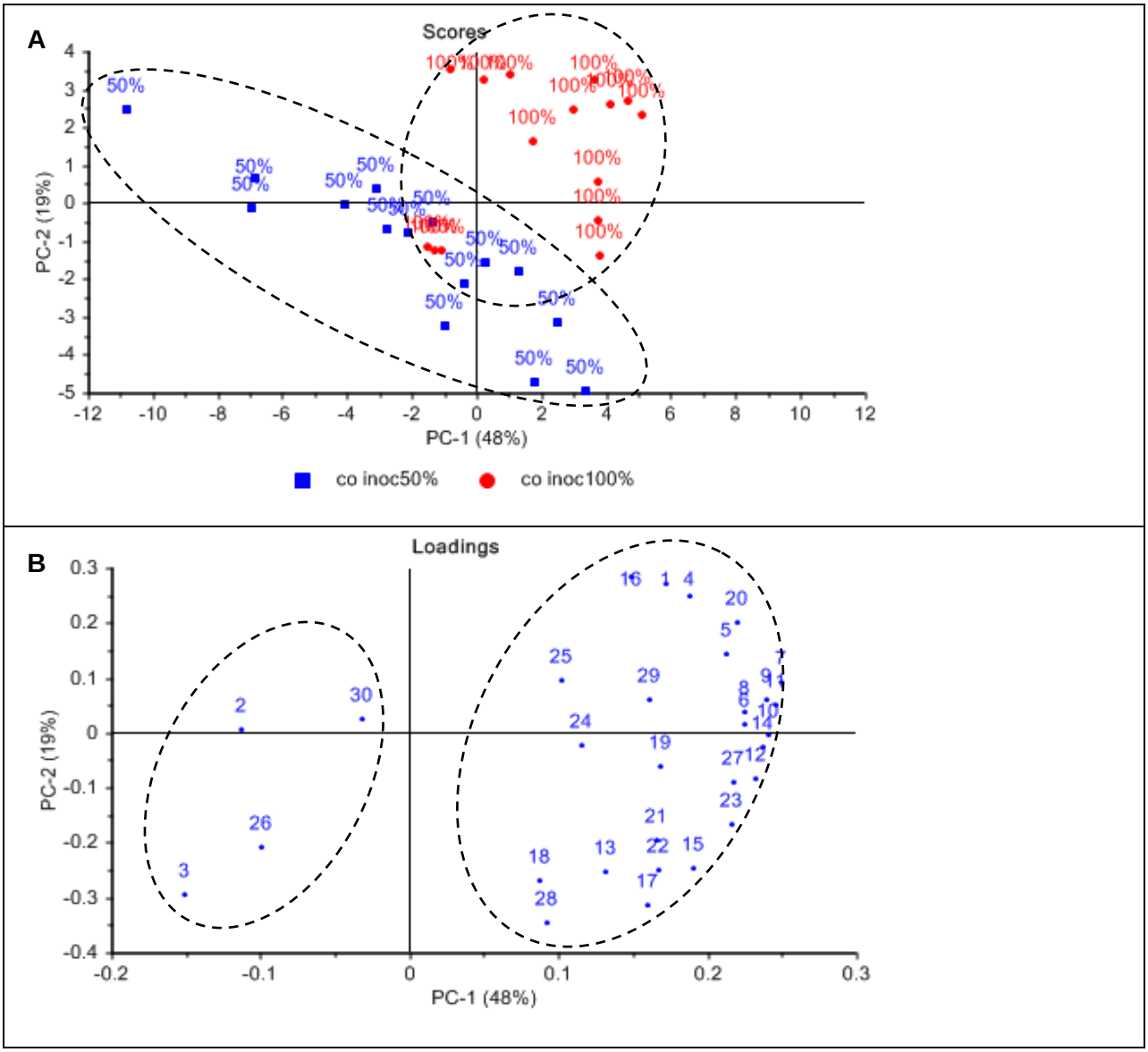

Figure 4.5 A) PCA score plot giving a visual overview of the changes in chemistry imparted by LAB metabolism in the co-inoculated treatments at the two different process stages. Broken lines indicate the groupings of scores based on the process stage (50% and 100% completion of MLF) and **B)** The corresponding loadings plot (PC1 vs PC2). Broken lines indicate the variables which are important for the separation.

The loadings plot (**Figure 4.5B**) was used to evaluate the specific variables which are important for the separation observed in the score plot (**Figure 4.5A**). The loadings plot of PC1 and PC2 shows a group of highly correlated variables separating to the right (**numbers of variables indicated in Tables 4.2 and 4.3**) of the PCA loadings plot while four variables including acetic acid (quantified by WineScan), decanoic acid, 2-phenylyethyl acetate and titratable acidity separate to the left (**Figure 4.5B**). The separation between these two groups of compounds is dominating the variation explained by PC1 (48%).

In order to improve the model for discrimination purposes certain aspects were considered in this data set namely variable selection and potential outlying samples.

Outlying samples were identified in the influence plots (data not shown). At 50% completion of MLF the samples which were identified as outlying samples included S5 A, S5 B, MX B and V2 B. Sample VP C at 100% completion of MLF was also identified as an outlier. These samples were characterised by a high residual X variance and in some cases a high leverage on PC1, PC2 and PC3 were not well described by the model and therefore contribute to the noise in the data set and contributes to the distortion of the model.

The results show that these samples are in some way different, however, further interpretation of these samples is necessary to establish what factors contribute to the differences observed in these specific samples and whether there is anything grossly abnormal or something interesting about these samples. Due to the complexity of wine and the variability between samples these possible outlying samples could be representative of the data rather than gross outliers.

The qualitative interpretation of the FT-MIR spectral data (data not shown) as well as the quantitative interpretation of the means and standard deviations of the quantified chemical data between the biological repeats showed nothing grossly abnormal in terms of these samples.

The identified outlying samples are somewhat different, however, these samples were kept in the data set as to be able to model the biological variability. Outlying samples were considered for each separate model during this study.

Variables identified on the loadings plot to have low loadings were subsequently removed from the model. These included the four variables separating to the left of the PCA loadings plot (**Figure 4.5B**) as well as 3-ethoxy-1-propanol and isovaleric acid which didn't significantly contribute to the separation between the LAB treatments at both time points as seen in the univariate study. The removal of these variables increased the explained variance from 67% to 75% on two PC's (data not shown).

The results showed that the removal of these specific variables didn't contribute any further to a better separation on the PCA score plot (data not shown) when comparing it to the preliminary model before variable selection (**Figure 4.5A**). With this said, however, the removal of these specific variables improved the explained variance of the model and subsequently models more important data and less "noise". The removal of variables in this case is therefore seen as advantageous for discrimination purposes.

Due to the clear separation between the two time points further data modelling was done separately for these two time points producing two separate datasets for discrimination purposes. Further investigation will evaluate the ability to discriminate between the LAB strains namely *O. oeni* and *L. plantarum* strains at a particular process stage. For these models the same aspects namely outlying samples and variable selection were taken into consideration.

50% COMPLETION OF MLF

The PCA score plot and the corresponding loadings plot in **Figure 4.6A** and **Figure 4.6B** respectively give an overview of the volatile profile (higher alcohols, esters, and fatty acids) and chemical composition (pH, titratable acidity and volatile acidity) associated with the metabolic activities of the five different co-inoculated LAB treatments at 50% completion of MLF.

The initial model captured 73% of the explained variance on two PC's, showing excellent discrimination between the LAB genera on the PCA score plot (**Figure 4.6A**). PC1 capturing 58% of the variance is explained mostly by the separation between these LAB genera. *O. oeni* separate to the left of the score plot while *L. plantarum* separate to the right. Treatment MX separates in the middle of these two treatments. PC2 explaining 15% of the variance explains the within class variability observed within the genera. The within class variability shows two distinct groups for *O. oeni* as well as for *L. plantarum* (**Figure 4.6A**). Further exploration into the within class variation shows that the *O. oeni* strains namely S5 and VP separate in the PC1 direction and slightly in the PC2 direction while the *L. plantarum* strains namely V2 and 56 show distinct separations in the PC2 direction (**Figure 4.6A**). The tight clustering of the scores of the different strains shows excellent biological repeatability with very little variation between the biological repeats (**Figure 4.6A**).

The separation between the LAB genera along PC1 is driven by a group of highly correlated variables (**Figure 4.6B**). These 18 variables (**see insert Figure 4.6B**) with very high discrimination abilities include amongst others hexanol, butyric acid, isoamyl alcohol and butanol (**See Tables 4.2 and 4.3 for the indication of variable numbers**). The compounds separating to the left of the loadings plot (**Figure 4.6B**) including acetic acid (quantified by the WineScan), ethyl lactate, decanoic acid and 2-phenylethyl acetate (**Figure 4.6B**) did not contribute to the separation between the LAB genera.

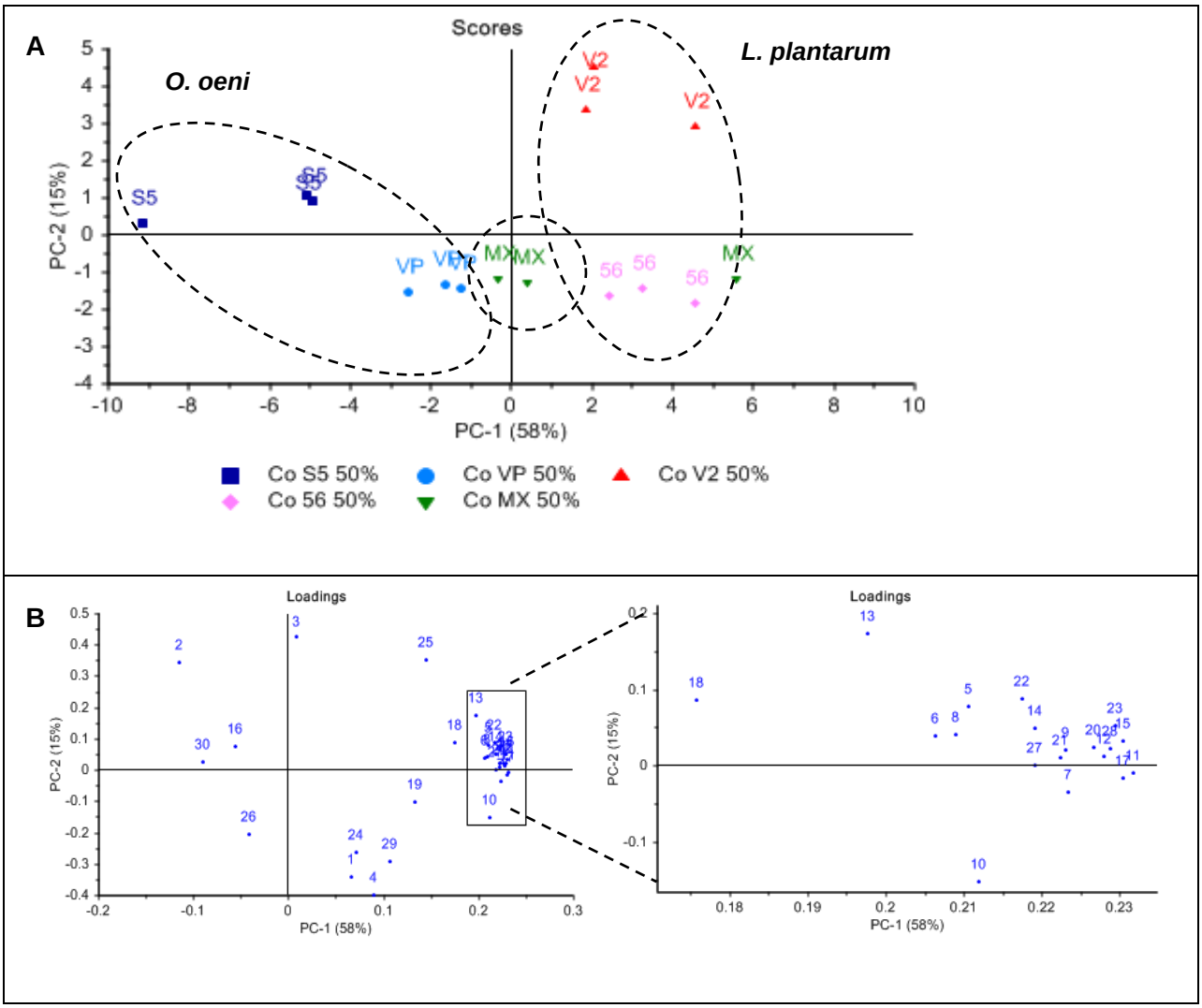

Figure 4.6 A) PCA score plot giving a visual overview of the changes in chemistry imparted by LAB metabolism at 50% completion of MLF in the co-inoculated treatments, showing within class variance and **B)** The corresponding loadings plot (PC1 vs. PC2) insert: 18 highly correlated variables.

Once again variable selection was evaluated and variables with low loadings were removed. The explained X variance improved from 73% to 89% on two PC's after the removal of these specific variables with PC1 explaining 84% of the variance (**Figure 4.7A**). The model was subsequently improved by the removal of certain variables. The subsequent PCA score plot (**Figure 4.7A**) shows excellent discrimination between the LAB genera with the variables distributed over the entire loadings plot (**Figure 4.7B**) all contributing to the separation observed.

The removal of variables in this case resulted in the loss of the within class variability specifically in the *L. plantarum* (**Figure 4.7A**) separation which was observed in the preliminary score plot (**Figure 4.6A**). These variables therefore contributed to the within class variability which was previously observed. These variables, however, didn't contain enough structured variation to be discriminating for the LAB genera.

This model therefore shows promise for the discrimination between *O. oeni* and *L. plantarum* in further PLS-DA and SIMCA work.

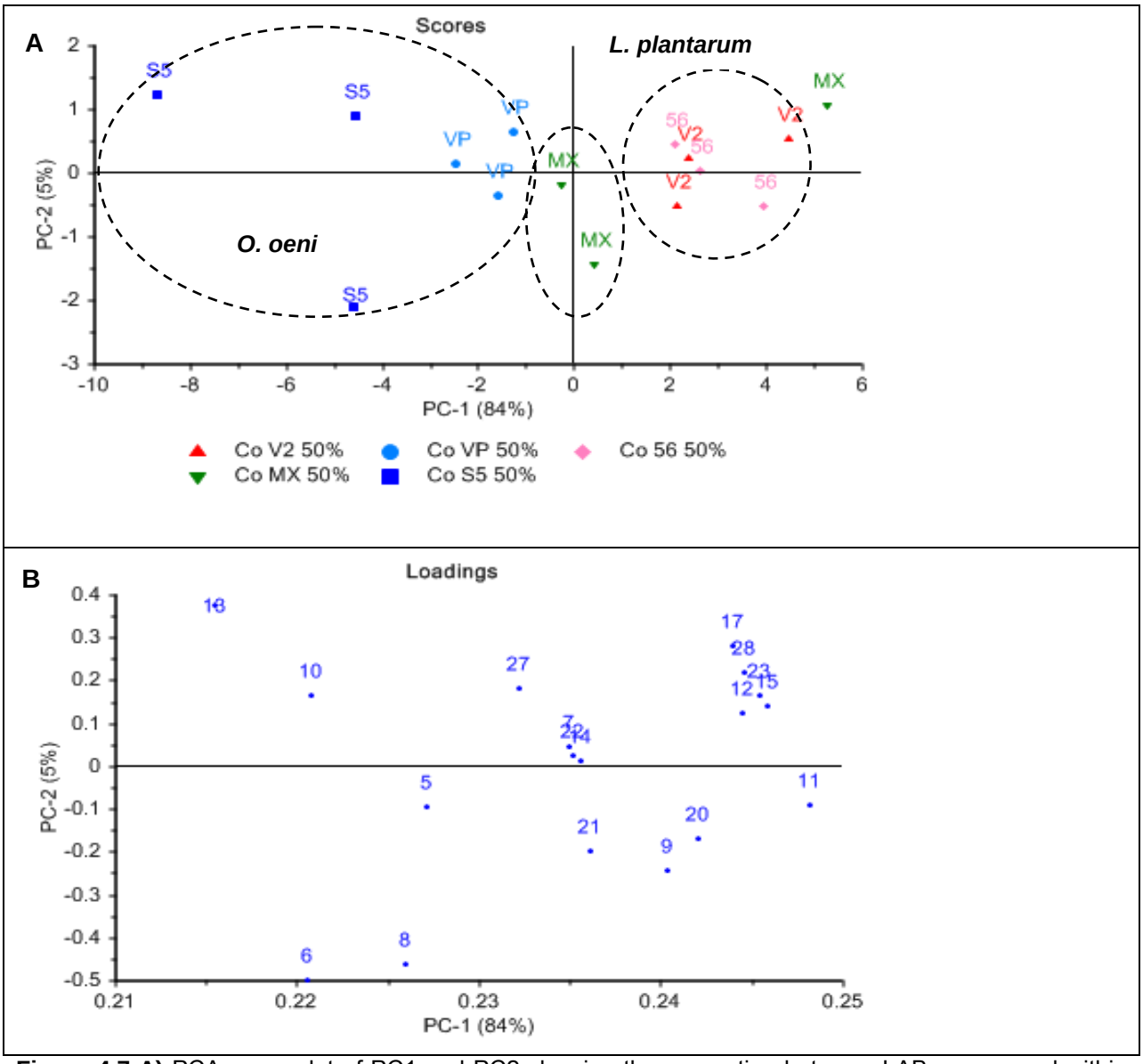

Figure 4.7 A) PCA score plot of PC1 and PC2 showing the separation between LAB genera and within class variance after the removal of variables and **B)** Corresponding loadings plot of PC1.

100% COMPLETION OF MLF

The PCA score plot and the corresponding loadings plot in **Figures 4.8A and 4.8B** respectively, give an overview of the volatile profile (higher alcohols, esters, fatty acids and carbonyl compounds) and chemical composition (pH, titratable acidity and volatile acidity) associated with the metabolic activities of the five different LAB treatments at 100% completion of MLF.

The PCA model explaining 92% of the variance on PC1 and PC2 shows discrimination between the LAB treatments on the PCA score plot (**Figure 4.8A**). PC1 capturing 82% of the variance is driven by the separation between *O. oeni* and *L. plantarum* while PC2 explains 10% of the variation.

The separation observed between *O. oeni* and *L. plantarum* strains was not as clear as that observed in the data set modelling the co-inoculated samples at 50% completion of MLF.

Treatment MX does not separate from the *L. plantarum* treatments (**Figure 4.8A**). This was previously established where we observed that the chemistry of the samples converge toward the end of the fermentation. The chemistry of these samples are more similar to each other than that of the samples at 50% completion of MLF, however, this model does show possible discriminant ability. **Figure 4.8B** shows a group of highly correlated variables which have very little contribution to the separation observed in the score plot (**Figure 4.8A**).

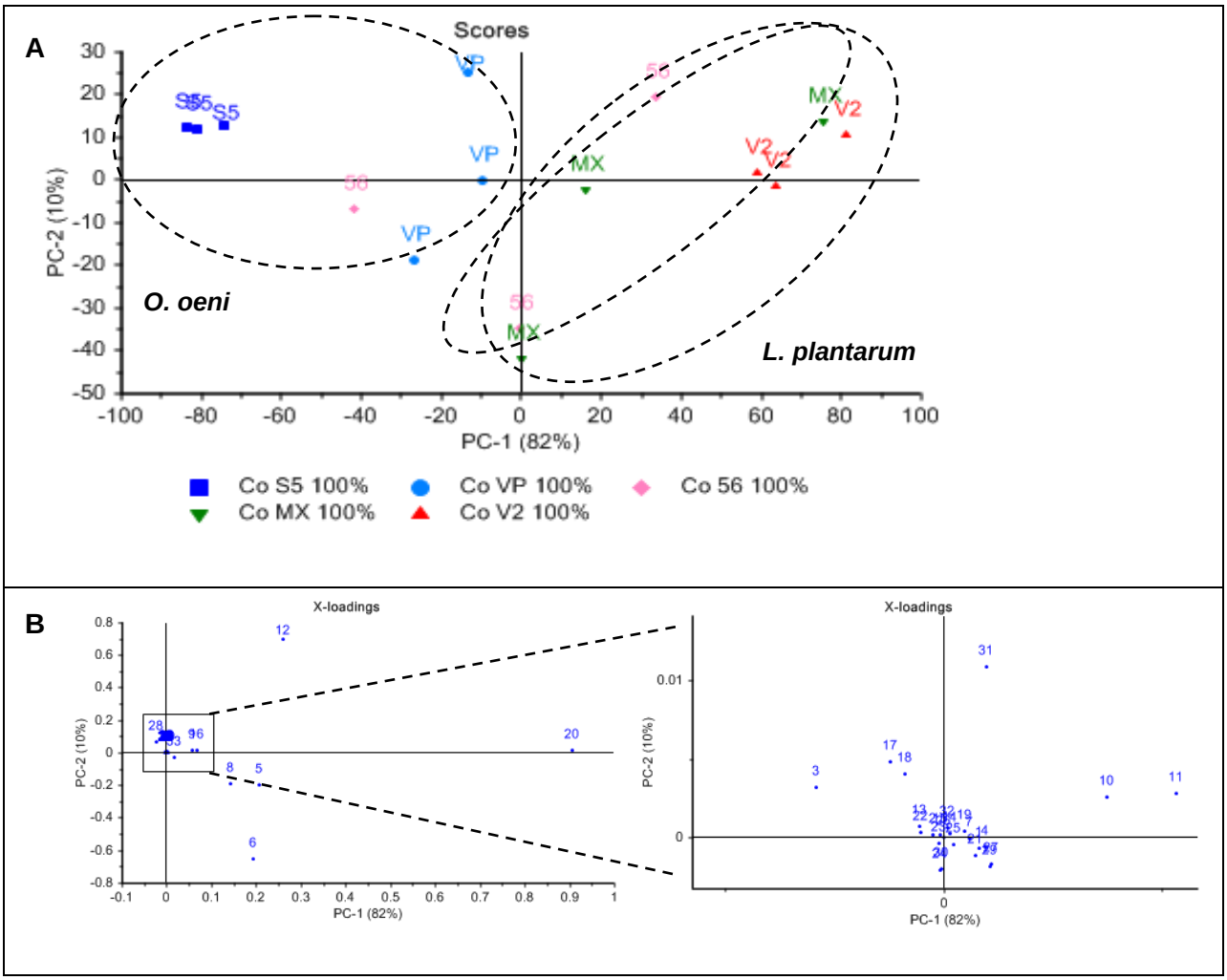

Figure 4.8 A) PCA score plot giving a visual overview of the changes in chemistry imparted by LAB metabolism at 100% completion of MLF in the co-inoculated treatments and **B)** The corresponding loadings plot (PC1 vs PC2). insert: highly correlated variables which have very little contribution to the separation observed in the score plot.

The removal of variables with low loadings did not change the variation captured by two PC's (92%) (**Figure 4.9A**), however, an increase in explained variation from 82% to 85% was observed for PC1. The resulting few variables namely propanol, isobutanol, ethyl lactate, ethyl acetate and acetic acid (quantified by GC-FID) distributed over the loadings plot (**Figure 4.9B**) showed clearer separation between the LAB genera on the PCA score plot (**Figure 4.9A**). Variable selection therefore improved the models discrimination ability.

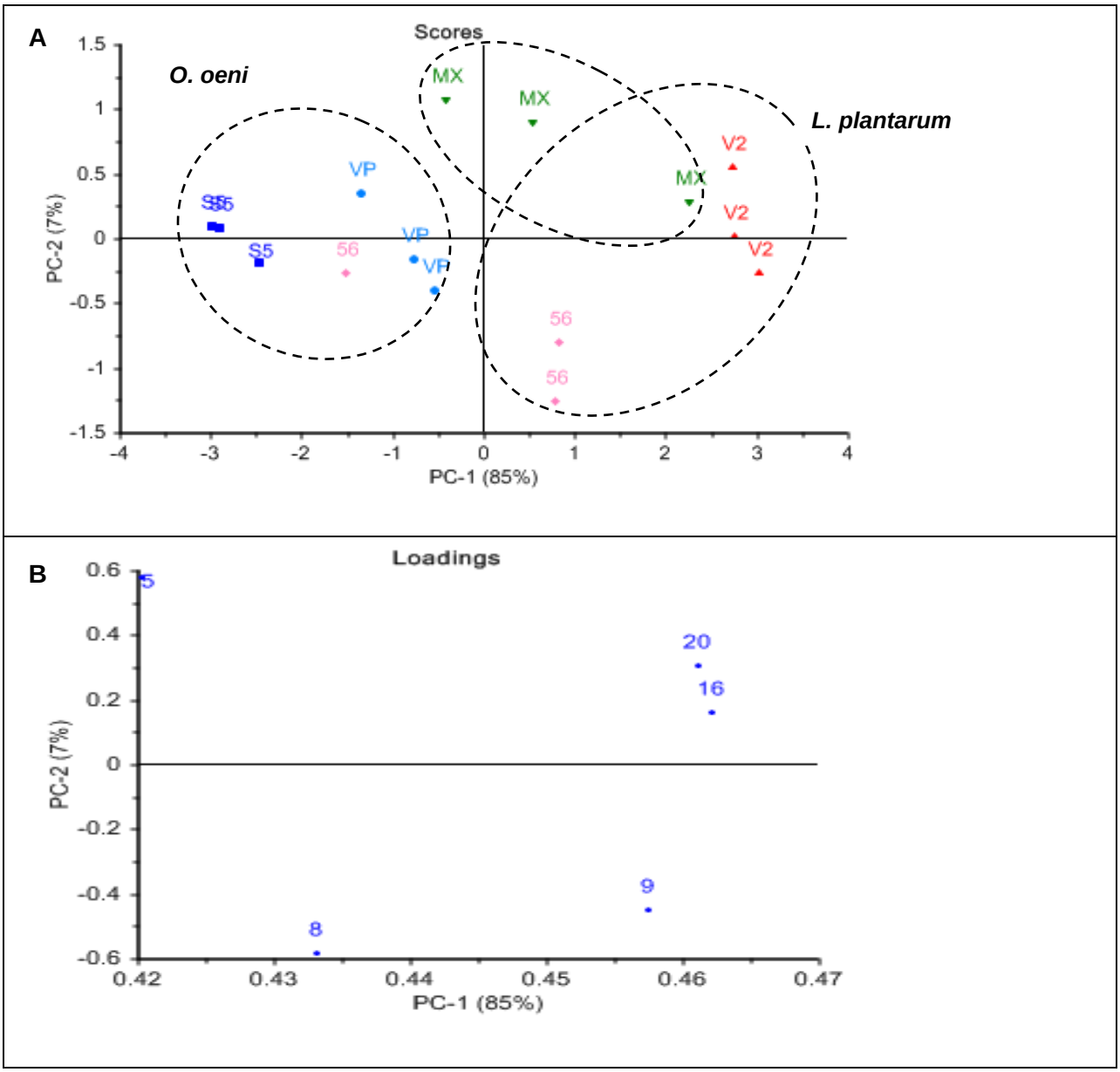

Figure 4.9 A) PCA score plot of PC1 and PC2 showing the separation between LAB genera after the removal of certain variables and **B)** Corresponding loadings plot of PC1.

SEQUENTIAL INOCULATION STRATEGY

The PCA score plot (**Figure 4.10A**) and the corresponding loadings plot (**Figure 4.10B**), give an overview of the volatile profile (higher alcohols, esters, and fatty acids) and chemical composition (pH, titratable acidity and volatile acidity) associated with the metabolic activities of the five different sequential inoculated LAB treatments obtained at 50% and 100% completion of MLF. The PCA score plot showed that this model captured 65% of the variation in the data set with PC1 explaining 43% of the variation while PC2 explains 22%. As observed in the co-inoculated strategy, distinct separation between the sequential inoculated samples is seen at both time points.

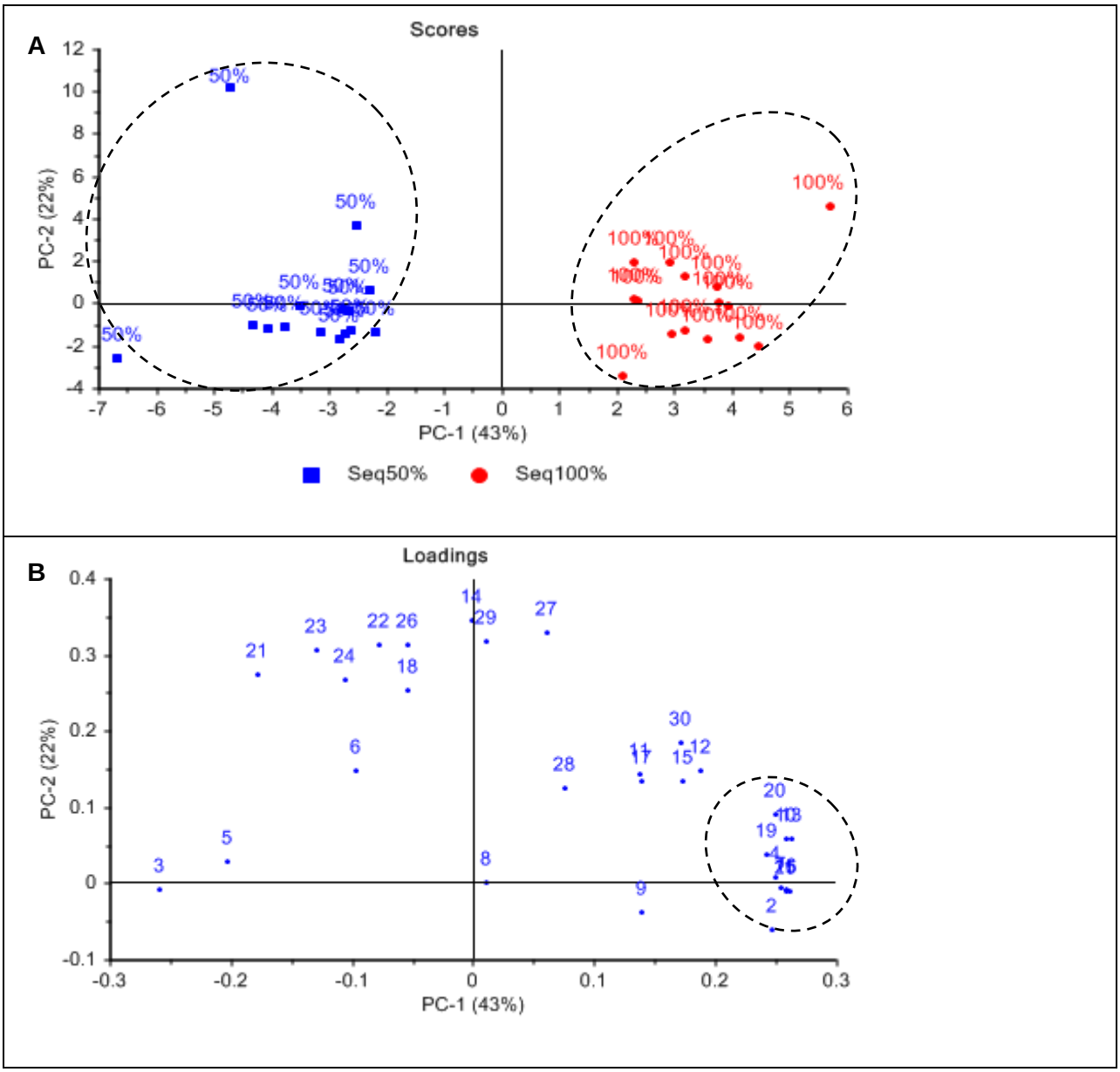

Figure 4.10 A) PCA score plot giving a visual overview of the changes in chemistry imparted by LAB metabolism in the co-inoculated treatments at the two different process stages. Broken lines indicate the groupings of scores based on the process stage (50% and 100% completion of MLF) and **B)** The corresponding loadings plot (PC1 vs. PC2). Broken lines indicate the highly correlated variables explaining the separation on PC1.

PC1 explains the separation observed between the samples at the two specific time points with the samples at 50% completion located to the left of the score plot while the samples at 100% completion are located to the right of the score plot. The tight clusters show that very little variation is observed between the LAB treatments at each specific time point in terms of their chemical profiles. With this said, however, certain samples lie far apart from the tight clusters and could possibly be outlying samples which are distorting the model mainly in the PC2 direction.

The PCA loadings plot (**Figure 4.10B**) shows a group of highly positively correlated variables (**See Tables 4.2 and 4.3 for the indication of variable numbers**) explaining the

separation on PC1 including amongst others acetic acid (quantified by GC-FID), ethyl caprylate, isoamyl acetate, ethyl lactate and diethyl succinate. The variables separating to the top of the loadings plot including amongst others hexanoic acid, octanoic acid and 2-phenylethyl acetate are most likely explaining the outlying samples which are mainly separating in the PC2 direction.

In both the co-inoculation and the sequential inoculation strategies PCA could distinguish between the specific process points namely 50% and 100% completion of MLF showing the clear different volatile profiles at these specific time points. Further exploration into the sequential data set for each particular process stage is not discussed, however, the results showed that the volatile profiles at a specific time point were dependent on the specific inoculation strategy as seen by the specific variables contributing to the separation. Further, PCA showed clear promise in the discrimination between the LAB genera in both inoculation strategies as well as discrimination on a strain level within *O. oeni* and *L. plantarum*. These results are in accordance with a study by Pozo-Bayón *et al*. (2005) who showed clear metabolic differences between *O. oeni* and *L. plantarum* species using PCA as well as a degree of dispersion among the different strains.

PCA also showed the biological repeatability and the potential outliers in the data sets. Variable selection improved the separation in some cases, however, further exploration into variable selection in these data sets could possibly improve the discrimination ability.

PROFILING USING PLS-DA

This preliminary PLS-DA study will explore the data set of the co-inoculated samples at 50% completion of MLF. PLS-DA models were established using quantified chemical data, FT-MIR spectral data as well as scores from the preliminary PCA study. PLS-DA was used as an exploratory tool to evaluate the potential ability for future classification purposes.

PLS-DA WITH QUANTIFIED CHEMICAL DATA

The preliminary PLS-DA score plot (**Figure 4.11A**) using the quantified chemical data as X variables shows good discrimination between wines fermented with *L. plantarum* and *O. oeni* and no overlap between the two classes. Four factors are optimal for explaining over 99% of variation between the two classes (data not shown). The separation on PC1 between the two classes explains 60% of the X variance while capturing 82% of the Y variance or the response, being the separation between *O. oeni* and *L. plantarum*. PC2 captures 11% of the X variance while capturing 13% of the Y variance. The results of the score plot show further separation between the specific strains within the two classes. *O. oeni* treatments S5 and VP show distinct separation while the separation between the *L. plantarum* treatments 56 and V2 is more subtle. Clustering's are also observed when evaluating the time aspect. Although these fermentations

are all at exactly the same stages of their fermentation (50% completion of MLF) separation between the days can be observed (**Figure 4.11A**).

A good discrimination can be observed on the predicted vs. measured plot (**Figure 4.12**) for *O. oeni* and *L. plantarum* using the quantified chemical data with *O. oeni* lying very close to the ideal value +1 and *L. plantarum* strains lying close to -1. Some separation can, however, be observed within the classes. The R^2 value of 0.93 for cross validation showed the excellent ability of this model for future prediction of samples.

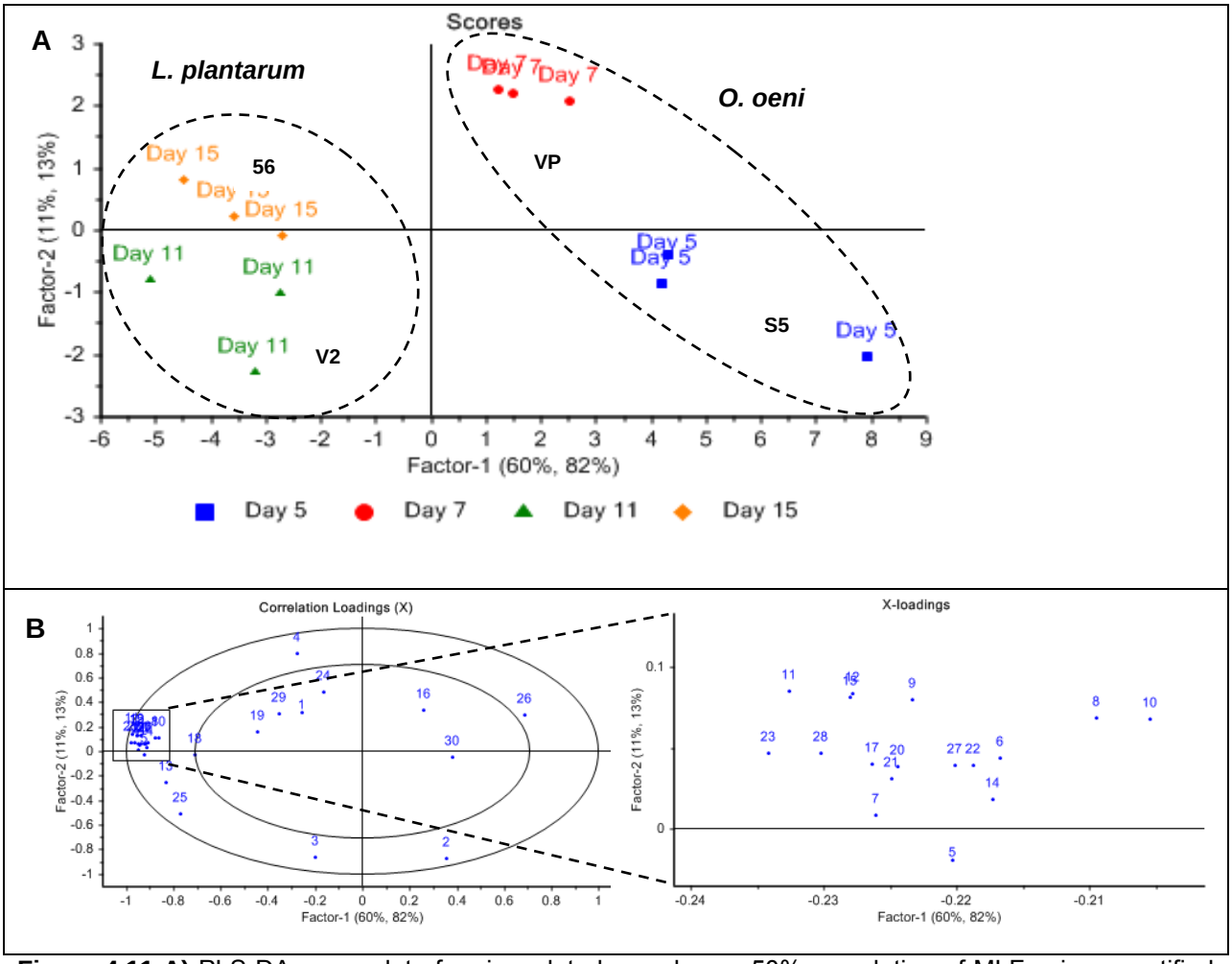

Figure 4.11 A) PLS-DA score plot of co-inoculated samples as 50% completion of MLF using quantified chemical data and **B)** Corresponding correlations loadings (X) plot. Insert: highly correlated variables describing the between class variability.

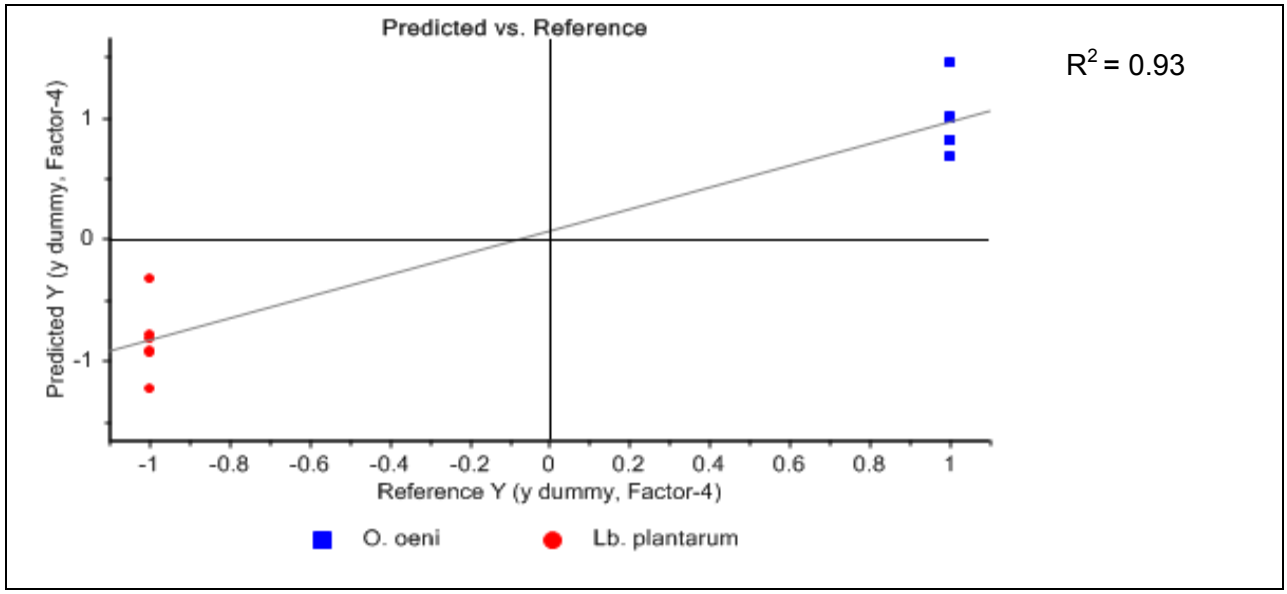

Figure 4.12 PLS-DA predicted vs. measured plot of quantified chemical data showing the separation between the two LAB classes at 50% completion of MLF in the co-inoculation strategy.

The correlations loadings (X) plot (**Figure 4.11B**) shows the important variables responsible for the separation between the classes. The group of highly correlated variables (**See Tables 4.2 and 4.3 for the indication of variable numbers**) falling to the left side of the loadings plot explain between 50% and 100% of the variance. These variables model the between class variability of this data set and best describe the discrimination between the two classes. All the other variables including amongst others isovaleric acid, decanoic acid and ethyl lactate are mainly modelling the within class variability (**Figure 4.11B**). These variables are contributing to noise in the PLS-DA model as this technique doesn't capture within class variance. These variables are similar to those noted in the exploratory PCA study. When these variables were removed in the PCA study the within class variability was lost.

The removal of variables contributing to the within class variability as identified in the correlations loadings plot (**Figure 4.11B**) resulted in an increase in the explained X variance from 60% to 88% on factor one. The explained Y variance, however, decreased from 82% to 76%. The models discrimination performance also decreased showing overlap in the two classes when looking at the predicted vs. reference plot (data not shown).

PLS-DA WITH FT-MIR SPECTRAL DATA

The preliminary PLS-DA score plot (data not shown) using the FT-MIR spectral data (noise due to water removed) as X variables showed good discrimination between the two classes. PC1 explained 91% of the X variation while only explaining 44% of the Y variation or the separation between the two classes while PC2 explains 8% of the X variance and 38% of the Y variation. The separation between the two classes was almost equally modelled by PC1 and PC2. Once

again when taking the time aspect into consideration the clustering could also be attributed to the specific day at which each treatment was at 50% completion of MLF (data not shown).

The PLS-DA explained variance plot of the FT-MIR spectra shows that five components was optimal for explaining over 98% of the Y variance (data not shown). A good discrimination can be observed in the predicted vs. measured plot for *O. oeni* and *L. plantarum* using the FT-MIR data with *O. oeni* lying very close to the ideal value +1 and *L. plantarum* strains lying close to -1 (**Figure 4.13**). No overlap between these classes could be observed. The R^2 value of 0.98 for cross validation showed the excellent predictive ability of this model for future samples using FT-MIR spectral data.

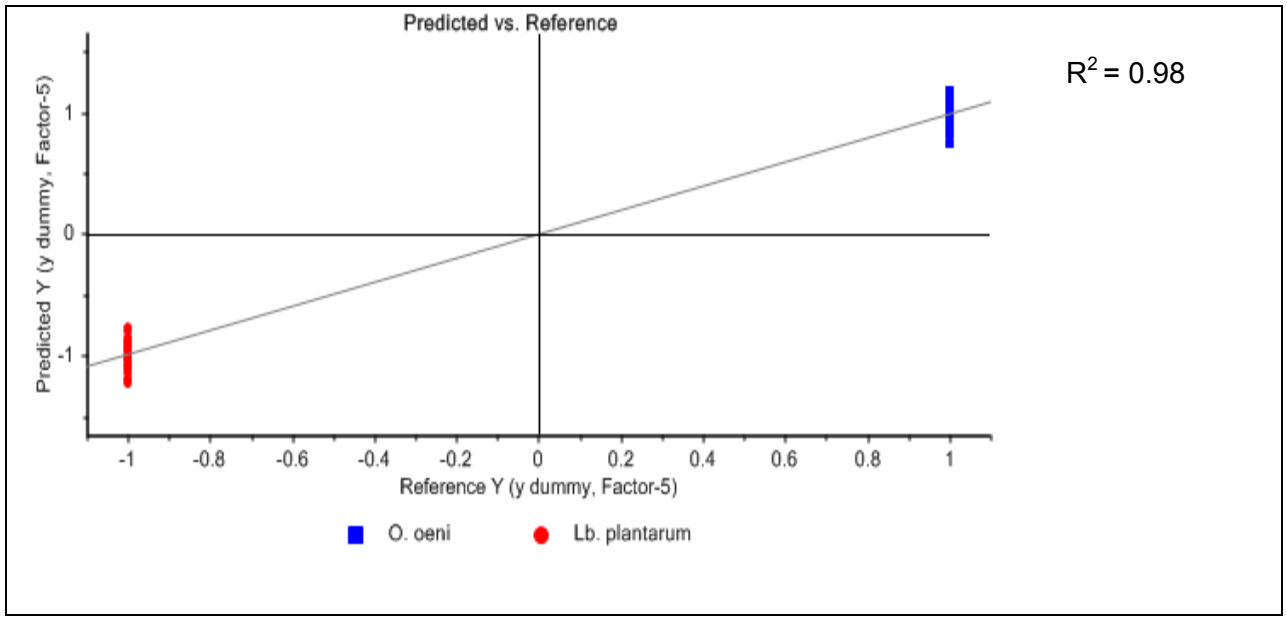

Figure 4.13 PLS-DA predicted vs. measured plot of FT-MIR spectra showing the separation between the two LAB classes at 50% completion of MLF in the co-inoculation strategy.

PLS-DA USING SCORES

In order to capture the within class variation a PLS-DA model was established using the scores from three PC's of the preliminary PCA study including the all the quantified chemical variables. The resulting score plot of the PLS-DA model (data not shown) showed excellent discrimination ability between the two classes as well as showing distinct within class variation. PC1 explained 70% of the X variance and 79% of the Y variance while PC2 explained 19% of the X variance and 3% of the Y variance.

The predicted vs. measured plot (**Figure 4.14**) shows good discrimination between *O. oeni* and *L. plantarum* classes using the scores. *O. oeni* samples lying very close to the ideal value +1 and *L. plantarum* strains lying close to -1. Some separation is, however, observed in the *O. oeni* treatments. This model with an R^2 value of 0.66 for cross validation showed relatively lower prediction ability to that of the models established with chemical data and the FT-MIR spectral data.

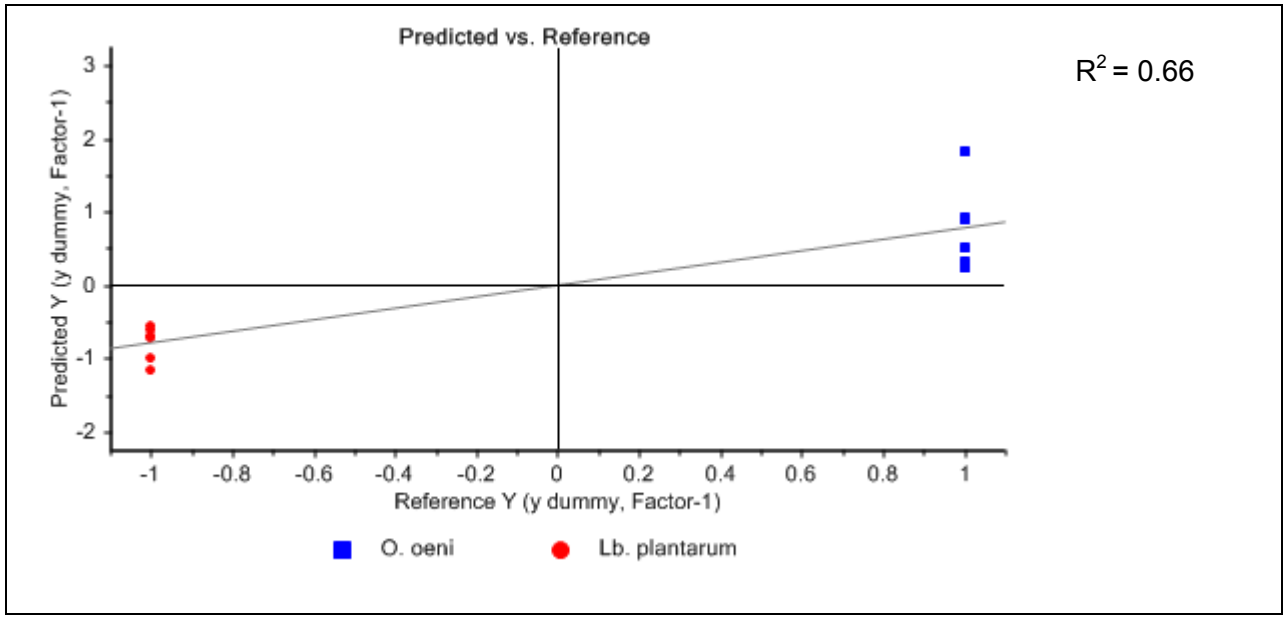

Figure 4.14 PLS-DA predicted vs. measured plot using PCA scores showing the separation between the two LAB classes at 50% completion of MLF in the co-inoculation strategy.

The three different data sets used for PLS-DA all showed excellent discrimination ability. The explained Y variance for the quantified chemical data was above 98% on two factors while when using the FT-MIR spectral data or the PCA scores of the chemical data the explained Y variance was 82% on two factors. Some separation was observed in the two classes when using the chemical data as well as the PCA scores while very little separation was observed when using the FT-MIR data.

SIMCA ANALYSIS

The SIMCA application in the Unscrambler Software was used as preliminary classification study on the co-inoculated samples at 50% completion of MLF. Two disjoint PCA class-models namely "*O. oeni*" and "*L. plantarum*" were made to classify test set samples at a significance level of 5% for quantified chemical data as well as the FT-MIR spectral data. The classification results are displayed in **Figure 4.15** and **Figure 4.16** respectively. The area below the horizontal line delimits membership of "*L. plantarum*" treatments whereas the area to the left of the vertical line delimits membership of "*O. oeni*" treatments. The area near the origin of plot delimits the samples which show non-membership to any of these models (Esbensen, 2006).

Promising results are shown for the chemical data (**Figure 4.15**) keeping in mind the size of the data set. The calibration samples classified correctly into the respective classes. One of the test samples (V2 A) showed 100% non-membership to both the models. The typical *O. oeni* test sample (VP A) classified correctly as an "*O. oeni*" sample (as can be seen from its position to the left of the vertical line). The typical *L. plantarum* test sample (56 B) also classified

correctly (seen by its position below the horizontal line). The non-typical test samples (MX A, B, C) classified as *O. oeni* samples.

The FT-MIR spectral results (**Figure 4.16**) are, however, not as promising despite the excellent separations seen with PLS-DA. Most of the *O. oeni* calibration samples classified correctly into the typical class (as can be seen from the position to the left of the vertical line). The *L. plantarum* calibration samples, however, showed 100% non-membership to either class. The test samples separate close to their respective "typical" classes. The "non-typical" tests samples (MX A, B, C) lie close to the *L. plantarum* strains, however, show 100% non-membership to any of the classes.

Future work should aim at enlarging these data sets as the size of this data set could be a limiting factor in these results.

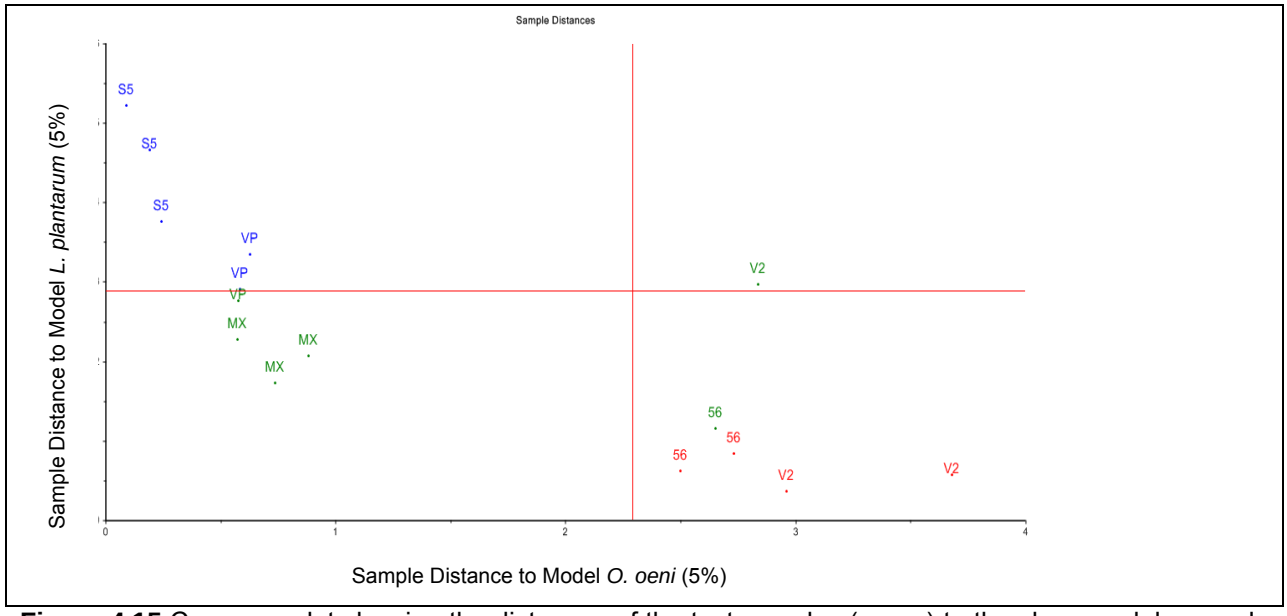

Figure 4.15 Coomans plot showing the distances of the test samples (green) to the class models namely "*O. oeni*" (blue) and "*L. plantarum*" (red) using quantified chemical data.

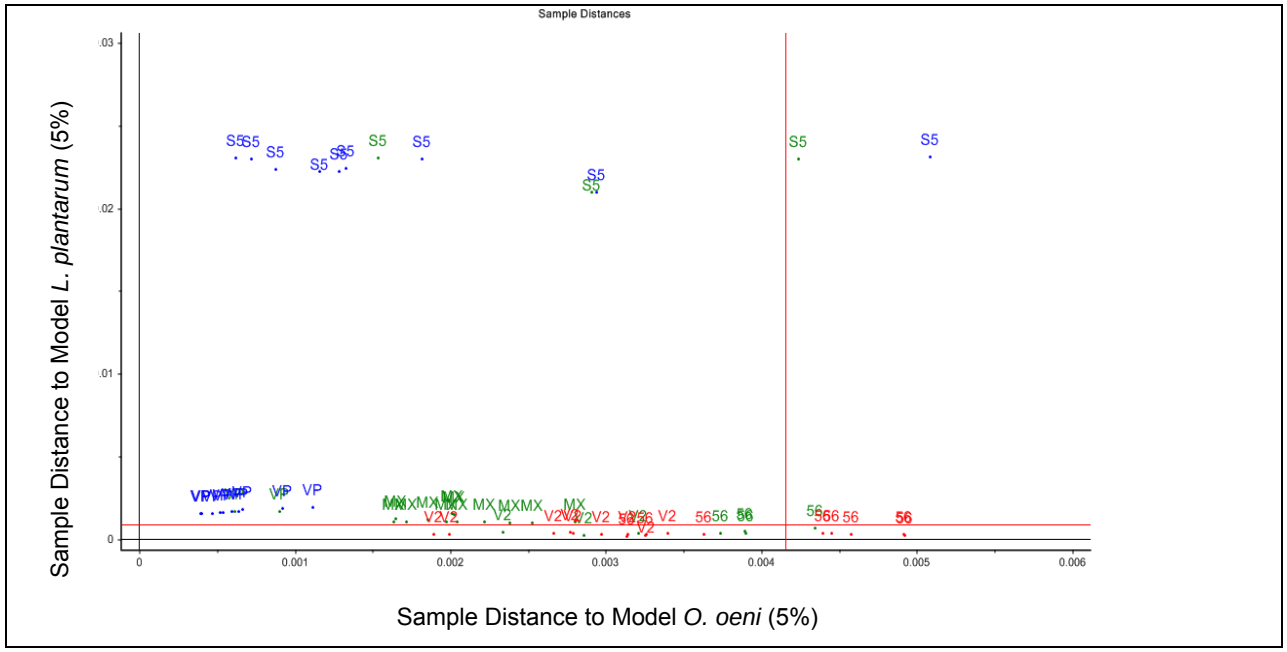

Figure 4.16 Coomans plot showing the distances of the test samples (green) to the class models namely "*O. oeni*" (blue) and "*L. plantarum*" (red) using FT-MIR spectral data.

4.4 CONCLUSIONS

In summary this study evaluated the ability of univariate and multivariate techniques to discriminate between wine LAB in South African Shiraz wines within an inoculation strategy using quantified chemical data as well as FT-MIR data.

These techniques show that strain related differences in terms of quantified volatile metabolites are present, however, these are specific to the inoculation strategy as well as the specific time process stage. With this said this study was on carried out during 2011 and would need to be repeated in subsequent studies in order to make more definite conclusions.

This study has shown that multivariate tools such as PCA and PLS-DA are powerful tools to discriminate between LAB treatments and has shown the importance of both chemical and spectral data for the discrimination between LAB. The quantified chemical data showed greater potential for discrimination, however, the use of FT-MIR spectra for discrimination should not be disregarded. It has been shown that the variability within samples can be uniquely influenced by different data sets such as spectroscopic measurements and chemical data (Skov *et al*., 2008). The simple and rapid FT-MIR technique with its time saving benefits should be considered as the technique of preference in further studies.

Further studies can explore the many data modelling tools available to optimize the discrimination between LAB treatments in wine. In order to improve the robustness of these specific models the data sets would need to be increased. This could involve including a larger number of LAB strains for investigation, using wines made with different process technologies, including other cultivars, including wines from different vintages as well as evaluating the

potential of these models for classifying LAB in matured wines. Further exploration into variable selection can also be employed. Near infrared technology should be included in extended studies as this analytical technique is widely used for on-line applications. Furthermore extended studies should include a sensorial evaluation of the wines to evaluate whether the chemical differences identified between the LAB treatments can be correlated to sensorial aroma descriptors for the different LAB treatments.

4.5 LITERATURE CITED

Abrahamse, C.E. & Bartowsky, E.J., 2012. Timing of malolactic fermentation inoculation in Shiraz grape must and wine: Influence on chemical composition. *World J. Microbiol. Biotechnol*. 28, 1-11.

Antalick, G., Perello, M.C. & de Revel, G., 2010. Development, validation and application of a specific method for the quantitative determination of wine esters by headspace-solid-phase microextraction-gas chromatography–mass spectrometry. *Food Chem*. 121, 1236-1245.

Bartowsky, E. & Henschke, P., 1995. Malolactic fermentation and wine flavour. *Aust. Grapegrower Winemaker* 378, 83-94.

Bartowsky, E.J., Francis, I.L., Bellon, J.R. & Henschke, P.A., 2002. Is buttery aroma perception in wines predictable from the diacetyl concentration?. *Aust. J. Grape Wine Res*. 8, 180-185.

Bartowsky, E.J., Henschke, P.A., Høj, P.B. & Pretorius, I.S., 2004. Chasing wine aroma - does *Oenococcus oeni* have the potential to release aroma compounds from authentic grape precursors?. *Austr. N.Z. Wine Indust J*. 19, 24-31.

Bevin, C.J., Dambergs, R.G., Fergusson, A.J. & Cozzolino, D., 2008. Varietal discrimination of Australian wines by means of mid-infrared spectroscopy and multivariate analysis. *Anal. Chim. Acta* 621, 19-23.

Boido, E., Medina, K., Fariña, L., Carrau, F., Versini, G. & Dellacassa, E., 2009. The effect of bacterial strain and aging on the secondary volatile metabolites produced during malolactic fermentation of Tannat red wine. *J. Agric. Food Chem*. 57, 6271-6278.

Cozzolino, D., Smyth, H.E. & Gishen, M., 2003. Feasibility study on the use of visible and near-infrared spectroscopy together with chemometrics to discriminate between commercial white wines of different varietal origins. *J. Agric. Food Chem*. 51, 7703-7708.

Cozzolino, D., McCarthy, J. & Bartowsky, E., 2012. Comparison of near infrared and mid infrared spectroscopy to discriminate between wines produced by different *Oenococcus Oeni* strains after malolactic fermentation: A feasibility study. *Food control* 26, 81-87.

Delaquis, P., Cliff, M., King, M., Girard, B., Hall, J. & Reynolds, A., 2000. Effect of two commercial malolactic cultures on the chemical and sensory properties of chancellor wines vinified with different yeasts and fermentation temperatures. *Am. J. Enol. Vitic*. 51, 42-48.

De Revel, G., Martin, N., Pripis-Nicolau, L., Lonvaud-Funel, A. & Bertrand, A., 1999. Contribution to the knowledge of malolactic fermentation influence on wine aroma. J. Agric. *Food Chem*. 47, 4003-4008.

de Villiers, A., Alberts, P., Tredoux, A.G.J. & Nieuwoudt, H.H., 2011. Analytical techniques for wine analysis: An African perspective. *Anal. Chim. Acta* 730, 1-22.

Drici-Cachon, A., Guzzo, J., Cavin, F., & Diviès, C., 1996. Acid tolerance in Leuconostoc oenos. Isolation and characterisation of an acid resistant mutant. *Appl Microbiol. Biotechnol*. 44, 785–789

du Toit, M., Engelbrecht, L., Lerm, E. & Krieger-Weber, S., 2010. *Lactobacillus*: The next generation of malolactic fermentation starter cultures-an overview. *Food Bioprocess Technol*. 4, 876-906.

Ebeler, S.E., 2001. Analytical chemistry: Unlocking the secrets of wine flavor. *Food Rev. Int*. 17, 45-64.

Edelmann, A., Diewok, J., Schuster, K.C. & Lendl, B., 2001. Rapid method for the discrimination of red wine cultivars based on mid-infrared spectroscopy of phenolic wine extracts. *J. Agric. Food Chem*. 49, 1139-1145.

Esbensen, K.H. (ed). 2006. *Multivariate Data Analysis – In Practice*. 5th Ed. Camo ASA, Oslo, Norway.

Fornachon, J. & Lloyd, B., 2006. Bacterial production of diacetyl and acetoin in wine. *J. Sci. Food Agric*. 16, 710-716.

Francis, I.L. & Newton, J.L., 2005. Determining wine aroma from compositional data. *Aust. J. Grape Wine Res*. 11, 114-126.

Herjavec, S., Tupajić, P. & Majdak, A., 2001. Influence of malolactic fermentation on the quality of Riesling wine. *Agric. Conspec. Sci*. 66, 59-64.

Izquierdo Cañas, P., García Romero, E., Gómez Alonso, S. & Palop Herreros, M., 2008. Changes in the aromatic composition of Tempranillo wines during spontaneous malolactic fermentation. J. *Food Compos. Anal.* 21, 724-730.

Jeromel, A., Herjavec, S., Orlić, S., Redžepović, S. & Wondra, M., 2008. Changes in volatile composition of Kraljevina wines by controlled malolactic fermentation. *J. Cent. Eur. Agric*. 9, 363-372.

Knoll, C., Fritsch, S., Schnell, S., Grossmann, M., Rauhut, D. & Du Toit, M., 2011. Influence of pH and ethanol on malolactic fermentation and volatile aroma compound composition in white wines. *LWT-Food Sci. Technol*. 44, 2077-2086.

Knoll, C., Fritsch, S., Schnell, S., Grossmann, M., Krieger-Weber, S., du Toit, M. & Rauhut, D., 2012. Impact of different malolactic fermentation inoculation scenarios on Riesling wine aroma. *World J. Microbiol. Biotechnol*. 28, 1143-1153.

Lambrechts, M.G. & Pretorius, I.S., 2000. Yeast and its importance to wine aroma-a review. *S. Afr. J. Enol. Vitic*. 21, 97-129.

Laurent, M.H., Henick-Kling, T. & Acree, T.E., 1994. Changes in the aroma and odor of Chardonnay wine due to malolactic fermentation. *Vitic. Enol. Sci*. 49, 3–10.

Lee, J.E., Hong, Y.S & Lee, C.H., 2009a. Characterization of fermentative behaviors of lactic acid bacteria in grape wines through ^{1}H-NMR- and GC-based metabolic profiling. *J. Agric. Food Chem. 57*, 4810-4817.

Lee, J.E., Hwang, G.S., Lee, C.H. & Hong, Y.S., 2009b. Metabolomics reveals alterations in both primary and secondary metabolites by wine bacteria. *J. Agric. Food Chem*. 57, 10772-10783.

Lerm, E., Engelbrecht, L. & du Toit, M., 2010. Malolactic fermentation: The ABC's of MLF. *S. Afr. J. Enol. Vitic*. 31, 186-212.

Lilly, M., Lambrechts, M.G. & Pretorius, I.S., 2000. Effect of increased yeast alcohol acetyltransferase activity on flavor profiles of wine and distillates. *Appl Environ. Microbiol*. 66, 744–753.

Liu, S.Q., 2002. Malolactic fermentation in wine - beyond deacidification. A review. *J. Appl. Microbiol*. 92, 589-601.

Lonvaud-Funel, A., 1999. Lactic acid bacteria in the quality improvement and depreciation of wine. *Antonie Leeuwenhoek.* 76, 317-331.

Louw, L., Roux, K., Tredoux, A., Tomic, O., Næs, T., Nieuwoudt, H.H. & van Rensburg, P., 2009. Characterization of selected South African young cultivar wines using FTMIR spectroscopy, gas chromatography, and multivariate data analysis. *J. Agric. Food Chem*. 57, 2623-2632.

Magerman, C.M., 2009. The evaluation of Fourier transform infrared (FT-IR) spectroscopy for quantitative and qualitative monitoring of alcoholic wine fermentation. Thesis, Stellenbosch University, Private Bag X1, 7602, Matieland (Stellenbosch), South Africa.

Maicas, S., Gil, J., Pardo, I. & Ferrer, S., 1999. Improvement of volatile composition of wines by controlled addition of malolactic bacteria. *Food Res. Int*. 32, 491-496.

Malherbe, S., Tredoux, A.G.J., Nieuwoudt, H.H. & du Toit, M., 2012. Comparative metabolic profling to investigate the contribution of *O. oeni* MLF starter cultures to red wine composition. *J. Ind. Microbiol. Biotechnol*. 39, 477–494.

Manley, M., Van Zyl, A. & Wolf, E., 2001. The evaluation of the applicability of Fourier transform near-infrared (FT-NIR) spectroscopy in the measurement of analytical parameters in must and wine. *S. Afr. J. Enol. Vitic*. 22, 93-100.

Martineau, B., & Henick-Kling, T., 1995. Formation and degradation of diacetyl in wine during alcoholic fermentation with *Saccharomyces cerevisiae* strain EC 1118 and malolactic fermentation with *Leuconostoc oenos* strain MCW. *Am. J. Enol. Vitic*. 46, 442-448.

Martineau, B., Acree, T.E & Henick-Kling, T., 1995. Effect of wine type on the detection threshold for diacetyl. *Food Res. Int*. 28, 139-143.

Matthews, A., Grimaldi, A., Walker, M., Bartowsky, E., Grbin, P. & Jiranek, V., 2004. Lactic acid bacteria as a potential source of enzymes for use in vinification. *Appl. Environ. Microbiol*. 70, 5715-5731.

Matthews, A., Grbin, P.R. & Jiranek, V., 2006. A survey of lactic acid bacteria for enzymes of interest to oenology. *Aust. J. Grape Wine Res.* 12, 235-244.

Næs, T., Isaksson, T., Fearn, T. & Davies, T. (eds). 2002. *A user friendly guide to multivariate calibration and classification*. NIR Publications. Chichester, UK.

Nieuwoudt, H.H., Pretorius, I.S., Bauer, F.F., Nel, D.G. & Prior, B.A., 2006. Rapid screening of the fermentation profiles of wine yeasts by Fourier transform infrared spectroscopy. *J. Microbiol. Methods*. 67, 248-256.

Osborne, C.D., 2007. Discriminating wine yeast strains and their fermented wines: an integrated approach. Thesis, Stellenbosch University, Private Bag X1, 7602, Matieland (Stellenbosch), South Africa.

Palma, M. & Barroso, C., 2002. Application of FT-IR spectroscopy to the characterisation and classification of wines, brandies and other distilled drinks. *Talanta* 58, 265-271.

Patz, C.D., Blieke, A., Ristow, R. & Dietrich, H., 2004. Application of FT-MIR spectrometry in wine analysis. *Anal. Chim. Acta* 513, 81-89.

Peinado, R.A., Moreno, J., Bueno, J.E., Moreno, J.A. & Mauricio, J.C., 2004a. Comparative study of aromatic compounds in two young white wines subjected to pre-fermentative cryomaceration. *Food Chem*. 84, 585-590.

Peinado, R.A., Moreno, J.A., Muñoz, D., Medina, M. & Moreno, J., 2004b. Gas chromatographic quantification of major volatile compounds and polyols in wine by direct injection. *J. Agric. Food Chem*. 52, 6389-6393.

Pozo-Bayón, M.A., Alegría, E.G., Polo, M.C., Tenorio, C., Martín-Álvarez, P.J., Calvo de la Banda, M.T., Ruiz-Larrea, F. & Moreno-Arribas, M.V., 2005. Wine volatile and amino acid composition after malolactic fermentation: Effect of *Oenococcus oeni* and *Lactobacillus plantarum* starter cultures. *J. Agric. Food Chem*. 53, 8729-8735.

Rapp, A., 1998. Volatile flavour of wine: Correlation between instrumental analysis and sensory perception. *Nahrung* 42, 351-363.

Ribéreau-Gayon, P., Dubourdieu, D., Doneche, B. & Lonvaud, A. (eds). 2006. *Handbook of Enology: The chemistry of wine stabilization and treatments*, Vol 2. 2nd Ed. Wiley, New York, USA. pp. 59

Roussel, S., Bellon-Maurel, V., Roger, J.M. & Grenier, P., 2006. Authentication of white grape must variety with classification models based on aroma sensors, FT-IR and UV spectrometry. *J. Food Eng. 60*, 407–419.

Skov, T., Ballabio, D. & Bro, R., 2008. Multiblock variance partitioning: A new approach for comparing variation in multiple data blocks. *Anal. Chim. Acta* 615, 18-29.

Son, H.S., Hwang, G.S., Park, W.M., Hong, Y.S., Lee, C.H., 2009. Metabolomic characterization of malolactic fermentation and fermentative behaviors of wine yeasts in grape wine. *J. Agric. Food Chem*. 57, 4801-4809.

Statsoft, Inc. (2011) STATISTICA (data analysis software system), version 10. www.statsoft.com

Swiegers, J.H., Bartowsky, E.J., Henschke, P.A. & Pretorius, I.S., 2005. Yeast and bacterial modulation of wine aroma and flavour. *Aust. J. Grape Wine Res*. 11, 139-173.

Ugliano, M. & Moio, L., 2005. Changes in the concentration of yeast-derived volatile compounds of red wine during malolactic fermentation with four commercial starter cultures of *Oenococcus oeni*. *J. Agric. Food Chem*. 53, 10134-10139.

Versari, A., Parpinello, G. & Cattaneo, M., 1999. *Leuconostoc oenos* and malolactic fermentation in wine: A review. *J. Ind. Microbiol. Biotechnol*. 23, 447-455.

WineScan FT 120 Type 77110 and 77310 Reference Manual, Issue 4 GB Foss Electric, Denmark, 2001. http://www.foss.dk

Chapter 5

Research Results

High-throughput Fourier transform mid-infrared (FT-MIR) and near-infrared (FT-NIR) spectroscopy calibrations for the quantification of malic acid and lactic acid

CHAPTER 5. RESEARCH RESULTS

High-throughput Fourier transform mid-infrared (FT-MIR) and near-infrared (FT-NIR) spectroscopy calibrations for the quantification of malic acid and lactic acid

Jessica Garlick[1], Maret du Toit[1], Hélène Nieuwoudt[1]

[1]Institute for Wine Biotechnology, Department of Viticulture and Oenology, Stellenbosch University, Private Bag X1, Matieland, 7602 South Africa

ABSTRACT

Fourier transform infrared (FT-IR) spectroscopy is known to be a fast cost effective alternative to traditional wet chemistry techniques used for routine monitoring of wine fermentations. The FT-MIR WineScan instrument used in our environment is supplied with commercial ready-to-use calibration models. However, to date no tested models have been established for malic acid and lactic acid in a South African wine matrix. For the purpose of monitoring of fermentations in this study there was a clear need to optimise these calibration models. The aim of this study was therefore to first evaluate the performance of the ready-to-use FT-MIR calibration model for the quantification of malic acid in the South African wine matrix (n=1239), as well as to develop new FT-MIR and FT-NIR calibration models for malic acid (n= 185 and n = 133) and lactic acid (n = 114 and n = 68) for the purpose of monitoring in a Shiraz wine matrix of this study. Samples from 11 Shiraz batch fermentations were collected at regular time intervals throughout alcoholic and malolactic fermentations and analysed with FT-MIR and FT-NIR spectroscopy and enzymatic reference methods. The results of this study showed that the global model gave a very poor prediction (SEP = 0.96 g/L, R^2 = 0.7867, bias = 0.91, RPD = 2.2) and was not suitable for the quantification of malic acid for this study. The newly established calibrations models for malic acid (SEP = 0.06 g/L, R^2 =0.9835, bias = - 0.00 g/L, RPD = 7.8) and lactic acid (SEP = 0.04 g/L, R^2 = 0.9923, bias = 0.00 g/L, RPD = 8.4) using FT-MIR spectroscopy showed very good performance for the quantification of these constituents, while NIR spectroscopy yielded fairly poor calibrations for malic acid (SEP = 0.10 g/L, R^2 = 0.95, bias = 0.01 g/L, RPD = 4.7) and lactic acid (SEP =0.11 g/L, R^2 = 0.91, bias = 0.03 g/L, RPD = 3.5) when evaluating the RPD values. However, these models were optimal for the monitoring purposes in our study. FT-IR therefore proved to be a useful technique for the quantification of these major organic acids for the off-line monitoring of malolactic fermentation.

5.1 INTRODUCTION

The use of Fourier transform mid-infrared (FT-MIR) and near-infrared (FT-NIR) spectroscopic techniques has for many years been recognised as powerful tools for the quantification of wine constituents for routine wine analysis purposes (reviewed by Bauer *et al*., 2008; De Villiers *et al*., 2012). Various organic and inorganic constituents present in wine exhibit optical properties which absorb in the infrared (IR) region of the electromagnetic (EM) spectrum. The MIR region usually ranges from 200 – 4000 cm^{-1} while the NIR region usually ranges from 12, 800 – 4, 000 cm^{-1} or 780 – 2,500 nm. Spectroscopic techniques therefore measure the frequencies of the vibrations of covalent bonds present in functional groups, for example C-C, C-H, O-H, C=O and N-H, upon absorption of radiation in the MIR and NIR regions of the EM spectrum. Through various mathematical calculations including Fourier transformation, the measured frequencies are processed to produce an absorbance- or transmittance spectrum (Smith, 1999; Pavia *et al*., 2009). Multivariate calibration techniques such as partial least squares (PLS) regression finds correlations between spectra and the actual concentrations of constituents in the wine matrix (Næs *et al*., 2002; Esbensen, 2006). Spectral pre-processing techniques such as first derivative and multiplicative scatter correction (MSC) are often applied to spectral measurements in order to optimize the multivariate calibration (Martens *et al*., 2003) by removing irrelevant information in the spectra that cannot be interpreted by the regression techniques (Nicolaï *et al*., 2007). The use of instruments such as the WineScan FT 120 (Foss Analytical, Denmark, http://www.foss.dk) to quantify wine constituents has shown excellent performance results in terms of speed of analysis, accuracy and good precision (Gishen & Holdstock, 2000; Nieuwoudt *et al*., 2004; Patz *et al*., 2004; Louw *et al*., 2009).

The routine monitoring of wine fermentations usually involves chemical analysis including enzymatic analysis and chromatography which require large extensive sample preparation, expensive equipment and often many purification steps, which delay obtaining the results in real-time (Cozzolino *et al*., 2006; Urtubia *et al*., 2004). IR spectroscopy as a quantification technique can, however, be used for monitoring purposes. IR spectroscopy is seen as a high-throughput, cost effective and non-destructive alternative to the traditional routine analysis techniques for the quantification of chemical constituents using calibration techniques (Urtubia *et al*., 2008). Both enzymatic analysis, as well as IR spectroscopy, is seen as high-throughput techniques, however, the establishment of IR calibration models allows for less wet analytical chemistry to be done in the future.

The WineScan instrument is specific for applications in wine and grape matrices and is issued with ready-to-use commercial calibrations. South African samples were, however, not included in the establishment of these models.

This poses as a problem when wanting to predict constituents in a South African must matrix. The wine matrix presents a large amount of variation in terms of cultivar, style, geographic origin, vintage, chemical composition and maturation periods and therefore these calibration models need to be evaluated in terms of their accuracy for predicting samples in a specific matrix (Nieuwoudt *et al*., 2004).

Malic acid and lactic acid are quantitatively major organic acids found in wine (Volschenk *et al*., 2006). The routine monitoring of malic acid concentrations in particular is used as an indicator of the progress of malolactic fermentation (MLF) and is therefore seen as an important quality parameter in winemaking. Several organic acids are present at varying concentrations in the wine matrix. The quantification of single organic acids by FT-IR presents several limitations due to the spectral similarities of these individual organic acids (Moreira & Santos, 2005). It is also known that sugars and organic acids share a carbonyl group as well as C-O and O-H infrared bands and therefore cause further spectral interferences when quantifying organic acids present at lower concentrations (Moreira & Santos, 2005).

The objective of this study was therefore to evaluate the ability of the ready-to-use FT-MIR calibration model to predict malic acid in South African samples as well as to establish new high-throughput FT-MIR and FT-NIR calibration models for the quantification of malic acid and lactic acid in a Shiraz wine matrix using an enzymatic technique for the generation of reference data. These quantitative models will be used for the purpose of monitoring for this particular study.

5.2 MATERIALS AND METHODS

5.2.1 FERMENTATION SAMPLES

The experimental design and sampling procedure carried out in this study follows that which has been reported in **Figures 3.1 and 3.2 in Chapter 3**. Sampling involved the collection of independent duplicate samples (30 ml) per fermentation at 12 hourly intervals where possible, throughout alcoholic and malolactic fermentation. The strategy was to obtain as many samples as possible for bioprocess monitoring purposes and to obtain the widest range of malic acid and lactic acid concentrations for calibration purposes. The total number of 1239 samples was obtained for the validation of the ready-to-use model.

5.2.2 FT-MIR AND FT-NIR SPECTROSCOPY

FT-MIR and FT-NIR spectroscopy was carried out as reported in **Chapter 3**. Duplicate FT-MIR spectra for each sample were generated using a WineScan FT 120 spectrometer

(FOSS Analytical A/S software version 2.2.1, Denmark, 2001) in transmission mode over the spectral range 5011 - 929 cm^{-1} at 4 cm^{-1} intervals (i.e, 1056 data points per spectrum). Each spectrum is based on 20 repeat scans. FT-MIR data were treated as reported in **Figure 3.2A in Chapter 3**.

A quartz cuvette with a 1 mm path length was used with a FT-NIR spectrometer (MPA, Multi Purpose FT-NIR analyser instrument, Bruker Optics, Ettlingen, Germany) to generate FT-NIR spectral data in transmission mode over the range 12,499 - 3,999 cm^{-1} (resolution of 8 cm^{-1}). Each spectrum is based on an average of 16 repeat scans. The FT-NIR data were treated as seen in **Figure 3.2A in Chapter 3** for further analysis.

5.2.3 REFERENCE METHODS

5.2.3.1 MALIC ACID AND LACTIC ACID

A total of 1239 frozen samples were thawed at ambient laboratory temperature (±20 °C) and thoroughly mixed before analysis. Reference values for malic acid and lactic acid were generated to establish calibration sets together with the corresponding FT-IR spectra. Malic acid (expressed as g/L) and lactic acid (expressed as g/L) were determined using an established in-house enzyme-linked assay using Enzytec™ kits for L- Malic acid (Id number, E 5280) and L-Lactic acid (Id number, E 5260) (Thermo Fisher Scientific Oy, Finland) on the automated Arena Konelab 20 XT Photometric analyser (Part number: 984163, Thermo Electron Oy, Finland).

5.2.4 MULTIVARIATE DATA ANALYSIS

5.2.4.1 PCA

The FT-MIR and FT-NIR spectral data were exported and reformatted (duplicate spectra averaged) in Microsoft excel and subsequently exported into The Unscrambler® X (version 10.2, Camo, Nedre Vollgate, Norway). PCA was used to reduce the dimensionality of the data to a smaller number of principal components (PC's) (Næs *et al*., 2002; Esbensen, 2006). PC's describe in decreasing order the maximum variance among the observations. This exploratory tool was used to examine groupings and trends in the data. PCA was used for the identification of spectral outliers using the score, residual, Hotelling T^2 and influence plots in The Unscrambler® X. PCA was performed using random cross validation (20 segments, 99 samples per segment).

5.2.4.2 PLS

PLS was the multivariate regression technique used for all the calibration work in this study. Independent test set validation was used for the validation of the calibration models. The full spectral set for each compound was divided into a calibration and a validation set consisting of 70% and 30%, respectively. The minimum and maximum values in the full spectral set were included in the calibration set. **Figure 2.8 in Chapter 2** shows the process followed for establishing and validating the calibration models.

PLS finds a relationship between two sets of data, an X-matrix and a Y-matrix by regression modelling. This algorithm can be used to predict the y variables in future samples. This method projects the original x variables onto a smaller number of PLS components also known as “latent variables” or “factors”. The factors are calculated in the same way as PC’s are calculated in PCA with the incorporation of the y variable into the calculation (Esbensen, 2006).

Before calibration sets were established outliers were detected using PCA and were confirmed by X-Y relation outlier plots (T vs. U scores) during PLS regression for each data set. Samples which deviated considerably from the straight regression line relationship in the X-Y relation plot were removed. Outliers include spectral outliers as well as poorly predicted samples, which are characterized by a large difference between predicted and reference values (also known as residuals). Samples with malic acid and lactic acid values below 0.09 g/L were removed from the respective spectral sets. These samples fall below the limit of accurate quantification by spectroscopic techniques.

5.2.5 VALIDATION OF READY-TO-USE MALIC ACID CALIBRATION MODEL

The ready-to-use malic acid model (**Table 5.1**) was evaluated on its ability to predict malic acid in South African fermenting must samples. The complete spectral set for malic acid was fitted as an independent validation set onto the ready-to-use calibration model. PLS was used to evaluate the goodness-of-fit using the Advanced Performance software module version 2.2.2 of the FT-MIR spectrometer (WineScan FT120 Type 77110 and 77310 Reference Manual, FOSS Analytical, Denmark, 2001).

Table 5.1 Descriptive statistics of the malic acid ready-to-use calibration model provided with the WineScan FT 120 instrument.

n[a]	Mean	Min[b]	Max[c]	Reference method	Reference[d]
2654	1.25	0.00	13.20	Enzymatic	Application note 159, P/N 1025297

[a]number of samples; [b]Minimum; [c]Maximum; [d]Application notes for WineScan FT120, Issue 2GB, October 2001, Foss Analytical, Denmark. http://www.foss.dk.

5.2.6 ESTABLISHING NEW FT-MIR AND FT-NIR MALIC ACID AND LACTIC ACID CALIBRATION MODELS

5.2.6.1 FT-MIR CALIBRATION MODELS

New FT-MIR calibration models for both malic acid and lactic acid were established using the Advanced Performance Software Module version 2.1.0, an extension of the basic WineScan FT 120 instrument software (WineScan FT 120 Type 77110 and 77310 Reference Manual, Foss Analytical, Denmark, 2001). The WineScan software by default automatically selects 15 "filters" (single wavenumbers or a small group of adjacent wavenumbers; 18 wavenumbers selected for malic acid and 22 wavenumbers selected for lactic acid in this study). The wavenumbers with the highest correlation between the measured absorbance and the corresponding reference value are therefore selected and collectively captures the maximum variation in the concentration of the y-variable in question (WineScan Reference Manual, Foss Analytical, Denmark, 2001).

Further calibration work was done on the FT-MIR spectra using The Unscrambler® X software. These calibrations included larger wavenumber regions than those proposed by the WineScan software in order to evaluate the influence of wavenumber selection on the predictive abilities of the calibration models. No spectral pre-processing techniques were used on the FT-MIR data.

5.2.6.2 FT-NIR CALIBRATION MODELS

The OPUS QUANT 2 software version 6.5 (Bruker Optics, Ettlingen, Germany) was used to develop FT-NIR calibration models for malic acid and lactic acid. The interactive region selection allowed for the removal of noise from the calibration models. More than 300 models involving different combinations of spectral pre-processing techniques and spectral ranges were tested by the software in the optimisation step for each component separately. The mathematical pre-processing treatments available for optimisation included no data treatment, constant offset elimination, straight line subtraction, vector normalization (SNV), minimum-maximum normalisation, multiplicative scatter correction (MSC), 1st derivative, 2nd

derivative, 1st derivative + straight line subtraction, 1st derivative + vector normalisation (SNV) and 1st derivative + MSC. The model with the most optimal combination [i.e. lowest root mean square error of prediction (RMSEP)] value was chosen. "Rank" refers to the number of PLS components.

5.2.7 EVALUATION OF THE PERFORMANCE OF CALIBRATION MODELS

The statistical indicators used to evaluate the calibration models included bias and the correlation coefficient (R^2). Furthermore the standard error of cross validation (SECV) and standard error of prediction (SEP) was used in the WineScan Advanced Performance Software and The Unscrambler® X software while the root mean square error of calibration (RMSECV) and root mean square error of prediction (RMSEP) was used in the OPUS software. Bias gives an indication of the systematic error in the predictive values and is calculated as the average of the residuals (difference between the reference values and the predicted values) (Esbensen, 2006). The SEP is the standard deviation of the predicted residuals and is equal to the RMSEP but corrected for bias. SEP measures precision of a prediction while RMSEP measures accuracy of the predictive ability of a model (Næs *et al*., 2002). The accuracy of the predictive ability of the calibration model, based on the reference data was expressed as SECV/RMSECV when based on the calibration samples, and as SEP/RMSEP when based on the independent validation set.

The residual predictive deviation (RPD) is defined as the ratio of the standard deviation of the reference values to the standard error of the predicted values when using independent test set validation (Esbensen, 2006). The higher the RPD value the higher the probability is of accurate prediction of future samples. The calculations of these indicators are standard statistical procedures reported by several references (Næs *et al*., 2002; Esbensen, 2006). A summary of the interpretation of RPD to evaluate the performance of a calibration model is described by Williams (2004) and is given in **Table 5.2**. The criterion categorizes the suitability of the calibration model for quantification purposes. This criterion, however, is subjective and will depend on the specific application.

Table 5.2 The evaluation of the RPD value to determine the performance of the calibration models in terms of quantification ability.

Performance parameter	Excellent	Very good	Good	Fair	Poor	Very poor
RPD[a]	>8.1	6.5 - 8.0	5.0 – 6.4	3.1 - 4.9	2.4 – 3.0	0 – 2.3

[a]Residual predictive deviation (Williams, 2004).

5.2.8 VALIDATION OF THE REFERENCE METHODS

An in-house validation procedure was followed to ensure the accuracy and repeatability of the appropriate reference methods. Calibrations in the range 0 - 1.65 g/L and 0 - 2 g/L were set up for malic acid and lactic acid respectively. When the concentrations of the specific constituents exceeded the calibration range in a specific sample, appropriate dilutions were carried out. Quality control samples of known malic acid and lactic acid concentration were run after every 10th sample and the average of these quality control results were reported as the quality control value for a specific run. A standard deviation of less than 8% for the quality control samples was the internal laboratory target.

5.3 RESULTS AND DISCUSSION

5.3.1 EVALUATION OF THE READY-TO-USE FT-MIR CALIBRATION MODEL FOR MALIC ACID

The performance of the malic acid calibration model provided with the WineScan FT 120 instrument was evaluated in terms of its ability to predict malic acid in fermenting must samples of this study. The complete malic acid spectral set (n=1239) was used as an independent test set to validate the global malic acid calibration model. These test samples were representative of South African fermenting red must samples but more specifically representative of future prediction samples for the purpose of this specific study. A summary of the validation statistics for the quantification of malic acid using the ready-to-use model is given in **Table 5.3**. Filters were deselected to ensure the lowest possible SEP based on the test set.

Table 5.3 The regression statistics evaluating the performance of the FT-MIR ready-to-use malic acid (g/L) calibration using an independent test set consisting of South African fermenting must samples.

n[a]	Min. – Max.[b]	SD[c]	PLS factors	SEC[d]	SEP[e]	Bias	R^{2f}	RPD[g]
1239	0.09–1.78	0.48	10	0.22	0.96	0.9121	0.7867	2.2

[a]Sample number; [b]Minimum - Maximum; [c]Standard deviation; [d]Standard error of calibration; [e]Standard error of prediction; [f]Coefficient of correlation; [g]Residual predictive deviation.

The range of the test set was between 0.09 and 1.78 g/L malic acid which fell within the range of the calibration set (0.00 - 13.20 g/L). The lowest SEP was determined using 10 PLS factors. The validation statistics for the unadjusted ready-to-use calibration model showed a large SEP and bias, respectively 0.96 g/L and 0.91 g/L, with a R^2 of 0.7867 (**Figure 5.1**). The prediction error of 0.96 g/L can be considered a fair estimate of the error level to be expected if we use this global model for the prediction of malic acid in our specific

samples. The RPD value less than three indicated that the ready-to-use model was not suitable for quantification of malic acid in South African fermenting must samples.

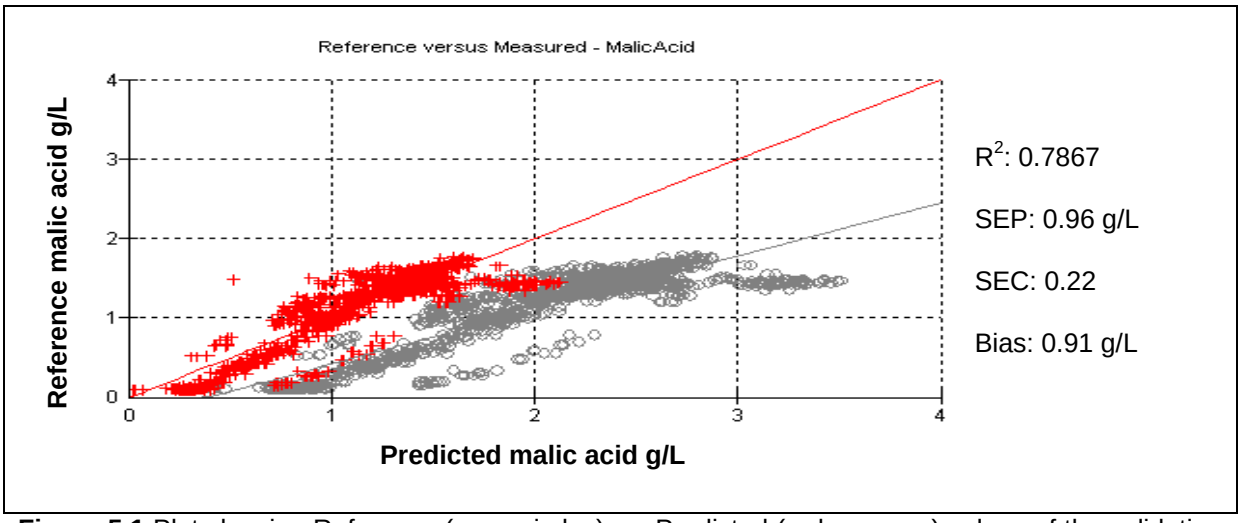

Figure 5.1 Plot showing Reference (grey, circles) vs. Predicted (red, crosses) values of the validation of the ready-to-use FT-MIR malic acid calibration using South African fermenting must samples. (**n=1239**)

The regression plot for the reference malic acid values vs. the predicted values showed a very poor fit of the South African malic acid samples onto the global calibration model (**Figure 5.1**).

The results of this validation show the importance of having a representative calibration set of the future prediction samples. The calibration set used to establish the global malic acid model was established using a large variety of must matrices from 11 different countries (Application note 159, P/N 1025297) but excluded SA samples. Although the malic acid range of the validation set fell within the calibration sets range the matrix of these two sets are very different. The range covered in the calibration set included exceptionally high malic acids values (0 - 13.20 g/L).

Fermenting must and wine samples can present a large amount of variation. Factors including, origin, vintage, cultivar, viticulture and vinification conditions vary and have a large influence on the matrix effect (Bauer *et al*., 2008). The large prediction error observed may therefore be due to a matrix effect which has been shown to affect the error of calibration models (Dambergs *et al*., 2002). For these reasons, the global model isn't suitable for the quantification of malic acid in the samples of this particular study.

5.3.2 ESTABLISHMENT OF NEW QUANTITATIVE CALIBRATION MODELS FOR MALIC ACID AND LACTIC ACID

It was therefore necessary to develop a new calibration model for the quantification of malic acid in our must samples. No previous lactic acid global calibration model was set up on the WineScan FT 120 instrument for fermenting must and thus new lactic acid calibrations were also established.

FT-MIR CALIBRATION MODELS FOR MALIC ACID AND LACTIC ACID

The new FT-MIR calibrations models were evaluated on their ability to predict malic acid and lactic acid in South African samples. The influence of wavenumber selection on the predictive ability of the models was evaluated. Thus two options were investigated, using the 15 highly correlated PLS filters proposed by the WineScan Advanced Performance Software Module as variables (spectral regions 964 - 1543 cm^{-1}, 1716 - 2732 cm^{-1} and 2434 - 2970 cm^{-1} are made available for selection of filters) and using the extended spectral region once water absorbance regions were deselected from the FT-MIR spectra (i.e. 311 wavenumbers). The extended spectral region included the wavenumber intervals 1582 - 965 cm^{-1}, 2006 - 1698 cm^{-1} and 2971 - 2701 cm^{-1} (Patz *et al*., 2004) as variables.

Filters which explained a small percentage of the variation in the sample set were deselected in a stepwise manner and the subsequent evaluation of the SEP was done to find the lowest number of filters giving the lowest possible SEP value.

Descriptive statistics for the calibration and validation sets using either filter selection or the extended spectrum region are given in **Table 5.4**.

Table 5.4 The descriptive statistics of the calibration and validation sets for establishing new FT-MIR calibration models for malic acid (g/L) and lactic acid (g/L).

Parameter	Calibration set			Validation set		
	N[a]	Min.– Max.[b]	SD[c]	N[a]	Min.– Max.[b]	SD[c]
Malic acid (g/L)	435	0.09±1.78	0.49	185	0.10±1.70	0.46
Lactic acid (g/L)	267	0.09±1.61	0.50	114	0.09±1.60	0.50

[a]Sample number; [b]Minimum - Maximum; [c]Standard deviation.

The 15 PLS factors selected for malic acid included 18 wavenumbers (**Table 5.5**). A total of 98.7% accumulated variance between the samples was explained by the 15 PLS filters for malic acid (**Table 5.5**). Similarly 22 wavenumbers were selected for lactic acid. A total of 99.36% accumulated variance between the samples was explained by 15 PLS filters for lactic acid (**Table 5.5**).

Table 5.5 Malic acid and lactic acid filters proposed by the WineScan Advanced Performance Software Module.

	Malic acid		Lactic acid	
Filter number	**From wavenumber to wavenumber**	**Accumulated explained variance**	**From wavenumber to wavenumber**	**Accumulated explained variance**
1	1153.542 - 1153.542	18.55	1103.388 - 1103.388	24.20
2	1728.384 - 1728.384	51.08	1728.384 - 1732.242	41.58
3	1381.164 - 1381.164	54.44	1130.394 - 1130.394	88.44
4	1130.394 - 1134.252	71.93	2881.926 - 2881.926	94.36
5	1018.512 - 1022.37	94.56	1022.37 - 1026.228	95.54
6	2878.068 - 2878.068	95.54	1388.88 - 1388.88	96.15
7	1516.194 - 1516.194	96.10	1516.194 - 1516.194	96.64
8	1246.134 - 1249.992	97.94	1458.324 - 1462.182	97.75
9	1720.668 - 1720.668	98.30	1238.418 - 1238.418	98.46
10	1346.442 - 1346.442	98.38	1165.116 - 1168.974	99.01
11	1365.732 - 1365.732	98.46	1720.668 - 1720.668	99.13
12	1469.898 - 1469.898	98.55	1342.584 - 1346.442	99.15
13	1396.596 - 1396.596	98.60	1365.732 - 1369.59	99.27
14	1535.484 - 1535.484	98.63	1469.898 - 1473.756	99.33
15	1184.406 - 1184.406	98.70	995.364 - 995.364	99.36

As discussed in **Chapter 3,** differences were observed between the filters selected for the two organic acids (**Table 5.5**). For malic acid, the three most prominent filters were at 1728 cm^{-1}, 1018 cm^{-1} to 1022 cm^{-1} and at 1153 cm^{-1}, collectively explaining 73% of the variation. The filters at 1130 cm^{-1}, 1103 cm^{-1} and at 1728 cm^{-1} to 1732 cm^{-1} were the three most prominent filters for lactic acid and explained 88% of the variation in lactic acid. These wavenumbers are therefore the most important for the quantification of malic acid and lactic acid respectively. By looking at the FT-MIR spectrum it is clear that these filters correspond to the prominent spectral peaks visually observed in the spectrum (**Figure 5.2**).

The only wavenumber which was common between the two organic acids was at 1728 cm^{-1} (**Figure 5.2**) which corresponds to the absorption of the C=O stretch band of carboxylic acids (Silverstein *et al*., 1991). The filter at 1728 cm^{-1} was the most prominent filter for malic acid explaining 32.53% of the variance while it explained 17.38% of the variance for lactic acid. These results correspond to a study carried out by Moreira & Santos

(2005) who reported wavenumber 1728 cm^{-1} to explain the highest variation for the determination of malic acid.

One study (Sivakesava *et al*., 2001) found high correlations bands at wavenumber region 1800 - 1625 cm^{-1} for lactic acid which corresponds to the filter at 1728 - 1723 cm^{-1} reported for the determination of lactic acid in our study (**Figure 5.2**).

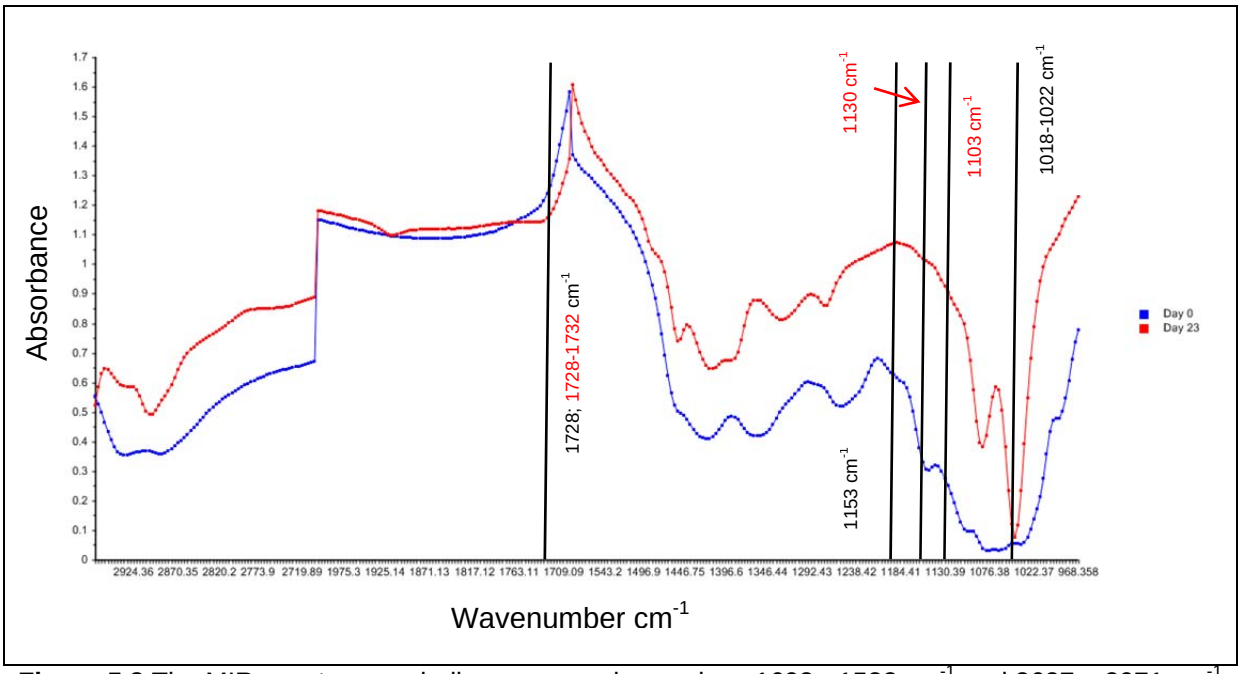

Figure 5.2 The MIR spectrum excluding wavenumber regions 1698 - 1582 cm^{-1} and 3627 – 2971 cm^{-1} which are characterised by the intense absorbance by water and region from 3627 cm^{-1} onwards containing very little useful information. Vertical lines indicate the filters which collectively explained 73% and 88% of the variation in malic acid (black wavenumbers) and lactic acid (red wavenumbers) respectively.

Table 5.6 shows the validation statistics of the new calibration models evaluating these different spectral regions.

Excellent statistics were obtained with the new malic acid and lactic acid FT-MIR calibration models. Very similar validation statistics were obtained when comparing the calibration models established using either the 15 filters or the extended spectral region for both malic acid and lactic acid (**Table 5.6**).

Table 5.6 The validation statistics for the evaluation of the new FT-MIR calibrations of malic acid and lactic acid.

Parameter	PLS Factors	R^{2a}	SEP[b] (g/L)	SEC[c]	RPD[d]	Bias (g/L)
Filter selection[e]						
Malic acid						
	9	0.9835	0.06	0.06	7.8	-0.0004
Lactic acid						
	10	0.9923	0.04	0.04	8.4	0.0017
Extended Spectrum[f]						
Malic acid						
	9	0.9860	0.06	0.06	8.5	-0.0013
Lactic acid						
	9	0.9934	0.04	0.04	12.2	-0.0020

[a]Coefficient of correlation ; [b]Standard error of prediction; [c]Standard error of calibration; [d]Residual predictive deviation; [e]Data analysis carried using the WineScan Advanced Performance Software Module; [f]Data analysis carried out using The Unscrambler X version 10.2 software.

The malic acid test set (n = 620) was divided into a calibration set (n = 435) and a validation set (n = 185) (**Figure 5.3**). The R^2 of 0.9835 indicated an excellent correlation between the malic acid concentrations measured with the reference method and the malic acid concentration predicted with the new calibration model. The RPD value of 7.8 and R^2 value both indicate a very good calibration model for the purpose of malic acid quantification. Nine PLS factors yielded the lowest SEP of 0.06 g/L with a bias value close to zero (**Figure 5.3**). The predictive ability of the new malic acid model performed exceptionally better than the global calibration model, however, this could be due to the smaller amount of variation in the sample matrix compared with that of the ready-to-use global model.

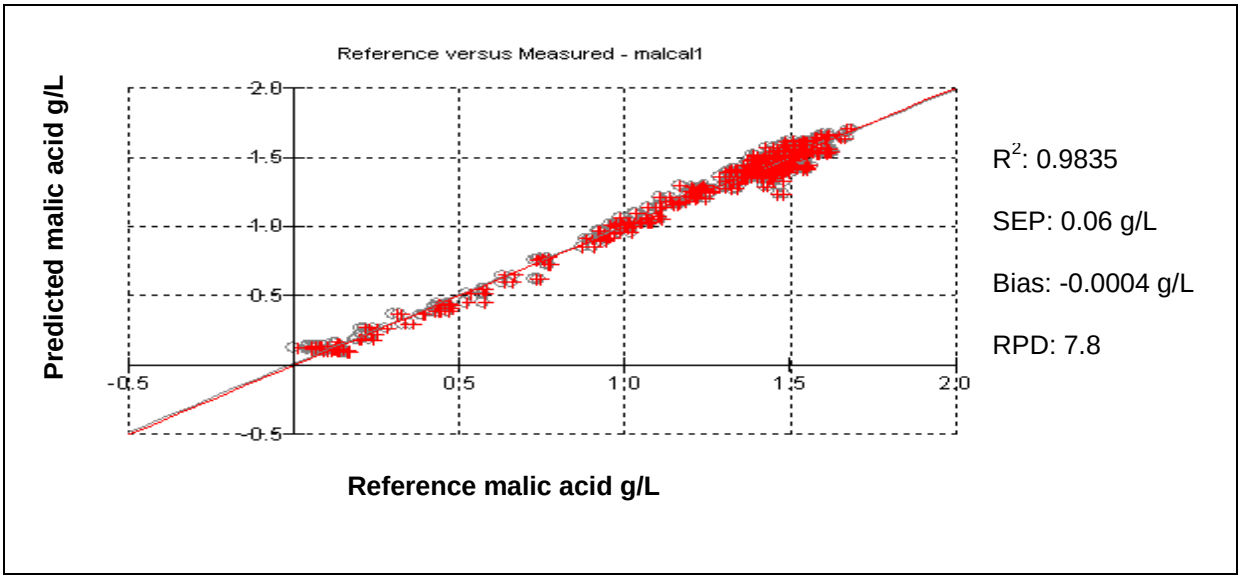

Figure 5.3 Plot showing the regression statistics of the FT-MIR calibration model for malic acid using PLS-regression with the 15 highly correlated wavenumber filters. (**n = 185**)

The histogram plot of the residual values for the new malic acid calibration shows that 97% of the samples had a prediction error smaller than 0.15 g/L while 94% of the samples had a

prediction error smaller than 0.1 g/L (**Figure 5.4**). These results indicate excellent calibrations for quantification purposes.

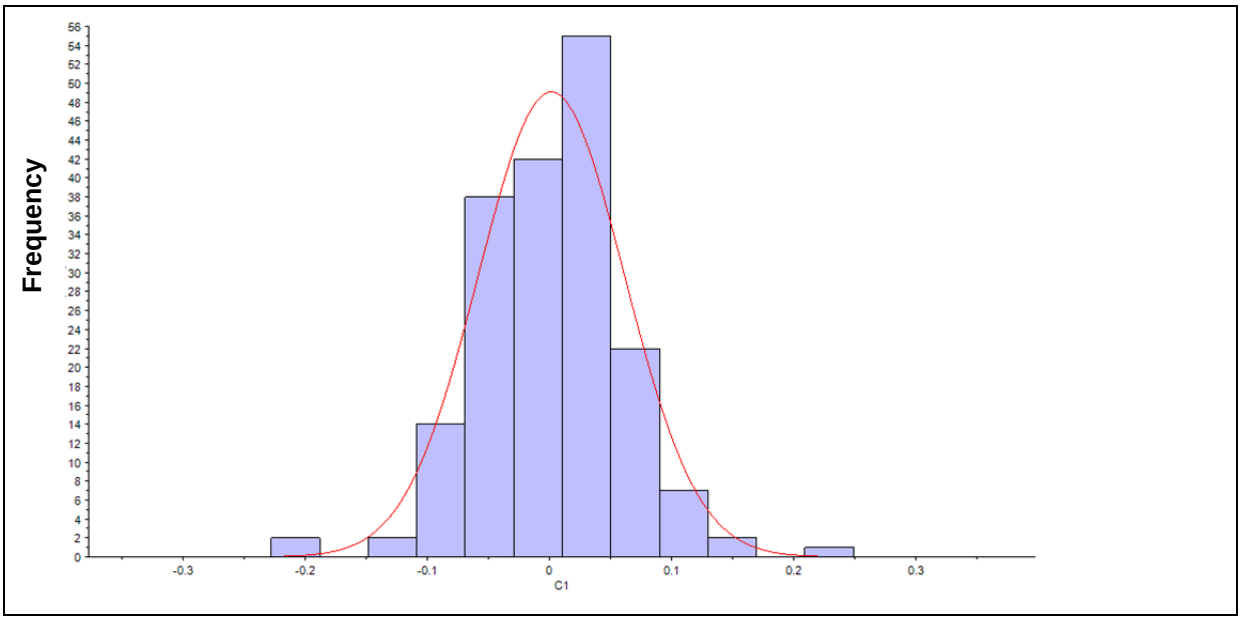

Figure 5.4 Histogram plot of the residuals for the FT-MIR malic acid calibration.

For the lactic acid calibration, the sample set (n = 381) was divided into a calibration set (n = 267) and a validation set (n = 114) (**Figure 5.5**). The calibration model for lactic acid prediction performed well, with the smallest prediction error of 0.04 g/L using 10 PLS factors. The correlation coefficient of 0.9923 and a RPD value of 8.4 indicate a very good calibration model for the purpose of lactic acid quantification (**Figure 5.5**).

The histogram plot of the residual values for the lactic acid calibration showed that 99% of the samples had a prediction error smaller than 0.1 g/L (**Figure 5.6**). These results indicated excellent calibrations for the quantification of lactic acid.

The results showed that the FT-MIR calibration models performed particular well for the purpose of monitoring malic acid and lactic acid in a Shiraz wine matrix.

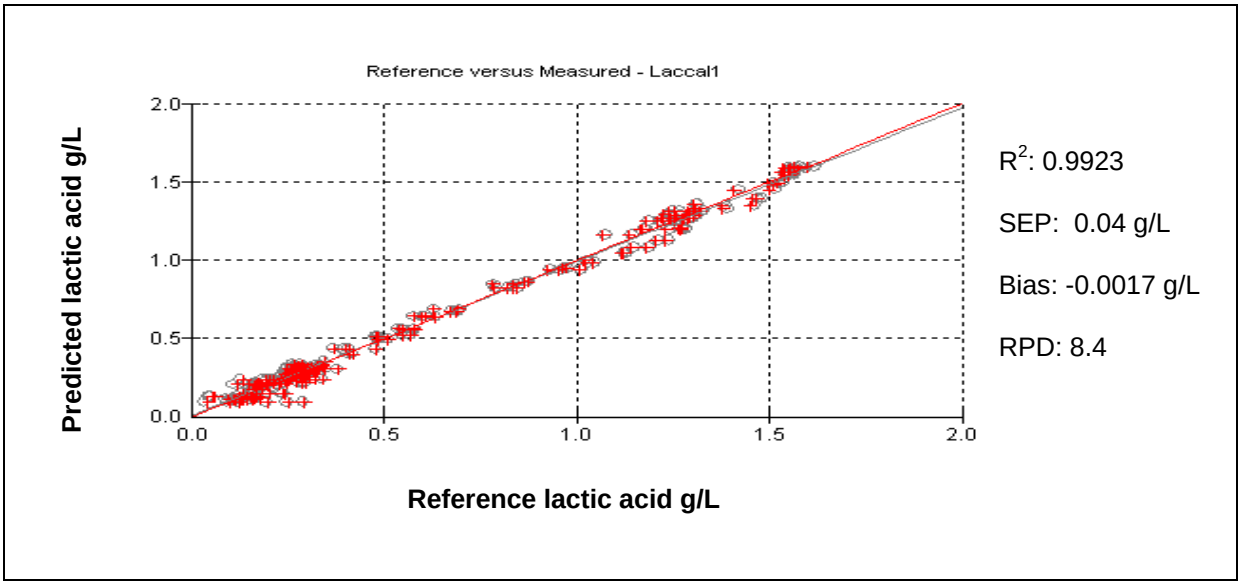

Figure 5.5 Plot showing the regression statistics of the FT-MIR calibration model for lactic acid using PLS-regression with 15 highly correlated wavenumber filters. (**n = 114**)

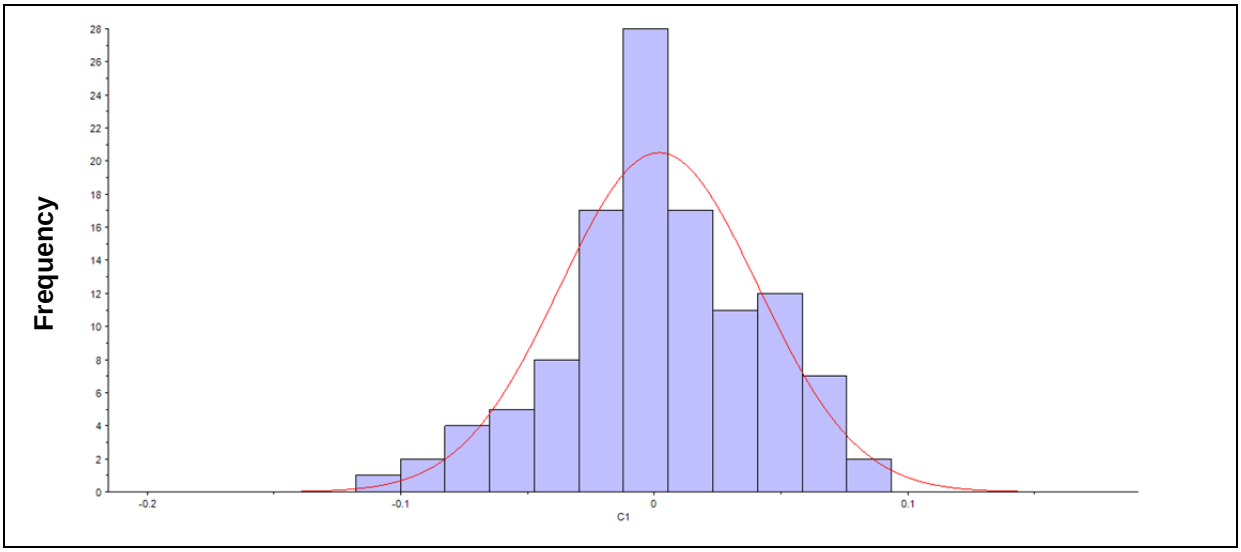

Figure 5.6 Histogram plot of the residuals for the FT-MIR lactic acid calibration.

FT-NIR CALIBRATION MODELS FOR MALIC ACID AND LACTIC ACID

The new FT-NIR calibrations models established using the OPUS software, were evaluated for their ability to predict malic acid and lactic acid. The following regions; 5264 - 5037 cm^{-1} and 4055 - 3999 cm^{-1} were removed for calibration purposes. Descriptive statistics for the calibration and validation sets of the FT-NIR calibration models are given in **Table 5.7.**

Table 5.7 The descriptive statistics of the calibration and validation sets for establishing new FT-NIR calibrations models for malic acid and lactic acid using the OPUS software.

Calibration			Validation		
Parameter	**Malic acid (g/L)**	**Lactic acid (g/L)**	**Parameter**	**Malic acid (g/L)**	**Lactic acid (g/L)**
n[a]	318	177	**n[a]**	133	68
Min. – Max.[b]	0.08-1.78	0.10-1.49	**Min.[b] – Max.[c]**	0.08-1.76	0.10-1.48
SD[c]	0.40	0.36	**SD[d]**	0.48	0.39

[a]Sample number; [b]Minimum - Maximum; [c]Standard deviation.

Table 5.8 gives the validation statistics of the various combinations of spectral regions and pre-processing treatments showing the lowest RMSEP values for malic acid.

Table 5.8 Validation statistics of the malic acid calibration models obtained from the optimisation using the OPUS software.

Spectral pre-processing	**Wavenumber region (cm^{-1})**	**Rank**	$\mathbf{R_{val}^{2a}}$	**RMSEP[b] (g/L)**	**RPD[c]**	**Bias (g/L)**
Constant offset elimination	6100 – 5449.2	10	0.95	0.10	4.7	0.0054
Minimum-maximum normalization	6100 – 5449.2	10	0.95	0.10	4.7	0.0077
MSC[d]	6100 – 5449.2	9	0.95	0.10	4.5	0.0029
No spectral pre-processing	6100 – 5449	10	0.91	0.14	3.3	0.0022

[a]Coefficient of correlation; [b]Standard error of prediction; [c]Residual predictive deviation; [d]Multiplicative scatter correction.

A high correlation between the NIR wavenumber region 6100 – 5449 cm^{-1} and the prediction of malic acid was proposed (**Table 5.8**). The combination of this region with three different spectral pre-processing treatments yielded the lowest SEP values. These included constant offset elimination, minimum-maximum normalisation and multiplicative scatter correction (MSC) which all yielded prediction errors of 0.10 g/L (**Table 5.8**). The validation statistics of these models were similar and showed only a very slight improvement in terms of the correlation coefficient (0.95) from that of the unprocessed data from the same spectral region (0.91) (**Table 5.8**).

These models all had R^2 values of above 0.9, however, the RPD values were between 3 and 4. These models therefore perform fairly for the purpose of quantification based on these RPD values. All these models were good enough for the purpose of quantification in this study. The model established with constant offset elimination pre-processing in the region 6100 – 5449 cm^{-1} showed the best performance for the prediction of malic acid (**Figure 5.7**).

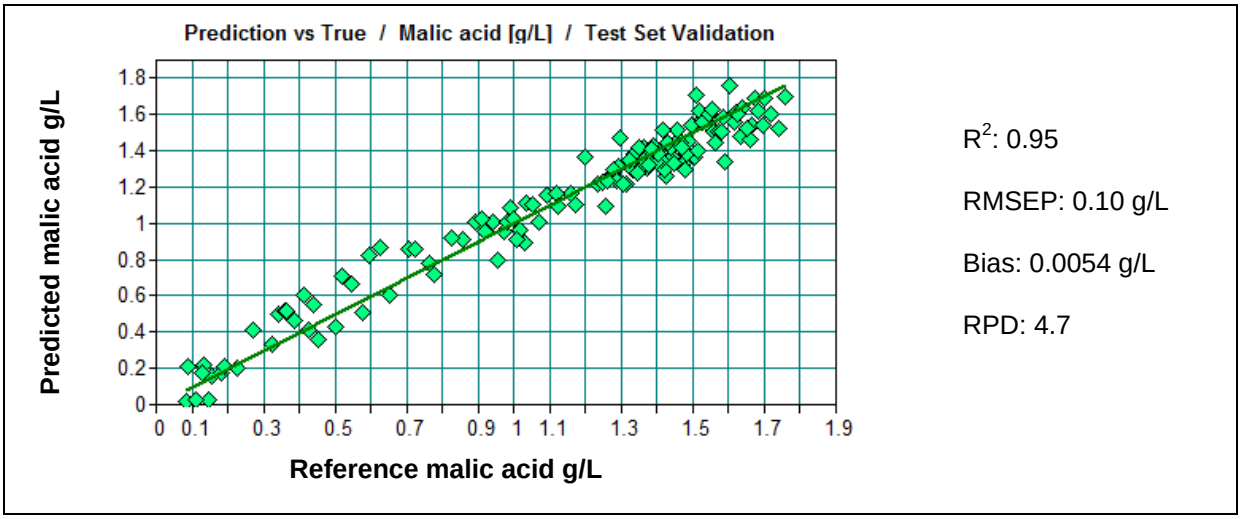

Figure 5.7 Plot showing the regression statistics of the FT-NIR calibration model for malic acid using PLS-regression. The model was established with a combination of constant offset elimination pre-processing in the region 6100 – 5449 cm^{-1}. (**n=133**)

Table 5.9 gives the validation statistics of the various combinations of spectral regions and pre-processing treatments showing the lowest RMSEP values for lactic acid.

Table 5.9 Validation statistics of the lactic acid calibration models obtained from the optimisation using the OPUS software.

Spectral pre-processing treatment	Wavenumber region (cm^{-1})	Rank	R^{2a}	RMSEP[b] (g/L)	RPD[c]	Bias (g/L)
1st derivative + vector normalization (SNV)[d]	6100 – 5449.2	10	0.91	0.11	3.5	0.0350
Vector normalization (SNV)[d]	6100 – 5449.2	10	0.89	0.12	3.2	0.0235
MSC[e]	6100 – 5449.2	10	0.89	0.12	3.2	0.0301
No spectral pre-processing	6100 – 5449		0.82	0.17	2.5	
MSC[e]	7500.2 – 5449.2; 4600.6 – 4291.1	10	0.87	0.13	3.0	0.0534
Constant offset elimination	7500.2 – 5449.2; 4600.6 – 4291.1	10	0.87	0.14	2.8	0.0309
No spectral pre-processing	7500.2 – 5449.2; 4600.6 – 4291.1	10	0.61	0.24	1.7	

[a]Coefficient of correlation; [b]Standard error of prediction; [c]Residual predictive deviation: [d]Standard normal variate; [e]Multiplicative scatter correction.

As with the malic acid results, a high correlation between the NIR wavenumber region 6100 – 5449 cm^{-1} and the prediction of lactic acid in the samples was proposed (**Table 5.9**). The spectral pre-processing treatments yielding the lowest SEP values of 0.11, 0.12 and 0.12 g/L respectively for lactic acid included first derivative + vector normalization (SNV), vector normalization (SNV) and MSC in this region (**Table 5.9**). The correlation coefficients of these models were very similar with first derivative and vector normalization (SNV) yielding

the highest R^2 of 0.91. The validation statistics of the pre-processed spectra showed only a slight improvement from that of the unprocessed data from the same spectral region (0.82) (**Table 5.9**). Although yielding slightly poorer results, the optimisation results also proposed a relatively high correlation between the NIR wavenumber regions 7500.2 - 5449.2 and 4600.6 - 4291.1 cm^{-1} and the prediction of lactic acid. The spectral pre-processing treatments yielding the lowest SEP values of 0.13 and 0.14 g/L lactic acid in these regions included MSC and constant offset elimination respectively (**Table 5.9**). The lactic acid calibration models using pre-processed spectral yielded RPD values slightly higher than the models without spectral pre-processing (**Table 5.9**). The FT-NIR calibration models performance in terms of the quantification of lactic acid can be reported as fair or even poor in some cases based on these RPD values. The model established with first derivative and SNV pre-processing in the region 6100 – 5449 cm^{-1} showed the best performance for the prediction of lactic acid (**Figure 5.8**).

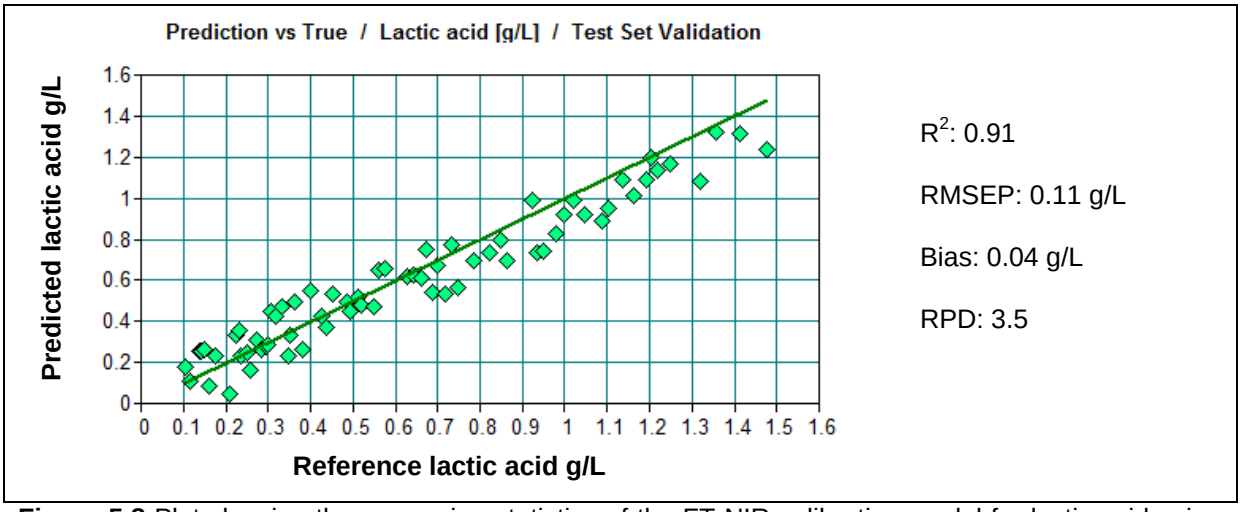

Figure 5.8 Plot showing the regression statistics of the FT-NIR calibration model for lactic acid using PLS-regression. The model was established with a combination of first derivative and SNV pre-processing in the region 6100 – 5449 cm^{-1}. (**n=68**)

Unlike the MIR calibration models which proposed single wavenumbers, the NIR calibration work established larger wavenumber regions and spectral pre-processings which were highly correlated to the prediction of malic acid and lactic acid. These proposed regions correlated to the variation which can be visually observed on the FT-NIR spectra (**Figure 5.9**). The regions which were proposed including 6100 – 5449 cm^{-1} and 7500.2 – 5449.2 cm^{-1} fall within the region where the C-H stretch, O-H stretch, C-O stretch and C=O stretch overtones of carboxylic acids are known to absorb (Shenk *et al*., 2008).

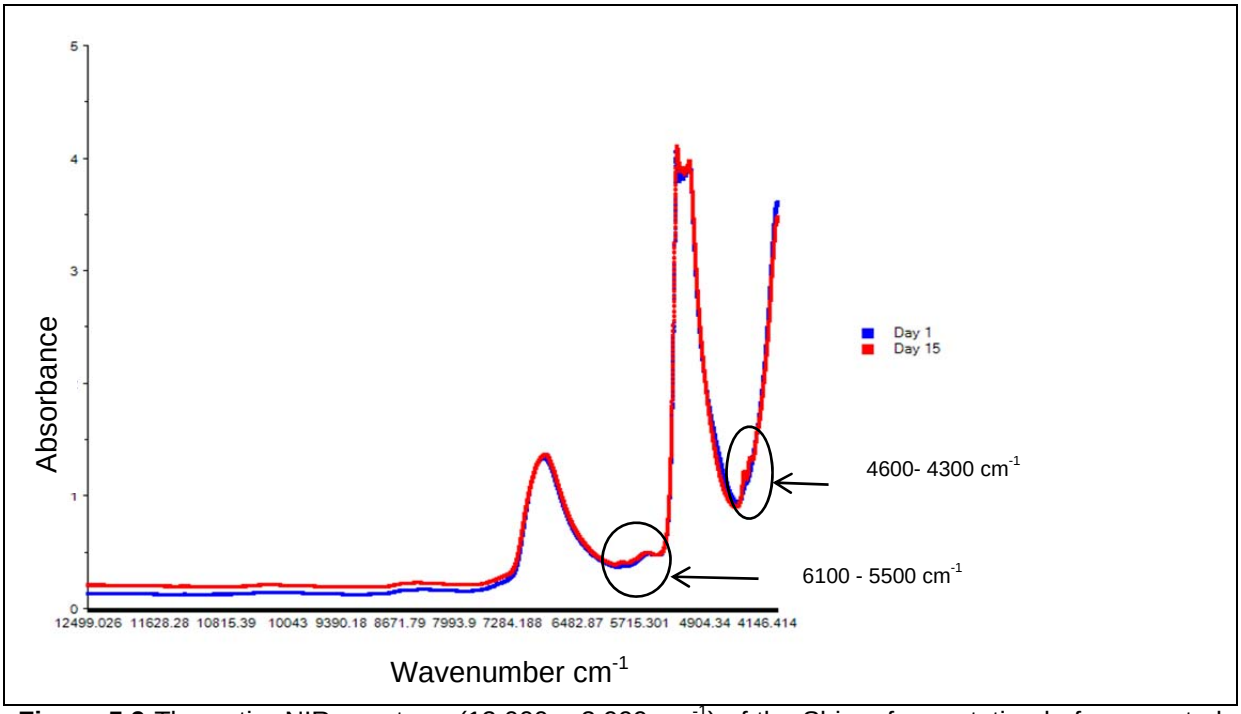

Figure 5.9 The entire NIR spectrum (12,000 – 3,999 cm^{-1}) of the Shiraz fermentation before spectral transformation. Circles show the wavenumber regions where visual variation was observed.

Very few comparative studies have reported on the quantification of malic acid and lactic acid using FT-MIR and FT-NIR spectroscopy. The quantification of malic acid and lactic acid by previous authors all used high performance liquid chromatography (HPLC) for the determination of reference values and showed varying results in terms of the infrared region yielding the best possible predictions. Using the MIR region SEP values of 0.56 g/L (Sivakesava *et al*., 2001), 0.55 g/L (Urbano Cuadrado *et al*., 2005) and 0.95 g/L (Picque *et al.,* 1993) for lactic acid have been reported. Studies using the NIR region have reported SEP values of 1.80 g/L (Sivakesava *et al*., 2001), 1.35 g/L (Manley *et al*., 2001) and 0.41 g/L (Urbano Cuadrado *et al*., 2004; 2005) for lactic acid and SEP values of 1.024 g/L (Manley *et al*., 2001) and 0.36 g/L (Urbano Cuadrado *et al*., 2004) for malic acid. Excellent correlations between MIR spectra and reference values were reported for the quantification of malic acid and lactic acid in a young wine matrix (Louw, 2007). The SEP values were reported as 0.26 g/L and 0.15 g/L for malic acid and lactic acid respectively. The calibration sets for these models were, however, extremely small, namely 36 samples for malic acid and 42 samples for lactic acid.

5.4 CONCLUSIONS

The calibration results of this study have shown great promise for the quantification of lactic acid and malic acid for the purpose of monitoring in a Shiraz wine matrix using both MIR and NIR spectral regions. While traditional monitoring techniques employed by the wine industry

are costly, time consuming and involve highly sophisticated equipment (Cozzolino *et al*., 2006) this study has shown the potential of IR spectroscopic techniques together with multivariate calibration as fast accurate alternatives for process monitoring and quality control.

To conclude the results of this study the RPD values for both malic acid and lactic acid calibrations models using FT-MIR spectroscopy showed very good calibration models for the purpose of quantification. These models yielded relatively low prediction errors confirming the potential for these calibration models to predict unknown samples in our study relatively accurately. The use of the 15 highly correlated filters and the extended spectrum yielded very similar results. The FT-NIR calibration models, however, had much lower RPD values and thus the calibration models for both malic acid and lactic acid were relatively poor. With this said, however, the prediction errors for these models were also relatively small but greater than the MIR calibration models.

Our calibrations models are surprisingly good when considering the spectral interferences which have been previously reported for the complex wine matrix (Moreira & Santos, 2005). It has been reported that the quantification of single organic acids presents difficulties due to the spectral similarities of the individual organic acids (Moreira & Santos, 2005). It is also known that sugars and organic acids share a carbonyl group as well as C-O and O-H infrared bands and therefore cause further spectral interferences when quantifying organic acids (Moreira &Santos, 2005; Bauer *et al*., 2008).

The promising calibration models established in this study would partly be due to the extremely accurate quantification of malic acid and lactic acid reference values using the high-throughput in-house developed spectrophotometric technique. The small calibration sets used for the development of these models can, however, can be seen as a limitation of these preliminary models.

The samples used for calibration purposes spanned the complete variation of malic acid and lactic acid concentrations of the specific fermentations carried out in this study. However, the range of the sample sets should be extended to include higher malic acid and lactic acid concentrations which would be found in wines and also to include other red cultivars as well as white wine samples. To build robustness into these preliminary calibration models it is necessary to extend the existing calibration sets. This involves including samples from other matrices, cultivars, origins and vintages.

Furthermore, the ready-to-use calibration model is easy to use for an untrained operator, however, the results of this study show how critical it is for the evaluation of this model for the suitability for quantification in different wine matrices.

5.5 LITERATURE CITED

Application note 159, 2001. Issue 2GB, P/N 1025297. Foss Analytical, Denmark. Must Under Fermentation Calibration- Malic acid.

Bauer, R., Nieuwoudt, H., Bauer, F.F., Kossmann, J., Koch, K.R. & Esbensen, K.H., 2008. FTIR spectroscopy for grape and wine analysis. *Anal. Chem*. 80, 1371-1379.

Cozzolino, D., Parker, M., Dambergs, R.G., Herderich, M. & Gishen, M., 2006. Chemometrics and visible-near infrared spectroscopic monitoring of red wine fermentation in a pilot scale. *Biotech. Bioeng*. 95, 1101-1107.

Dambergs, R.G., Kambouris, A., Francis, I.L. & Gishen, M., 2002. Rapid analysis of methanol in grape-derived distillation products using near-infrared transmission spectroscopy. *J. Agric. Food Chem. 50, 3079*.

de Villiers, A., Alberts, P., Tredoux, A.G.J. & Nieuwoudt, H.H., 2011. Analytical techniques for wine analysis: An African perspective. *Anal. Chim. Acta* 730, 1-22.

Esbensen, K.H. (ed). 2006. *Multivariate Data Analysis – In Practice*. 5th Ed. Camo ASA, Oslo, Norway.

Foss Electric, Denmark. http://www.foss.dk.

Gishen, M. & Holdstock, M., 2000. Preliminary evaluation of the performance of the Foss WineScan FT 120 instrument for the simultaneous determination of several wine analyses. *Aust. Grapegrower Winemaker 438a,* 75-81.

Louw, L., 2007. Chemical characterisation of South African young wines. Thesis, Stellenbosch University, Private Bag X1, 7602, Matieland (Stellenbosch), South Africa.

Louw, L., Roux, K., Tredoux, A., Tomic, O., Næs, T., Nieuwoudt, H.H. & van Rensburg, P., 2009. Characterization of selected South African young cultivar wines using FTMIR spectroscopy, gas chromatography, and multivariate data analysis. *J. Agric. Food Chem*. 57, 2623-2632.

Manley, M., Van Zyl, A. & Wolf, E., 2001. The evaluation of the applicability of Fourier transform near-infrared (FT-NIR) spectroscopy in the measurement of analytical parameters in must and wine. *S. Afr. J. Enol. Vitic*. 22, 93-100.

Martens,H., Nielsen, J.P., & Engelsen, S.B., 2003. Light scattering and light absorbance separated by extended multiplicative signal correction. Application to near-infrared transmission analysis of powder mixtures. *Anal. Chem*. 75, 394-404.

Moreira, J.L. & Santos, L., 2005. Analysis of organic acids in wines by Fourier transform infrared spectroscopy. *Anal. Bioanal. Chem.* 382, 421-425.

Næs, T., Isaksson, T. Fearn, T. & Davis, T. (eds). 2002. *A user-friendly guide to multivariate calibration and classification*. NIR Publications, Chichester, UK.

Nicolaï, B.M., Beullens, K., Bobelyn, E., Peirs, A., Saeys, W., Theron, K.I. & Lammertyn, J., 2007. Nondestructive measurement of fruit and vegetable quality by means of NIR spectroscopy: A review. *Postharv. Biol. Technol*. 46, 99–118.

Nieuwoudt, H.H., Prior, B.A., Pretorius, I.S., Manley, M. & Bauer, F.F., 2004. Principal component analysis applied to Fourier transform infrared spectroscopy for the design of calibration sets for glycerol prediction models in wine and for the detection and classification of outlier samples. *J. Agric. Food Chem*. 52, 3726-3735.

Patz, C.D., Blieke, A., Ristow, R. & Dietrich, H., 2004. Application of FT-MIR spectrometry in wine analysis. *Anal. Chim. Acta* 513, 81-89.

Pavia, L.P., Lampman, G.M. & Kriz, G.S. (eds). 2009. *Introduction to Spectroscopy: A Guide for Students of Organic Chemistry*. 4th Ed. Harcourt College Publishers, Belmont, USA. pp. 15-104.

Picque, D., Lefier, D., Grappin, R. & Corrieu, G., 1993. Monitoring of fermentation by infrared spectrometry: Alcoholic and lactic fermentations. *Anal. Chim. Acta* 279, 67-72.

Shenk, JS, Workman, J.J & Westerhaus, M.O., 2008. Application of NIR Spectroscopy to Agricultural Products. In: Burns, D.A. & Ciurczak, E.W. (eds). *Handbook of Near-Infrared Analysis*. 3rd Ed. Marcel Dekker, New York, pp. 347-386.

Silverstein, R.M., Clayton Bassler, G. & Morrill, T.C. (eds). 1991. Infrared spectrometry. In: *Spectrometric identification of organic compounds*. 5th Ed. Wiley, New York. pp. 91-164.

Sivakesava, S., Irudayaraj, J. & Ali, D., 2001. Simultaneous determination of multiple components in lactic acid fermentation using FT-MIR, NIR, and FT-Raman spectroscopic techniques. *Process Biochem*. 37, 371-378.

Smith, B.C. (ed.). 1999. *Infrared spectral interpretation: A systematic approach*. CRC Press LLC, Boca Raton, Florida, USA. pp. 67-152.

Urbano-Cuadrado, M., Luque de Castro, M., Pérez-Juan, P., García-Olmo, J. & Gómez-Nieto, M., 2004. Near infrared reflectance spectroscopy and multivariate analysis in enology: Determination or screening of fifteen parameters in different types of wines. *Anal. Chim. Acta* 527, 81-88.

Urbano Cuadrado, M., Luque de Castro, M., Perez Juan, P. & Gómez-Nieto, M., 2005. Comparison and joint use of near infrared spectroscopy and Fourier transform mid infrared spectroscopy for the determination of wine parameters. *Talanta* 66, 218-224.

Urtubia, A., Ricardo Pérez-Correa, J., Meurens, M. & Agosin, E., 2004. Monitoring large scale wine fermentations with infrared spectroscopy. *Talanta* 64, 778-784.

Urtubia, A., Pérez-correa, J.R., Pizarro, F. & Agosin, E., 2008. Exploring the applicability of MIR spectroscopy to detect early indications of wine fermentation problems. *Food control* 19, 382-388.

Volschenk, H., van Vuuren, H.J.J. & Viljoen-Bloom, M., 2006. Malic acid in wine: Origin, function and metabolism during vinification. *S. Afr. J. Enol. Vitic*. 27, 123-136.

Williams, P.C., 2004. Implementation of Near-Infrared Technology. In: Williams, P. & Norris, K. (eds). *Near Infrared Technology in the Agriculture and Food Industries*. 2nd Ed. Am. Assoc. Cereal Chem., St. Paul, MN. pp 145-169.

WineScan FT 120 Type 77110 and 77310 Reference Manual, Issue 4 GB Foss Electric, Denmark, 2001. http://www.foss.dk.

Chapter 6

General Discussion & Conclusions

CHAPTER 6. GENERAL DISCUSSION AND CONCLUSIONS

Ideally, effective monitoring techniques should be fast, non-destructive, require little sample preparation and be cost effective in order to deliver real-time information. These techniques should provide easily interpretable graphical displays which would allow the winemaker to gain insight into the metabolic state of a fermentation at any specific process stage for the complete control of a process.

The conventional monitoring techniques used by the wine industry are often laborious and unreliable. The research presented in this thesis therefore addressed the current need for alternative fermentation monitoring strategies. More specifically, the overall objective of this study was to develop a platform of methods of both a qualitative and quantitative nature for the monitoring and trend identification of alcoholic fermentation (AF) and malolactic fermentation (MLF) in wine production. Furthermore, very little published work exists on the profiling of different lactic acid bacteria (LAB) treatments and inoculation strategies. Thus, the experimental design was carefully set up in such a way to explore the differences and/or similarities in the fermentation trends of *Oenococcus oeni* (*O. oeni*) and *Lactobacillus plantarum* (*L. plantarum*) treatments, used in both a co-inoculation and a sequential inoculation scenario. Since several of these LAB cultures are in the developmental stages of being tested prior to possible commercialisation, the evaluation of their fermentation performance was of critical importance.

Fourier transform mid-infrared (FT-MIR) and near-infrared (FT-NIR) spectroscopy were the techniques of choice in this study. Based on the measurement of the response of chemical bonds in wine constituents, upon the exposure to infrared radiation, these techniques provided information rich spectra which could be seen as a metabolic fingerprint/snapshot of a sample. By using partial least squares (PLS) regression, the information captured in the spectra was used as a quantitative method where by spectra were correlated to the actual concentration of specific constituents (measured with appropriate reference methods) for the prediction of unknown samples.

The first major objective involved the development of quantitative methods for fermentation monitoring. The ready-to-use FT-MIR calibration model was evaluated for its ability to quantify malic acid in South African fermentation samples. Automated enzyme-linked spectrophotometric analysis allowed for the high throughput of samples and the generation of malic acid and lactic acid reference values with a high precision and accuracy. The standard deviation of repeat measurements of these reference values was less than 8%, thereby rendering a very accurate analytical platform from which the calibration work could be initiated. The global ready-to-use commercial malic acid calibration model on the WineScan instrument performed poorly when evaluated with our fermentation samples, giving a prediction error of 0.96 g/L. New calibration models for both malic acid and lactic acid were therefore established using both FT-MIR and FT-NIR spectroscopy. The aim with these models was to facilitate the

handling of large volumes of samples generated in this study, therefore only the Shiraz wine matrix was included. In this respect, these developments made a significant contribution towards efficient handling of the large volumes of analytical requirements of this project. Based on the positive outcomes of this objective, the models can also serve as a basis from which further expansions of the models can be done to include other red and white cultivars, in order to increase the application and robustness of the models.

To date, the rapid monitoring of MLF in our environment was problematic, due to the absence of accurate PLS calibration models. Malic acid in particular is of critical importance as a quality parameter for monitoring the progress of MLF in red wine production, as well as in certain white cultivars and thus, it was of paramount importance to establish the most robust calibration model, while ensuring the best analytical precision is maintained for further research purposes as well as for practical industrial application. The addition of this model to the existing platform of PLS models developed in earlier studies by our laboratory, particularly those for glucose, fructose, pH, volatile acidity, ethanol and residual sugar, makes a huge contribution towards our capacity for comprehensive metabolic profiling. Indeed, the generation of quantitative data provided a means for the critical evaluation of exact compound concentrations at critical important process stages like end of AF and end of MLF. Using these quantitative values non-linear fitted graphs were fitted to compare the rate of the different fermentation scenarios investigated in this study and showed that the co-inoculated fermentations proceeded significantly faster than the sequential fermentations in terms of sugar degradation and ethanol production. The potential use of these techniques for future online applications as excellent graphical displays of data should be considered for predicting the rate of different fermentation processes.

It is clear that the generation of quantitative data involves an extensive amount of wet analytical chemistry to generate robust calibration models for the accurate prediction of compounds. The quantitative approach is therefore extremely time consuming and expensive during the calibration model development stage. The generation of calibration models also restricts the user to evaluate trends only in constituents that have been calibrated for. For this reason, we shifted emphasis to a qualitative approach for fermentation monitoring in the second objective.

This study clearly also showed the powerful nature of the application of chemometric modelling techniques with both MIR and NIR spectra to monitor the time course trends of the fermentations while bypassing the need to generate quantitative data. In both the MIR and NIR spectra significant variation was observed relating to the time of fermentation. The variation observed was mainly ascribed to the major AF process whereby sugar is degraded to produce ethanol. The same trends were observed when evaluating the spectral scores and loadings using the multivariate technique, principal component analysis (PCA). A clear time course trend was observed on PC1 for both the MIR and NIR spectral data. The trend was clear at the

beginning of fermentation with a large amount of variation between the samples from a specific day while towards the end of fermentation the chemistries of the different fermentations showed apparent similarities. PCA also clearly showed the deviation of certain samples from the time course trend. No trend was seen in terms of LAB treatments or inoculation strategies using the chemometric methods applied here and in future mining of the data generated in this study, the variation on higher-order PC's should be investigated. A simple spectral conformity test based on comparison of the standard deviation of the absorbance recorded at each wavenumber in the infrared spectra, showed excellent potential to be used for future online and industrial applications for the prediction of a specific process stage. This technique is a fast and easy test which by-passes the need for spectral interpretation such as PCA to evaluate the state of a process.

IR spectroscopy can therefore be seen as an excellent alternative to the traditional methods used for monitoring fermentations. With this said, however, this technology comes with challenges which need to be considered for the successful application for fermentation monitoring. Representative sampling remains a challenging factor, however, it is a critically important factor to consider in order to model the biological variability of a ferment and produce the most accurate representation of a whole batch fermentation. In this study the issue of representative sampling was addressed to the best of our ability. During AF, punching down of the fermentation cap was carried out before sampling, while during MLF, the fermentation canisters were thoroughly swirled to mix the ferment prior to sampling. Duplicate independent technical repeats of biological triplicates were sampled in order for us to capture the biological variance within this experiment. However, the biological variability of the LAB should also be tested in subsequent vintages, due to the variation in grape chemical composition, particularly the amino acid content. The specific timing of sampling during fermentation as well as the accuracy of the respective reference data used for calibration are two factors which also need to be considered.

Furthermore, the interpretation of the evolution of the fermentation processes was extended in this study, through the third objective that involved an exploratory, broad range metabolic profiling approach, to evaluate the influence of different inoculation strategies and MLF starter cultures, on the Shiraz wine matrix. GC-FID and GC-MS techniques were used for the accurate quantification of volatile and carbonyl compounds respectively at two critical stages of fermentation, namely 50% completion of MLF and 100% completion of MLF (referring to 50% and 100% completion of malic acid degradation respectively). For several of the LAB cultures tested in this study, the results presented for the aroma compounds here, are the first rounds of chemical testing of the fermentation profiles associated with each of the cultures.

Both a univariate approach involving analysis of variance (ANOVA) and a multivariate data analysis strategy that involved PCA, were successfully applied to profile different inoculation strategies as well as MLF starter cultures using quantified aroma compound data. Both these

techniques showed excellent potential as profiling techniques to differentiate between two critical process stages, namely the 50% MLF completion stage and the final fully completed stage. In both cases the results showed clearer differentiation between the MLF starter cultures at 50% completion of MLF, compared to the data at 100% completion of MLF. While the univariate approach looks at absolute values and significant differences the results of the PCA gave a good graphical representation of the data at the different process stages.

Despite the fact that both the univariate and multivariate technique showed degrees of discrimination between the fermentation profiles of the differently elaborated wines, the use of the multivariate approach exposed more apparent differences. The distinct differences between MLF starter cultures, in particular the differences between *O. oeni* and *L. plantarum* were clear with PCA. Furthermore, PCA also showed clear differences between the strains within these genera.

ANOVA results showed that different metabolic profiles between different MLF species and strains are present. However, these differences are influenced by the specific inoculation strategy and process stage. As mentioned before, it is important to note that these fermentations were only done for one particular year and thus further repetitions would need to be carried out to make more definite conclusions.

The supervised classification technique, PLS-discriminant analysis (PLS-DA) was successfully used for the profiling of *O. oeni* and *L. plantarum* species using quantified chemical data, spectral data and PCA score values. The FT-MIR spectral data showed the least separation within the two specie classes. Soft Independent Modelling of Class Analogy (SIMCA) models using quantified chemical data and FT-MIR spectra showed promise for the classification of MLF starter cultures into their respective classes however these data sets would need to be increased in future studies. This exploratory study evaluating the metabolic differences between MLF starter cultures once again shows the power of IR spectroscopy as an information rich technique.

From this study it is clear that all these analytical techniques together with various data analysis techniques, give critically important insight into the metabolic state of a fermentation process as well as evaluating the differences between different LAB treatments and inoculation strategies. However infrared spectroscopy remains the technique of choice due to its speed and accuracy of analysis, low cost and generation of information rich spectral data.

The next step following this study should be to evaluate the spectral data using software such as SIMCAP+ to produce models for batch process monitoring and the subsequent identification of deviating and problematic fermentations. This off-line study should be consequently be followed by an on-line study whereby these infrared spectroscopy models are applied for the real-time monitoring of AF and MLF. Near-infrared spectroscopy is seen as the ideal tool for these online applications due to its suitability to fibre optics as well as the availability of cheaper more robust instrumentation available compared with MIR spectroscopy.

Furthermore the applications of this study should be applied to an industrial fermentations to evaluate these techniques on a larger scale.